

# CONCRETE STRUCTURES

ANNUAL TECHNICAL JOURNAL



Tassi – Balázs L. G.  
**Naples and Hungary**

Vörös  
**Railway bridges**

Tassi – Wellner – Becze – Mihalek – Barta  
**Highway bridges**

Teiter  
**Composite bridges**

Orbán  
**Masonry arch bridges**

Farkas J. – Kocsis – Németh – Bodor – Bán  
**Flyover constructed of HSC/HPC**

Képes – Novák – Polgár  
**Commercial and industrial buildings**

Gonda  
**Concert hall**

Farkas Gy. – Kovács – Szalai – Lovas  
**Probability based design**

Sipos – Domokos  
**Deformation of RC members**

Balázs G.  
**Creep law for concrete**

Kausay – Simon  
**Particle size distribution**

Nemes – Józsa  
**Mix design of LWAC**

Borosnyói – Balázs L. G.  
**Members prestressed with FRP**

# 2006



ÉMI-TÜV

Notified Body  
1417

Competence  
Certainly  
Quality

[www.emi-tuv.hu](http://www.emi-tuv.hu)

By using the services of the  
**team of ÉMI-TÜV Bayern Ltd.**

your work will be crowned with success in the  
fields of quality systems and safety techniques.

**We offer testing, quality control,  
certification, assessment of conformity and  
expertise in the following fields:**

- elevators, escalators, stage technical equipment
- hoisting machines, cranes and conveyor equipments
- pressure vessels, boilers and gas-containers
- welding technologies, welders, welding plants
- load-bearing structures and non-load-bearing building structures
- amusement rides
- playground equipments
- assessment of conformity and **CE** marking
- design approval
- TÜV CERT, MRTI and TÜV MS certification (according to TGA and NAT accreditation) of Quality Management Systems and Environmental Management Systems; Hospital Supply Standards (KES); Labour Health and Safety Technique Systems (MEBIR); Food Safety System (HACCP / IFS / EUREPGAP); Integrated Corporate Systems

ÉMI-TÜV Bayern Ltd. TÜV SÜD Group • H-2000 Szentendre, Dózsa György út 26.  
Tel.: (+36) 26 501-120 Fax: (+36) 26 501-150 • E-mail: [igazgatosag@emi-tuv.hu](mailto:igazgatosag@emi-tuv.hu)

**Editor-in-chief:**  
Prof. György L. Balázs

**Editors:**  
Prof. Géza Tassi  
Dr. Herbert Träger

**Editorial board:**  
János Beluzsár  
Assoc. Prof. István Bódi  
László Csányi  
Dr. Béla Csiki  
Assoc. Prof. Attila Erdélyi  
Prof. György Farkas  
Gyula Kolozsi  
Dr. Károly Kovács  
Ervin Lakatos  
László Mátyássy  
László Polgár  
Antonia Teleki  
Dr. László Tóth  
József Vörös  
Péter Wellner

**Board of reviewers:**  
Prof. György Deák  
Prof. Endre Dulácska  
Dr. József Janzó  
Antónia Királyföldi  
Dr. Jenő Knébel  
Prof. Péter Lenkei  
Dr. Miklós Loykó  
Dr. Gábor Madaras  
Prof. Árpád Orosz  
Prof. Kálmán Szalai  
Prof. Géza Tassi  
Dr. Ernő Tóth  
Dr. Herbert Träger

Founded by: Hungarian Group of *fib*  
Publisher: Hungarian Group of *fib*  
(*fib* = International Federation for Structural Concrete)

**Editorial office:**  
Budapest University of Technology  
and Economics (BME)  
Department of Construction Materials  
and Engineering Geology  
Műegyetem rkp. 3., H-1111 Budapest  
Phone: +36-1-463 4068  
Fax: +36-1-463 3450  
WEB <http://www.eat.bme.hu/fib>  
Editing of online version:  
László Bene

Technical editing and printing:  
RONO Bt.

Price: 10 EUR  
Printed in 1500 copies

© Hungarian Group of *fib*  
ISSN 1419-6441  
online ISSN: 1586-0361

Cover:  
The first Hungarian extradosed bridge.  
Design and contact: Hídépítő Co.  
Bartók Béla Concert Hall in the  
Budapest Palace of Arts.  
Concrete structure design: Dékettő Ltd.  
Contract: Arcadom Co.

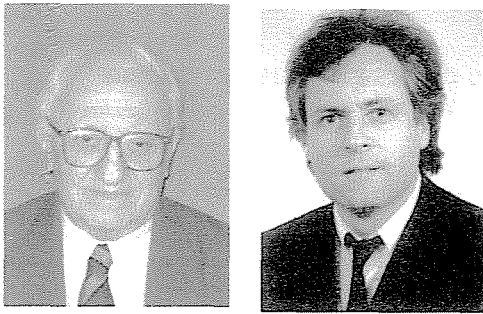
## CONTENT

- 2** Prof. Géza Tassi - Prof. György L. Balázs  
**HISTORICAL LINKS BETWEEN NAPLES AND HUNGARY -  
CONCRETE AND THE fib CONGRESS**
- 6** József Vörös  
**100 YEARS OF REINFORCED CONCRETE RAILWAY BRIDGE  
CONSTRUCTION IN HUNGARY**
- 11** Prof. Géza Tassi - Péter Wellner - János Becze - Tamás Mihalek - János Barta  
**DEVELOPMENT OF CONCRETE HIGHWAY BRIDGE  
CONSTRUCTION IN HUNGARY**
- 17** Zoltán Teiter  
**RENEWED DESIGN PRACTICE OF REINFORCED CONCRETE DECK  
SLAB OF COMPOSITE BRIDGES IN HUNGARY**
- 22** Zoltán Orbán  
**CONDITION ASSESSMENT AND REHABILITATION  
OF MASONRY ARCH RAILWAY BRIDGES**
- 31** Dr. János Farkas - Ildikó Kocsis - Imre Németh - Jenő Bodor - Lajos Bán  
**MOTORWAY FLYOVER CONSTRUCTED OF HSC/HPC**
- 38** József Képes - László Novák - László Polgár  
**PREFABRICATED CONCRETE STRUCTURES FOR  
COMMERCIAL AND INDUSTRIAL BUILDINGS IN HUNGARY**
- 49** Ferenc Gonda  
**CONCRETE STRUCTURE ON ELASTIC PADS - THE BARTÓK BÉLA  
NATIONAL CONCERT HALL IN THE PALACE OF ARTS, BUDAPEST**
- 54** Prof. György Farkas - Tamás Kovács - Prof. Kálmán Szalai - Assoc. Prof. Antal Lovas  
**HISTORICAL BACKGROUND OF PROBABILITY-BASED  
DESIGN IN HUNGARY**
- 64** András Árpád Sipos - Prof. Gábor Domokos  
**SPATIAL DEFORMATIONS OF RC MEMBERS**
- 70** Prof. György Balázs  
**VALIDITY OF LINEAR CREEP LAW FOR CONCRETE**
- 75** Prof. Tibor Kausay - Dr. Tamás Simon  
**GRAPHO-ANALYTICAL CALCULATION OF PARTICLE SIZE  
DISTRIBUTION CHARACTERISTICS OF CONCRETE AGGREGATES**
- 82** Dr. Rita Nemes - Assoc. Prof. Zsuzsanna Józsa  
**ASPECTS OF MIX DESIGN OF LIGHTWEIGHT AGGREGATE  
CONCRETE**
- 88** Dr. Adorján Borosnyói - Prof. György L. Balázs  
**SERVICEABILITY ASPECTS OF CONCRETE MEMBERS  
PRESTRESSED WITH FRP - HUNGARIAN EXPERIENCES**

### Sponsors:

Railway Bridges Foundation, ÉMI Kht., HÍDÉPÍTŐ Co.,  
MÁV Co., MSC Hungarian SCETAUROUTE Consulting Co.,  
Pfleiderer Lábatlani Vasbetonipari Co., Pont-TERV Co., UVATERV Co.,  
MÉLYÉPTERV KOMPLEX Engineering Co., Betonmix Consulting Ltd.,  
BYM Épelem Ltd., CAEC Ltd., Pannon Freyssinet Ltd., STABIL PLAN Ltd.,  
UNION PLAN Ltd., DCB Consulting Ltd.,  
BME Dept. of Structural Engineering,  
BME Dept. of Construction Materials and Engineering Geology

# HISTORICAL LINKS BETWEEN NAPLES AND HUNGARY – CONCRETE AND THE *fib* CONGRESS



Prof. Géza Tassi – Prof. György L. Balázs

*Naples played a significant role at particular times throughout Hungarian history having definitive influence in architecture and the fine arts. For example, the first Hungarian concrete structures utilised the volcanic tuff which originated from the Naples region. Additionally the second part of the Fourth Congress of FIP (an ancestor of *fib*) took place in Naples in 1962. This event gave a boost to the evolution of the Hungarian FIP Group.*

**Keywords:** Anjou kings, Queen Beatrix, Italian art, Pozzuoli, Roman cement, early concrete structures, FIP, *fib*

## 1. INTRODUCTION

The FIP congresses as well as the plenary sessions of CEB were very important milestones in the worldwide development of structural concrete during the second part of the 20th century. The merger of FIP and CEB, which was declared in 1998 and the first *fib* Congress in 2002, gave new impulse to specialists in improving this important sector of the building industry. The successful *fib* Symposium 2005 in Budapest has indicated the importance of international technical-scientific meetings, and we are therefore looking ahead with great expectation to attending this important meeting, the Second International *fib* Congress 2006, to be held in Naples, Italy.

We, the people of Hungary, have always been proud to the relationships between our homeland and other nations which have shaped the events of our culture during the course of our 1100 year history after the settlement of Magyars in our land located in the Carpathian Basin of Central Europe. We consider it to be of great importance to keep in step with the technical developments of our time, to learn from engineers internationally, to exchange ideas and to share our experiences with them.

## 2. NAPLES AND HUNGARIAN HISTORY

First let us mention that there are many historical relics in Naples which are connected to Hungary, for example the Donna Regina Closter which was reconstructed by our Queen Mary (Mária). The monastery includes a room with frescos illustrating the legend of Saint Elisabeth (Erzsébet), member of the Hungarian Árpád royal dynasty.

Hungarian prince Andrew (Endre), son of Robert Charles (Róbert Károly), brother of King Louis the Great (Nagy Lajos) is buried in the San Luigi Chapel of Naples.

The royal archives of Naples contains a great number of documents originating from the last period of the Hungarian Árpád royal dynasty (late 13<sup>th</sup> century) until the death of Ladislav of Naples (end of 14<sup>th</sup> century) and later, from the second part of the 15<sup>th</sup> century (Szilágyi, 1896).

Queen Beatrix (Point 2.2) was born in Castello Nuovo in Naples. She was the daughter of King Ferdinand of Naples from the Aragonia dynasty and married the Hungarian King Mathias (Mátyás). After the death of the King Mátyás, Queen Beatrix returned to her Naples where she died and lies buried in the Church San Pietro.

### 2.1 The Anjou era

Princess Mary (Mária) was daughter of King Stephen (István) V of the Árpád dynasty. She married Charles II (also known as Charles the lame), king of Naples and of the Anjou dynasty (1285-1309). Their son was Charles (Martell), born 1271 who married Clementia, a Habsburg princess. Their son was Robert Charles (Róbert Károly) (1288-1342, *Fig. 1*, drawing by K. Vagyóczky) who was elected as king of Hungary after the Árpád dynasty produced no male heir. He was crowned in 1310. His son Louis the Great (Nagy Lajos) reigned from 1342 to 1382 and was also king of Poland. His younger brother Andrew (Endre) married Queen Johanna from Naples (granddaughter of King Robert of Naples). Andrew (Endre) was also crowned as king but because of various intrigues and the interest of the queen in different matters, Andrew (Endre) was killed.

**Fig. 1:** Hungarian King Robert Charles (Róbert Károly) of the Anjou Dynasty originated from Naples



A military campaign led by the Hungarian king was the revenge for the brutal death of Andrew. King Louis could have occupied the throne of the Kingdom of Naples (Sicily), but for specific reasons, he didn't wish to accept.

The Toldi-trilogy, a story in verse written by the greatest Hungarian epic poet János Arany (1817-1882), was written about this historical battle.

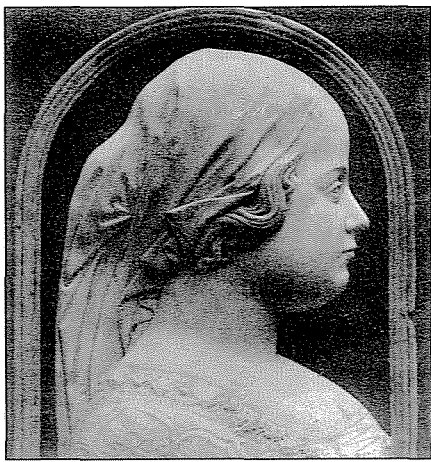


**Fig. 2:** Born in Naples Queen Beatrix, wife of Hungarian King Matthias

Louis the Great was followed on the throne by his daughter Queen Mary (Mária) born 1370, and reigned from 1382 to 1395. Her husband was Prince Sigmund of Luxemburg. Queen Mary could not maintain her wealth and the Anjous of Naples took steps to gain the Hungarian crown. The great-grandson of Mary (Mária) of

the Árpád dynasty and of Charles II (the lame), king of Naples became the king of Hungary and was named Charles the Little. (Kis Károly) (1354-86). He was of the Durazzo branch of the Anjou Dynasty and sat on the throne of Naples as well. Charles the Little was killed shortly after his coronation in December 1385 and his son Ladislas was the last Anjou king of the Naples (Sicily) Kingdom. With his death the Anjou dynasty was ended.

The Anjou era had both glorious and troublesome times both in the Naples (Sicily) and the Hungarian Kingdoms. None-the-less, the culture of medieval Italy spread throughout Hungary.

The map of a part of the Kingdom of Naples and of the Hungarian Kingdom can be seen in Fig. 2.

**Fig. 3:** Map of a part of the Kingdom of Naples and the Hungarian Kingdom in the Anjou era (14<sup>th</sup> century)



## 2.2 The Hungarian Kingdom at the time of King Matthias

King Matthias (Mátyás) of Hungary reigned 1458-1490. After being widowed for twelve years, he decided in 1476 to marry. He sought the hand of Beatrix (Beatrice) (1457-1508), the daughter of King Ferdinand of Naples of the Aragon Dynasty. Matthias sent a splendid delegation to Naples of the most noble Hungarian people comprised of viscounts, members of the clergy and members of the royal family. Princes and episcopes of Bohemia and Silesia joined the delegacy. The deputation was accompanied by 800 horse soldiers (20 Turks among them). They travelled triumphantly across Italy. Beatrix was accompanied by the Archbishop of Naples and many noble gentlemen and ladies of Naples followed the royal bride. At the border of Slavonia, they entered Hungary where they were welcomed by the king's mother, Erzsébet Szilágyi, widow of János Hunyadi.

She accompanied the delegation to Székesfehérvár (Roman name Alba Regia). Matthias awaited them with more foreign rulers and Hungarian noblemen. Beatrix alighted from her six-horse tied coach and prepared to genuflect before the king, but Matthias did not allow this and reached out his arms to his future queen. The coronation took place on the third day after her arrival, and some weeks later they moved to Buda Castle.

The youth, beauty and multidiscipline education of Beatrix (Fig. 3, relief of contemporary Italian sculptor) created a deep impression in the king. Matthias had an enduring interest in renaissance culture and consequently many Italian artists, architects and scientists came to the Hungarian Kingdom. Their merciful and humanist influence would continue to be an influence despite the much tormented history of Hungary.

The queen returned to Naples after the death of Mathias, but the progressive spirit of Italian culture remained for centuries to come.

## 2.3 The Habsburg dynasty and Naples

Two centuries after the reign of King Mathias and prior to the reestablishment of a united Italy, the Habsburg kings of Hungary once again developed a close relationship with Naples. As the Austrian emperors had to abdicate their throne in Spain and Flanders, by way of modest compensation, were granted the seat of Naples. Thus Charles III (Károly) (Austrian emperor named Karl VI) (1685-1740, reigning from 1711) became the king of Naples in 1713. He was the last Habsburg male to rule and was succeeded by Mary Theresa (Mária Terézia).

## 3. INFLUENCE OF NAPLES ON THE DEVELOPMENT OF CONCRETE

### 3.1 Ancient Italy

Construction activity in ancient Italy was marked by a very important feature. Earlier binding materials were only used which hardened in open air. As a result new types of mortar and artificial stone were introduced. The significant property of the bonding material was that it hardened by adding water, and

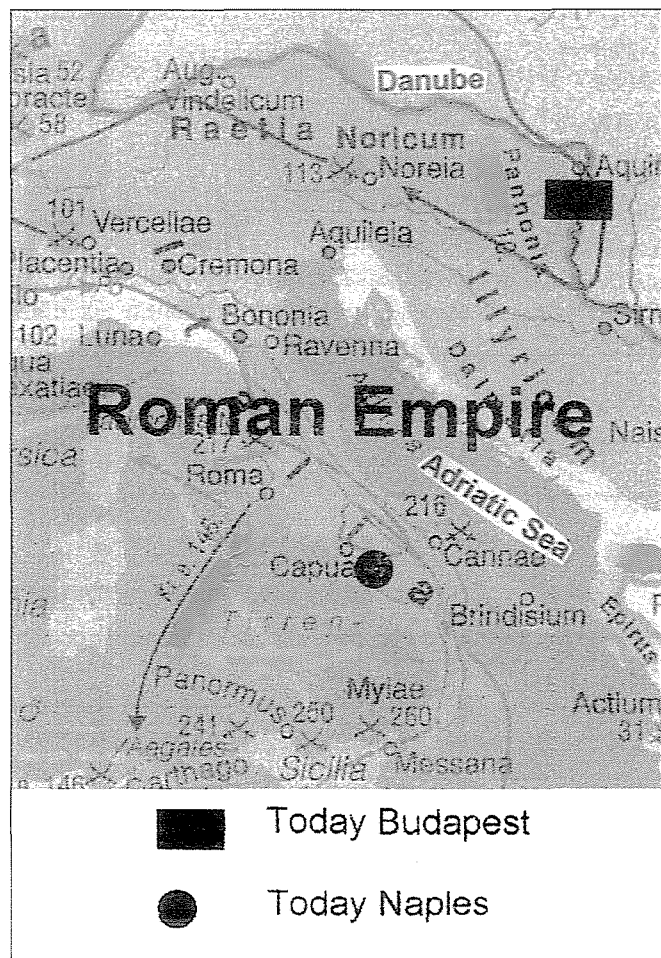
even under water. This hydraulic bonding material originates from the region of Naples. The powder of volcanic tuff was used and mixed with water and other materials (Balázs, 1984). The volcanic material was found in the Naples region at Pozzuoli. Marcus Vitruvius Pollio described the artificial stones, which were called *betonium*, as being used in the era of Julius Cesar and Cesar Augustus (Palotás, 1961). *Betonium* was a collective noun for all such materials, but in many European languages this became the root of the name of concrete (béton, Beton, beton, betón, betong). It is therefore not surprising that the breakwater of Naples was constructed using such material in the 4<sup>th</sup> decade of the 1<sup>st</sup> century AD.

### 3.2 Relics of the Roman Empire in Pannonia (today known as Transdanubia, Hungary)

There was a period of world history when the region of Naples and the region of Buda (Pannonia, Western Hungary of today) belonged to the same empire. Many historic relics of the Roman Empire can be found in our country, among them such buildings, roads, hydraulic works which contained hydraulic binding material. Constructed in the 4<sup>th</sup> century AD in the Roman city of Sopianae in the present time Hungarian town Pécs are the world theritage listed early Christian crypts (Lenkei, Schubert, Temesi, Vörös, 2005).

Approximately 70,000 km of roads, starting from Rome and going in many directions, were constructed using Puzzolan mortar and artificial stone, built in bridges and other structures, too. A remnant of such a road is still to be seen in Szombathely, where the Roman City of Savaria was situated.

**Fig. 4:** Map of a part of the Roman Empire (3<sup>rd</sup> Century AD) with today Naples and Budapest



The first bridge-like structure in the Hungarian capital is an aqueduct in Aquincum (at old Buda) where, among other buildings, two amphitheatres from the 2<sup>nd</sup>-3<sup>rd</sup> century AD remained and were explored. All of these examples utilised materials originating from Naples. (The map of a part of the Roman Empire containing of the today Naples and Budapest is to be seen in Fig. 4).

### 3.3 Later Hungarian concrete structures where Puzzolan was applied

Construction in the first centuries of the Hungarian Kingdom has incorporated hydraulic bonding material for mortar. Later, at the end of the 18<sup>th</sup> century a burnt marl based material was invented in Britain. It was called Caementum Romanum (i. e. Roman cement) and had similar properties to Puzzolan (Palotás, 1961).

The first plain concrete structures in Hungary were realised when Roman cement was introduced. Thus these applications can be considered as “great-grandchildren” of the ancient works which used the first hydraulic bonding materials found near Naples. In Hungary an early application of Roman cement was in the 1839 foundation of the Széchenyi Chain Bridge (Fig. 5), the first permanent connection across the Danube. It is an interesting coincidence that the marl burning furnace

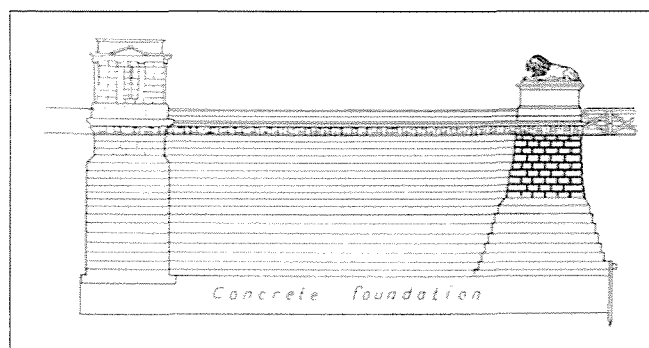


**Fig. 5:** Foundation (1839) of the Chain bridge across the Danube connecting Buda and Pest

was established in close proximity to the Pest abutment of the bridge, where later the Hungarian Academy of Sciences was built (Mihailich, Haviár, 1966). This building was subsequently the venue for the 2005 *fib* Symposium in Budapest.

After the foundation of the Chain bridge, plain concrete structures were built. The largest volume (19,000 m<sup>3</sup>) of such concrete was used in the navigation lock of the Franz Joseph canal (1852).

Certainly, Italian concrete construction techniques had a definitive and enduring role in Hungarian building science and industry during the permanent boom of technology; however it would be difficult to attach these to defined cities of regions.

## 4. NAPLES PROVIDING A VENUE TO MEETINGS ON STRUCTURAL CONCRETE

Italian specialists in concrete construction contributed much to facilitate better exchange of experiences between engineers throughout the world. Italy hosted many events of parent associations of *fib*. There were CEB plenary sessions (Rome 1957, 1979; Treviso 1987); the FIP Congress (Rome-Naples, 1962);

numerous commissions and task groups meeting and other events. Presidents of international associations were elected from Italy: F. Levi (FIP and CEB), G. Mancini (*fib*). Commissions and task groups were chaired by Italian colleagues and several Italian engineers were given high awards by these associations.

Let us review events in Naples.

## 4.1 FIP Congress in 1962

The fourth FIP Congress was held in Rome and Naples. The meeting which was opened in Rome on 26<sup>th</sup> May 1962 continued on 31<sup>st</sup> May in Naples and lasted till 2<sup>nd</sup> June. Participants were hosted by the Municipality of Naples in the splendid Royal Palace (Palazzo Reale). The working sessions were at the Mostra d'Oltremare – Teatro Mediterraneo. The closing banquet took place in the Nuova Piscina Coperta.

The outstanding structures sessions were attractive, and all other technical sessions were informative and useful. The sight-seeing and visits to noteworthy places, among them Pozzuoli and Solfatara, made Naples and surroundings unforgettable.

The FIP Congress in 1962 was the first such event where a Hungarian professional group participated. The Hungarian delegation consisted of 12 professionals, among them such internationally known personalities as E. Bölcskei, P. Csonka, L. Palotás and J. Thoma, plus four accompanying persons. The Hungarian presentations and published papers have proved to be a good entrance into international concrete life (Tassi, 2003).

## 4.2 The Second International *fib* congress 2006.

It was a great honour for the Hungarian Group of *fib* to have the Italian *fib* delegation, under the leadership of President G. Mancini, announce their invitation to the Naples congress at the *fib* Symposium 2005 held in Budapest. We are proud and pleased that both the Advisory Committee and the Scientific Committee of the congress in Naples co-opted Hungarian members.

Looking at the circular distributed by the organisers, we are convinced that our Italian friends follow our slogan of 2005 to "Keep Concrete Attractive". We are confident that the organisers and contributors will do their utmost to ensure the benefits of international meetings as we tried to formulate it last year (Tassi, Balázs, Borosnyói, 2005).

The venue, "Mostra d'Oltremare", reinforces the experience to everyone who has ever been at this grand conference centre: the supreme value and high level professional benefit as well as noble entertainment for delegates and accompanying persons.

## 5. CONCLUSION

When delegates from different countries gather in a city of the host country, it is worthwhile to look into the past and search for common historical backgrounds. Hungarians are fortunate to have common roots with Italy in culture, art and science. Italy produced many noteworthy civil engineering and architectural objects and added much to the science of concrete.

We have seen huge developments over more than four decades and particularly during the last four years since the first *fib* congress. We hope that the congress will be a triumph for concrete science and technology. By means of this issue of "Concrete Structures" we can show a segment of the activity of Hungarian concrete engineers over the last four year period.

We wish success to all participants of the congress at Mostra d'Oltremare.

## 6. REFERENCES

- Balázs, Gy. (1984) "Construction materials and chemistry", Tankönyvkiadó, Budapest (in Hungarian)
- Lenkei, P., Schubert, J., Temesi, E., Vörös, G. (2005). "Functional or architectural attractiveness of concrete structures for archaeological remains (Harmony or controversy under the earth)", "Keep Concrete Attractive", Proceedings of the *fib* Symposium Budapest 2005 (eds. G. L. Balázs and A. Borosnyói), pp. 69-73, ISBN 963 420 838 X
- Mihailich, Gy., Haviár, Gy. (1966), "The beginning and the first achievements of reinforced concrete construction in Hungary", Akadémiai Kiadó, Budapest (in Hungarian)
- Palotás, L. (1961), "Construction materials II.", Akadémiai Kiadó, Budapest (in Hungarian)
- Szilágyi, S. (editor) 1896, "History of the Hungarian nation" Athenaeum, Budapest (in Hungarian)
- Tassi, G. (2003), "History of the Hungarian FIP Group from the beginning to 1998", Vasbetonépítés (special issue 2003) (in Hungarian)
- Tassi, G., Balázs, L. Gy., Borosnyói, A. (2005) "Benefit of technical/scientific symposia" Concrete Structures 2005, Vol. 6, p. 2.

**Prof. Géza Tassi** (1925) Civil Eng., PhD, Doctor of Techn. Sci. (Hung. Acad. Sci.) (1976), professor (semi retired) at the Dept. of Struct. Eng. of Budapest Univ. of Techn. and Econ. (BME). Awarded Golden Ring (1979) and Golden Diploma (2000) of the BME, FIP Medal (1992), awarded at the first congress of *fib* (2002), Palotás László-award (2005). Lifetime honorary president of Hungarian Group of *fib*. Author of 240+ publications, mainly on RC and PC structures.

**Prof. György L. Balázs** (1958) Civil. Eng., PhD, Dr.-habil., Head of Dept. of Constr. Materials and Eng. Geology of the Budapest Univ. of Tech. and Econ. (BME), Member of the Presidium of *fib*, president of the Hungarian Group of *fib*, convener of *fib* Task Group on "Serviceability Models" and "*fib* Seminars". Member of several *fib*, ACI and RILEM task groups or commissions. Author of 200 publications mainly on structural concrete, non-metallic reinforcement, fibre reinforced concretes and various other construction materials.

# 100 YEARS OF REINFORCED CONCRETE RAILWAY BRIDGE CONSTRUCTION IN HUNGARY



József Vörös

The first reinforced concrete railway bridges on the network of Hungarian Railways were built 100 years ago. On this centenary we commemorate the history and development of the first reinforced concrete railway bridges by briefly describing some of the most significant structures. This commemoration, however, would not be complete if we did not mention those plain concrete constructions that were built before the reinforced concrete bridges or at the same time and, in fact, could be considered as their predecessors.

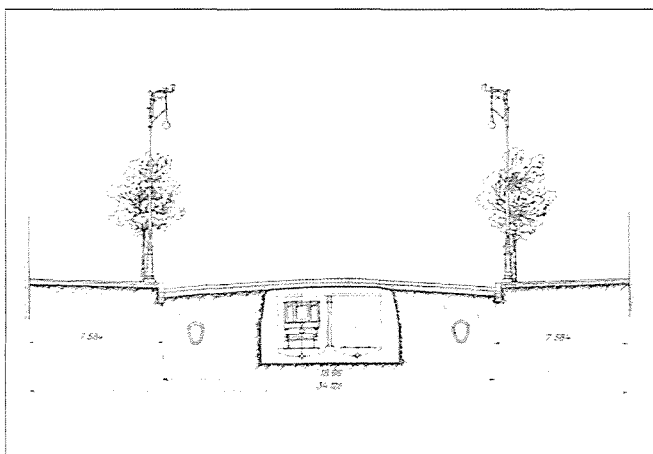
**Keywords:** Reinforced concrete, railway, bridges

## 1. INTRODUCTION

The building of concrete culverts and concrete abutment walls along the lines of Hungarian Railways started in the 1880's. In the field of bridge construction the application of concrete, which was a new building material at the time, was accepted with reservations. This is why bridges with concrete elements were first built in the first decade of the 20th century. At that time regulations concerning the production of concrete or the building of railway bridges did not exist yet. In 1909, the Hungarian Association of Engineers and Architects issued its booklet entitled the "Design and Construction of Concrete Structures with Iron Reinforcement" which was published again unabridged in 1914. At Hungarian Railways these regulations were in use at the beginning of the 1900s for composite trough bridges and reinforced concrete bridges with various structures.

Concrete structures were also built in other fields of transport development at the time. One of these structures is, for example, the wall of the tunnel of the European continent's first underground railway in Budapest named after Emperor and King Franz Josef and the pedestrian bridge built on the surface section of the underground (Fig. 1).

**Fig. 1:** The cross section of the underground railway built in 1896



## 2. CONCRETE CULVERTS, ARCHES AND BRIDGES

Concrete culverts with 0.6 to 1.0 m spans were rarely built at the end of the 1800s. The first plans for building concrete culverts were made in 1894. In 1908 new constructions were designed with so called "frog mouth" profiles with a spans ranging from 0.6 m to 2.0 m. These culverts were laid directly on the ground without rigid foundations where subsoils provided adequate



**Fig. 2:** The first concrete bridge (designed by Robert Wünsch)

strength. Culverts with spans of 1.0 m or more incorporated steel tyings which were placed in the bottom part of the pipe body in order to resist tensile forces. These steel elements were 0.4 to 0.5 m far from each other with dimensions of 25/10 to 30/15 mm, depending on the size of the span.

At present there are still about one thousand different arch culverts and bridges along the lines of Hungarian Railways. However, only about 10% of these are concrete structures. Most of the concrete arches were built in the first half of the last century, usually with semicircular arch design (Fig. 3). Some of the larger barrels of the concrete arch bridges were provided with minimum reinforcement in order to avoid cracking due to shrinkage of the concrete. These reinforced structures, however, were specified as plain concrete structures.



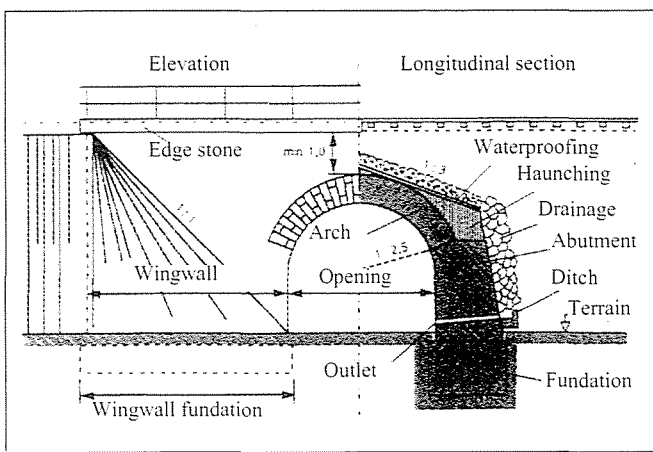
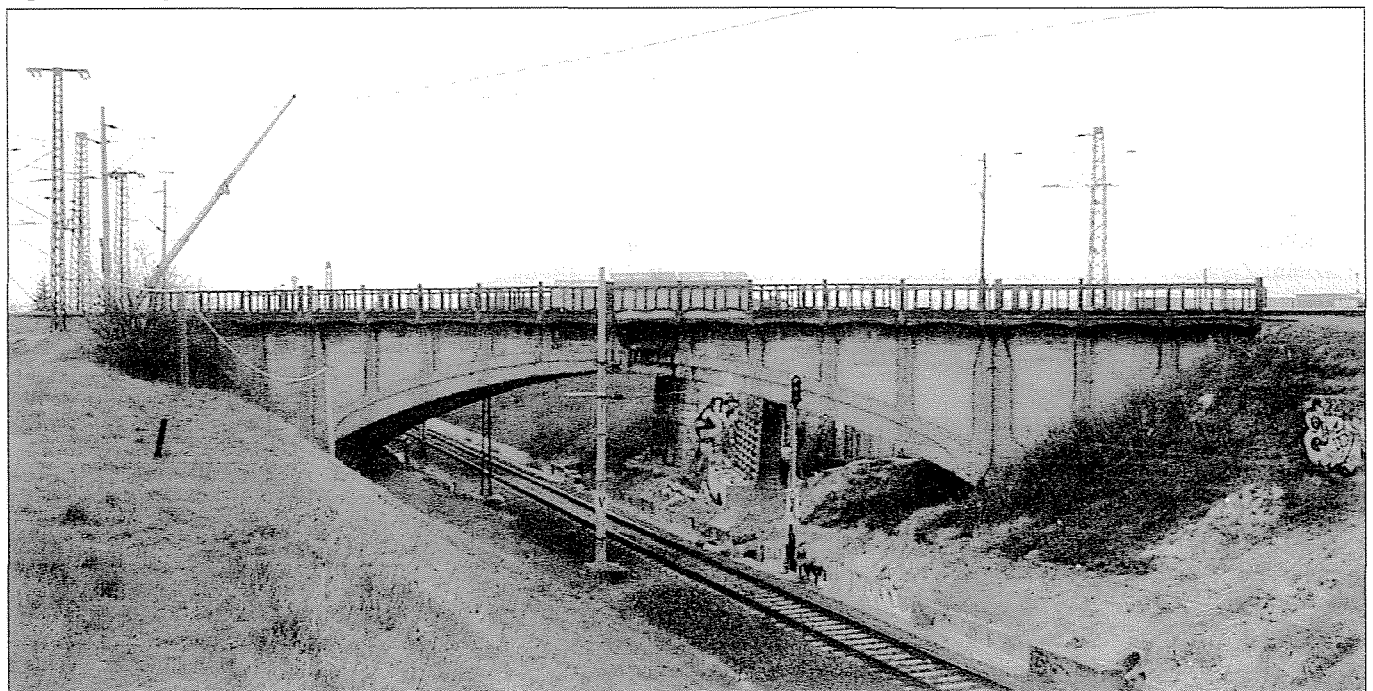


Fig. 3: General configuration of semi-circular arch bridges

The first composite trough bridges with concrete structures were built at the very beginning of the 1900s along the Hungarian railway lines. The first designs for these bridges appeared in Ignác Spitzer's work, chief engineer at Hungarian Railways, entitled "Transition of Superstructure Ballast on Railway Bridges" in 1904. According to the presumptions of the design, concrete has merely a filling role in composite trough bridges, all the load is borne by the concreted rails or steel beams.

In addition to the great number of advantages, composite bridges also had their drawbacks, such as the need for a huge amount of steel components because the composite action of the integrated load bearing structures and the filling concrete was not taken into consideration when determining their sizes. Nowadays, the dimensions of such bridges are based on the planning directives from the Bridge Department of the Railways which were in turn developed according to suggestion from the Research and Development Institute (ORE) of the International Railway Union (UIC). These directives paid attention to the composite action of the concrete and the steel elements which resulted in significant savings regarding the amount of steel material used. The first bridge built according to the new directives was the Rinya Bridge on the Dombóvár-Gyékényes railway line. The bridge has 10.5 m span and was designed by the Designing Institute of the Hungarian Railways. The construction was carried out by the Bridge Building Di-

Fig. 4: Three-hinged concrete arch at Érd



rectorate of the Hungarian Railways in 1974.

The concrete arch bridge with the largest effective span was built in 1913 near Érd railway station on the Budapest-Kelenföld-Szentlőrinc line arching over the Budapest-Nagykanizsa line. The structure is a three-hinged concrete arch bridge with a 27.0 m effective span. The construction of this bridge was necessitated due to corrosion of the iron arch of the earlier bridge because of the steam of steam engines. There is 900 m<sup>3</sup> of concrete built in to the bridge. The sandy gravel used for concreting was improved by adding crushed stone. It was the first time that pneumatic tampers were used for the compaction of the concrete. During the last few decades significant cracks have appeared on the surface of the concrete arch and speed limit had to be introduced on the bridge. The railway traffic on the bridge came to an end in 1999 when a new bridge was erected next to it to replace the old one. The old, out-of-date bridge will be demolished in the near future (Fig. 4).

### 3. REINFORCED CONCRETE BRIDGES

#### 3.1 The first reinforced concrete railway bridges

The first three reinforced concrete bridges on narrow gauge railway lines were built in the Debrecen and Nyíregyháza region nearly at the same time in 1905. One of these was blown up during the war, another had been demolished earlier. The portal bridge with slab-and-girder deck and with 4.7 + 8.4 + 4.7 m spans, however, is still standing on the 92/3 section of the Nyíregyháza-Dombrád railway line. The bridge was designed by Szilárd Zielinski, professor of the Technical University of Budapest. The design calculations were carried out by Zsigmond Jemnitz, chief engineer in Zielinski's designing office. They calculated with allowable stress values of 3.5 N/mm<sup>2</sup> of pressure in concrete and 10 N/mm<sup>2</sup> of tension in the steel reinforcements. The first load test of the bridge was carried out on 7 September 1905. They detected hairline cracks on the main

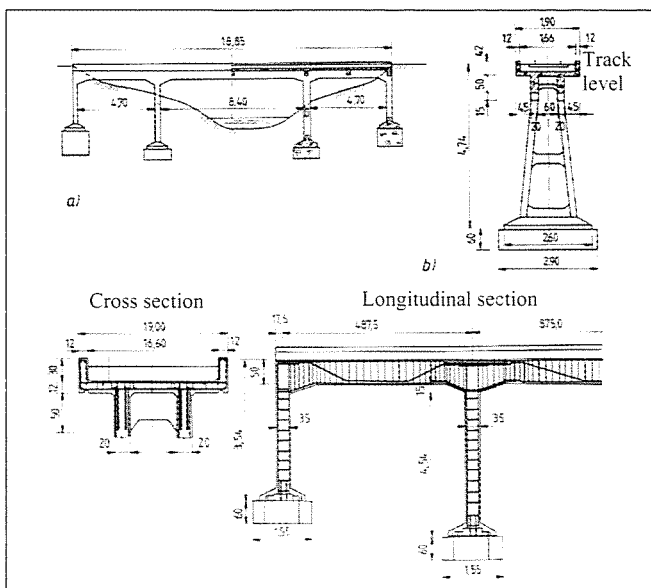


**Fig. 5:** The first reinforced concrete bridge at narrow gauge railway, 1905

girders which were corrected. Five years later in 1911, there was a further load test carried out again on the bridge where no further cracks were found. Railway traffic on the bridge ceased in 1972 when there was a new bridge built next to the old one. The bridge has not been demolished it is still in use as a footbridge of monumental value (Fig. 6).

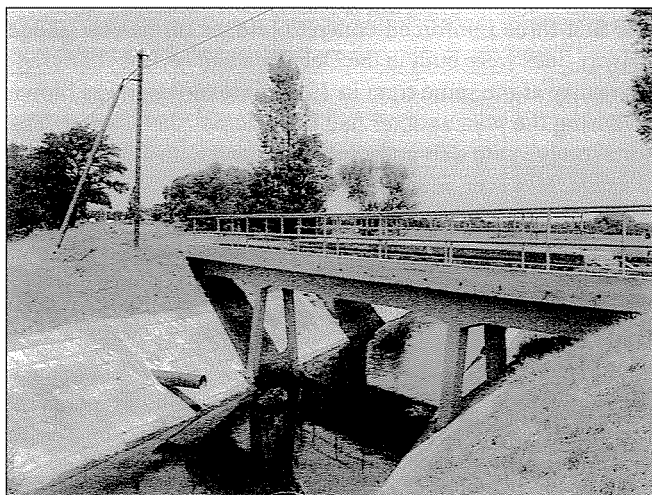
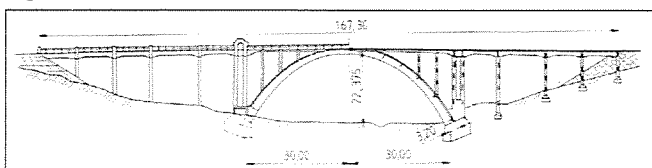


**Fig. 6:** The first reinforced concrete bridge at narrow gauge railway, 1905

The first two reinforced concrete bridges on standard gauge railway lines were built in 1908 on the Brassó-Fogaras railway line. When building the railway lines two viaducts had to be erected between sections 290 and 310 on the line. The original concept was to build high banks on these sections, but after the evaluation of economic calculations they decided to build viaducts instead of the banks. The design work was also done in Szilárd Zielinski's office, under the direction of Professor János Kossalka. The effective span of the bigger viaduct is 60.0 m, and that of the smaller viaduct is 36.0 m. The two load bearing elements of the bridges are arches leaning on plates (Fig. 7).

The superstructure of the viaduct situated near the railway station of Sinka is laid on a 30 cm thick crushed stone bedding.

**Fig. 7:** General plan of the viaduct at Sinka, 1908



The bridges were loaded with two engines with a 10.1 ton axle load, which were the heaviest engines at the time, and attached carriages with an 8.6 ton axle load.

### 3.2 The first prestressed concrete bridges.

The first prestressed concrete bridge of Hungarian Railways was built in 1966 over the Tarna river near the railway station of Recsk on the Kisterenye-Kápolna railway line. The 17.0 m span bridge was designed by the Hungarian Road and Railway Designing Company (Uvaterv) and was built by the Bridge Construction Directorate of the Hungarian Railways. The bridge was built with two main box girders that are not connected to each other. Each main girder consists of three prefabricated reinforced concrete elements which already had the ducts of prestressing cables. The specified concrete grade was B 450.

The bridge elements were manufactured in the Budapest Manufactory of the Bridge Construction Directorate and were transported to the building site on the railway. The threading of

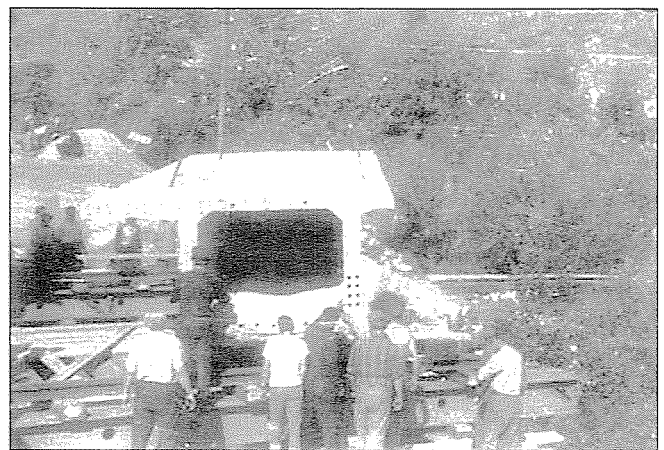
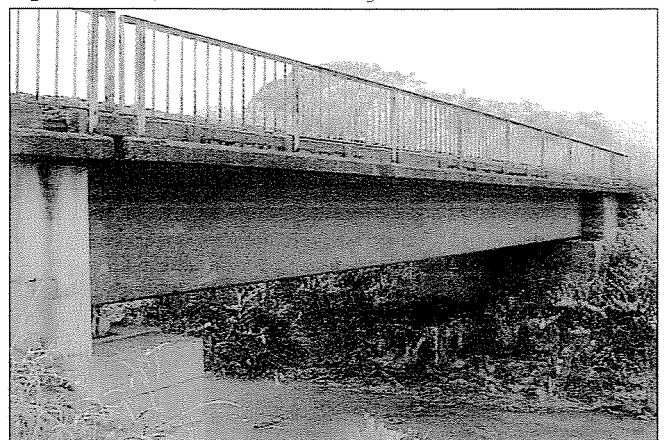


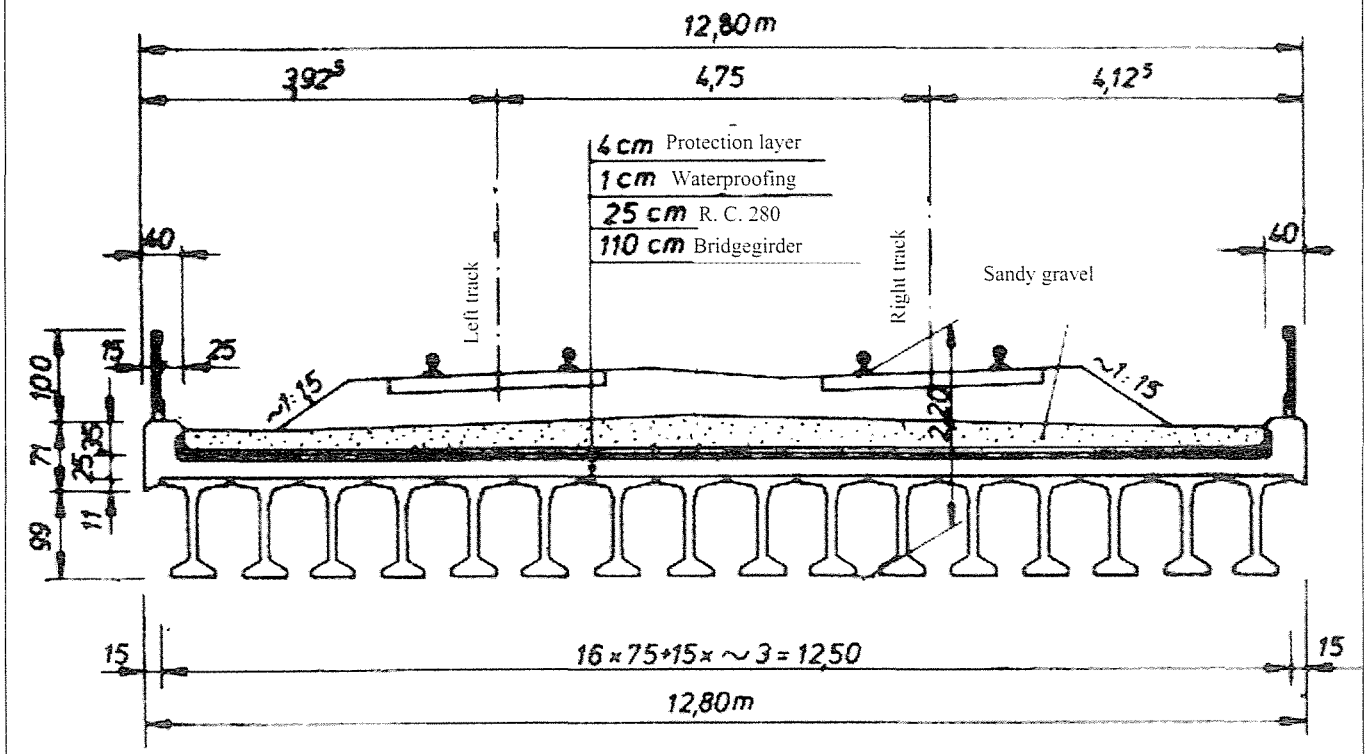
**Fig. 8:** Elements of the first prestressed concrete bridge at Recsk

the prestressing cables, their tension and later the injection of the cable ducts was carried out by the specialists of the Bridge Construction Company (Hidépítő). Each prestressing cable consists of 18 wires with the diameter of 5 mm, the cables were stressed by Freyssinet prestressing jacks. The prefabricated reinforced concrete elements were mounted by railway cranes (Fig. 8). In the course of test load stress measurements were carried out on the bridge by the Technical University in cooperation with Central Structure Testing Directorate of the Hungarian Railways. The results proved that the design calculations were correct. The bridge was opened to the public on 16 December 1966 (Fig. 9).

**Fig. 9:** The first prestressed concrete bridge at Recsk over Tarna river



# Cross section



The first bridge of the Hungarian Railways designed with prefabricated and prestressed concrete girders was built on the 661/2 section of the Budapest-Hegyeshalom railway line. The bridge, that is situated near Tatabánya railway station, had to be built in the course of track correction and to serve as a road overpass. Based on the Railway Bridge Regulations of 1976 the design was made by Uvaterv, the construction was carried out by the Bridge Construction Directorate of the Hungarian Railways. 16 prestressed concrete bridge girders were used for the 14.0 m span two-track bridge with ballast lead through. 25 cm thick B280 grade reinforced concrete floor slabs were constructed that work together with the bridge girders. The bridge was supplied by waterproofing with asphalted aluminium foil. The bridge was opened on 20 October 1979 after load test with two M62 engines (Fig. 10).

floor structure were filled with concrete. During the course of prestressing, compressive stresses developed in the stiffening structure, which later decreased the tensile stresses deriving from the live load.

The bridge was put into operation on 2 February 1949 (Fig. 11). In 1956 there was an earthquake with its epicentre in near-

## 4. CONCRETE ARCH BRIDGE AT DUNAHARASZTI

The first Langer System concrete railway arch bridge was built in 1949 on the railway line between Dunaharaszti and Ráckeve. This bridge was based on the plans by Hugó Székely to replace the former steel bridge with a span of 50 meters which had been destroyed during World War II. The tied arch bridge built with a ballasted track has a span of 52 metres.

The load bearing structure was built in two phases. In the first phase, a 3-hinged arch structure was built, which had an interim crownhinge built on the top of the arch, the discontinuity in stiffening structure was built together with the bridge deck structure the middle of the span.

The ties were released into concrete at the ends of the stiffening girders. In the second phase, when the stresses caused by the permanent loads were formed in the structure of the stripped bridge, the ties were prestressed using built-in hydraulic presses. After the completion of the prestressing, the interim hinges of the arches and the gaps left in the reinforced

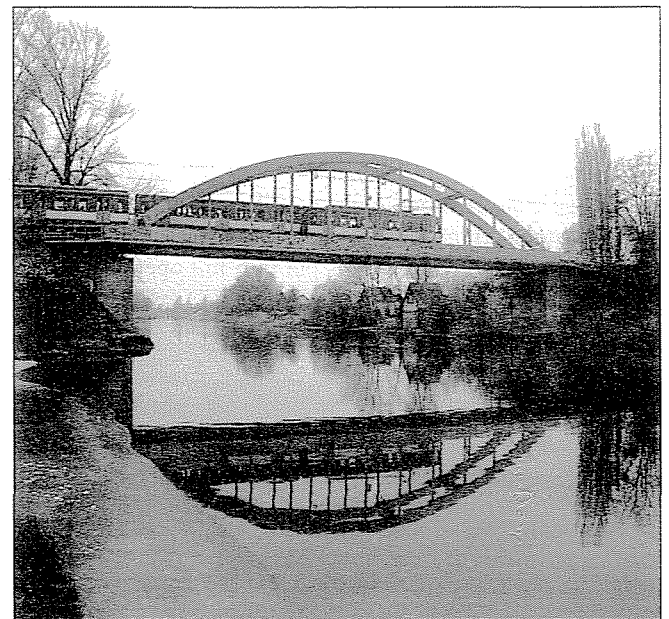


Fig. 11: Reinforced concrete arch bridge at Dunaharaszti

by Dunaharaszti, and as a consequence, the bridge went through a comprehensive test, where no adverse structural change was detected. In the subsequent years significant corrosion damage developed in the concrete structure of the bridge which was eliminated by epoxy resin treatment.

## 5. REINFORCED CONCRETE UNDERPASS IN BÉKE STREET, BUDAPEST

The extension of Béke Street in the direction of Újpest was prevented by a traverse cross section of the circular-railway running along the left bank of the Danube River. Under the 13 tracks of the Budapest-Angyalföld railway station only the two tracks of the tram were transferred. During World War II - at the end of 1944 - the steel tyings of the old bridge were blown up. The demolished bridge was rebuilt as an emergency bridge in 1945 reusing the concrete abutment walls of the old bridge.

The reconstruction plans of the bridge were made by the Municipal Engineering Institute of Budapest. The new bridge is an underpass with three spans of 11.0 + 8.0 + 11.0 metres, where the two side-spans are for cars and pedestrians, and the middle span is for trams. The bridge transfers 13 railway tracks, as well as the traffic of Balzsam Street. In addition, a loading station owned by the Hungarian State Railways was located over the underpass (Fig. 12.).

During construction the Bridge-Construction Directorate of

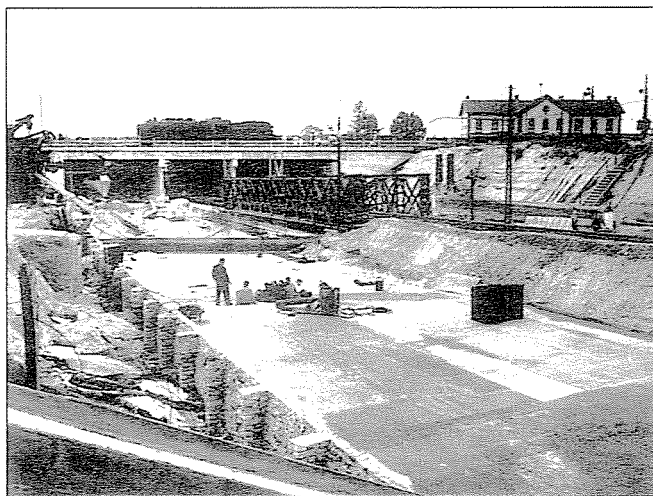


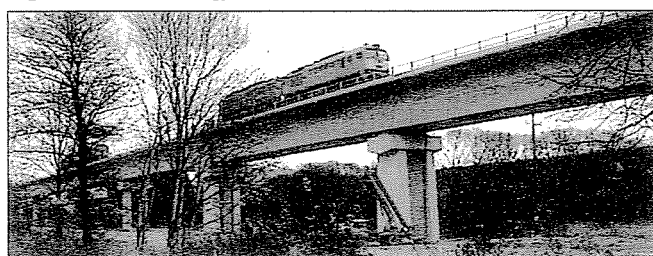
Fig. 12: Construction works at Béke street underpass

the Hungarian State Railways built in 10,500 m<sup>3</sup> of concrete, the Bridge-Construction Company added a further 5,500 m<sup>3</sup> of concrete at the bridge. The Béke Street underpass was opened to the traffic in phases, but was put into full operation on 15 May 1957 (Fig. 13).

Fig. 13: Underpass at Béke street



Fig. 14: Viaduct at Nagyrákos



## 6. POST-TENSIONED CONCRETE BRIDGE CONSTRUCTED WITH INCREMENTAL LAUNCHING

The longest bridge currently owned by the Hungarian Railways is the 1,400 metre-long viaduct at Nagyrákos, which is also a post-tensioned concrete bridge. 16-spans of the bridge are straight, 4 are levelling curves and 16 spans are with an arc of 2,400 m radius. The spans are 37 m, 38.5 m and 45 m. The closed, 3.75 m deep, 4.5 m wide box-casting units were prefabricated and installed opposite each other with incremental launching. In the middle of the bridge, two 38.5 m span structures with a convex rounding-off curve were needed due to changes in level. The prestressing cables are of straight, arched and broken-line alignment. For the possible future reinforcement of the bridge two spare points were formed. A collection of computer programs assisted the dimensioning of the bridge. The bridge, to which so much attention was paid at conferences and technical journals, was finally put into operation in 2000. As the designer of the structural drawings, also the building contractor of the viaduct, the Bridge Construction and Engineering Stock Company was awarded several professional awards (Fig. 14). Simultaneously to the construction of the 1400 m long viaduct, another 200 m post-tensioned concrete bridge with 5 spans was built, which in the shadow of its big brother was almost thrust into the background. At this latter bridge the same dimensions of cross section, technologies and dimensioning principles were employed as with the 1,400 m viaduct.

## 7. SUMMARY

In the previous units we have given an overview of the history and evolution of concrete and reinforced concrete railway bridges in Hungary by introducing the structures we consider as important landmarks. When comparing the evolution of reinforced concrete construction in Hungary with other European railway companies, we can assume that Hungarian engineers have been at the forefront of the expertise in this period. The portal bridges built in the Debrecen-Nyíregyháza axis (1905), the arch bridges between Fogaras and Brassó (1908), the newest post-tensioned concrete bridge with incremental launching, and the consistent modernisation of the general-purpose plans are only a few to mention out of the many examples of their achievements. These were possible to reach by the high standard of education in technical engineering, the competence and innovative spirit of our engineers and the industry of the Hungarian workers.

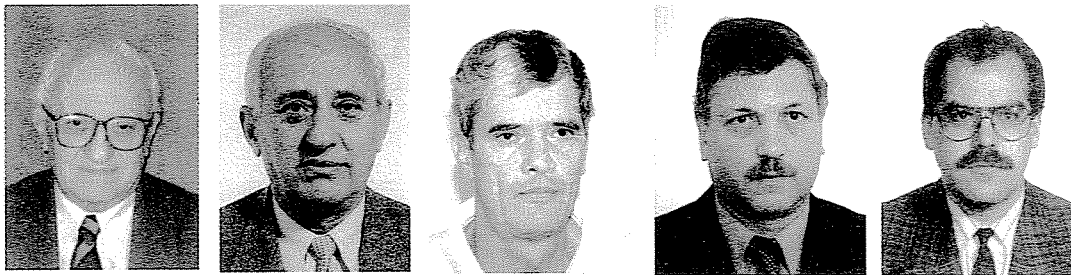
## 8. ACKNOWLEDGEMENTS

We would like to give our thanks and at the same time acknowledge the hundreds of unknown bridge builders who have been in the forefront of reinforced concrete railway bridge building during the last century, and contributed to safe railway transport with their expertise.

József VÖRÖS (1946) qualified civil engineer, director of the Bridge Division of MÁV Rt. The national introduction of prestressed concrete bridges characterises his effective professional work. His activity in connection with the first balanced cantilevered bridge is recognised with a State Prize. He controlled the construction of the first balanced cantilevered prestressed concrete bridges.

He has been teaching at the Construction Execution Department of Technical University of Budapest since 1992 and is a member of the Hungarian Group of *fib*.

# DEVELOPMENT OF CONCRETE HIGHWAY BRIDGE CONSTRUCTION IN HUNGARY



Prof. Géza Tassi - Péter Wellner – János Becze – Tamás Mihalek – János Barta

Reinforced concrete has been applied in Hungary for highway bridges since early 1890s. There was a boom in the first decade of the 20<sup>th</sup> century. A further development proceeded between World War I and II. The time of the reconstruction work after the insane destruction of bridges by the end of World War II was blended with the introduction of prestressing and prefabrication. A few examples are shown from among classical concrete bridge structures built in Hungary, furthermore of up-to-date technologies like construction with precast bridge girders, segmental and monolithic free cantilevering, incremental launching and application of cable stays.

**Keywords:** Classical RC bridges, prefabrication, free cantilevering, incremental launching, cable stays.

## 1. INTRODUCTION

It would be difficult to give a complete review on the Hungarian concrete bridges which were constructed for highways in the last approximately 120 years. In this paper, we try to describe some significant bridges constructed till the end of the 1960s, then the main trends of the recent technologies

## 2. CLASSICAL EXAMPLES OF RC HIGHWAY BRIDGE CONSTRUCTION

The first road bridge in Hungary, constructed of reinforced concrete was completed in 1890 on the main road Budapest-Belgrade. It is a 2×5 m span structure built in Monier system (Tassi, 1994). The first RC bridge in the capital is a 10.70 m span pedestrian overpass built in 1896 above the former surface section of the first underground line of continental Europe (Balázs, Borosnyó, Tassi, 2004).

In the first decade of the 20<sup>th</sup> century a rapid development started. As a summit of that time, the Temesvár Parkway Bridge was established. In 1908 it had the worldwide longest span of girder bridges, close 40 m; it is a compound structure, skew arrangement and the neighbourhood of the piers form a box girder (Mihailich, Haviár, 1966, Jancsó, 2001).

After World War I, in spite of cruel losses of the country, Hungary has shown a further development in the field of concrete bridge construction. As an example let us mention the 100 m long viaduct at Veszprém with a 45 m span middle arch, which was erected in 1938 (Bölcskei, 1968). To the conditions of the Hungarian Plain, arches with tie were very convenient. Such bridges were implemented in 1930s and early '40s among other types (slabs, simply supported and continuous girder bridges etc.).

At the end of World War II the great majority of bridges were destroyed. Late 1940s and early '50s the reconstruction proceeded at a quick pace. New traces for roads were also



Fig.1: Viaduct at Mecseknádasd

installed. Numerous traditional short and middle span concrete bridges were built. Besides these an approx. 100 m span arch, the Mecseknádasd-Varasd viaduct was completed (Fig. 1, Bölcskei – Csaba – Láng-Miticzky, 1959). New canal-system for long-range irrigation project was carried out. The arches with tie were stepwise developed. The hot rolled steel profiles tie rods were replaced by high tensile steel cables (Bölcskei, 1957).

A special type of arches was developed in Hungary; this is the arch with prestressed concrete deck slab. The slab serves also as tie, decreasing the structural depth to a minimum. An example is a bridge across the Bodrog River. The slab is continuous over 20+70+20 m spans, the arch is over the river bed, and the structural depth is 500 mm (Huszár, 1968, Fig. 2).

It is to be mentioned, that the V-shaped support – which later was spread all over the world – has been applied first in Hungary (Fig. 3, Bölcskei, 1951). Another example is a pedestrian overpass across a motorway, where the rear stay of the V-support is behind the plane of the slope (Fig. 4, Királyföldi, 2000, construction in the 1960s).

A great many other monolithic concrete bridges of different types were erected on motorways, highways and at urban transport lines. The first larger (30 m span) site prefabricated, non-prestressed girders were applied at the Bolond-út viaduct (Fig. 5). The first steps in post-tensioning were also done in the

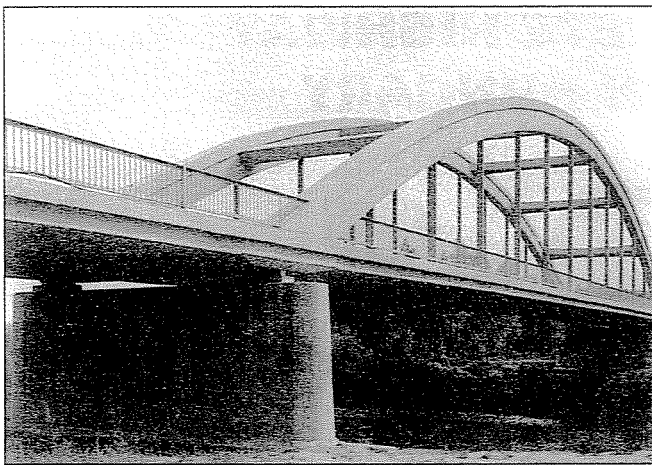


Fig. 2: Arch bridge with deck slab working as tie

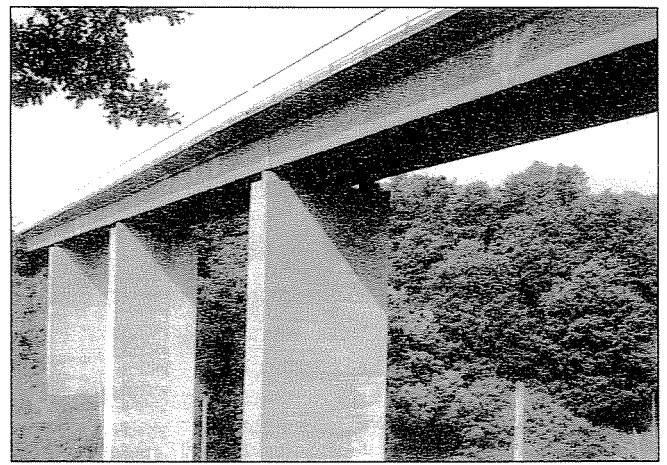


Fig. 5: Highway bridge constructed with precast girders



Fig. 3: V-shape supported bridge

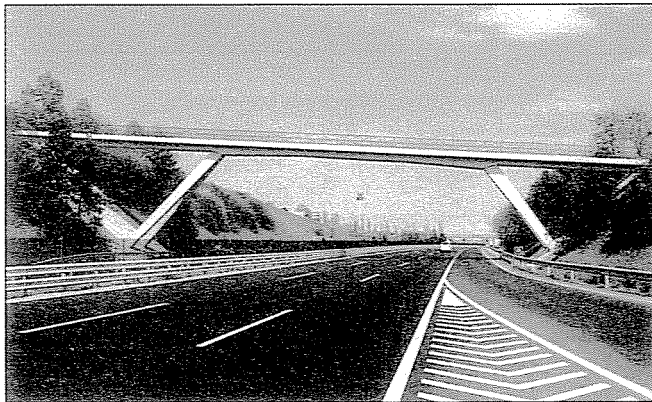


Fig. 4: Pedestrian motorway overpass with hidden V-shape supports

early 1950s using original Hungarian prestressing equipment (Böröcz, 1952).

### 3. BRIDGES CONSTRUCTED BY UP-TO-DATE METHODS

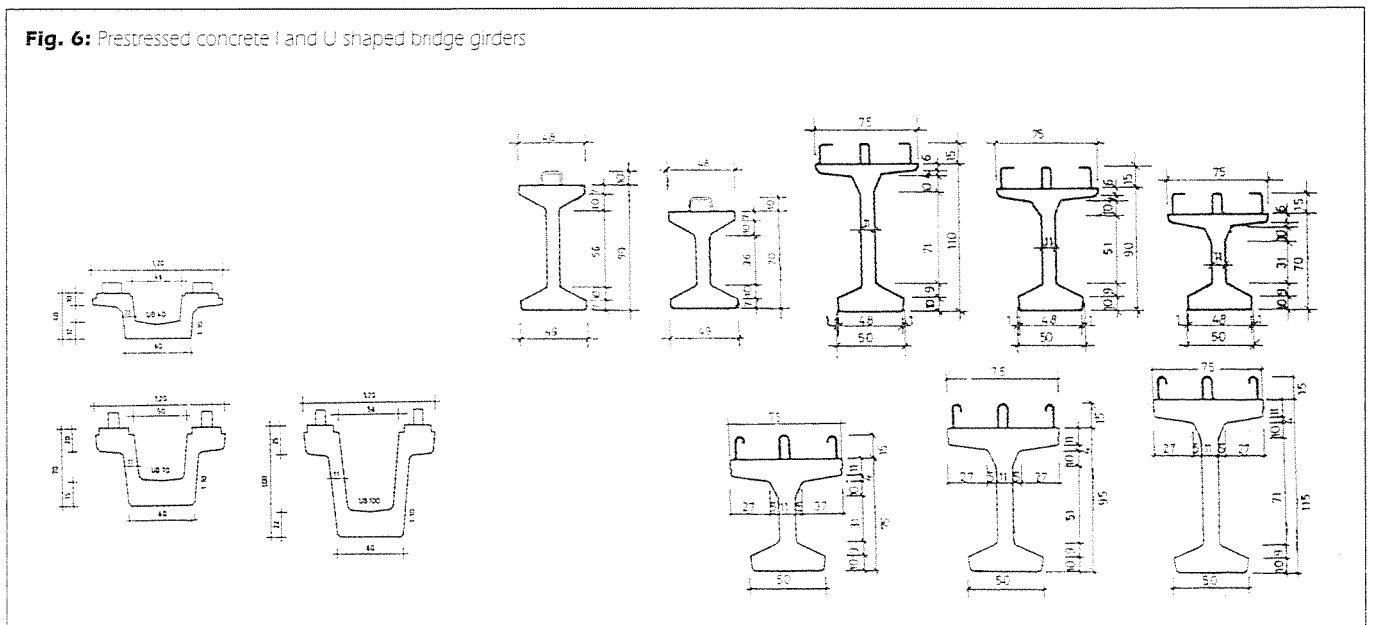
#### 3.1 Prefabrication in highway bridge construction

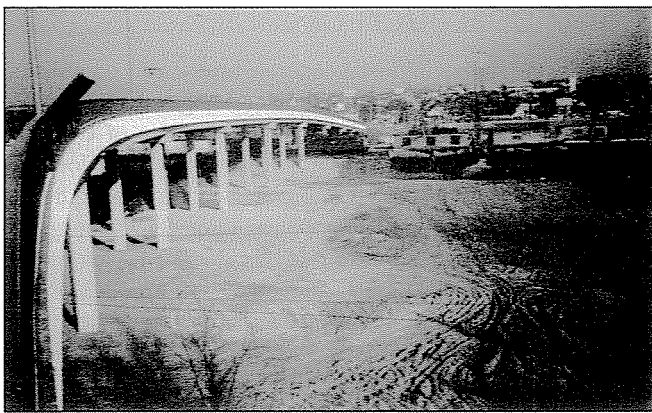
As mentioned, there were some bridge girders by site prefabrication and post-tensioning. For others, prestressed pre-tensioned concrete girders were applied. These were manufactured at temporary prefabrication plants.

The first series of precast prestressed concrete bridge elements made in mass production were of upset T cross section shape. These beams work together with site concrete. Dozens of thousand such elements were used for the construction of large sections of the Budapest underground lines.

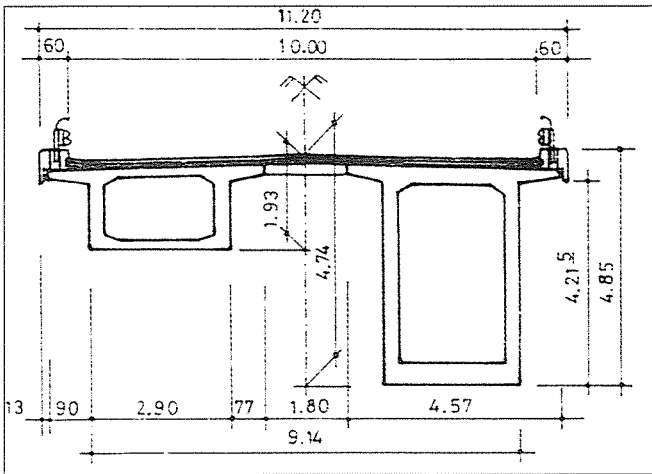
Factory produced prestressed pre-tensioned concrete girders were introduced for short and medium span bridges. These 12~30 m long members are produced with I and U cross sections (Fig. 6, Sigray, Tápai, 1990). The girders were fit to create simply supported and continuous bridges, also curved in ground plan (Fig. 7).

Fig. 6: Prestressed concrete I and U shaped bridge girders





**Fig. 7:** Bridge superstructure using prefabricated girders with curved ground plan



**Fig. 8:** Cross section of a segmental free cantilevered bridge

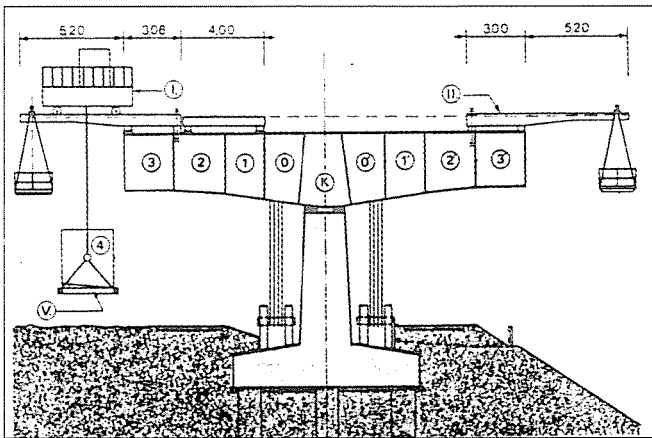


**Fig. 9:** Arrangement of free cantilevering

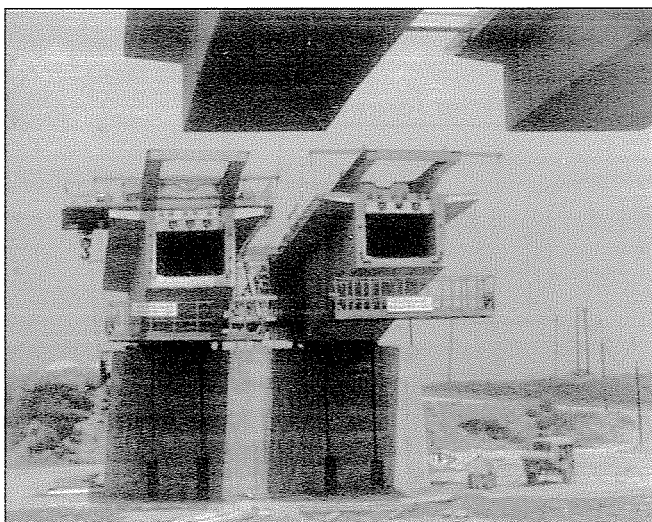


**Fig. 10:** View of segmental free cantilevering

## 3.2 Segmental free cantilevering

Several river bridges were constructed of approximately same span ( $\sim 37+72+37$  m). The typical cross sections of the twin box girders at midspan and above the piers respectively, are shown in *Fig. 8*. The segments were precast at a temporary plant not far away of the construction site using the *contact* method. This enabled the joint epoxy layer to be not wider than 2 mm. The rotation round the starting 'k' element before closing was prevented by temporary supporting or anchoring of the '0' segments (*Fig. 9*). The segments were systematically post-tensioned and the ducts were grouted. After casting the middle gap and the tensioning of the cables working for positive moments, the temporary anchoring was released. A phase of the assembly can be seen in *Fig. 10*, (Reviczky, 1978).

## 3.3 Free cantilevering using travellers

A series of free cantilevered monolithic concrete highway bridge structures were realised in Hungary. The main openings vary between 75 and 120 m. The travellers used and the post-tensioning are of Freyssinet system (György, Szigyártó, 1992). The twin box girders are separately built by two travellers each. A 1.20 m wide non-prestressed concrete slab connects the parallel box girders. In *Fig. 11* the cross section can be seen with the traveller while *Fig. 12* shows the photo of the erection. The St. Stephen bridge across the Tisza River at Szolnok has been built in a complex way. Along the full length of 667.60 m the structure is one monolithic unit. The river bed part spans  $69+120+69$  m are constructed by free cantilevering, while the flood area parts were completed by incremental launching (see Chapter 3.4), at the western bank three bays, at the eastern side 8 bays spanning 28.8–36 m (*Fig. 13*, Varga, 1993).

## 3.4 Incremental launching

The incremental launching bridge construction has gained a wide range of popularity in the last decades in Hungary. The first bridge where this method was applied is in use across the Berettyó River. The spans are  $32.25+50.00+32.25$  m. The permanent casting place, the formwork and the cross section of the box girder is shown in *Fig. 14*.

At the further application of the incremental launching two Hungarian specialties were introduced. A very advantageous novelty was the omitting of the original concrete assembly, casting and launching, finally lost bed. Instead of this, a transportable steel trough is used. The mass of the full equipment is about 100 t, and parts of it can be used more times. *Fig. 15* shows the steel manufacturing unit and *Fig. 16* the launching with the steel nose at the Dulácska valley bridge.

The other Hungarian specialty is the solution of the applicability of the method at such bridges where no place is available behind the abutment. In this case the manufacturing trough can be placed at the bridge side of the abutment and when the full launching is completed; the structure can be pushed back towards the starting abutment.

The most effective Hungarian application of incremental launching was at the giant railway bridge at Nagyrákos (see Vörös, 2006 in this issue and Wellner, Mihalek, 2002).

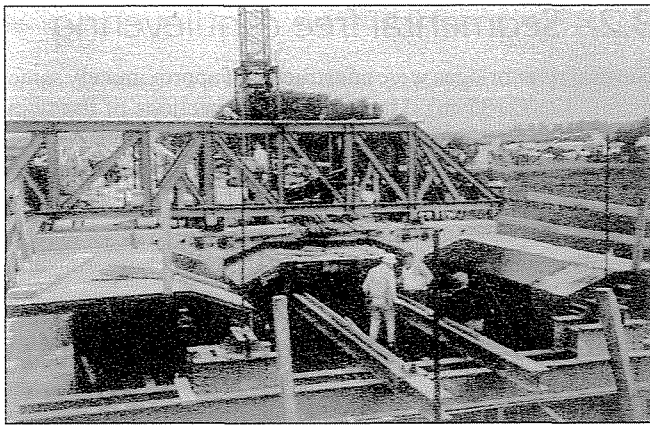


**Fig. 11:** The arrangement of free cantilevering resulting in monolithic structure

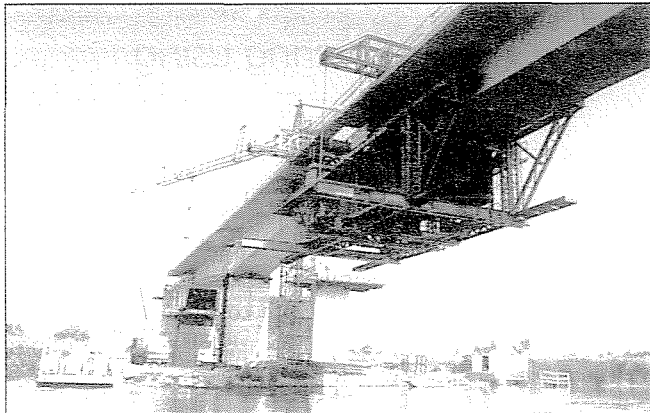


**Fig. 12:** View of free cantilevering with travellers

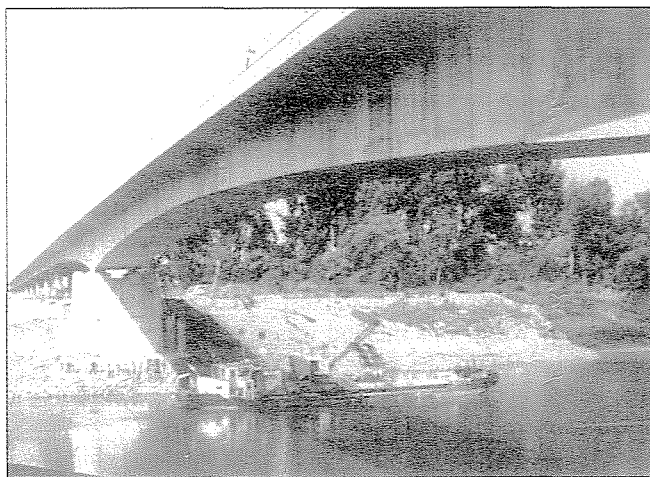


**Fig. 13:** The St. Stephen bridge across Tisza River at Szolnok

### 3.5 Application of cable stays

Recently, the first extradosed concrete bridge was completed in Hungary. The object is at the interchange of motorways M7 and M70, at Letenye, close to the border of Croatia. The superstructure is monolithic; the assembly was done by means of full scaffolding. The cross section width is 15.84 m. The box girder is 1.60 m deep and has three cells. The spans are 52.26 + 61.98 m. The skew is 39.56°. The height of the two I-type pylons is 11.05 m above the bottom edge of the stiffening girder. There are grouted tendons in the spines and sliding cables which run along a part of the stiffening girder and after a deviation they are elevated to the top of the pylons (Fig. 17, Becze, 2006).

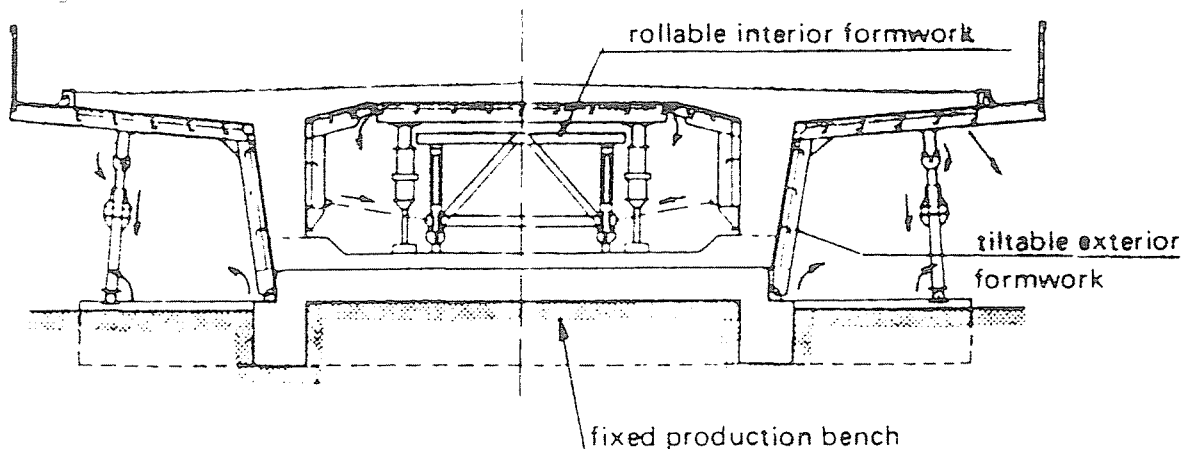
No major cable stayed bridge has been constructed till now. In the near future, such a huge bridge will be implemented for the northern sector of the M0 motorway around Budapest. The full length will be 1847 m. The flood area bays will be supplied by concrete structures to be built by incremental launching. The large spans will be served by cable stayed structures with a maximum span of 300 m. The towers are of concrete, the stiffening girders are of steel (Fig. 18, Hunyadi 2006).

## 4. TRENDS OF FURTHER DEVELOPMENT

The trend can be seen from the above description. For short and medium (up to ~30 m) span bridges the application of factory produced girders are fit. It is worthwhile to improve these structures, to increase the durability and the variability. The incremental launching method seems to be proved till the range of 70 m. Above this span till 120+ m spans the free cantilevering and above this the cable stayed bridges can be taken into consideration. The extradosed structures find an intermediate place at the various technologies. It is also clear that concrete finds place at different mixed structures. The improving of construction materials as well as the production and execution technology has to be in highlight. There is a development in the field of composite bridges, in substructures, towers, etc., where the role of concrete is significant. The increasing Hungarian highway and motorway construction needs more bridges of various types. Giant concrete bridge works, such as the 1872m long and 85m high Köröshegy viaduct (Fig. 19, Wellner, Mihalek, Barta 2005), are going on even at the time of the Second Congress of *fib*.

**Fig. 14:** Cross section and manufacturing arrangement of highway bridge built by incremental launching

### Shaping of formworks





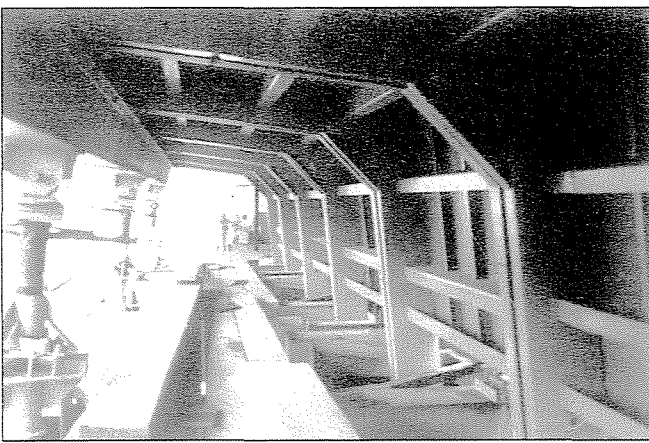


Fig. 15: Steel manufacturing trough for incremental launching

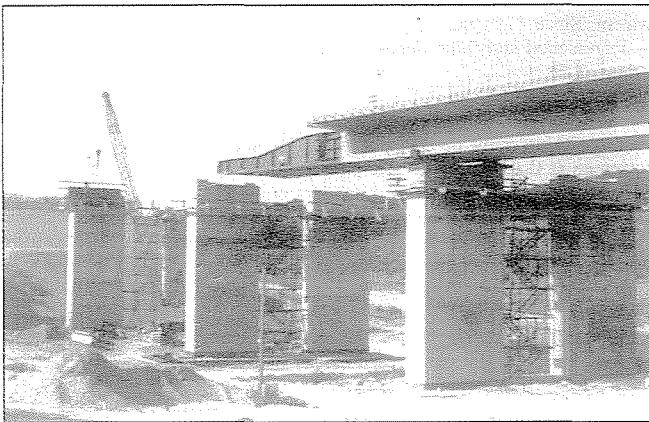


Fig. 16: Dulačska valley bridge constructed by incremental launching

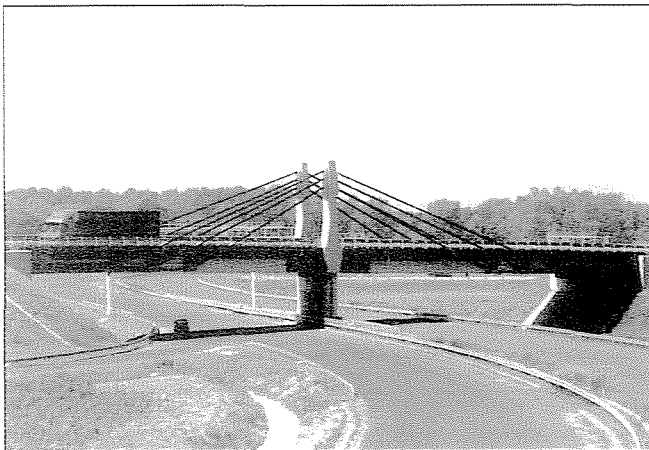


Fig. 17: The first Hungarian extradosed bridge

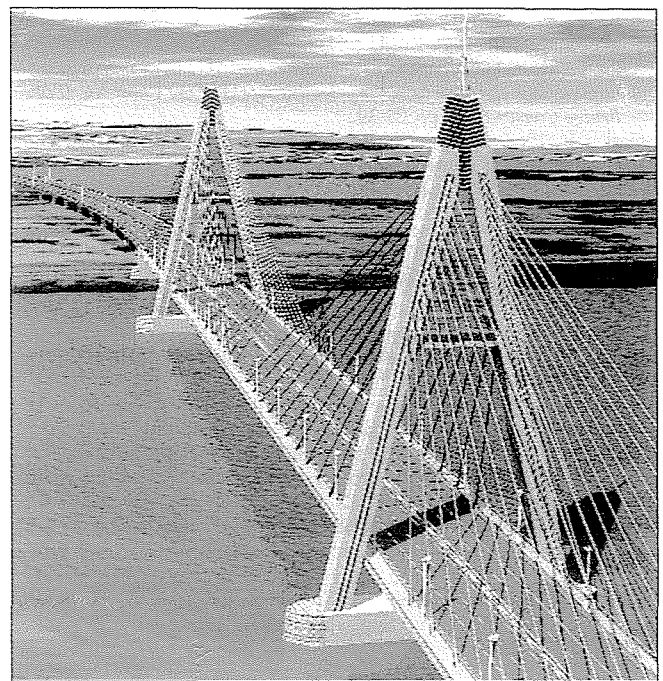


Fig. 18: Future view of the bridge crossing the Danube at the northern section of the M0 motorway around Budapest

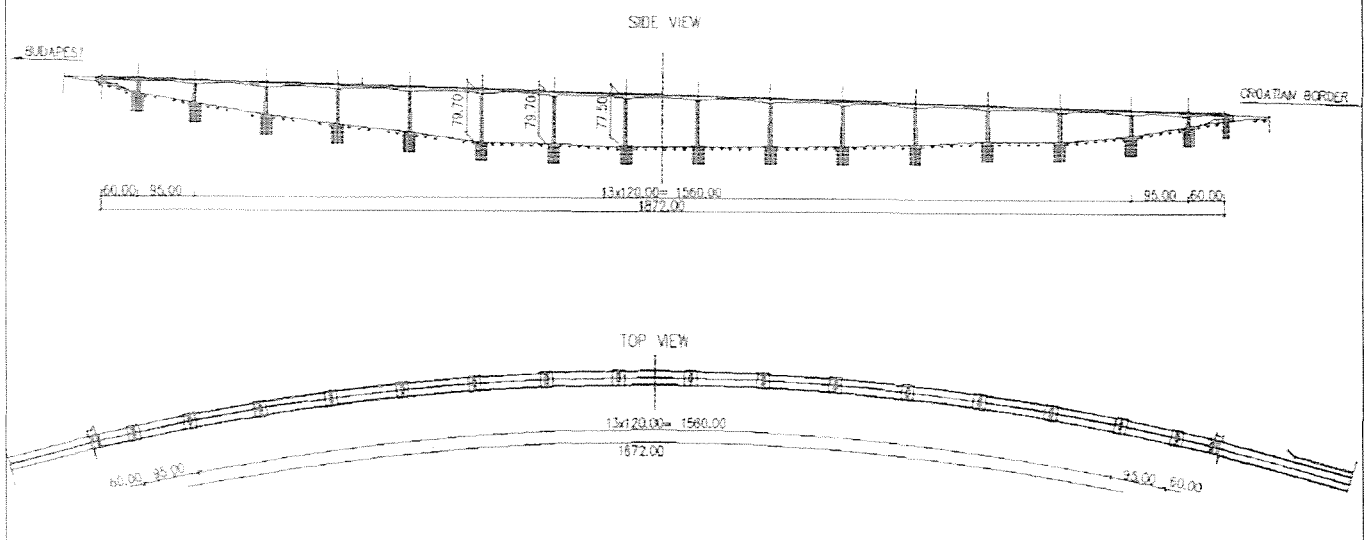
## 5. CONCLUSION

Hungarian concrete highway bridge construction has rich traditions. There were many outstanding results, novelties at the time of the construction work. This paper was not aiming at the full evaluation of achievements in the field of theory of structures, organisation and material research. No doubt, the short description of implemented works shows the permanent progress in the Hungarian concrete technology, in which Hidépítő Company contractor of most of the mentioned structures have been taking a rather prominent part in the last decades.

## 6. REFERENCES

- Balázs, L. Gy., Borosnyói, A., Tassi, G. (2004), "Keep Concrete Attractive - towards the fib Symposium 23-25 May 2005 in Budapest", *Concrete Structures*, pp. 2-4.
- Becze, J. (2006) "Designing of an extradosed motorway bridge (in Hungarian)", *Vasbetonépítés*, 1. 12-15.
- Böleskei, E. (1951). "Structures with 'V'-footing. (In Hungarian), *Mélyépítés*-

Fig. 19: Elevation and ground plan of the Köröshegy viaduct



- tudományi Szemle*, pp. 202-208.
- Bölskei, E. (1957), "High-tensile cable tie-rods", Scientific Publications of the Technical University of Architecture, *Building, Civil and Transport Engineering. Extracts from the scientific works of the Chair No. II of Bridge Construction*, pp. 29-39.
- Bölskei, E. (1968), "Concrete, reinforced concrete and prestressed concrete bridges" (In Hungarian), Tankönyvkiadó, Budapest.
- Bölskei, E., Csaba, L., Láng-Miticzky, T. (1959), "Reinforced concrete bridges" (In Hungarian), Műszaki Könyvkiadó, Budapest.
- Böröcz, I. (editor), (1952), "Prestressed concrete structures, Vol. 2" (In Hungarian), Műszaki Könyvkiadó, Budapest.
- György, P., Szigyártó, L. (1992), "A survey of post-tensioned bridges in Hungary and development tendencies concerned", Proceedings of the FIP '92 Symposium, Budapest, Vol. 2, pp. 663-669.
- Hunyadi, M. (2006), "The northern bridge of the circular road", *Mérnök Újság*, XIII. 2, pp. 4-6.
- Huszár, Gy. (1968) "Designing of the Bodrog River bridge at Alsóberecki", (in Hungarian) *Mélyépítéstudományi Szemle*, pp. 97-100.
- Jancsó, Á. (2001), "Bridges across the Bega river", Mirton, Timișoara.
- Királyföldi, A., (2000), "Pedestrian bridge at Kápolnásnyék" (In Hungarian), *Az Országos Műemlékhivatal Katalógusai*, p. 29.
- Huszár, Zs., "Investigations connected to the design, sizing and prestressing of the Bodrog River Bridge at Alsóberecki." (in Hungarian), *Mélyépítési Szemle*, pp. 71-79.
- Mihailich, Gy., Haviár, Gy. (1966) "The beginning and the first achievements of reinforced concrete construction in Hungary" (In Hungarian), Akadémiai Kiadó, Budapest.
- Reviczky, J. (1978) "Free cantilever bridge erection from precast segments in Hungary" FIP VIII Congress, London, Hungarian Group.
- Sigrai, T., Tápai, A. (1990), "Manufacture and use of plant prefabricated bridge girders", *Achievements in prestressed concrete in Hungary The Hungarian Building Industry*, Special Edition, pp. 33-38, 33-38.
- Tassi, G. (1994), "Main features of the development of concrete bridge construction", *Proceedings of the US-Hungarian Bridge Conference at the Technical University of Budapest*, pp. 15-34.
- Varga, J. (1993), "The designing of the St. Stephen Tisza River bridge at Szolnok", (In Hungarian), *Közlekedéscsépítés- és Mélyépítéstudományi Szemle*, pp. 258-266.
- Vörös, J. (2006), "100 years of reinforced concrete railway bridge construction in Hungary", *Concrete Structures*, pp. 6-10.
- Wellner, P., Mihalek, T. (2002), "One of the longest prestressed concrete railway bridges of Europe – executed by incremental launching method in Hungary", *Concrete Structures*, pp. 7-10.
- Wellner, P., Mihalek, T., Barta, J. (2005), "Köröshegy viaduct - the biggest in size, prestressed, concrete bridge in Hungary", *Concrete Structures*, pp. 56-59.
- Prof. Géza Tassi** (1925), Civil Eng., Doctor of Technical Sci. (Hungarian Academy of Sciences), Professor (1976) at the Department of Structural Engineering, Budapest University of Technology and Economics. FIP medallist, awarded at the first Congress of *fib*, lifetime honorary president of Hungarian Group of *fib*, Palotás prize holder. Main field of interest: theory and investigation of prestressed concrete structures, concrete bridges.
- Péter Wellner** (1933) M. Eng. is Head of Technical Department at Hidépitő Co. Designing of prestressed concrete bridges and the associated institutions involved in their technology in Hungary indicates his successful professional background. He received a National Prize for his involvement in first bridge built in cantilevered system in Hungary. The incremental launching method was initiated in his homeland by him. Such structures are now continuously used. He is a member of Hungarian Group of *fib*, and he was awarded the Palotás prize.
- Tamás Mihalek** (1950) MSc, structural engineer, He started his designing work at Hidépitő Co. He took part in technological design works for monolithic superstructures and ones made of precast elements. He participated in the design of the first Hungarian bridge built in incremental launching system. Since 1996 the Hidépitő Co. has been constructed many bridges by incremental launching under his direction. He is member of Hungarian Group of *fib*.
- János Becze** (1948) graduated from the Civil Engineering Faculty of the Technical University of Budapest in 1973. Started his activity in bridge designing at the Uvaterv Co. He participated in the design work of major bridges; he was responsible for important projects. In 1987 he changed for the Technical Dept. of Hidépitő Co., where he participated in the realisation of the first Hungarian bridge constructed by incremental launching. He also worked in the technological design of the St. Stephen bridge at Szolnok, where he had lion part in solving foundation problems, too. He was involved in different tasks on the long railway bridge built by incremental launching. Recently, he designed in frame of his department the first extradosed concrete bridge in Hungary. Based mainly of this outstanding result he was awarded the Palotás-prize of the Hungarian Group of *fib*, where he is an honoured member.
- János Barta** (1968), MSc. Civil Eng. is design engineer at the Technical Department of Hidépitő Co. Graduated at the Civil Engineering Faculty of the Budapest University of Technology. After designing building structures in 1997 he moved to Hidépitő. There he took part in the design works of the sub- and superstructures of several bridges and a pier structure of the Port of Ploče, Croatia. Some of the designed bridges had prestressed reinforced concrete superstructures and were constructed with the incremental launching technology such as the Viaducts on the Hungarian-Slovenian railway line, the Homokkert overpass in Debrecen and two viaducts on the M7 highway. He was the statical designer of Hungary's first extradosed bridge structure at Leteny. He is member of the Hungarian Group of *fib*.

# RENEWED DESIGN PRACTICE OF REINFORCED CONCRETE DECK SLAB OF COMPOSITE BRIDGES IN HUNGARY



Zoltán Teiter

*Based on the design practice of composite bridges constructed already and to be constructed the paper gives an outline of the changes taken place during the last years in Hungary in connection with the calculation of this type of superstructures. Spanning our two major and some minor rivers, bridges consisting of steel main girder in composite action with reinforced concrete deck slab were designed by the Department for Bridge and Technology Design of UVATERV Engineering Consultants Ltd. With the successful construction of these bridges the use of the cracked reinforced concrete deck slabs as structural units became a routine also in Hungary. Due to the above circumstances this economic type of structure that had been undeservedly pushed into the background for a long time could come into the limelight again.*

**Keywords:** composite bridge, cracked deck slab, sequence of concrete casting, bridge shape, moving supports

## 1. INTRODUCTION

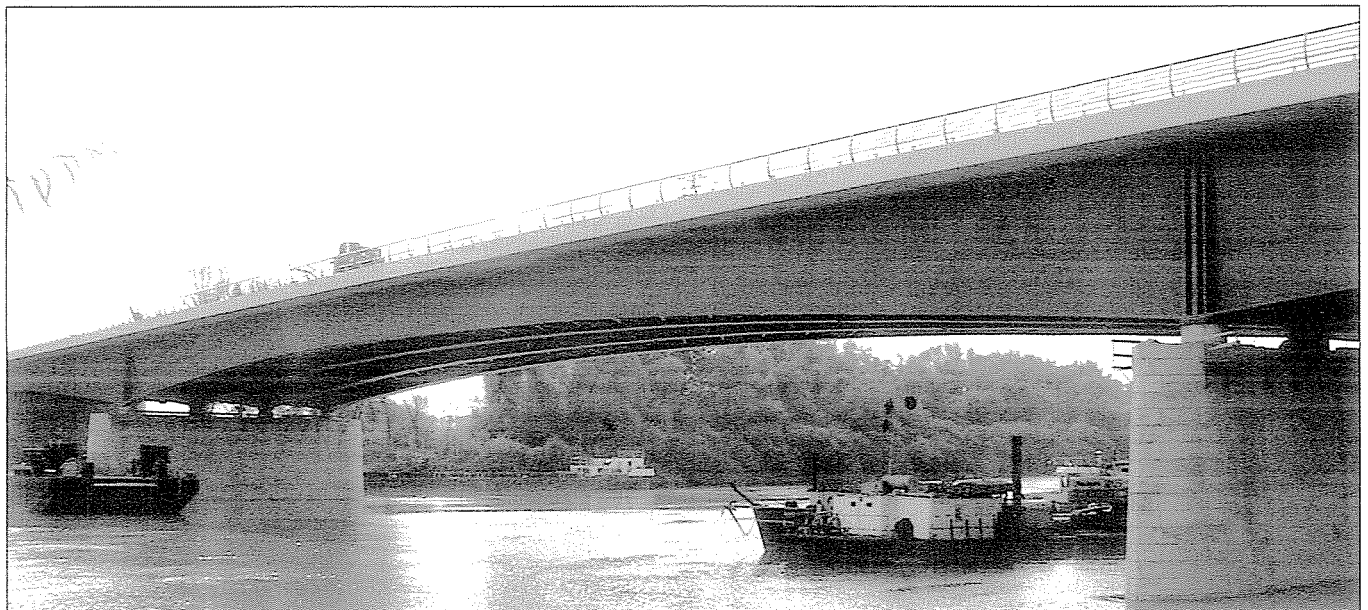
At the end of the past millennium, moreover in its last decade the design and construction of composite bridges almost entirely stopped in Hungary. It was partly owing to a mysticism mixed with fear that questioned the possibility of designing the shapes of composite bridges. However foreign examples proved that composite bridges are competitive in their own category although there was a need for a break-through in the field of design there as well in the last decade (Saul, 1999; Saul, Lustgarten, Rinne, Aschrafi, 1992).

In the last years the development of the motorway and expressway network of Hungary has got an upswing. The construction works have been accelerated all over the country.

This situation has been favourable to the use of the quickly and economically erectable bridge structures thus the bridges with composite superstructure have also come to the front. We would like to show some examples of motorway bridges designed by UVATERV Ltd. Some of them are already constructed and others are under construction or still exist in designs only. A common feature of these bridges is that they have a composite superstructure of reinforced concrete and steel. It is because of the expressed demand of our client on the one hand and the consequence of preferring the aspect of cost saving related to spans on the other hand.

The Tisza Bridge at Oszlár on motorway M3 was opened to traffic in 2001, so the bridge over the Danube on motorway M9 at Szekszárd in 2003. The bridge of motorway M35 over Keleti Főcsatorna (Eastern Main Canal) is under construction. Establishing a connection with Croatia a bridge of motorway

**Fig. 1:** Tisza Bridge at Oszlár, view of river bridge



M7 crossing river Mura has been designed and the preparation of designs for approval of bridge of motorway M44 over river Körös is in progress.

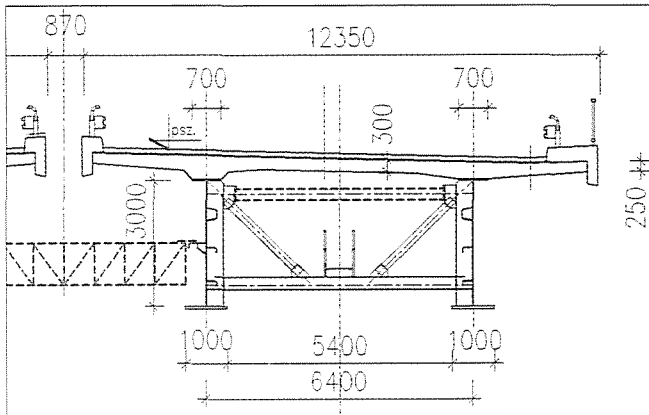
## 2. BRIEF DESCRIPTION OF THE BRIDGES

### 2.1 Tisza Bridge at Oszlár, bridge over river bed

The motorway M3 running towards Ukraine crosses river Tisza near the village Oszlár. The motorway of a reduced total width (26.50 m) required two bridge structures of identical arrangement erected side by side.

The river bridge is a three-span composite structure consisting of two open and haunched steel main girders (Fig. 1). Arrangement of spans of the river bridge: 72-112-72 m. Width of the two bridges is 25.57 m that includes 2×2 traffic lanes and 2×1 emergency lanes (Fig. 2). The distance between

Fig. 2: Tisza Bridge at Oszlár, cross-section of river bridge



the main girders is 6400 mm. The height of the parabolically haunched web plate is 2565 mm at the end cross beams, 5600 mm at the intermediate supports and 3000 mm in the middle of the main span.

### 2.2 Bridge over Danube at Szekszárd, bridge over flood area

In the south of Hungary a new expressway that can be developed to the future motorway M9 completes the connection

Fig. 3: Danube bridge at Szekszárd, view of flood bridge



between the eastern and western parts of the country. The road has 2×1 traffic lanes and 12 m total width. The new bridge over the Danube at Szekszárd with its total length of 916 m is an organic part of the project. The flood bridges are 196.5 m and the river bridge is 520 m long.

As far as the forms of flood bridges are concerned they are identical with that of the river bridge. From structural aspect these are composite girder bridges with closed steel box main girders. Spans of the flood bridges: 65.5-65.5-65.5 m (Fig. 3). The width of the bridge is 14 m that includes 2×3.75 m traffic lanes together with the emergency lanes and a walkway with cycle track on one side (Fig. 4). The web-to-web distance is 5500 mm at the bottom flange and 7250 mm at the top.

### 2.3 Bridge over Eastern Main Canal

The connection of newer areas of the eastern region into the circulatory system of the country becomes possible by the section of M3 motorway branching towards Debrecen and marked as M35. The motorway crosses the Eastern Main Canal before Debrecen. A new motorway bridge with composite structure has been designed here.

Total width of the road is 28.73 m, which gives place for 2×2 traffic lanes and 2×1 emergency lanes (Fig. 5). Arrangement of bridge spans: 44-60-44 m. The main canal is navigable in the main span and service roads are constructed along both of the outer spans on the top of the flood protection dams together with game passes nearby. The axis of the supports encloses an angle of 70 degrees with the tangent drawn to the motorway axis.

The distance between the open main girders is 7300 mm. The height of the parabolically haunched web plate is 2100 mm at the end cross beams, 3000 mm at the intermediate supports and 2100 mm in the middle of the main span.

### 2.4 Mura Bridge

The M7 motorway is destined for establishing a connection with Croatia in the western part of the country. Over the river

Fig. 4: Danube bridge at Szekszárd, cross-section of flood bridge

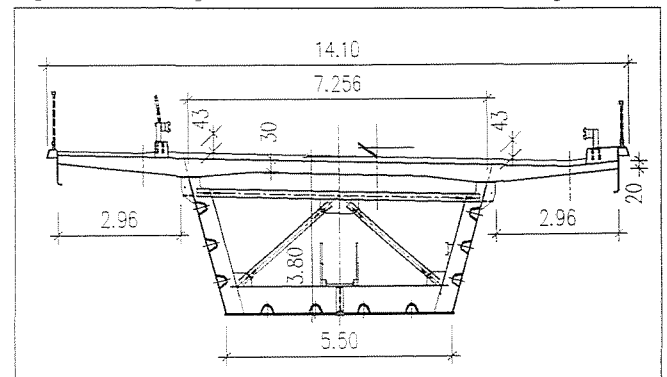
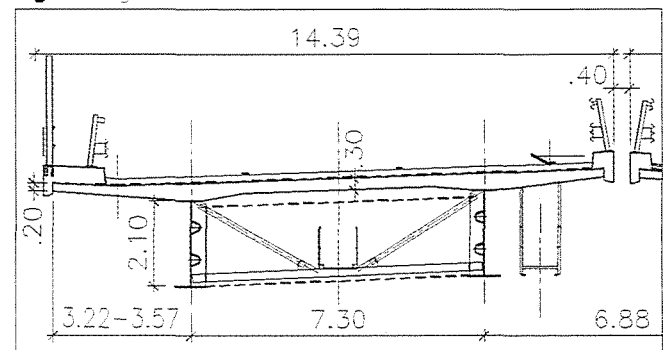


Fig. 5: Bridge of Eastern Main Canal, cross-section



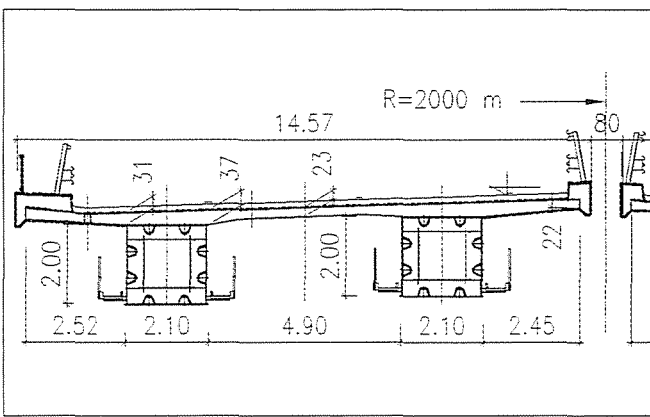


Fig. 6: Mura Bridge, cross-section of river bridge

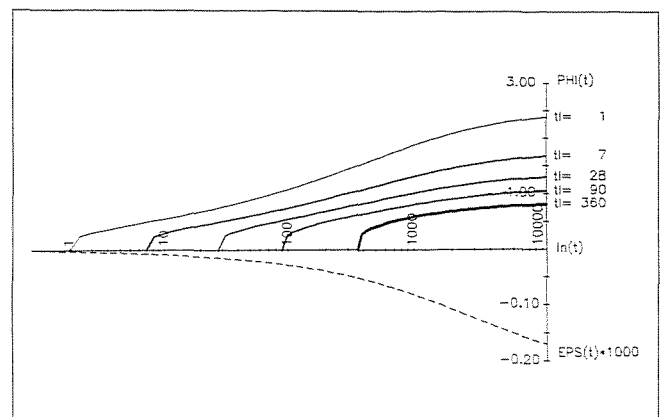


Fig. 8: Variables of creep and shrinkage of a concrete unit in the programme

Mura that separates the two countries as a boundary a bridge had to be designed with regard to the restrictions due to the existing and joining road alignment. The site was determined as a result of long-lasting negotiations between the two countries. Geometric features of the site had to be taken into account during the preparation of the designs.

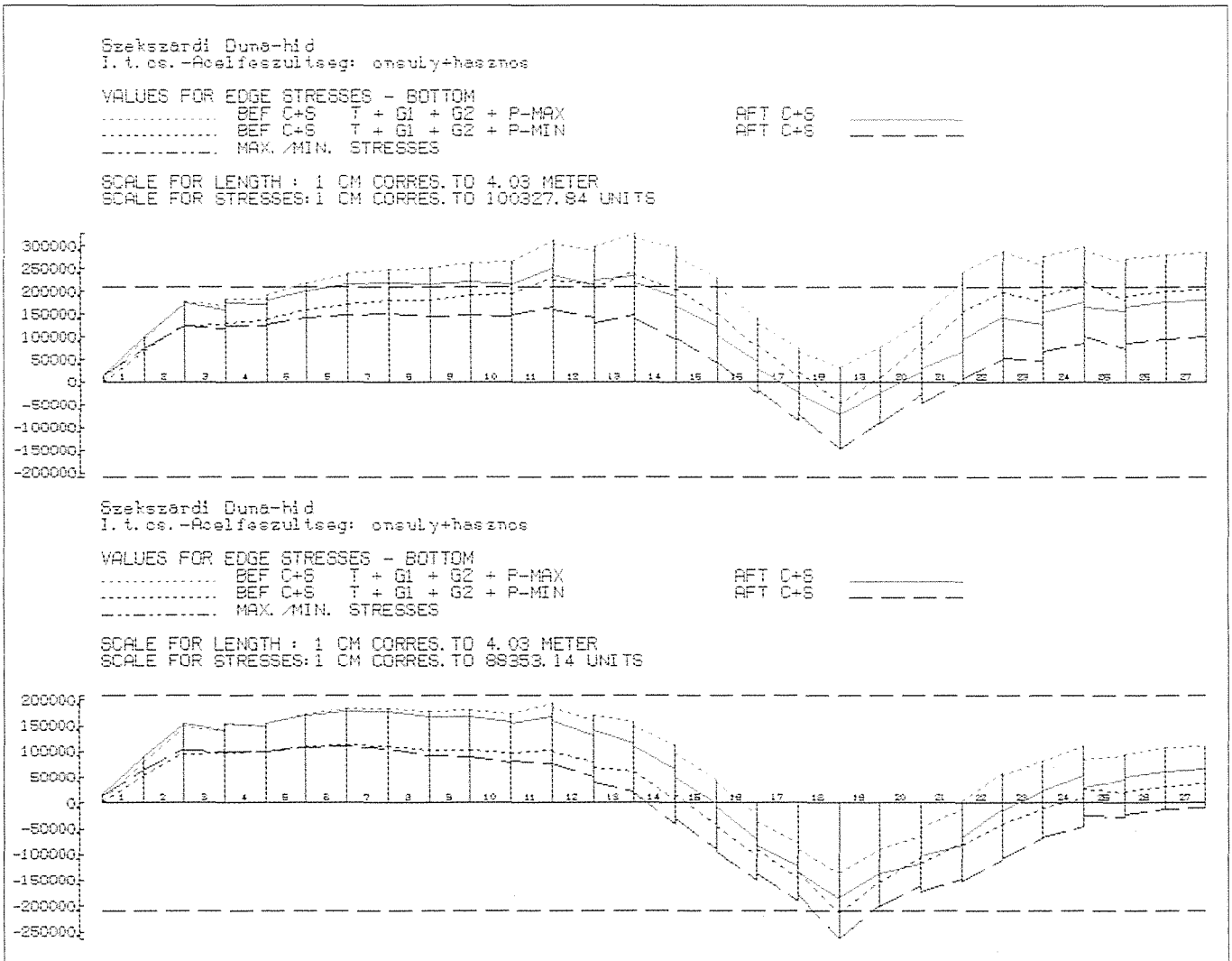
The structure comprising a continuous bridge of five spans with an arrangement of 36-48-48-48-36 m and a total length of 216 m is constructed with a reinforced concrete deck slab and steel main girders. The reinforced concrete deck slab rests on two steel closed box main girders (Fig. 6). The axis of the supports encloses an angle of 75 degrees with the tangent drawn to the motorway axis.

### 3. UP-TO-DATE DESIGN

#### 3.1 Camber and sequence of concrete casting

In the case of Tisza Bridge at Oszlár the reinforced concrete deck slab has been constructed on the steel main girders lifted already onto their places without the use of auxiliary supports (Fig. 9). In such cases the structure rests upon the final supports and the supports themselves will not be lowered or lifted. From the aspect of bridge shape it can be declared that

Fig. 7: Stresses of steel main girder in case of traditional and up-to-date design



the changing in the sequence of casting of sections involves different consequences.

The classic casting order starting in the midspans and terminating above the supports requires a rather significant camber, in case of which the error of calculation due to a difference between the considered and the real values of the dead load of the structure in longitudinal direction and of its rigidity, may result in deviations of tens of mm. This is unfavourable for the designer because he/she should specify a determined form of camber although the definition of the length of the cracked zone and the consideration of the rigidity of this section causes less uncertainty.

Nevertheless the sequence of concrete casting starting above the supports and ending in the midspans involves the deck slab into the structural system more intensively and for a longer term. Although the length of the cracked section is significant, the uncertainty of calculation divides into two components. The first part obviously comes from the estimation of the length of the cracked zone and the second one is the uncertainty of calculation mentioned above. In this way the impact of this latter part is not so significant that might cause any risk to the determination of the final shape with proper accuracy. The error deriving from the inaccuracy of length and rigidity of the cracked reinforced concrete deck slab can be kept within the construction tolerance. Even if the reinforced concrete deck slab needs additional reinforcement in the cracked sections this fact is highly compensated by the reduced amount of steel needed for the main girder.

### 3.2 Reduction of steel material

Calculating with the same steel material distribution stresses arising in the lowest extreme fibre are much higher at the version with no cracks and including support moving than in the case which requires no support moving but allows cracking.

This is represented by the stress diagrams of *Fig. 7* we

got when calculating the flood bridges of Danube bridge at Szekszárd. Under the same conditions in the case of uncracked deck slab and support moving the stresses in the steel exceed the ultimate stress value, while in case of cracking and without support moving the stresses remain below it. It can be observed on the *Figure* that with allowing some cracking the steel demand may be reduced in the section of the long lasting and moderately decreasing "positive" bending moment and we might need some additional material only in the section of the short and intensely decreasing "negative" bending moment.

After all, allowing some cracking in the composite reinforced concrete deck slab above the support considering the control of cracking can result in saving steel material and also the moving of support can be avoided.

### 3.3 Creep and shrinkage

In case of composite structures the most significant question is how we can control the shape of the bridge. The use of computer programmes for this purpose is widespread all over the world. UVATERV purchased the RM Spaceframe programme developed by the firm TDV located in Graz. The software can take into account the different ages of various sections of concrete casting in addition to the variable static frame and the time-dependency of concrete. This programme is able to compute the time-dependency of concrete not only according to Hungarian Standard but on the basis of the recommendations of CEB-FIP Model Code 78 and 90.

While building up the model a specified time should be assigned to each event, so to the creation of the particular concrete sections and to the application of the permanent loads as well. Later in a given time the physical features of these concrete sections will be taken into calculation with different values according to the ages (*Fig. 8*).

Making use of the advantages of computer calculation sometimes we have analysed the same bridge supposing several construction methods. On the above-mentioned *Fig. 7* it can be

**Fig. 9:** Deck slab of Tisza Bridge at Oszlár during construction



seen that due to the creep and shrinkage the effect of support moving will almost entirely disappear in time and because of the time-dependency of concrete the stress conditions of steel structure will significantly change during the bridge lifetime. In our calculations we have already experienced a change reaching even the half of the ultimate stress and observed also such case when in particular sections of the bridge, beside 50% utilization, the stress has changed its sign. Although these changes require long time and the structure can be considered adequate even under these conditions, in our opinion such bridges may only be designed very cautiously.

Our analyses have shown that the creep and shrinkage of the reinforced concrete deck slab will increase the value of deflection more intensely when we analyse a non-cracked structure. This happens despite the fact that in case of a cracked deck slab the concrete zones considered cracked, due to their nature, eliminates the reinforced concrete sections together with their creep and shrinkage quite according to an influence diagram thus in the midspans the latter effect resulted in form of deflection in a concentrated way.

### 3.4 Control of cracking

Requirements related to the control of cracking had been complicated to justify for the first bridges because some circumstances to be treated had not been yet recognized or allowed by the Hungarian Standards being effective that time. The approach applied by us is outlined as follows.

After cracking the force represented by the reinforced concrete deck slab is taken up not only by the reinforcing bars but also by the top flange of the steel structure below the deck slab. (This results from the continuous connection between the reinforced concrete and the steel structure and from the principle of turning of plane cross section. Due to the fact that structural steel is already loaded at the moment of casting of the deck slab and its elastic modulus is identical with that of the reinforcement, the top flange must be considered as determining when designing.)

With the help of the main girder model in serviceability state we calculated the maximum stress developing in the reinforcing bars after cracking (and elimination) of the deck slab. After that we searched for the crack width of such a reinforced concrete element whose forces taken up before cracking are not transferred directly to the reinforcing bars but also to the upper flange of the continuously connected steel structure which constrains the element, and so the width of cracks. This crack width was calculated in an indirect way that means that we loaded the deck slab as a purely tensioned reinforced concrete element by such a fictitious tensile force that we could get a proper crack width – which is around 0.20 mm in our case. This fictitious state resulted in a higher steel stress for the bars than their maximum calculated stress. The crack width belonging to the effective value of steel stress was calculated by proportionality. We were allowed to use this method of calculation because in the after-cracking state of the purely tensioned reinforced concrete element the reinforcing

bars are only working and strains of them are proportional to the crack widths. The value calculated in this way approximated the actually occurring crack width from above.

## 4. CONCLUSIONS

When constructing the deck slab of a composite bridge, in addition to the traditional sequence of casting starting in the midspans and ending above the supports the method of casting starting from the supports and ending in the midspans can also be used in a justifiable way, additionally in some cases it can give more favourable results. According to the newer calculations the significance of the usual support moving has considerably decreased to such an extent that it seems to be advisable avoiding with regard to the expensiveness.

Nowadays the cracking of the deck slab is allowable, designable and can be well controlled. With introducing cracked zones of concrete a significant amount of material can be saved in the steel main girder and the influence of creep and shrinkage of concrete can be reduced in the aspect of the deflections under permanent loads on the one hand and of the changes of stresses in the steel main girder in time on the other hand. Crack width of the cracked zones can be well controlled on the basis of the considerations of the previous section.

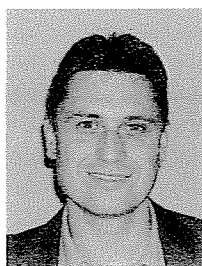
Measurements have proven that the shape of our bridges designed according to the above-mentioned principles show a difference within 10 mm compared to the designed/calculated values and this remains under the construction tolerance.

## 5. REFERENCES

- CEB-FIP (1978), "Model Code for Concrete Structures", Paris, London, Berlin
- CEB-FIP Model Code(1990), "Design Code", Comité Euro-International du Béton
- Iványi, M. (1998), "Theory of Construction of Bridges, Steel Structures", *Műegyetemi Kiadó*, Budapest (in Hungarian)
- MSZ-07-3710-87 (1987), "Design of Highway Composite Bridges", *Hungarian Standard Institute*, 20 p. (in Hungarian)
- Platthy, P. (1990), "Composite of Steel Girder and Reinforced Concrete Slab", *Tankönyvkiadó*, Budapest (in Hungarian)
- Saul, R. (1999), "Fritz Leonhardt als Stahlbrücken-Ingenieur", *Stahlbau*, 1968/7, pp. 486-493. (in German)
- Saul, R., Lustgarten P., Rinne, K.-D., Aschrafi, M. (1992), "Verbundbrücke mit Rekordspannweite über den Rio Caroni/Venezuela", *Stahlbau*, 1961/1, pp. 1-8. (in German)
- Szalai, K. (1998), "Reinforced Concrete Structures, Theory of the Strength of Reinforced Concrete", *Műegyetemi Kiadó*, Budapest (in Hungarian)

**Zoltán Teiter** (1968) MSc structural engineer, senior design engineer at the Department of Bridge and Technology Design of UVATERV Consultants Ltd. After graduating he worked for two years at the Department of Reinforced Concrete Structures, Faculty of Civil Engineering, Technical University of Budapest. His research fields were the theory and the strength of reinforced concrete and the second-order behaviour of reinforced concrete columns. He has been working for UVATERV since 1994 taking part in designing bridges mostly by modeling and force analyses. Responsible designer of several bridges. He is in a good contact with the Department of Structural Engineering of BME contributing to publications, design handbooks and standards. Member of the Hungarian Group of *fib*.

# CONDITION ASSESSMENT AND REHABILITATION OF MASONRY ARCH RAILWAY BRIDGES



Zoltán Orbán

The paper presents new methods of assessment, inspection and rehabilitation of masonry arch railway bridges. Some results of a test programme are demonstrated where the efficiency of non-destructive testing methods for the inspection of arches was studied. A multi-level assessment procedure is proposed with the adaptation of advanced tools for structural analysis and testing. Repair solutions are also demonstrated where the basic principle of the methods is the utilisation of the existing bridge capacity.

**Keywords:** masonry arch bridges, non-destructive testing, rehabilitation

## 1. INTRODUCTION

Masonry arch bridges form an integral part of the railway infrastructure in Hungary and worldwide. They are the oldest structure types in the railway bridge population with thousands still in service. *Fig. 1* demonstrates two outstanding masonry arch viaducts constructed in the 19<sup>th</sup> century by the Hungarian Railways. Today the majority of arches on the railway network are single span structures with a semi-circular shape (*Fig. 2*).

In order to promote interoperability between European railway networks and provide that the railways can accommodate increased axle loads, train speeds and a greater volume of freight traffic, it is necessary to assess the load carrying capacity of existing masonry arch bridges (*Orbán, 2003*). Assessment of masonry arch bridges is difficult as the structural behaviour of arches is very complex, there is little knowledge or experience of design of these structures, and a large part of the structures is hidden from view.

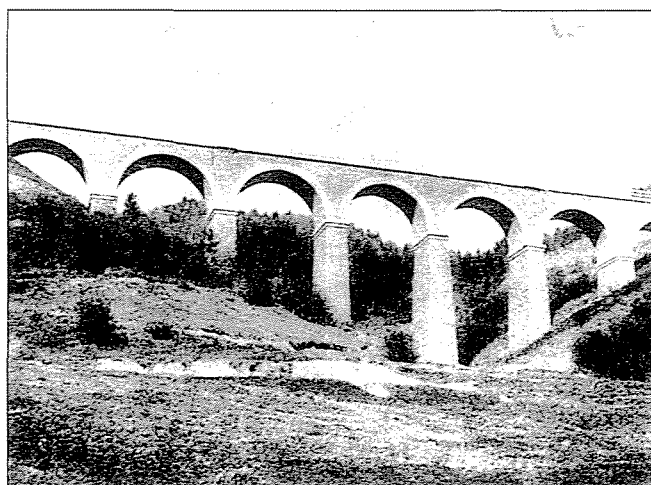
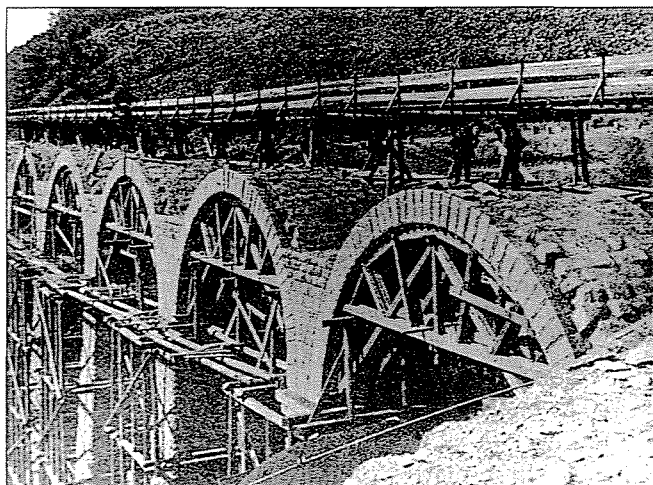
To provide confidence in the assessment result, reliable input parameters are required for the calculations. Accordingly effective inspection and measuring methods to establish the parameters are necessary. As well as the predominant use of visual inspections, and destructive investigation there is

a tendency in recent years towards using non-destructive testing techniques.

The current condition of masonry arch bridges varies from good to very bad, although statistics show that there are a relatively large number of bridges in a medium or bad condition with a tendency for accelerated deterioration (*Orbán, 2004*). Accordingly there is a potential doubt as to the adequacy of masonry bridges to withstand increased axle loads, train speeds and a greater volume of freight traffic. The design of these structures was based on empirical rules and contemporary railway loads, which has resulted in structures with an inherent ability to withstand greater loads and extreme weathering conditions. Today many masonry arches carry a load that is radically different from that which existed when they were constructed.

Contrary to doubts masonry arch bridges are proving durability with life-cycle costs significantly more economical than for the majority of other structure types. In addition, they belong to the civil engineering heritage of the railways, and their substitution or refurbishment requires careful consideration with maintenance strategies adopted to promote solutions that preserve and restore these structures instead of their replacement.

**Fig. 1:** The Ladok viaduct in Transylvania during construction (left) and after (right)





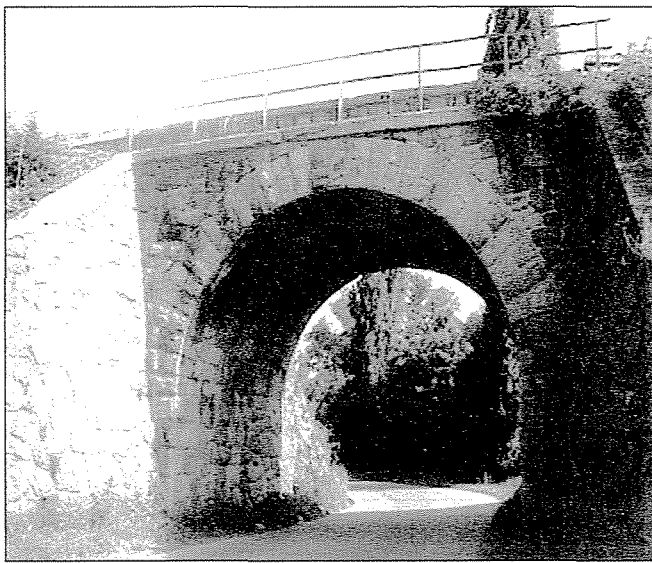


**Fig. 2:** Typical stone and brickwork arch bridge at the Hungarian Railways



## 2. METHODS AND PROCEDURE OF ARCH ASSESSMENT

Several methods are available for the assessment of masonry arch bridges. These include simple conservative methods (such as MEXE) and recently developed computerized methods (such as adaptations of the mechanism method and FEM systems). Besides their particular limitations, conservative methods often underestimate the load carrying capacity, which may result in uneconomical or unnecessary mitigation measures being taken to maintain or replace bridges. Conversely the use of sophisticated new methods is generally hindered by the difficulty in provision of input parameters or prolonged data processing.

*UIC Code 778-3R (1994)* gives guidelines for the use of the most widely applied approximate method, MEXE. Experience shows that in a large number of situations the method seriously underestimates the actual load-carrying capacity of the bridges. On the other hand in some other cases MEXE has been found to provide non-conservative results. The method is generally used as a first sieve for the initial assessment and preliminary determination of load capacity. As MEXE can provide unreliable and highly conservative values for the load carrying capacity of masonry arches, some railway administrations proposed modifications to the method in order to achieve better conformity with their experience (*Orbán, 2003*).

The use of advanced computerised techniques in the analysis of masonry arch bridges is a relatively new concept. Several computational techniques have been developed for this purpose including 1D frame or 2D and 3D non-linear finite element (FE) models, discrete element-based (DE) models and combined finite element-discrete element models (FE/DE). These methods were developed to describe the complex nature of arch deformation, cracking processes and arch-backfill interaction phenomena. Methods based on the lower bound mechanism or upper bound mechanism approaches are considered simple and promising tools for arch assessment.

Assessment of serviceability is becoming more and more important with increasing traffic volumes on masonry arches. Currently there is however no suitable method for the serviceability assessment of masonry arches nor any criteria against which such an assessment could be made.

The assessment of masonry arches is generally carried out at various levels. Example for a multi-level assessment procedure is detailed in *Table 1*.

## 3. INSPECTION AND TESTING OF ARCHES

### 3.1 Review on arch testing methods

Preservation of masonry arch bridges and their repair can successfully be accomplished only if careful diagnosis of the state of damage has been carried out. Before any intervention the observed damage (symptoms) needs to be evaluated and the possible causes determined. Effective inspection and measuring methods are therefore required. The link between the symptoms and their causes can only be found if the corresponding experimental and analytical procedures are used in a harmonised system.

Several inspection methods are used to investigate the condition or to determine the structure of masonry arch bridges. The most common method is still the pure visual inspection. Destructive testing is also used although there is a tendency in recent years towards using non-destructive testing techniques.

Most assessment procedures require the masonry strength and some other mechanical properties as the major input parameters for assessment. Destructive testing (DT) of masonry bridges is therefore necessary in many instances, although it should be noted that the results of most destructive tests are affected by significant uncertainties and they may provide only local information on some part of the structure, and cannot be directly extended to the whole bridge.

Semi-Destructive Testing (SDT) methods are based on in-situ localised measurements and considered as surface or small penetration techniques which can provide only qualitative information on the masonry condition and be used only for preliminary investigation.

While conventional DT methods focus mainly on the mechanical characteristics of the materials, Non-Destructive Testing (NDT) methods can provide an overall qualitative view on the arch condition. NDT methods on the one hand seem to be most promising tools for the inspection of masonry arch bridges but on the other hand need a great deal of further study and research.

Monitoring systems are occasionally installed on masonry arch railway bridges in order to follow the evolution of damage

**Table 1:** Description of multi-level assessment procedure for arch bridges

<b>1<sup>st</sup> Level:</b>	<b>Preliminary assessment</b>
Range of structures:	General
Method used for assessment:	MEXE or other simplified method
Input parameters are based on:	Visual inspection, Bridge records, Former assessments.
Results used for:	First ranking of bridges, Pointing at structures that are presumably under-strength or risky
<b>2<sup>nd</sup> Level:</b>	<b>Secondary assessment</b>
Range of structures:	Structures failed at preliminary assessment, Structures precluded from MEXE or other methods used for preliminary assessment (e.g. complex, oversize or structures with unique characteristics).
Method used for assessment:	Thrust line analysis, rigid-block analysis, 2D frame models, other simple methods.
Input parameters are based on:	Bridge records, visual inspection, Simple measurements (geometry, material composition and quality, approximate strength measurements, etc.), Default assumptions by similar structures
Results used for:	Verification of preliminary assessment results, Determination of structural parts and parameters where further investigation should be focused.
<b>3<sup>rd</sup> Level:</b>	<b>Revised (secondary) assessment</b>
Range of structures:	Structures failed at secondary assessment.
Method used for assessment:	Same as for secondary assessment, but the use of more than one method is advised in order to mitigate the effect of model uncertainty.
Input parameters are based on:	Destructive, slightly destructive and non-destructive testing carried out in-situ and in laboratory, Default assumptions for some other parameters.
Results used for:	Verification of secondary assessment, Gaining better understanding of arch behaviour, Ranking of damaged structures, Decision making on the mode of intervention.
<b>4<sup>th</sup> Level:</b>	<b>High-level assessment</b>
Range of structures:	Structures failed at revised secondary assessment with a moderate degree and a more sophisticated assessment might reveal the real extent of danger, Structures where the damage pattern requires more sophisticated methods to be applied in the analysis, Structures with unique characteristics (e.g. skew bridges, previously strengthened bridges, attached structures, bridges with a static system that have unique boundary conditions).
Method used for assessment:	2D and 3D finite element and discrete element models which can accommodate the unique features of masonry arch behaviour (e.g. non-linearity, very limited tensile strength, interaction between the arch and fill, transverse effects, etc.).
Input parameters are based on:	Further tests on bridges (if necessary), Default assumptions.
Results used for:	Verification of previous assessments, Gaining better understanding of arch behaviour, Verifying serviceability or loss of serviceability, Ranking of damaged structures, Decision making on necessary intervention, Planning of strengthening measures.

**Table 2:** Principles of Non-Destructive Testing methods

<b>Georadar (impulse radar)</b>	
Description of the method:	The method is based on the propagation of electromagnetic impulses, which are transmitted into the material using a dipole antenna. The impulses are reflected at interfaces between materials with different dielectric properties. The results are based on the correlation between the dielectric constants and the material characteristics.
Information obtained are used for:	Detecting voids, inclusion of different materials, detachment of rings, Detecting the morphology of the masonry, structural irregularities, Detecting backfill conditions, Defining geometry, Detecting the state of damage, Defining the presence and level of moisture, Controlling the effectiveness of repair intervention.
<b>Infrared thermography</b>	
Description of the method	The measurement is based on the thermal conductivity of the masonry material. The thermal radiation is collected by a camera sensitive to infrared radiation. The result is a thermographic image where each tone corresponds to a temperature range. Correlation to the mechanical and physical properties of the masonry can be established by calibration tests.
Information obtained are used for:	Survey of cavities, Detection of inclusions of different materials, Presence of moisture (the camera finds the cold parts where is a continuous evaporation, transpiration).
<b>Sonic test</b>	
Description of the method:	The technique is based on the generation of sonic impulses at a point of the structure. A signal is generated by a percussion or by an electro-dynamics or pneumatic device (transmitter) and collected through a receiver which can be placed in various positions of the structure. The resulting data is based on the wave velocity by measuring the time the impulse takes to cover the distance between the transmitter and the receiver. The velocity of the stress wave passing through the masonry material is proportional to the density, dynamic modulus and Poisson's ratio of the material. Some further developments of the method: <i>seismic tomography, seismic reflection, impact-echo method.</i>
Information obtained are used for:	Detection of voids, flaws, Finding damaged parts, Controlling the effectiveness of repair intervention.
<b>Boroscopy</b>	
Description of the method:	Boreholes are drilled in representative parts of the structure. A small camera is inserted into the borehole allowing a detailed study of its surface. The results of this study may be recorded for further analysis.
Information obtained are used for:	Detection of large cavities, General view of the materials,

patterns such as cracks or deformations. The knowledge of this evolution can help preventing more serious damage or a total collapse of the structure. Monitoring may also provide information that can be used to determine the root causes of the defects. These may be from visual inspection or electronic data collection. Load tests are carried out only in special cases on masonry arch bridges. However load tests are considered to provide the 'most reliable information' on the real structural behaviour.

The following list summarises testing methods that are frequently used on masonry arch bridges:

• Destructive Testing Methods:

- Mechanical tests on cored samples,
- Physical and chemical tests on cored samples,
- Tests on soil, backfill properties,

• Semi-Destructive and Non-Destructive Testing methods:

- Boroscopy,
- Flat-jack test,
- Hammering (sounding)
- Surface measurements (Hardness, Schmidt hammer, penetration, pull-out tests),
- Georadar,
- Infrared thermography,
- Sonic methods,
- Conductivity measurements,

• Monitoring methods:

- Crack monitoring,
- Deflection and relative displacement measurements,
- Dynamic tests,
- Load tests (in special cases)

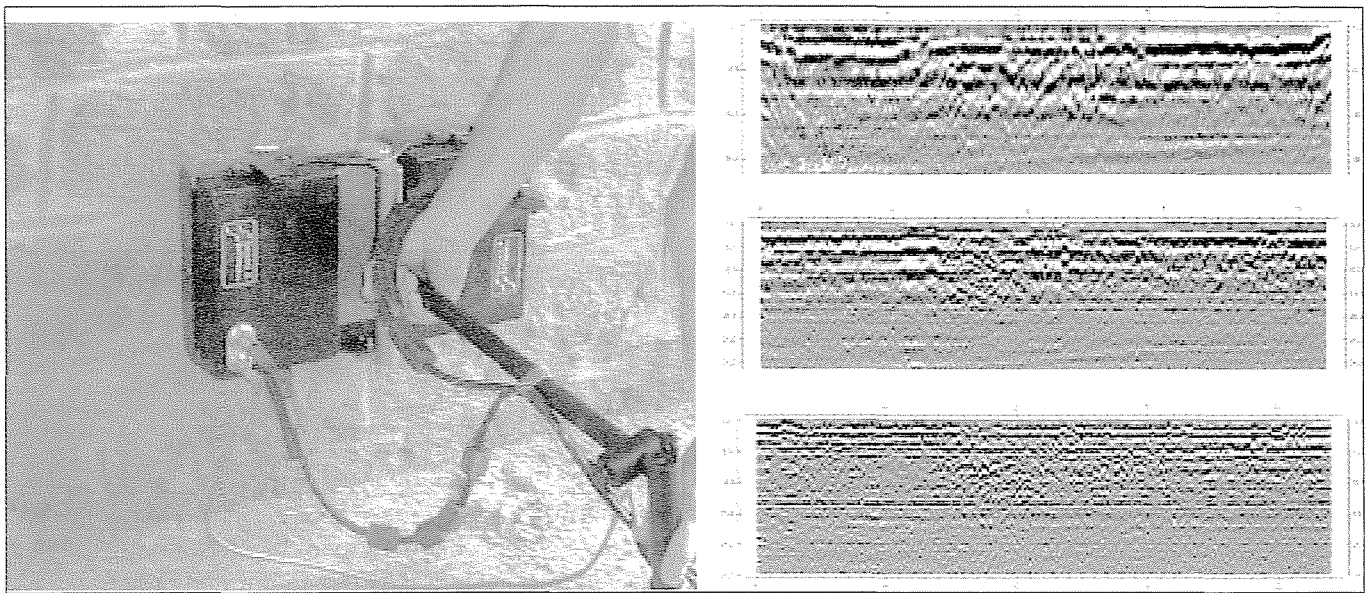


**Fig. 3:** Survey of a masonry bridge abutment with georadar (left)  
Radargrams recorded with different frequency antennas (right).

### 3.2 TEST PROGRAMME WITH DIFFERENT NDT METHODS

The number of references and projects that have utilized NDT methods on masonry arches is very low and only a few calibration tests have been carried out until now. A testing programme has been therefore initiated by the Hungarian Railways that is aimed at working out an inspection system for masonry structures with the utilisation of the potential in non-destructive testing. This testing programme was part of a multi-phase research project that is partially supported by the International Union of Railways and the Hungarian Research Fund (OTKA, Grant Nr. T046691). In addition to the testing capacities at the University of Pécs Faculty of Engineering the site tests were carried out with the technical support and assistance of various organisations, such as the Hungarian Institute of Geophysics, Inframed Ltd., Kompetenta Ltd., Bomix Ltd., and Vertikor-Alpin Ltd.

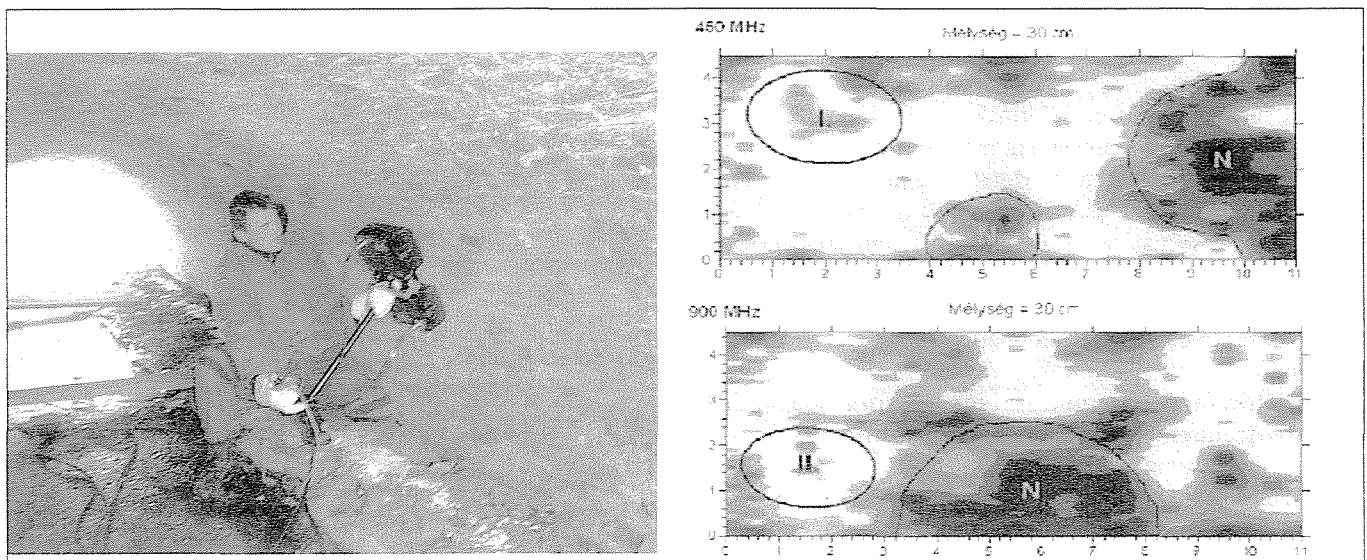
The following testing methods are involved in the programme: georadar, infrared thermography and seismic methods together with calibratory core drillings and boroscopy survey. The principles of these non-destructive methods are described in *Table 2*. Besides testing the efficiency of the above

mentioned methods on masonry arches it was also important to find forms of representing measured data that are meaningful for engineers.

Examples for some possible ways of representation are seen in *Fig. 3 to 7*.

Results of a survey of a masonry bridge abutment with georadar are seen on *Fig. 3*. The radargrams were recorded with different frequency antennas (450MHz, 900MHz, 1,5GHz). The distance measured lengthwise is on the horizontal axis while the depth scale is on the vertical. Using higher frequency antennae results in higher resolution but the penetration depth is lower. Lower frequency antennae provide greater depth of penetration but lower resolution. The recorded radargram highlights the constructional anomalies along a given profile plotted against the depth of the measurement. Due to the different frequencies used in the measurements the radargrams have different resolutions at different structural depths. Further option for processing radar data, when the density of the grid allows, is to plot the amplitude values of the individual radargrams in time and depth sequences to get an anomaly map for various depth levels (slice technique). The anomaly map shows, at a given depth level, the changes in the amplitude values. The resolution of the anomaly map depends on the grid density

**Fig. 4:** Survey of the barrel of a masonry arch bridge with georadar (left).  
Anomaly maps recorded at 30 cm depth with different frequency antennas (right). Different colours refer to anomalies in reflection.



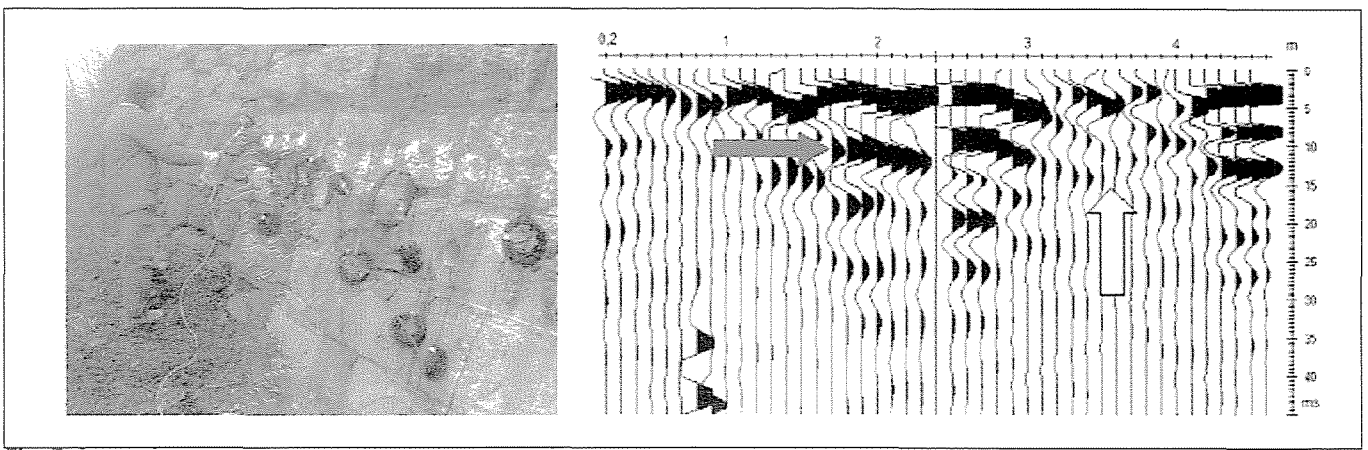


**Fig. 5:** Survey of a masonry abutment with seismic method (left). Recording of seismic reflections, where arrows indicate anomalies (right).

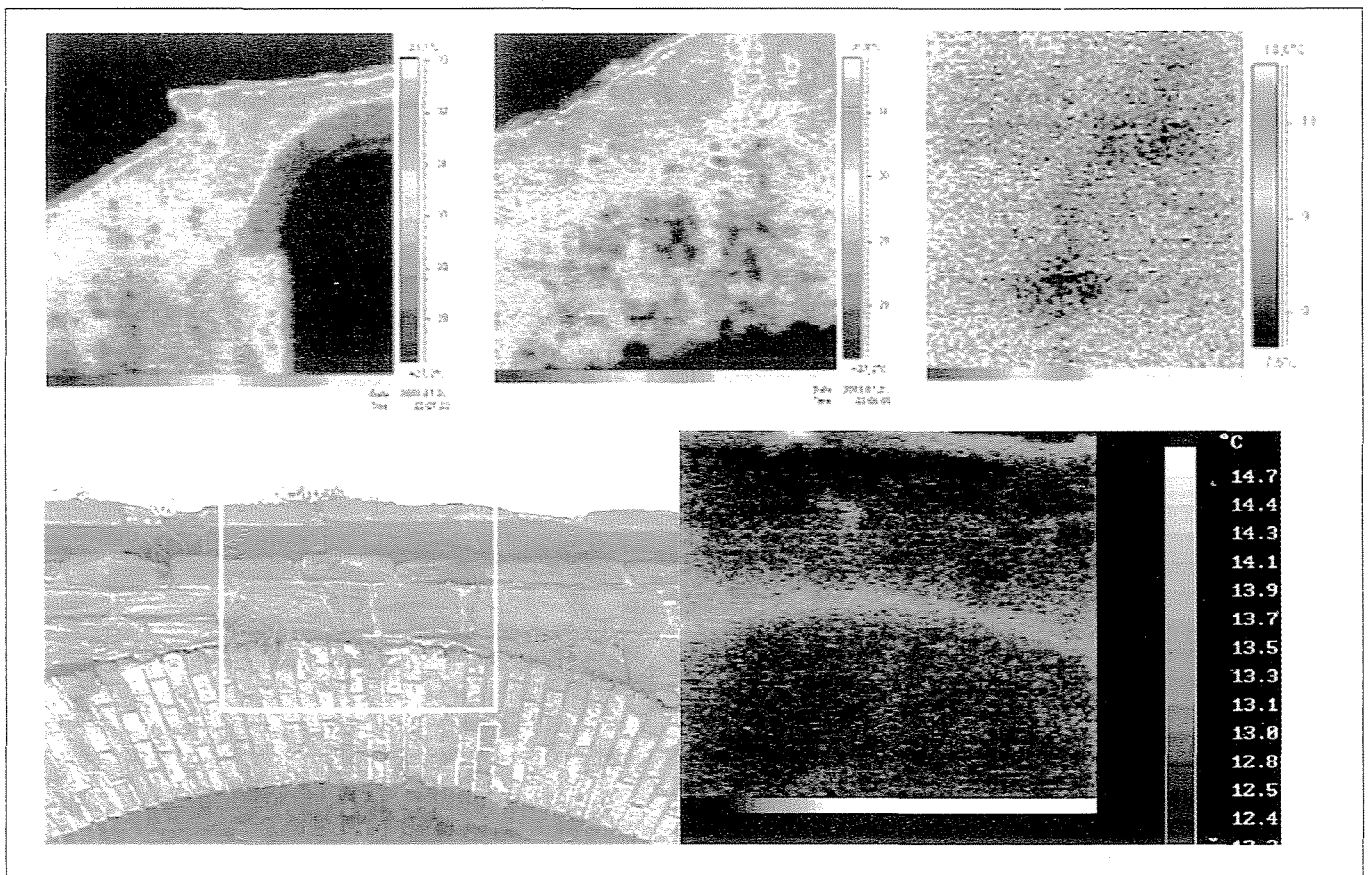
during the measurement. The anomalies mark the areas from where the electro-magnetic waves are reflected differently. Fig. 4 shows examples for anomaly maps measured on an arch barrel at two different frequencies. The maps are plotted against the penetration depth of the waves in a flat sheet form. Higher amplitudes (seen in reddish colours on the map) refer to cavity or other highly reflecting material, e.g. larger blocks of stone). Lower amplitudes (bluish colour) generally refer to an increase in moisture level or to rocks and soil with smaller compactness (e.g. fill material). The smaller, local anomalies may refer to small joint gaps, voids, or the presence of harder, highly reflecting material divergent from its environment.

Seismic tests were carried out on the stonework abutment of a viaduct with a computer-controlled seismic measuring system (Fig. 5, left). The distance between the geophones was 20 cm, and a hammer was used as a signal source. Fig. 5 (right) shows the recordings of seismic reflections where the image reveals two distinctive anomalies.

Test series have been performed with the use of infrared

thermography. The aim of the survey was to explore the application possibilities of this remote sensing method in non-destructive testing of masonry arch bridges, to help integrating this method into a more complex frame of analysis of masonry structures and to point out the currently conceivable directions of further research. The significance of research is confirmed by the fact that during the periodical inspection of masonry arch bridges, especially those with difficult or costly access, more and more importance must be given to remote sensing methods. The main task of periodical damage identification procedures based on 'in situ' remote sensing methods is to gain technical information by means of striking concomitant signs of possible damages which justify the necessity of further detailed investigation of the given structural area or section. The surface temperatures are represented on the thermal images by colours where lighter colours refer to higher temperature while darker colours refer to colder temperature (examples are seen on Fig. 6). The procedure is capable to point at wet areas, defects near the surface and presence of vegetation

**Fig. 6:** Selected images from the infrared thermographic survey of masonry arch bridges. Different colours or tones refer to different surface temperatures.



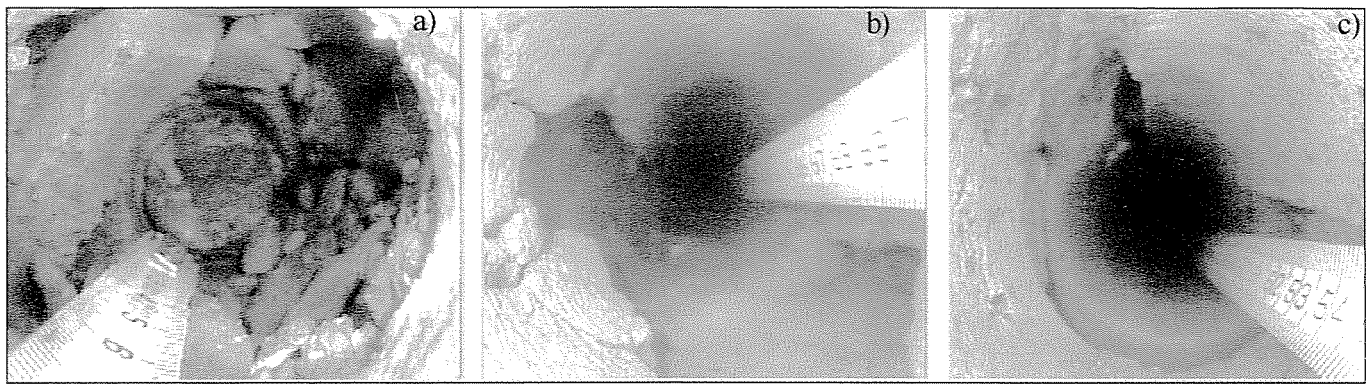


**Fig. 7:** Selected images from boroscopy survey.  
a) viewing backfill b) damaged zone c) separation

or other anomalies in the construction material that are invisible or hardly visible to the human eye.

Calibratory survey was carried out with a boroscopy camera that was inserted into boreholes drilled in representative parts of the structures. Digital recordings were made during the operation that allowed a detailed study of the internal parts of the structure in the boreholes. The objective of the survey was to help interpreting the results of the non-destructive measurements. The cores taken out from the drillings were further utilised for testing the physical and mechanical properties of the masonry. The collection of boroscopy images in *Fig. 7* demonstrates some representative findings during this survey.

### 3.3 Conclusions from the non-destructive tests

The radar survey was able to identify some internal geometrical features of the structures, such as structural thickness, the multi-ring nature of the barrel, presence of large cavities inside the masonry, etc. At some points these observations have been confirmed by boroscopy tests. Variations in the fill properties may cause different reflections also that can be seen on the radar images. However interpreting radar recordings is sometimes difficult. It is clear that boroscopy confirmation is indispensable for the successful interpretation of the radar images.

Infrared thermography was able to identify some of the characteristics of the masonry structure and to differentiate between the basic construction materials such as stones, bricks and mortars. Local anomalies have been recognised at some of the thermal images such as wet regions, cracks, weathered stones and remarkable mortar loss in the joints. However interpretation of the temperature variations on the images is sometimes fraught with difficulties due to the boundary effects.

Interpretation of seismic recordings is even more difficult than that of the radar images due to the highly inhomogeneous nature of masonry. However, the received seismic data might have been more meaningful if the resolution had been increased by applying higher frequency during the measurements.

## 4. REPAIR AND STRENGTHENING OF ARCHES

### 4.1 Review on the most frequently used methods

The following methods are used for the repair and strengthening of masonry arch bridges as the most frequent solutions:

- Methods for the restoration of waterproofing and drainage:
  - Drainpipes placed through the barrel, restoration of drainpipes,
  - Concrete saddle over the arch with bonded waterproofing,
  - Unbonded waterproofing on extrados,
  - Injection of arch barrel,
- Methods for the restoration and strengthening of arch barrels:
  - Injection of arch barrel,
  - RC shotcrete lining under the arch,
  - Concrete saddle over the arch,
  - Stitching of cracks and low pressure grouting,
  - Supporting barrel with steel rings,
- Methods for the restoration and strengthening of abutments, piers and foundations:
  - Underpinning through the abutment,
  - Scour protection (jacketing, sheetpiling, rock armour around pier),
  - Stitching and grouting of abutment cracks,
  - Installation of props or invert slab,
  - Injection of soil under foundations,
- Methods for the restoration of 3D integrity of arches:
  - Tie rods and patress plates,
  - Tying spandrel walls to new saddle on barrel,
  - Load dispensing concrete slab over the arch.

### 4.2 Repair preferences

As the most frequent source of masonry bridge problems is inadequate water drainage, there should be special emphasis on repair strategies that restore the integrity of waterproofing and drainage systems.

The most serious damage to arches relate to foundation problems therefore special attention should be given to their proper maintenance and repair.

Repair and strengthening techniques of arches should provide sufficient resistance against possible future loads and effects (e.g. permanently increasing axle loads, speeds, dynamic effects, other physical-chemical effects, etc.).

Preference should be given to maintenance strategies that promote solutions that preserve and restore masonry structures instead of replacing them. Repair works that do not take account of the fundamental modes of structural behaviour are unlikely to be beneficial.

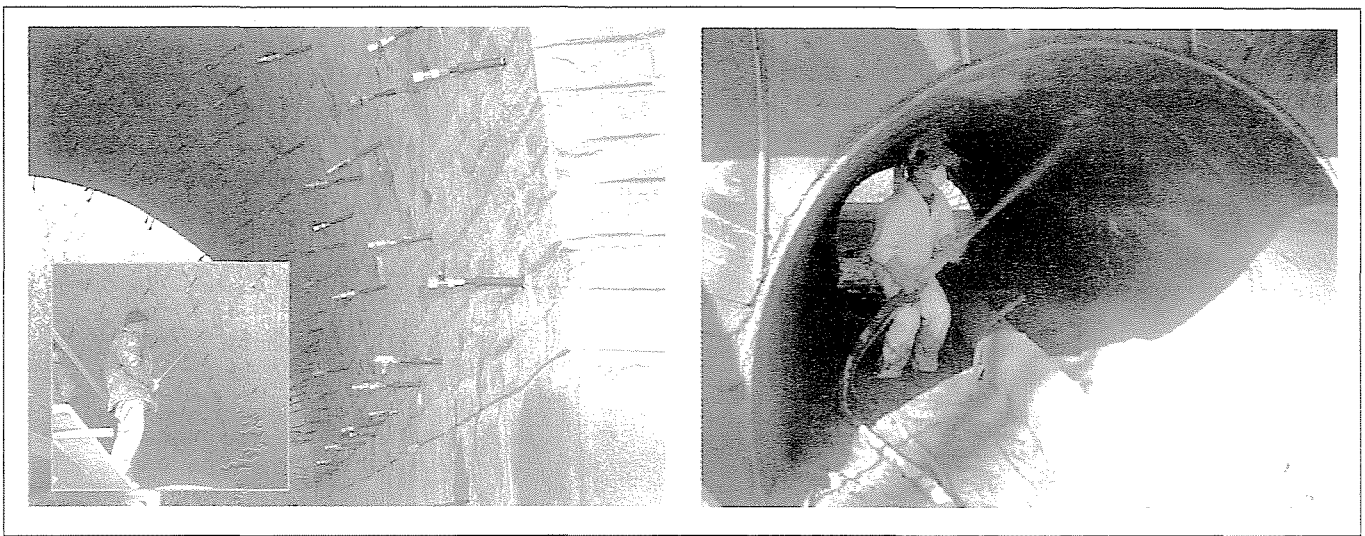


**Fig. 8:** Repair of arches with injection (left) and flexible shotcrete lining (right).

### 4.3 New concept of arch rehabilitation

Recent codes and guidelines for assessment of old structures dominantly focus on two main aspects: safety and serviceability. A variety of calculation procedures have been evolved in order to estimate the existing level of structural safety. These include both deterministic and probabilistic methods. According to recent practice assessment of safety is generally based on the load-bearing capacity: safety refers to the probability that the structural loads will not exceed the structure's capacity to resist them.

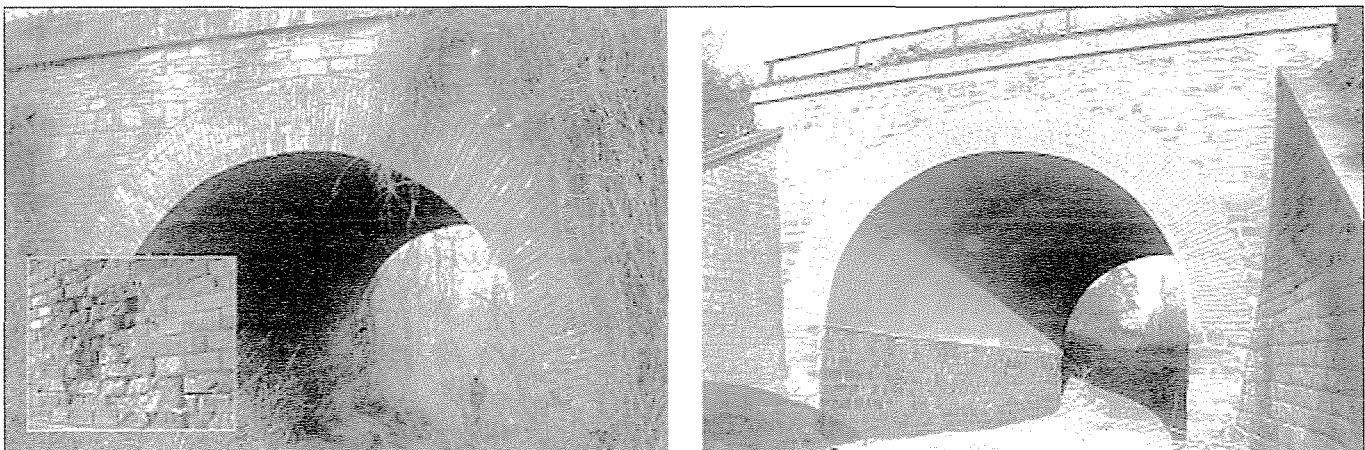
In case of an insufficient degree of safety strengthening operations are completed in order to provide an acceptable risk level by enhancing the load-bearing capacity. These measures often commit the error of concentrating only on increase in resistance, and modify the original load-carrying system, resulting in undesired extra loads on adjacent elements, or crack formation in other parts of the structure due to the stress re-distribution. Since risk is normally defined as a combination of the likelihood of occurrence of a defined hazard and the magnitude of its consequences, a similarly effective way of reducing the risk is the mitigation of the consequences.

Structural robustness is a measure of the structure's ability to mobilise alternative load paths and bridge over damaged parts in the event of overloading or under exceptional circumstances. Failure of masonry arches is usually preceded by the loss of robustness as a result of material deterioration or local damage making the structure susceptible to a mechanism-

like collapse. A key-element of structural robustness is the structural ductility that implies the structure's ability to undergo inelastic deformations and absorb large amounts of energy without substantial reduction in its resistance. In case of a mechanism-like failure structural ductility relies on the deformation capacity of plastic hinges or yield lines (sectional ductility). Therefore strengthening techniques of arches should focus more on the restoration of the structural integrity and ductility rather than strength increase only. Stabilisation of deformations would revive these structures' inherent ability to support themselves.

Examples are shown on *Fig. 8 and Fig. 9* for an arch repair technique where the structural integrity was provided by injection and an approximately 50mm thick fibre reinforced shotcrete lining. The resistance of this thin layer of shotcrete was enhanced by high-ductility welded steel mesh reinforcement. The bond between the concrete and the masonry surface was provided by the appropriate treatment of the masonry surface prior to shotcreting and by additional stainless steel bonding elements. Flexibility of the concrete lining, to maintain bond between the old and new structural parts, was achieved both by fibre reinforcement and by additives reducing the stiffness of the concrete. Lime-based mortar was used for injection in order to ensure compatibility with the existing structural materials. The mentioned repair solution is recommended when the arch surface is so degraded that patch repairs and repointing would not mean a long-lasting solution. It is also recommended when due to existing defects the arch needs no major strengthening only the stabilisation of the existing structural system. It should be noted however that durable repair solution is only possible if sufficient drainage is provided and maintained.

**Fig. 9:** Masonry arch bridge before (left) and after (right) repair.



## 5. CONCLUSIONS

Several methods are used for the assessment and structural analysis of masonry arch bridges. As the correlation between assessment results and measurements on arches is very limited, further research targeted towards a better understanding of their structural behaviour is considered essential. There is a need for new simple, reliable and user-friendly assessment methods to be developed and established in practice. To establish reliable input data for the analysis the application of effective inspection and measuring methods are needed.

In order to minimise damage to the structure destructive testing methods should be complemented and replaced by NDT methods wherever possible. There is a need therefore to increase the reliability of NDT measurements and to gain consistent results for the assessment of masonry arches. Unlike conventional destructive testing NDT methods provide mainly an overall qualitative information on the condition of the bridge. The results of the performed test programme have confirmed that NDT is a promising tool in finding hidden characteristics of masonry structures such as the presence of internal voids, flaws, layering condition, mapping of non-homogeneity, moisture content, etc. which may otherwise be detected only by destructive tests. However a great deal of further research is needed to increase the reliability of the interpretation of NDT results.

As many masonry arches belong to the civil engineering heritage of the railways their substitution or refurbishment requires careful consideration. It was concluded that maintenance policies and repair measures for masonry bridges should rely more on existing structural capacity and give preference to stabilization rather than substitution or replacement.

## 6. REFERENCES

- UIC Code 778-3R (1994), "Recommendations for the assessment of the load carrying capacity of existing masonry and mass-concrete arch bridges", Paris.
- Orbán Z. (2003): "Assessment, reliability and maintenance of old masonry arch bridges" UIC International Union of Railways. Research Project Report. Paris.
- Orbán Z. (2004): "Assessment, Reliability and Maintenance of Masonry Arch Railway Bridges in Europe", 4th International Conference on Arch Bridges, Barcelona, 2004 November 19-21.

**Zoltán Orbán** (1970) civil engineer, assistant professor at the Department of Structural Engineering at the University of Pécs, bridge expert at the Hungarian Railways. His main fields of activities are: assessment of concrete and masonry bridges, non-destructive testing of bridges, refurbishment of structures with high-performance concrete. He is member of the Panel of Structural Experts at the International Union of Railways (UIC) and leader of the international research project 'Improving assessment, optimisation of maintenance and development of database for masonry arch bridges'.





Dr. János Farkas



Ildikó Kocsis



Imre Németh



Jenő Bodor



Lajos Bán

According to the results of suitably prepared domestic studies and the favourable conclusions of foreign construction projects the application of high strength and high performance (HS/HP) concretes is expected to increase in the future. In the case of road surface pavements with reinforced joints (that, by the way, eliminate a common problem in Hungary, namely the rutting of asphalt roads) is the easiest way to construct bridges without a waterproofing and an asphalt finish. Such bridges exploit all the beneficial characteristics of HS/HP concretes. The design and the implementation of such a bridge involve a number of new problems that have to be solved. The present article offers an overview of the concrete technological experiments, the design and construction circumstances of the discussed flyover and the conclusions gathered in the course of the implementation of the project.

**Keywords:** high strength, high performance concrete, EC-based design processes, prestressing by unbonded tendons, tilting technology

## 1. DESIGN

### 1.1 General description of the structure

The bridge leads road No. 6707 over the M7 motorway (Figs. 1, 2, 3 and 8).

The main dimensions are as follows:

- crest width of connecting road: 12.00 m
- bridge opening between supports: approx. 11.00 m + 18.00 m + 18.00 m + 13.00 m
- cross-sectional arrangement: 0.565 m + 11 m + 0.565 m = 12.13 m
- lateral slope: 6 per cent in one direction
- design of the longitudinal section: slope of 2.43~0.72 per cent in one direction
- design of the horizontal layout: the bridge axis traces an arc with a radius of R=300m, the angle between the bridge axis and the motorway axis is 85.36°.

Load-bearing class of the bridge:

- $Q_{1k} = 600$  kN gross weight (2 × 300 kN twin axle) + 9 kN/m<sup>2</sup> on lane 1
- $Q_{1k} = 400$  kN gross weight (2 × 200 kN twin axle) + 2.5 kN/m<sup>2</sup> on lane 2
- $Q_{2k} = 200$  kN gross weight (2 × 100 kN twin axle) + 2.5 kN/m<sup>2</sup> on lane 3

Calculations were made for combinations of load bearing and serviceability limit states derived from vertical (LM1) and horizontal load models in accordance with KTI Rt. et al (2004) and MSZ ENV 1991-3 (Eurocode 1).

Structural layout of the bridge: 5-support, 4-rib monolithic superstructure made in two stages of C50/60 monolithic reinforced and cast-in-situ concrete applying longitudinal and transverse prestressing by means of unbonded tendons, with

crossbeams above the supports, individual piers and abutments made of C35/40 concrete and C25/35 flat foundations under the abutments and piers. There is an inspection chamber behind the abutments to enable the inspection of the watertight expansion joints.

### 1.2 New structural solutions devised during the design stage

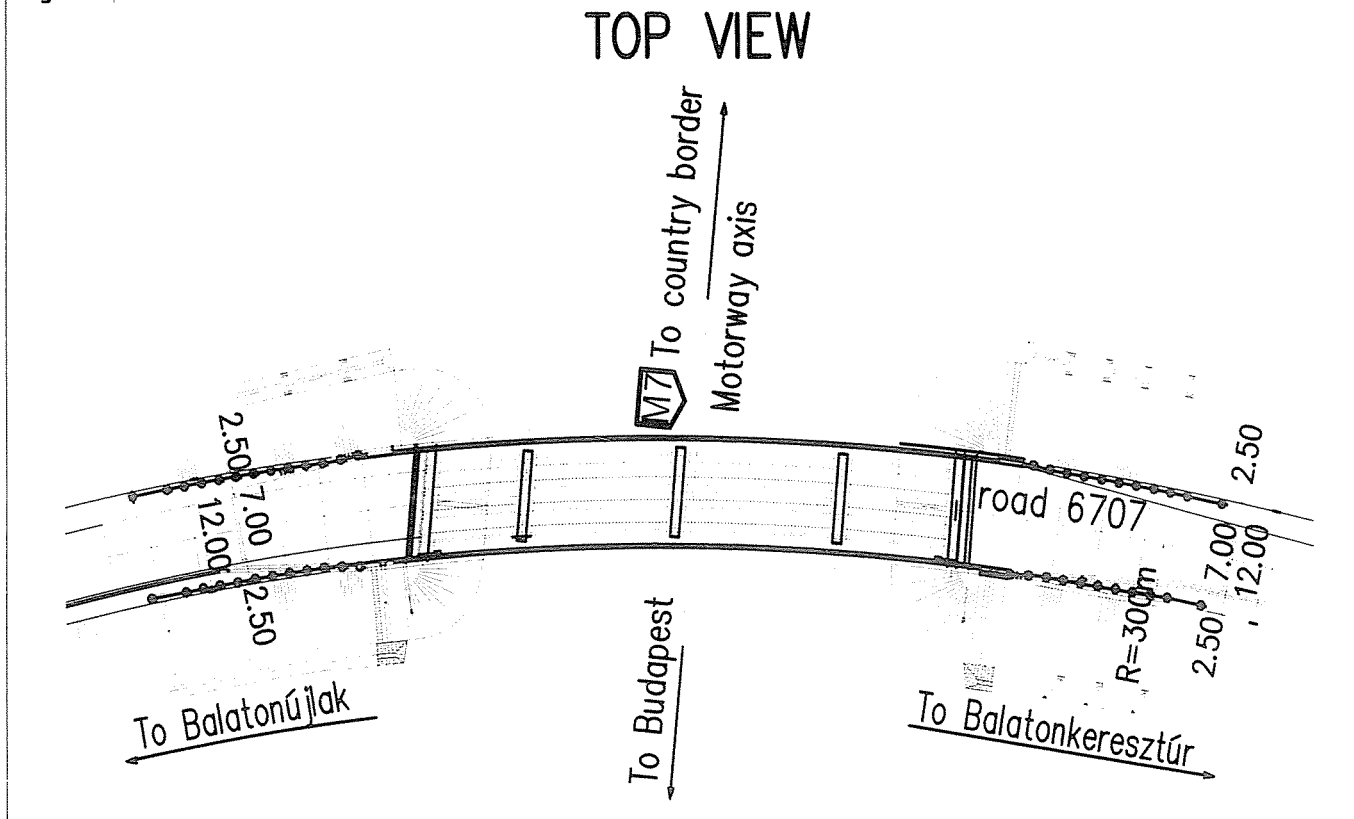
As a result of the omission of the waterproofing an array of new, non-standard structural solutions had to be devised. (We were released from the application of relevant standards by the Roadwork Main Department of the Ministry of Economy and Transport.)

- We omitted the waterproofing, the asphalt finish and the drainage system.
- Instead of an approach slab a reinforced concrete deck slab supported by the abutment was implemented.
- We designed a trapezoidal backfill to reduce subsidence.
- For reasons of the strict serviceability criteria a longitudinal and transverse prestressing was employed.
- We omitted the standard reinforced concrete curb and used a steel one instead.
- We implemented steel safety fence H3.

### 1.3 Design tasks related to maintenance and use

The owner insisted on the compilation of a “repair plan” so that it can identify the bridge in accordance with the current standards in case any structural alterations become necessary in the future. This made it necessary to design the bridge once in accordance with the regulations based on EC (KTI Rt. et al, 2004) and once in line with the technical requirements of the relevant roadwork regulations in force, to meet the strictest requirements in both cases. Regarding this particular bridge, this led us to the interesting conclusion (with a pronouncedly

Fig. 1: Top view



relative validity) that while the forces due to load bearing are almost the same under the different standards, the forces according to the serviceability requirements are some 60 per cent higher than normal service forces.

Previous structures of similar background were studied (Lindlbauer et al., 1988, Zilch et al. 2006).

### 1.4 Calculations of the new structure

On the one hand, the EC-based requirements of KTI Rt. et al. (2004) that are rather different from current bridge-design rules had to be considered. On the other hand, we wanted to do the additional calculations resulting from the new structure as accurately as possible, i.e. on very sophisticated models. Furthermore, we had to do calculations that were made necessary by the tilting method which we employed because at the preliminary tests we found that concrete flowed like honey.

#### 1.4.1 Summary of the calculations of the superstructure

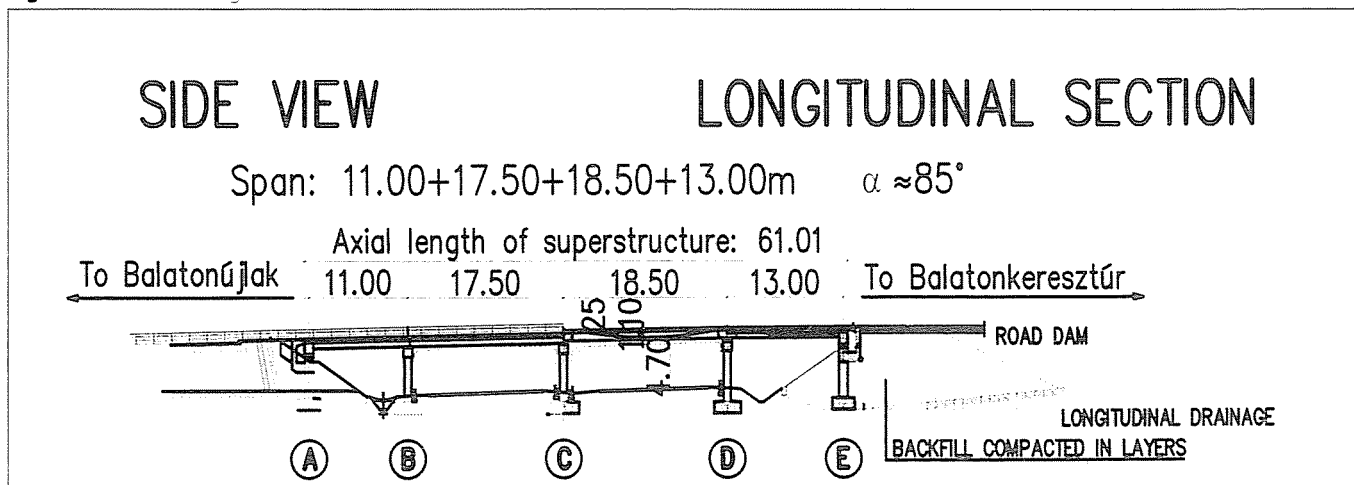
The calculation according to KTI Rt. et al. (2004) was completed as follows.

We made the calculations of the traditional super- and substructures in accordance with the Hungarian regulations in force since 2004.

The general regulations pertaining to prestressed concrete structures were extended to *non-waterproof superstructures* as follows:

- Under service conditions the stresses arising in all elements of the superstructure are under pressure (the decompression state in accordance with EC applied to a quasi permanent combination and for the most common combination).
- For the characteristic (and rather rare) combination we limited the maximum admissible tension at  $1.2 \text{ N/mm}^2$ , which is 40 per cent of the  $f_{ctk5\%} = 2.9 \text{ N/mm}^2$  of C50/60 concrete.

Fig. 2: Side view and longitudinal section



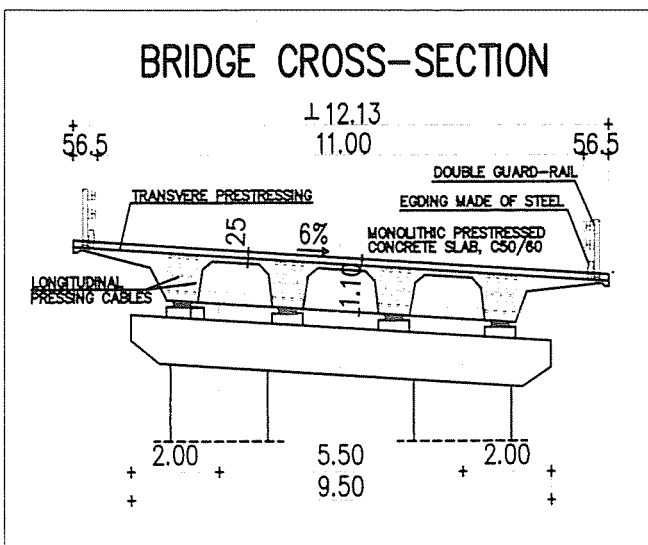


Fig. 3: Bridge cross section

- During prestressing the local tension remains below the  $f_{ctk}$  tension with a quantile of 95 per cent.
- We had to prove the failure and brittle failure safety under ultimate limit state.

Regarding the HS/HP concrete superstructure we applied the following calculation method that fulfils the above requirements:

- By means of a grid model we defined the transverse distribution of the four-main girder bridge and then investigated the side and intermediate main girders separately as bar structures (Fig. 4).
- We calculated the degree of indispensable longitudinal unbonded tendons for the main girders (comprising singly extruded "internal" tendons marked VT-CMM 4×150) so that the entire superstructure remains under pressure as a result of the service loads defined in accordance with KTI Rt. et al, (2004).
- We calculated the necessary normal reinforcement for all combinations in accordance with the load-bearing limit state.
- As a result of the Poisson-effect the longitudinal compressive stresses of the main beams cause a transverse tension which is added to stresses resulting from the traffic loads. We counteracted such transverse tension by means of crosswise prestressing at 1 m intervals using VT M 01-150 "internal" unbonded strands.
- To test the end anchorages we performed spatial finite element calculations on an elastic system.
- We made the calculations of the bearings, expansion joints, railings etc.
- In the case of this short-span bridge we deliberately omitted fatigue and dynamic calculations (which may, however, become necessary in the case of large spans and small structural heights).

#### 1.4.2 Calculations made necessary by the new structural designs

- To ensure a suitable layout of the backfill, the bridge and of the connecting earth embankment we performed plane nonlinear finite element calculations.
- To check the concrete slabs we performed finite element calculations on a two-layer paving system on an elastic support assuming compressed springs between the layers.

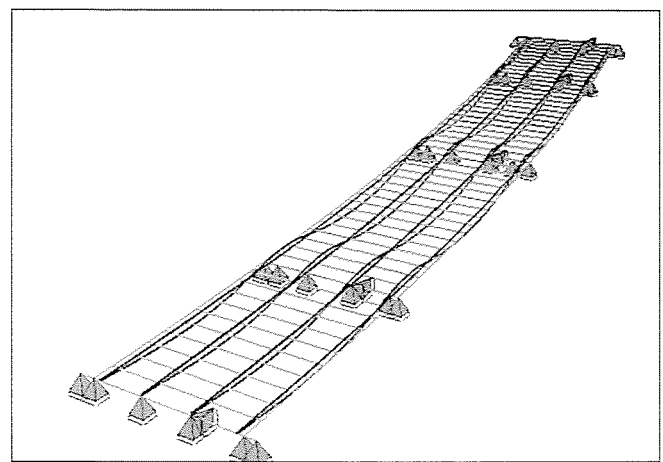


Fig. 4: The bar system model and the strands

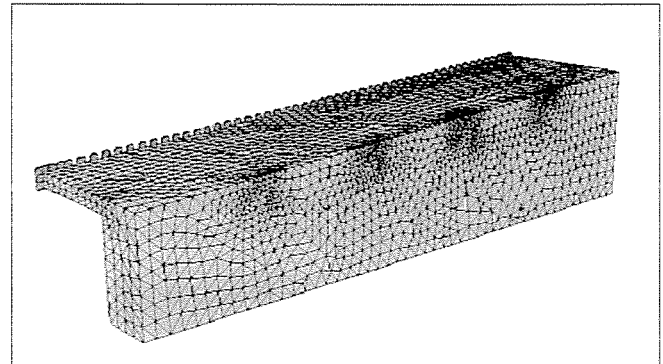


Fig. 5: Spatial model of the end cross beam

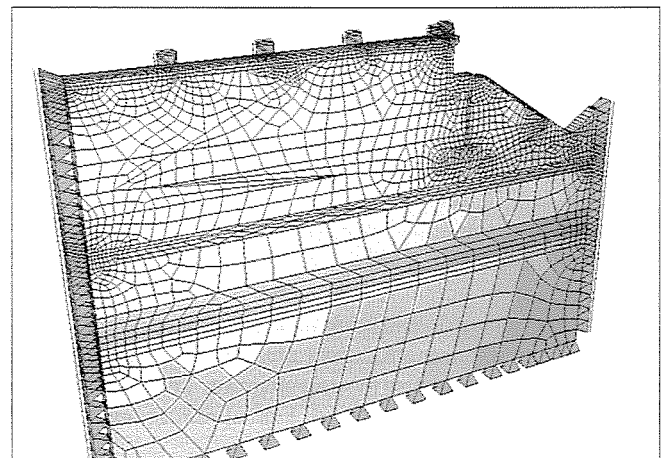


Fig. 6: The model of the back fill and the surrounding area in final state

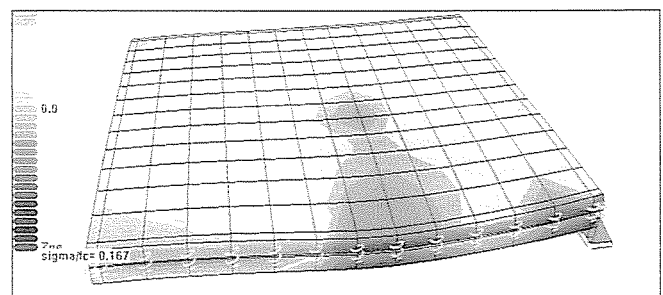


Fig. 7: One of the load positions and stress distribution of a 5×4m deck slab supported by a two-layer (concrete road slab + cement bonded soil) and by the bridge itself

#### 1.4.3 Technology-related calculations

- We controlled the displacements and stresses resulting from the tilting of the prestressed concrete superstructure on a grid model, calculated the additional reinforcements needed and the step-by-step asynchronous sinking of the needed points.
- Regarding load tests we calculated the deflection of

the loading conditions specified and the parameters of characteristic vibration.

Calculations were made using the *Sofistik* software of Mahid 2000 Co.

#### 1.4.4 Description of FEM calculations

Calculations of the end anchorages by FEM and considering construction conditions (*Fig. 5*) were carried out as follows:

The form of the main girder end built together with the cross beam has raised certain questions regarding the classic manual calculations of the end zone as a disc.

The spatial finite element calculations were made necessary by the investigation of the post-tensioning states and to ensure the optimum design of the anchoring devices.

Loads were transferred in nodes, which naturally resulted in errors on the safe side. Forces transmitted over a given limited surface would have resulted in smaller stresses. Anchorage zone length is equal to approx. 2 times the depth. Exact demoulding reaction forces were modelled by increasing the bare depth.

Prestressing followed at the age of 3 days for concrete with a compressive strength of 40 MPa and assuming full scaffolding:

- The two side main girders are prestressed one after the other by means of the central straight strand bundles.
- The two intermediate main girders are prestressed simultaneously by means of the central straight post-tensioning tendons.
- Prestressing of the two side main girders, by sinusoidal tendons
- Prestressing of the strands of the two intermediate main girders by sinusoidal tendons
- Removal of scaffolding.

By means of the above post-tensioning sequence we attempted to enforce the principle of uniform prestressing.

The results indicated that in the case of concentrated loads the maximum principal tensile stress is 3.0 MPa in the top plane of the slab extremities which is less than that  $f_{ctk}$  0.95 of C40 concrete (strength during prestressing). After having examined the stress distribution diagram and in line with applicable design principles both helical reinforcements and additional stirrups were installed.

After the completion of the prestressing process the proximity of the anchorage was inspected repeatedly and no cracks were discovered.

Examination of the soil behind the bridge according to FEM and considering construction conditions (*Fig. 6*) was performed as follows:

The main task was to reduce the occurrence of subsidence under the rigid pavement structure, to limit the stresses of the bridge deck concrete and to avoid cracks in the concrete deck slabs. As a result of a design-related re-thinking of the role of the approach slab and by means of its removal we could employ a larger backfill mass that can distribute forces more evenly and better backfill materials. To specify the additional consolidation settlement we multiplied the elastic settlement by 0.5. We calculated using the non-linear Mohr-Coulomb theory and the standard soil parameters.

The design of the deck slabs (*Fig. 7*) was performed as follows:

The 20 cm concrete and 20 cm cement bonded soil layer were laid on a soil with a bedding coefficient of  $C=70\ 000$  kN/m<sup>3</sup>. A vehicle with an ideal mass of 60 tons (with 4 loading surfaces of  $40 \times 40$  cm each) in accordance with KTI Rt. et al, (2004), a simultaneous live load of 9 kN/m<sup>2</sup> and a heat effect of  $\pm 5^\circ\text{C}$  above the lower and upper edge of the concrete slabs were alternately applied, i.e. the vehicle was placed on the edge, in the middle etc. of the system. If there was any tension detectable between the finite elements of the slab layers, the spring acting between them ceased to cooperate with the system. This means that the system is non-linear.

## 2. CONSTRUCTION

General view of the bridge is shown in *Fig. 8*.

### 2.1 Preliminary laboratory tests

The composition of the mixed transport concrete with a minimum specification of C 50/60 HS/HP required for the superstructure of the bridge was determined by means of a series of experiments using the materials available in the organisational radius of the construction site, also considering the technical parameters of the concrete mixers servicing the site. We have examined the characteristics of the fresh concrete, the compressive strength, water-tightness, frost resistance, de-icing salt resistance, resistance against the intrusion of chloride ions and abrasion resistance of the hardened concrete at the age of 2, 7, 28 and 90 days.

The water-tightness and abrasion resistance of high performance concretes is better, its frost resistance, de-icing salt

**Fig. 8:** General view of the bridge under construction



resistance, resistance against the intrusion of chloride ions is significantly better than that of ordinary concretes (Fig. 9).

The water-tightness, frost resistance, resistance against de-icing salt and the resistance against the intrusion of chloride ions of HP concretes made of CEM II/A 42.5 N blast furnace slag cement is on par with that of a concrete mixture made of CEM I 42.5 N Portland cement.

## 2.2 Preliminary test mixtures at a proportioning plant

Following the laboratory tests trial mixtures were made at the proportioning plants at the site. We had two 0.5 m<sup>3</sup> and one 1.0 m<sup>3</sup> mixer at our disposal. The mixers' control computer algorithms had to be modified (we changed the charging sequence, the discharge timing of the scales and worked out a way to charge water in multiple stages), we arranged the way the silica fume is charged and found a way to automatically monitor the moisture content of the concrete inside the mixer.

During the trial mixes we measured the moisture content of the aggregate, tested the proportioning accuracy of the aggregate, the cement, the water, the silica suspension and the admixtures, the mixing duration, the air and fresh concrete temperature and the consistence, bulk density and water content of the fresh concrete.

We made test specimens to know the compressive strength, water-tightness, frost-resistance, abrasion resistance, de-icing salt resistance, the resistance against chloride ions of the concrete.

The test results of the mixes performed at the mixing plants were similar to those of the laboratory tests, which led us to the conclusion that high strength and high performance concretes can be manufactured under industrial conditions.

The two concrete samples made at different proportioning plants and having different compositions were analysed for their characteristics relevant to their strength and durability. Based on the results of the trial mixes made at the proportioning plant we selected the concrete mixture made with CEM II/A-S 42.5 N cement for the construction trials.

## 2.3 Construction tests preceding the actual construction works

We performed construction tests at the concrete plant in Marcali, at one of the approach slabs of two flyovers of the M7 motorway and on the deck slab of a smaller bridge.

During the construction tests we determined the mixing time required and the cycle time of the mixers and tested the following parameters:

- the uniformity of the concrete mixture;
- the consistence endurance of the concrete mixture;
- the transportability of the mixture in mixing trucks;
- the pumpability of the concrete;
- the compactability of the concrete;
- and the way a uniform concrete surface can be created.

After the processing of the surface layer had to be compacted with a beam screed (Fig. 10). The beam vibrator also created the final level and surface of the concrete slab.

The behaviour of HS/HP concretes is rather different from that of ordinary concretes. When moved or vibrated, the concrete remains plastic, however, setting starts within a short time under static conditions. We prevented the evaporation of

the moisture content of the concrete by keeping the surface of the individual layers wet with water spraying.

For the roughening of the concrete surface we tried several methods:

- roughening of the fresh concrete by means of stone chipping vibrated into the surface;
- roughening of the fresh concrete by means of various types of brooms;
- roughening of the fresh concrete by means of artificial grass;
- roughening of the solid concrete by means of flushing out the fine particles from the surface;
- roughening of the hardened concrete by applying a thin Whisper-Grip layer.

Roughening of large areas with the above methods was not entirely satisfactory, so we tried a new method using a roller covered with artificial grass. The concrete surface treated this way has a homogeneous texture; its roughness is 0.8-1.0 mm (expressed as sand depth).

For the concrete works of the superstructure of the bridge a separate concrete technological manual was compiled. For the composition of the concrete see Table 1. A total amount of 484 m<sup>3</sup> of such concrete was used.

## 2.4 Construction

0.9 kg/m<sup>3</sup> polypropylene fibre was added in situ to the concrete mixture in the mixer. The consistency was measured at the proportioning plants and at the worksite for each mixing truck prior to and after the addition of the fibre. The temperature of the fresh concrete was 20-25 °C. Air temperature was 6-8 °C.

The construction sequence of the superstructure of the bridge comprised the following stages:

- Design of a near-horizontal bridge formwork in accordance with the plans considering the tilting.
- Construction of the formwork.
- Reinforcement fixing, placing of anchoring devices of prestressing cables, railings and steel borders (Fig. 11).
- Concreting, surface finishing, curing (Fig. 12).
- Prestressing (Fig. 13).
- Placing of hydraulic presses needed for the lowering/tilting of the structure after the partial removal of the formwork.
- Removal of the formwork.
- Lowering/tilting of the bridge into its final position.
- Placing and grouting of the horizontal gap of bearings.
- Placing of the bridge on the bearings, removal of hydraulic equipment.

The near-horizontal construction and the subsequent

Table 1: Concrete mixtures

		Concrete mixtures				
		A	B	C	D	
Aggregate	OH 0/4	[m%]	43	39.4	30.4	39.4
	OK 4/8	[m%]	21			
	UKZ 5/12	[m%]		19.2	25.6	19.2
	UKZ 12/20	[m%]			44.0	
	OK 8/16	[m%]	36	41.4		41.4
Water	[liter]	148	114.5	129	115	
Cement I 42.5 N	[kg]	360			420	
Cement II/A-S 42.5	[kg]		420	460		
Silica fume	[kg]		50	50	50	
Fluxing agent	[kg]	3.60	7.14	5.24	8.4	
Retarding admixture	[kg]	1.08	1.26	1.38	1.26	
Air-entraining agent	[kg]			1.15		
Planned bulk density	[kg/m <sup>3</sup> ]	2424	2457	2425	2459	
Water-cement ratio		0.42	0.35	0.35	0.35	

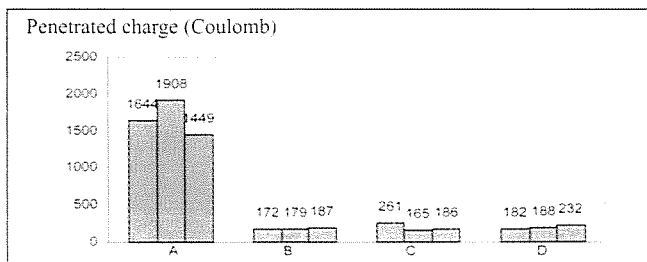


**Fig. 9:** Concrete resistance against intrusion of chloride ions



**Fig. 10:** Surface finishing with Tremix SVE beam screed

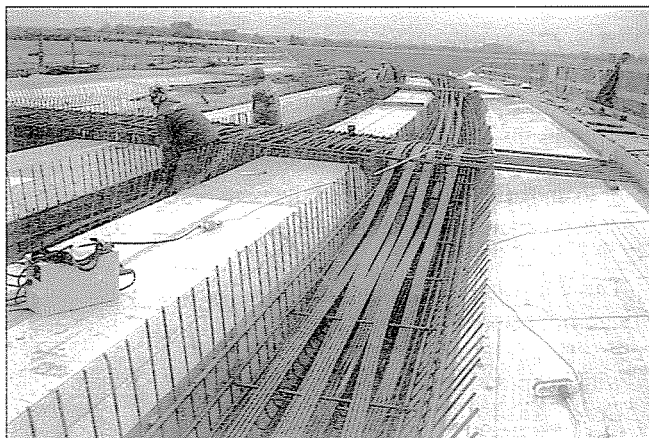


**Fig. 11:** Layout of prestressing strands



**Fig. 12:** Concreting the girders

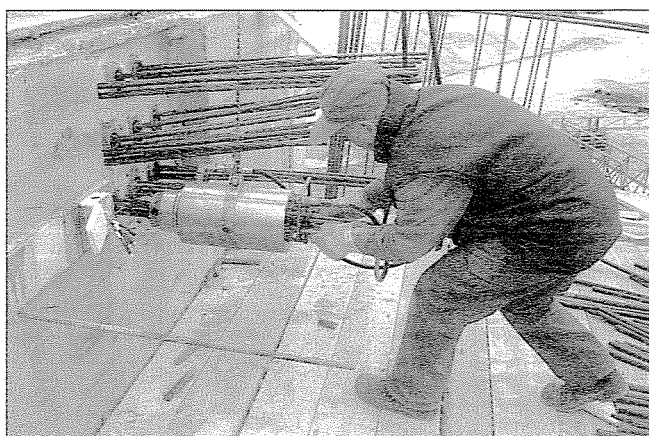


**Fig. 13:** Prestressing

lowering and tilting of the superstructure to its final position was necessary because of the initial fluidity of the fresh concrete and of the high (6 %) transversal slope of the superstructure.

In order to eliminate the unevenness problem encountered during the previous tests and construction trials the screed beam was placed on a steel profile outside the formwork.

Concrete casting took place in two stages. During the first stage we prepared the longitudinal and cross girders and then the slab. This was necessary in order to ensure a high capacity concrete supply during the preparation of the slab and a continuous progress of the work.

Beam screeding was followed by floating and roughening. The surface was roughened with a roller covered with artificial grass. The advantage of this method is that it enables an almost instantaneous preparation of the final finish after floating is completed.

The concrete surface was cured by means of a vapour barrier agent, one day later it was covered with a terfil (screen mesh) and a foil layer.

We measured the hydration heat generation process in the main girders during and after concrete casting and found that within 20 hours the temperature of the concrete rose from the initial 20 °C to a maximum of 65 °C. Premature shrinking was limited by means of appropriate and immediate curing.

The superstructure was prestressed longitudinally and transversally in accordance with a pre-defined sequence and prestressing forces. Prior to prestressing test cubes were used to determine the strength required for prestressing.

As mentioned, after the removal of the scaffolding the superstructure was tilted and lowered to its final position in accordance with the plans. The near-horizontal construction and the subsequent lowering and tilting of the superstructure to its final position was necessary because of the initial fluidity of the fresh HS/HP concrete and of the high (6 %) transversal slope of the superstructure.

In order to determine the movement coordinates of the formwork we constructed the 3D model of the bridge in Autocad and made step-by-step calculations of the geometric data using this model. To facilitate tilting of the structure raising presses were installed above the supports and below the cross beams of the superstructure. The raising presses were not installed to the geometrically most favourable positions but where they did not obstruct the installation of the final bearings.

During tilting, the level difference between two neighbouring supports had to be kept below 10 mm.

In the course of the work we were monitoring the shifts occurring at the individual supports and the reaction forces arising at the hydraulic presses. Even though the bridge was moved in accordance with a pre-calculated chart, actual values were fed back to a calculation software installed in situ and controlled the momentary stresses arising in the superstructure as a result of the movement to compare calculated and actual values of stresses.

After the positioning of the bridge as planned, bearings were installed and grouting the gaps was also completed. At this point the hydraulic presses could be relieved and subsequently removed.

In order to discover the problems related to the connection of the bridge and the connecting road two road sections were built behind the bridge with a length of 35 m each. The CP 4/3 concrete was delivered by dumping lorries and a WIRTGEN finisher was used for preparing the pavement. The road was built in two stages on a lane-by-lane basis.

### 3. CONCLUSIONS

In the course of the construction of the motorway flyover with a HS/HP concrete superstructure we gathered invaluable experience from the design process through the definition of the concrete structure to the actual construction works. We employed novel calculation and structural methods, performed concrete technology experiments and applied construction technologies while improving our professional skills in the construction phase.

By reducing the water-cement ratio and employing a plastifier and the suitable concrete composition a superstructure was devised that is more durable than normal concrete. Our experiments supported what foreign studies have already reported, namely that there is a significant increase in the compressive strength, water-tightness, de-icing salt and chloride ion resistance of this concrete compared to normal concrete while the abrasion resistance of the concrete did not decrease either. By means of improving the durability characteristics of the concrete and a suitable selection of the prestressing force (and controlling the cracking process) we could favourably influence the durability of the structure.

The HS/HP concrete with a fluid consistence can be processed by using a near-horizontal formwork (i.e. with a slope of not more than 2-3 %). If a lateral slope larger than this is required, a special technology should be devised.

We could prove that the tilting/lowering technology that we were the first to employ in Hungary, HS/HP concrete can be applied even for sophisticated bridge structures.

The application of HS/HP concrete for the purpose of bridge construction requires that current standards and road construction regulations are updated and extended and new ones are drawn up.

Drawing the conclusions of operation and maintenance is also important because any improvement of the structural designs and joints of bridges, the enhancement of concrete technology and of processing methods can only be achieved in possession of such experience. The experience gathered through the operation and maintenance also have an effect on the economy of such bridges.

Further studies are necessary to establish the time dependence of hardening, creep, shrinkage and hydration heat build-up and the effects thereof on the structure itself.

The high strength of HS/HP bridges results in reduced structural depth and a more slender form factor but also in a lower ductility, which prompts for more accurate dynamics and fatigue calculation methods.

The issue of decreasing the 30~50 mm concrete cover thickness common for normal concretes is also raised. In case of a large-scale application of this technology we believe a power surface finishing technology should also be devised.

Current research results show that the application of HP concretes has the following advantages in bridge-building:

1. Less concrete and reinforcing/prestressing steel is required

for the construction of a bridge with better performance characteristics.

2. Aesthetically more appealing structures can be constructed with smaller cross-sections and lower weight structural elements.
3. Deck slabs can be constructed without waterproofing.
4. Protection against salt corrosion can be omitted.
5. It is easy to connect to roads with a concrete pavement.
6. As a result of the HP concrete the durability of the bridge is increased, the cycle time between reconstructions is multiplied, the expected costs decrease and the life span of the bridge increases.

### 4. REFERENCES

- KTI Rt., Budapest University of Technology and Economy, Department of Road and Railway Construction; Budapest University of Technology and Economics, Department of Structural Engineering; Hungarian Academy of Sciences, Research Group of Structural Engineering; Orka Engineering Consulting Kft. (5/2004). "Civil Engineering Construction Permit and Technical Delivery Conditions for the construction of bridge superstructures connecting to rigid pavement structures of roads with a concrete finish, reinforced joints or a composite structure" (In Hungarian)
- Lindlbauer, W., Zehetner, K., Steigenberger, J., Handler, H (1998), "Directly-Trafficable High Performance Concrete Bridge Structures – Practical utilisation demonstrated by the example of the Badhausbrücke" *Österreichischer Betonverein-Schiffenreihe*, 32, pp. 15-20.
- Zilch, K., Essl, R., Hennecke, M. (2006). „Der Neubau der Innbrücke Gars - Hochleistungsbeton B85 im Grossbrückenbau“; *Bauingenieur*; pp. 14-21.
- Dr. János Farkas** (1958), civil engineer. Earned his PhD in the domain of bridge structures. Production designer of Vegyépszér Co. and Mahid 2000 Co. Member of the Hungarian Group of *fib* and of the Hungarian Engineers' Chamber. Main professional interests: reinforced concrete and prestressed concrete bridge structures, HS/HP concretes, structural engineering of bridge construction technologies, and bridge dynamics.
- Ildikó Kocsis** (1956), civil engineer, engineering specialist in concrete technology, chief production engineer of Vegyépszér Co. and of Mahid 2000 Co. Member of the Hungarian Scientific Society of Silicate Industry and of MAÚT, the Hungarian Road Association. Main professional interests: reinforced concrete and prestressed concrete bridge structures, concrete technology, HS/HP concretes, and R&D.
- Imre Németh** (1957), civil engineer, engineering specialist in structural engineering and concrete technology. Director of bridge construction of Vegyépszér Co. and General director of Mahid 2000 Co. Member of the Hungarian Group of *fib* and of the Hungarian Engineers' Chamber. Main professional interests: reinforced concrete and prestressed concrete bridge structures, bridge construction, structural engineering, construction technologies of large bridges, and subway construction.
- Lajos Bán** (1962), civil engineer, concrete technology chief engineer, head of the development team of Mahid 2000 Co., chief production engineer of the bridge construction department of Vegyépszér Co. and project manager of the M6 motorway construction. Main professional interests: information technology and concrete technology.
- Jenő Bodor** (1972), civil engineer, superintendent of Mahid 2000 Zrt., a bridge construction specialist. Main professional interests: reinforced concrete and prestressed concrete bridge structures, HS/HP concretes, bridge construction technologies.

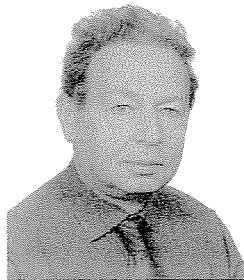
# PREFABRICATED CONCRETE STRUCTURES FOR COMMERCIAL AND INDUSTRIAL BUILDINGS IN HUNGARY



József Képes.



László Novák.



László Polgár

*In Hungary, there has been a long tradition of industrial prefabrication of concrete structural elements. Hungary's EU accession has further increased the number and volume of construction projects. The timeframe and the number of skilled workers available for the individual projects are getting more and more limited. The primary function of buildings is changed frequently; therefore there is an increasing demand for a flexible adaptability of structures to the new and altered functions. One of the consequences of this tendency is that clients require larger and larger spans and larger and larger load capacity. The overview below of the past four years reflects these changing requirements.*

**Keywords:** prefabrication, prestressed concrete beams, load bearing structure, halls

## 1. BRIEF HISTORICAL OVERVIEW

The manufacturing of concrete elements reached its peak in Hungary at the end of the 1970s. By 1980 the factories of precast concrete residential buildings reached their peak output and the manufacturing of load bearing elements, exterior building panels and civil engineering units reached new and newer highs, too. From the beginning of the 1980s volumes manufactured have been decreasing with the bottom around 1992. During this period of 12 years the quantity manufactured shrunk to about one fourth to one fifth of previous values. Because of the large amount of prefabricated residential panels precast concrete has become a quasi-symbol of the socialist regime, so at the time of the change of the political system many believed it was time to bury prefabrication, too.

The first successes of the new era arrived when foreign investors envisaged steel structures and it turned out that in Hungary the prefabricated concrete structures are more competitive than those made of steel, e. g.:

1988: Float Glass Factory, Orosháza (American client)

1990: Suzuki Car Manufacturing Plant, Esztergom (Japanese client)

Development has been almost constant since the entry of the METRO wholesale chain-store into the Hungarian market at the end of 1993. The share of prefabricated concrete structures has been increasing every year. The purpose of the present essay is to give an account of the most significant structures erected and the development tendencies of the past few years.

Hungarian manufacturers of concrete structures are represented by the Association of Hungarian Concrete Element Manufacturers (MABESZ, [www.webforum.com/mabesz/](http://www.webforum.com/mabesz/)), who's membership comprises about 80 per cent of the total Hungarian manufacturing capacity.

## 2. PREFABRICATED CONCRETE STRUCTURES OF THE PAST FEW YEARS

### 2.1 Hall-type skeleton structures

The most spectacular structures are single storey frameworks, mainly built for department stores, manufacturing plants and supermarkets. Development of warehouses was especially fast: in the past five years the floor area of new warehouses built was about 120,000 sq. m. annually. Large warehouses (with a floor area of 2000–3000 sq. m. and above) almost exclusively have concrete structures. There is an increasing demand for ever larger spans and clear heights.

Currently, the maximum span available in Hungary is 34.00 m; the clear height varies between 6.00 and 18.00 m, though clients sometimes specify even larger clear heights. The maximum floor area per column is 500 sq. m. (see the Lidl warehouse with a floor area of 14×32 m, i.e. 448 sq. m. per column).

#### 2.1.1 Warehouses

During the past 16 years approximately 1,200,000 sq. m. of new warehouses have been built in Hungary, which means that by the end of 2005 the warehouse floor (Fig. 1) area built since the change of the political system was almost two times as much as that of the warehouses built previously. In the meantime, many of the old warehouses have been demolished; still, the total warehouse capacity has doubled during this period.

The majority of these modern warehouses were built



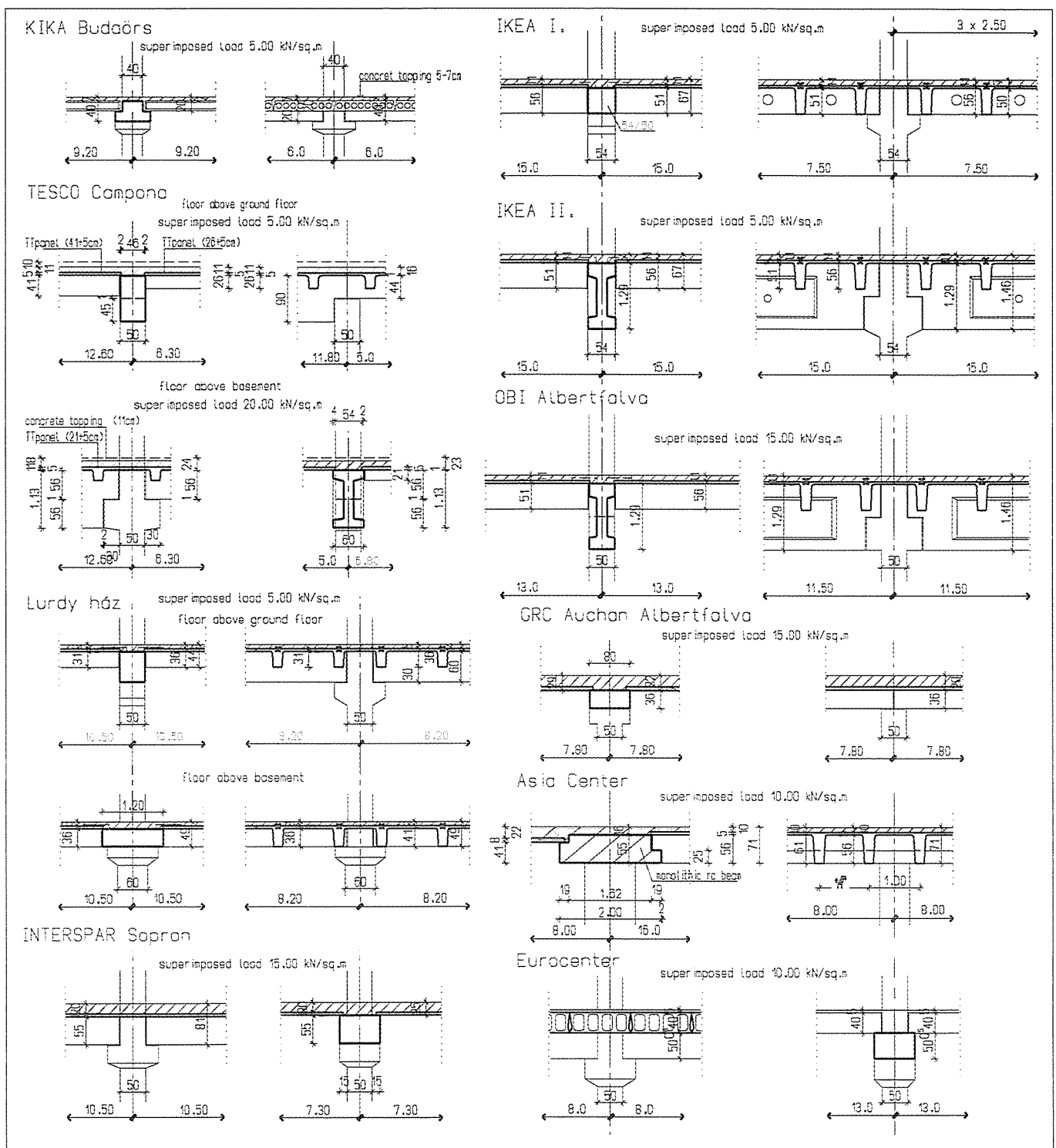


Fig. 1: Hypermarket floors

between 1995 and 2005. The past five years saw approximately 100,000 sq. m. of new warehouses built with a prefabricated concrete structure. Warehouses with steel structures mainly have a floor area of 1000~2000 sq. m. These figures do not include the warehousing capacities owned by the manufacturing companies (Audi, Bosch, Electrolux, etc.). Large warehousing facilities with a floor area of 50,000~100,000 sq. m. comprising several warehouse halls within one single plot are often built by developers for leasing purposes.

Hungarian companies active in the field of concrete prefabrication passed the test with flying colours, as demonstrated by the fact that large warehouse halls (those with a floor area of 3000 sq. m. and above) all have prefabricated concrete structures. *Table in next page* illustrates these tendencies. Clear heights and spans are constantly increasing.

Beams and purlins with a length of 15 m and more (and often less) are mostly made of prestressed concrete with a T or TT cross-section. Load bearing structures are characterised by the mass/sq. m. of the beams and roof purlins, which is normally between 120 and 150 kg/sq. m. In 2005 the characteristic selling price of concrete structure assembled and erected was EUR 0.2/kg (based on a price of EUR 500/cu. m.), which is below the customary average price in the EU. Considering the fact that these structures are highly streamlined with a high proportion of reinforcement steel and prestressing strands, such low prices hardly seem justified. The main reason is that wages are still extremely low in the construction industry. Supposing that the load bearing concrete framework of a hall costs HUF 180/sq. m., then based on a price of EUR 0.2/kg this still converts to a mere EUR 36/sq. m. The same with a steel structure would amount to

40 kg/sq. m. × EUR 1.6/kg, approx. EUR 64/sq. m., which explains why warehouses are made of prefabricated concrete in Hungary. Later on we shall take a closer look at some of the structures that have actually been built.

## 2.1.2 Industrial manufacturing plants

Ever since the change of the political system developers and clients of industrial manufacturing plants have almost exclusively been foreign investors. The first ones arrived before the change of the political system (Float Glass Factory, Orosháza; Suzuki, Esztergom), to be followed by numerous well-known companies like Philips, Audi, Bosch, Electrolux, Samsung, Alpine to name just a few of the bigger ones. The majority of these companies already had their tried and tested construction preferences, but their factories abroad mainly had supporting structures made of steel. These companies were surprised to find that in Hungary the cost of concrete structures was normally lower than that of steel ones.

The halls below are characterised by their respective column grids:

Float glass factory	21.0×21.0 m	40,000 sq. m.
Suzuki	12.0×18.0 m	60,000 sq. m.
Philips	14.4×21.6 m	30,000 sq. m.
Audi	20.0×20.0 m	70,000 sq. m.
Bosch	12.0×24.0 m	80,000 sq. m.
ADA	12.5×25.0 m	30,000 sq. m.
Sanyo	7.5×30.0 m	30,000 sq. m.
Asahi	18.0×30.0 m	50,000 sq. m.
Ibiden	12.0×20.0 m	60,000 sq. m.

These buildings could almost be labelled boring because they are mostly built upon the same construction scheme:

- concrete columns restrained at the bottom and free at the top end
- pre-stressed concrete simply supported roof main beams
- prestressed concrete simply supported roof purlins
  - concrete purlins are covered with corrugated steel roofing, topped with a heat insulation made of mineral wool and mechanically fixed roofing sheet
  - façades: coffered or cladding panel built and almost exclusively lightweight steel fronts with concrete laminated panel footings and anti-frost aprons.

The formworks and manufacturing technologies available at Hungarian concrete prefabrication plants are rather uniform and well adapted to these uniform requirements; this is why the products of the various manufacturing plants hardly differ from each other. This may come very handy: sometimes there are two or three plants delivering precast elements for the same project simultaneously. One memorable example of such cooperation was the Asahi hall built in 2004 in Tatabánya which was constructed with a column grid of 18×30 m and a floor area of 50,000 sq. m. by three cooperating companies in 3 months' time (a detailed description follows).

Today 70 per cent of the products of Hungarian manufacturing plants come from factories built by the Hungarian construction industry after the change of the political system. We are proud to add that the vast majority of the structures of these plants have been built by members of the Association of Hungarian Concrete Element Manufacturers since 1990, including some 800,000 sq. m. of manufacturing halls with a prefabricated concrete structure.



Fig. 2: IBIDEN 2 Hall framework exterior

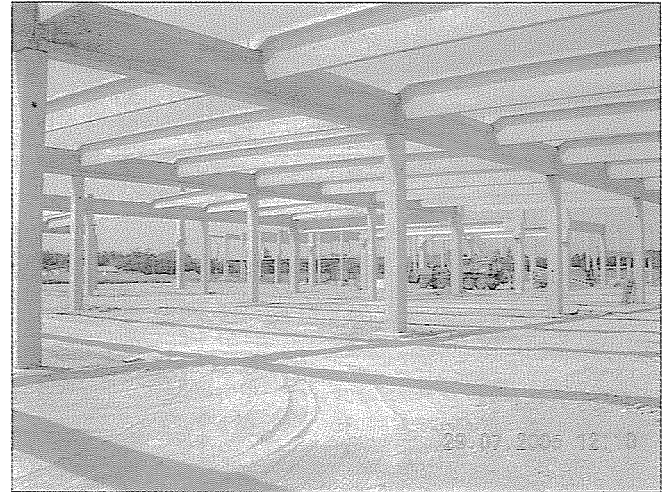


Fig. 3: IBIDEN 2 Hall framework general view



Fig. 4: IBIDEN 2 Intermediate floor's placement

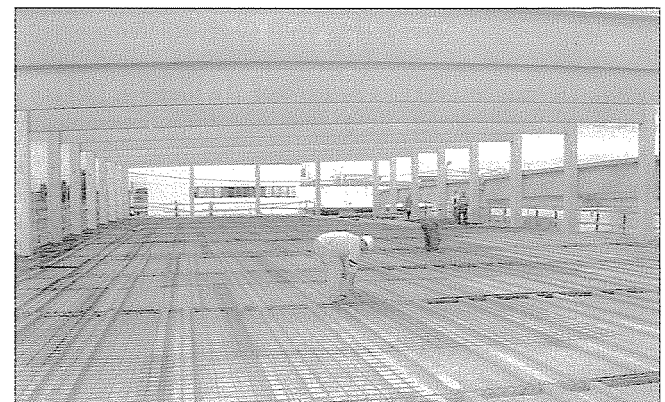


Fig. 5: IBIDEN 2 Reinforcement of Intermediate floor

## 2.1.3 Shopping centres, hypermarkets

The hypermarket construction boom started in 1994 with the appearance of the METRO chain-store company. At first, the single-storey hall frames of these department stores were mainly built at the outskirts of towns and cities (METRO, TESCO, CORA, AUCHAN, PRAKTIKER, OBI, BRICOSTORE etc.). The characteristic column grids are  $10 \times 20$  m,  $12 \times 20$  m,  $18 \times 24$  m and  $18 \times 26$  m with larger and larger spans as time progresses. Framework structures are similar: the connected columns fixed at the bottom and connected free at the top end, the prestressed concrete, simply supported beams, the purlins, and the reinforced concrete sandwich anti-frost aprons all made of prefabricated concrete elements. Extreme construction speed is of utmost importance. Roofs and fronts are clad with profiled steel coated sheet steel panels or - on the façades - with coffered cladding panels, glass wool, and corrugated steel sheet external covers or, as seen ever so often lately, with steel sandwich panels on the roofs and façades.

From 1998 onwards multi-storey shopping centres such as EUROPARK, DUNA PLAZA, MAMMUT, ÁRKÁD, ASIA CENTER and the like appear one after the other. These, too, are characterised by construction technologies that facilitate rapid completion by means of using as much prefabricated structural elements as possible. These major shopping centres are, however, a lot more sophisticated architecturally than the single-storey "tin can" hypermarkets of the outskirts. However,



**Fig. 6:** IBIDEN 2 Construction of the hall framework with intermediate floor

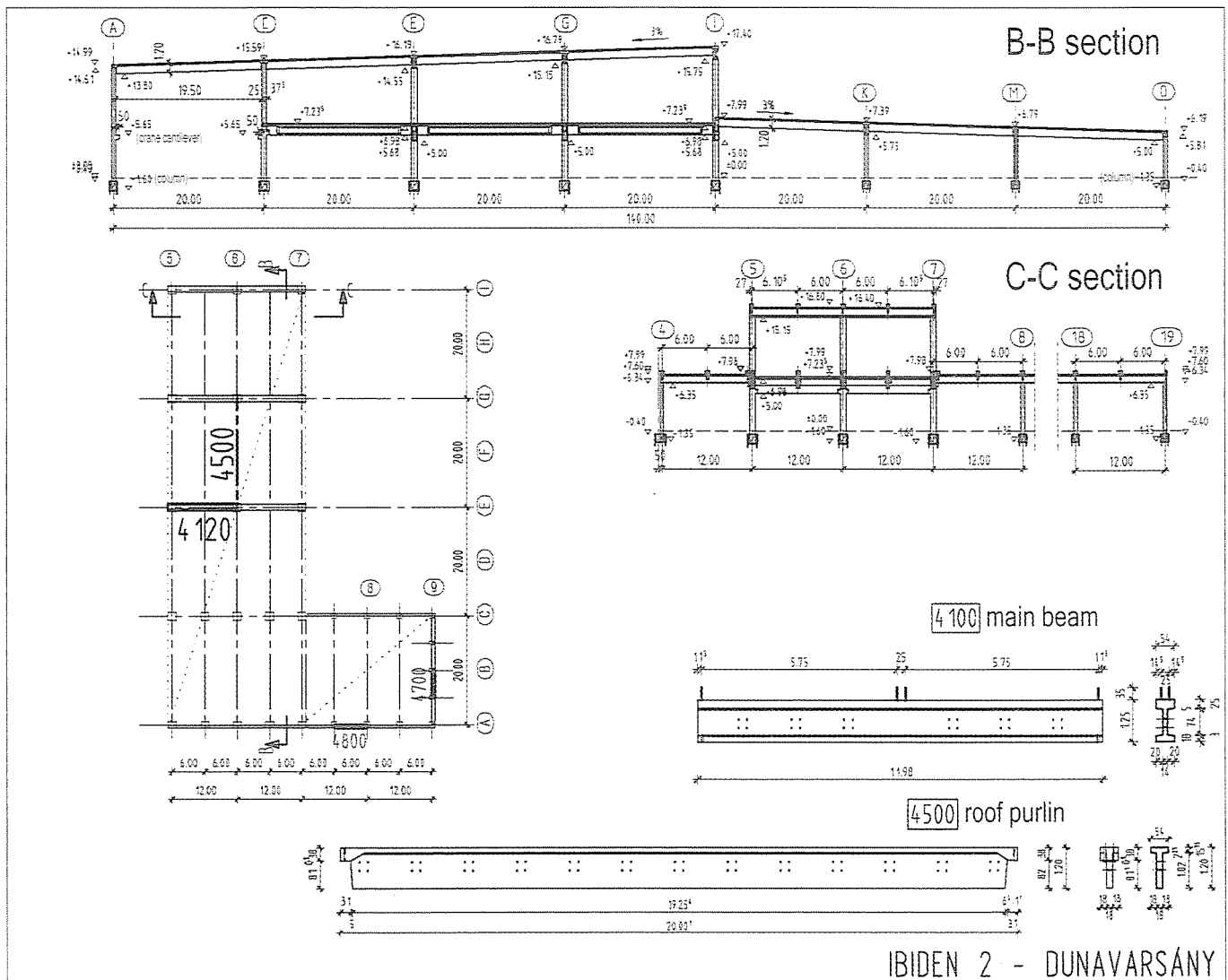
such architectural sophistication means that it is sometimes hard to find suitable prefabricated elements. Monolithic and prefabricated elements are often mixed.

The basement of these shopping centres normally comprises a parking facility, frequently with a denser column grid than in the commercial spaces upstairs. To name just a few:

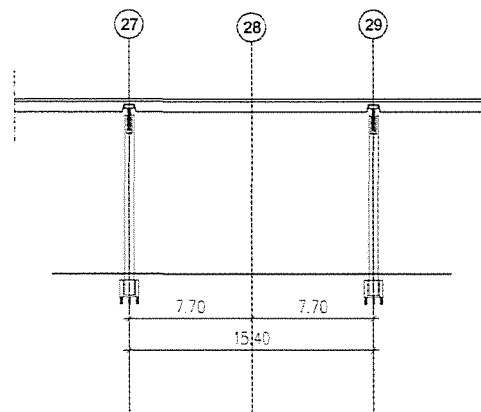
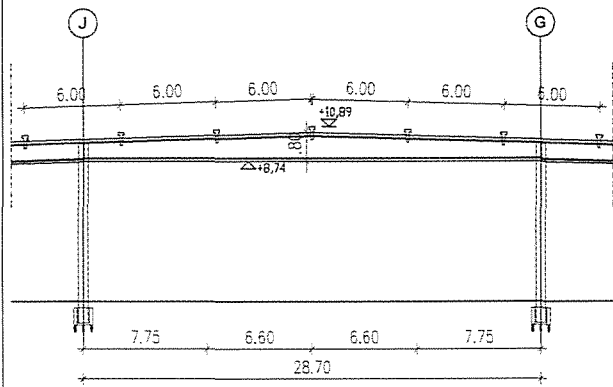
- Europark 8.00×10.50 m
- Lurdy Ház 8.00×10.50 m
- Árkád 10.00×16.00 m
- Asia Center 8.00×16.00 m
- IKEA 15.00×15.00 m

Fig. 1 shows department store floors

**Fig. 7:** IBIDEN 2 Sections and member drawings



Configuration with long main beam



Configuration with short main beam

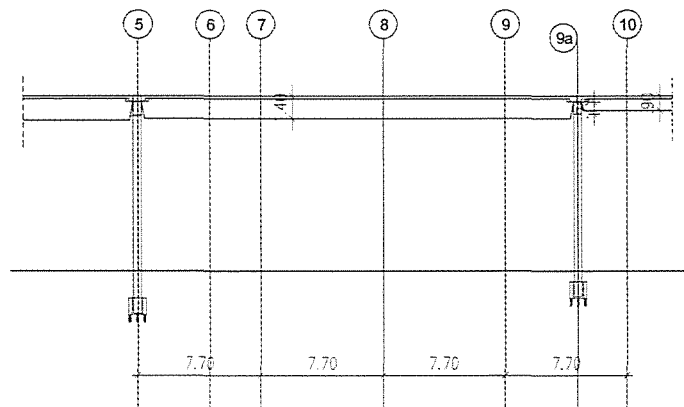
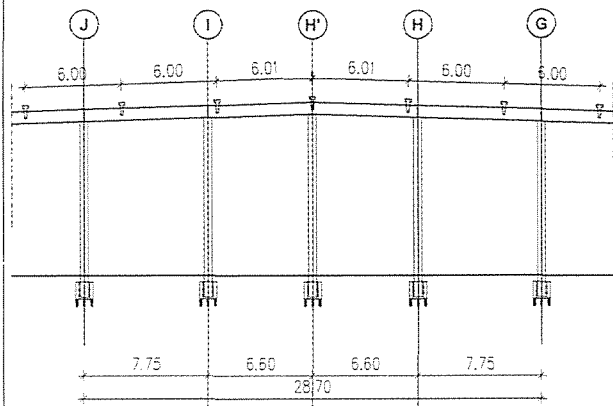


Fig. 8: LIDL Structural configurations

Formwork of main beam No. 4100

A-A section  
(M=1:25)

B-B section  
(M=1:25)

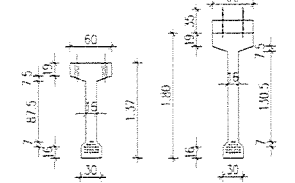
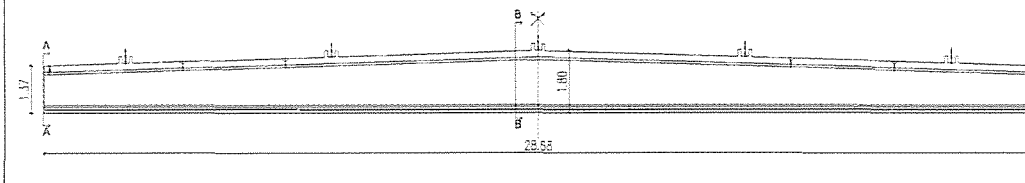


Fig. 9: LIDL Main beam configuration

Formwork of main beam No. 4070

A-A section

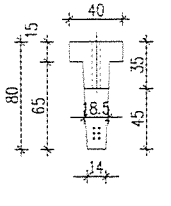
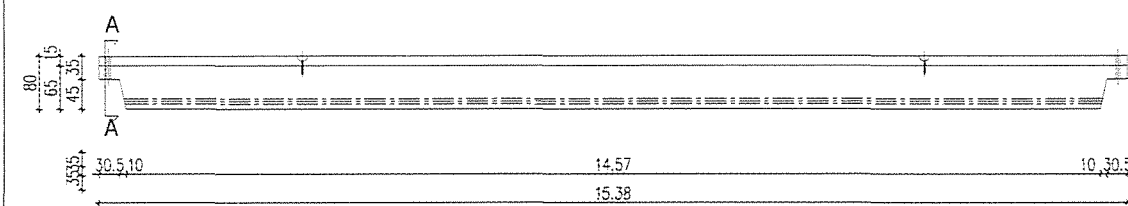


Fig. 10: LIDL Roof purlin configuration

## 2.2 Two storey buildings

### 2.2.1 IBIDEN Manufacturing Hall, Dunavarsány

The largest manufacturing facility projects of 2004-2005 were the two halls with a prefabricated concrete structure and a floor area of 26,000 sq. m. and 30,000 sq. m., built in 2004 and 2005, respectively (Fig. 2).

For further details of the IBIDEN project please visit [www.ibiden.co.jp/eng](http://www.ibiden.co.jp/eng).

The roofs of the halls with a characteristic column grid of 12.00×20.00 m are prestressed pre-tensioned, simply supported I-beams with a span of 12.00 m on which roof purlins rest at 6.00 m centres as prestressed pre-tensioned concrete T-beams with a constant depth (Fig. 3).

One of the most significant technological feats is the intermediate floor of the two-storey part also with a column grid of 12.00×20.00 m. which comprises prefabricated, prestressed concrete top ribbed floor elements together with the monolithic concrete topping resting on dragon beams placed at 6.00 m centres. This monolithic reinforced concrete slab also forms the upper compression flange of the prefabricated beams (Figs. 4

and 5). The first hall was inaugurated and commissioned during the summer of 2005. The second hall will be commissioned in 2006 and the preparations of the third hall with a floor area of 17,000 sq. m. are in progress.

Fig. 6 shows the construction and Fig. 7 the plans.

## 2.2.2 LIDL Logistics Centre, Hejőkürt

The Hungarian subsidiary of LIDL erected a new logistics centre with a floor area of more than 40,000 sq. m. at the Hejőkürt exit of the new leg of the M3 motorway. The new project helps reduce unemployment rates in the region and is a great gratification for the local government of Hejőkürt.

The main contract was awarded to GROPIUS Co. which, as one of the major main contractors of the market, had already completed a LIDL logistics centre in Székesfehérvár. Foundation works and the construction of the prefabricated structure were completed by STRONG & MIBET Construction elements Ltd., a subcontractor of GROPIUS Co.

A problem emerged during the design process of the prefabricated concrete structure. The German client intended to implement a technology in Hejőkürt that had originally been designed for a specific column grid. It turned out that the prefabricated structure of a similar hall that had already been built in Germany could not be constructed economically in Hungary and had to be redesigned while leaving the column system unchanged.

The framework is divided into the hall itself and the office building. The overall dimensions of the warehousing hall were extended during the construction phase and reached 335×122 m. The warehouse is subdivided into two sections, a refrigerated warehouse with short main beams and a warehouse with five bays and long main girders (Fig. 8). The two-story office building has a floor area of 12×16 m. One of the specialities of the warehouse section with a column grid of 7.7 m at the front façade and 15.4 m in the inside of the building is the main girder of the central bay with a span of 28.70 m – the design value of the moment of the two-slope (1.80 m deep) main girder was 6,400 kNm.

One of the characteristics of construction industry and of prefabrication industry in particular is that more and more buildings have a main girder span of 30–32 or even 36 m.

A few years ago prefabrication was dominated by main girders with a span of 24 m and the manufacturing of the few elements with a span of 30 m or more was considered a rare and memorable feat. Today, as a result of the introduction of European standards and the development of the concrete construction culture, of cement types, and chemicals, trailers delivering members with a length of 30 m or more and bearing the logo of one of the prefabrication factories to indicate the origin of the product are familiar sights on the roads.

In conformity with clients' requirements, designers strive for creating larger and larger free spaces. Current grids of 15×29 m are considered simple roof structures compared to those with a grid of 18×30 m, 20×24 m or 24×30 m (Fig. 9).

The total number of 360 main girders had to be manufactured within two months. The only way to achieve this was by means of a highly productive TT panel cross-section (Fig. 10).

Construction companies trying to figure out the most economical cross-section have been facing a serious dilemma because of the significant fluctuation of the price of reinforcing steel during the past two years.

In the case of LIDL steel economy was optimal because

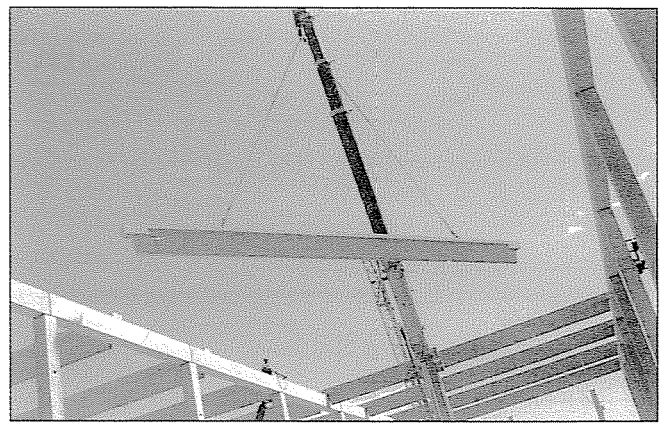


Fig. 11: LIDL Lifting and installing roof beam 1.

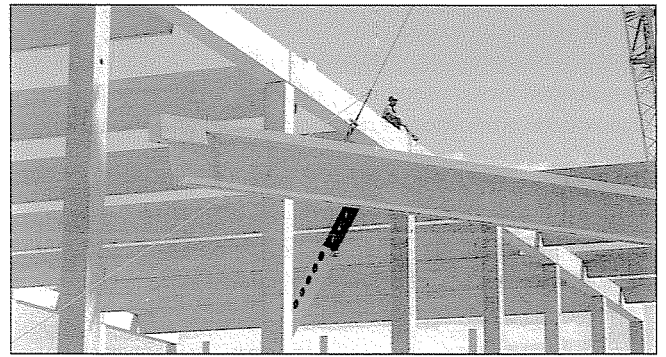


Fig. 12: LIDL Lifting and installing roof beam 2.

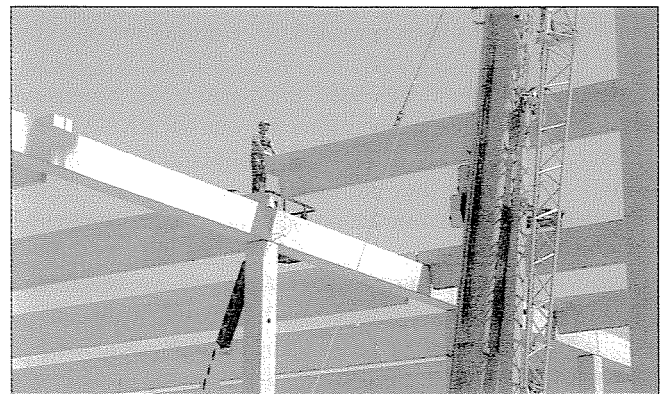


Fig. 13: LIDL Lifting and installing roof beam 3.

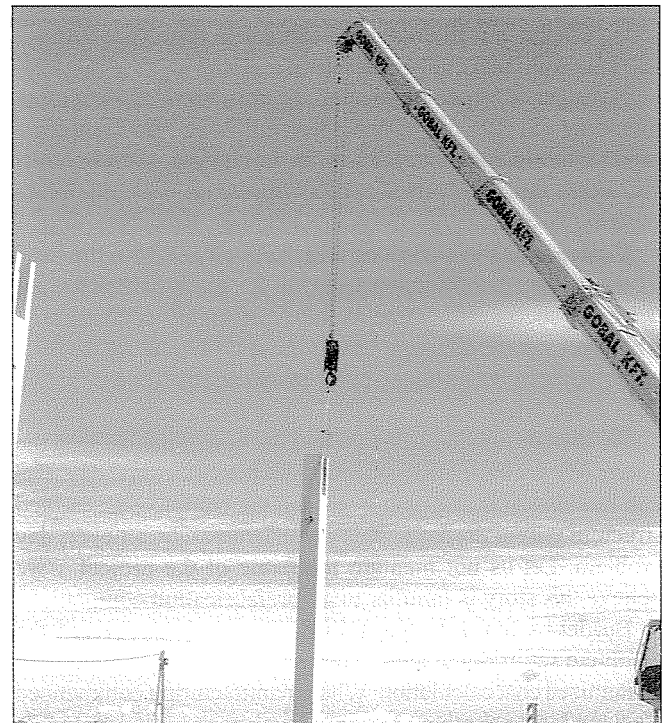


Fig. 14: LIDL Lifting and erecting column.

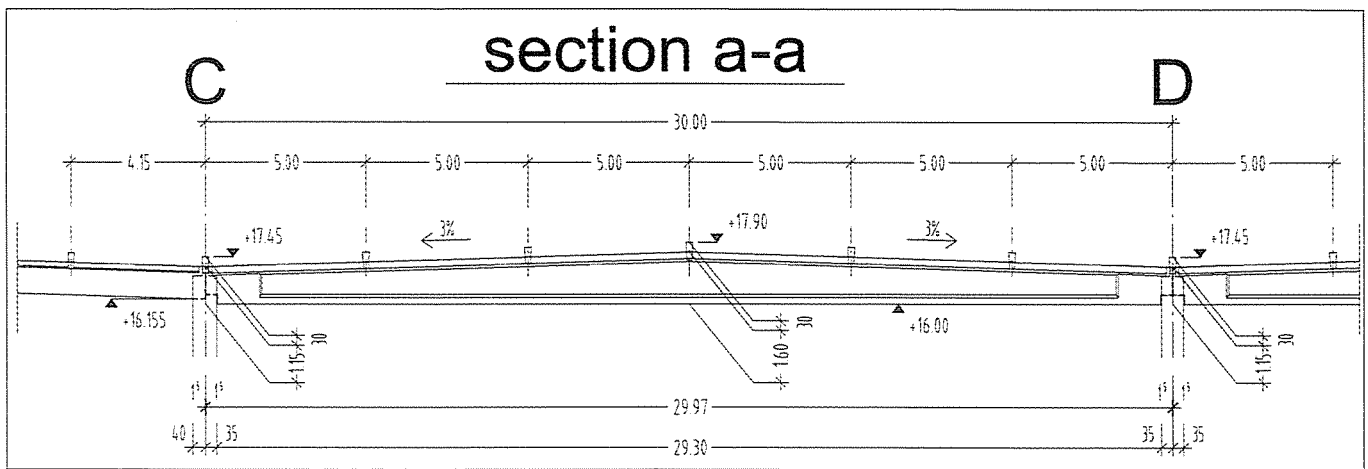


Fig. 15: AUDI Section detail

columns had a cross-section of 600×600 mm and a length of 11 m and the proportion of reinforcing steel was still not more than 120~130 kg/cu. m.

We believe we have a reason to call this building a classic example of prefabrication: many identical elements, no need to re-erect formworks very often, limited number of penetrations, low reinforcement steel ratio (Fig. 11 to 14).

### 2.2.3 Another extension of AUDI

The Audi plant has been extended twice during the past two years. The first project led by German construction company WALTER-BAU had hardly been completed when the second one was started. The main contractor was MERKBAU, the structure was completed by a sub-contractor, STRONG & MIBET Ltd. (or, as they are called from 2<sup>nd</sup> January 2006, STRONG-ROCLA Construction elements and environmental techniques Ltd.)

The G-40 manufacturing hall was hugely oversized: the columns with a cross-section of 1.20×1.00 and 1.00×0.80 m weighed almost 40 tons (Fig. 15). The German client did not economize on concrete, even though the tendering procedure it was proved through the revision of the structural calculations of some of the bidders that the structure would meet Hungarian requirements and international standards even if the cross-sections were reduced significantly.

However, it turned out that all the structural, architectural, plumbing and even the working drawings have been completed prior to the bidding process and after we had signed the contract we were, much to our surprise, furnished with complete working designs.

Compare this to situations where all we get from the head of the project coordination team of the main contractor are three A4 sheets with some sketches of highly sophisticated structures and the message "this is the sort of building we have in mind, please let us have a competitive price offer within two days at the latest".

We then design the structure and the news hits: we won the tender. We are expected to meet the architect the next day. The cup foundation is due next week and the complete assembled structure within 30 days. This is, unfortunately, an everyday problem. Let us not mention the name of the project – we believe this story is familiar to all prefabrication companies.

But let us return to the Audi-project. So we received the complete set of documents. The contract, of course, required an itemized cost calculation. When manufacturing commenced we were facing another problem: the plans specified materials

Fig. 16: AUDI The column

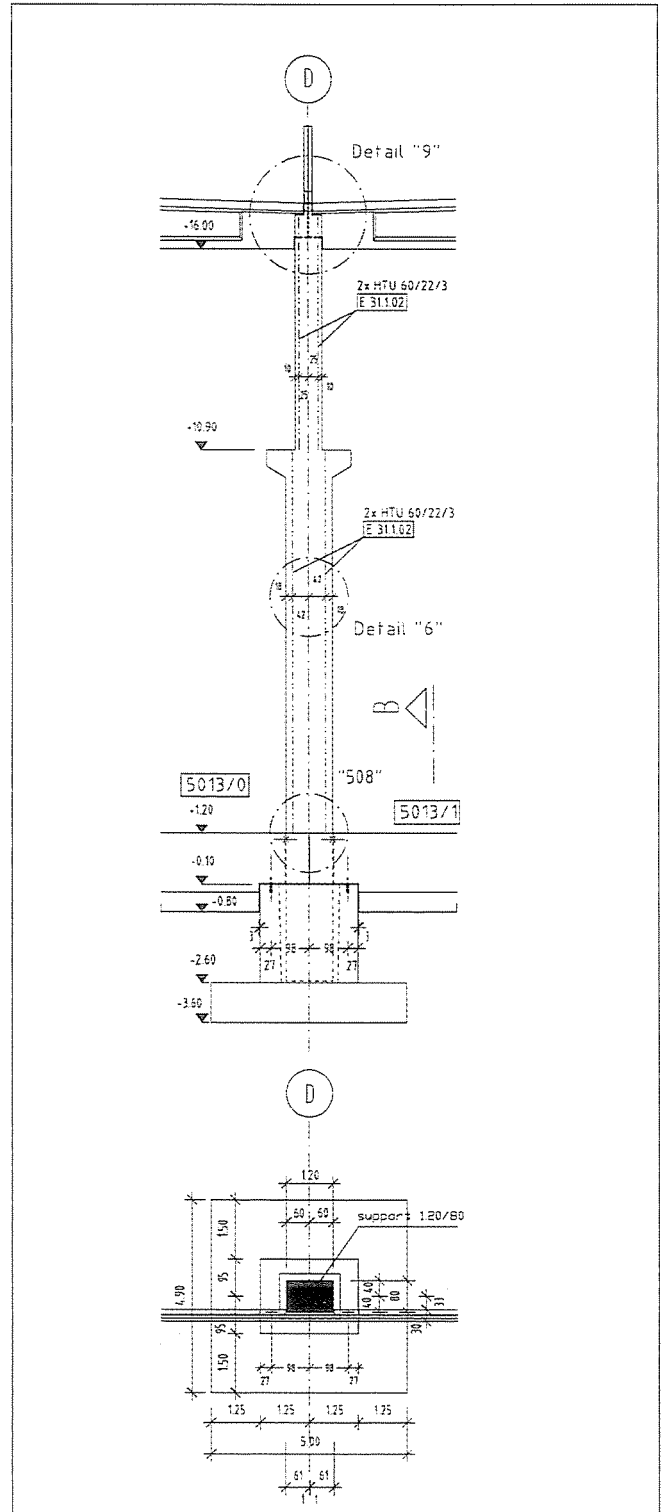




Fig. 17: AUDI Hall assembly 1.



Fig. 18: AUDI Hall assembly 2.

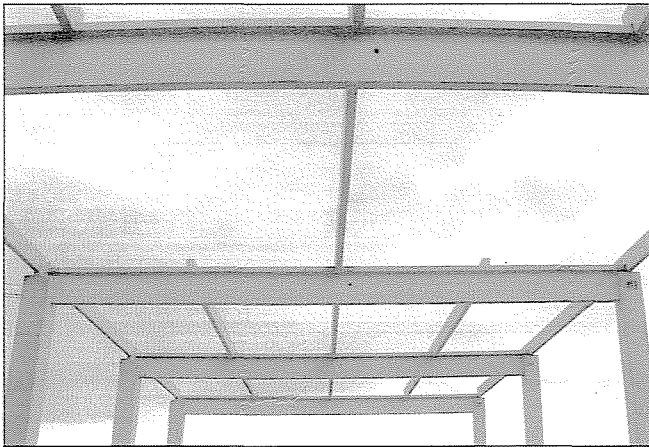


Fig. 19: AUDI Hall assembly 3.



Fig. 20: AUDI Hall assembly 4.

that were not available in Hungary. Quite a few items were imported from Germany and Austria, including the reinforcing steel splices, protruding bolts, lightning protection boxes etc.

Regarding auxiliary materials, apart from quality specification, price was another issue to be dealt with. The German client declared that “good quality has its price” and they refused to accept cheap aftermarket products, only original items (Fig. 16).

This year we erected building part G-12, G-20 which is an extension only. Nevertheless, the issues described above ceased to exist, things suddenly returned to normal.

This was a lump sum contract with ordinary Hungarian technology – which is by no means poor – and compared to the earlier project we can declare that it was not AUDI that had extreme demands: the German main contractor was somewhat too exacting.

Still, one thing cannot be denied. Together with foreign investors foreign main contractors appeared, too. And, however hard it may be to admit, they brought with them a different set of requirements, a demand based on the principle of value for money – and the readiness to pay for such quality.

A structure does not need to cost HUF 300 million for the client to demand the quality it is accustomed to in Western Europe. This rather depends on the client itself (Fig. 17 to 20).

## 2.2.4 LIEGL & DACHSER Logistics Centre, Pilisvörösvár

LIEGL & DACHSER is a forwarding and warehousing company based in Germany. Their first warehousing facility in Pilisvörösvár was built in 1999 and was extended in 2003 and 2005.

Preparation of bidding documents was commissioned by DACHSER GmbH, in Germany. The task was the construction of a hall structure with a floor area of  $92 \times 76.5 \text{ m} = 7038 \text{ sq. m.}$  and a useful height of 13.5 m. The characteristic grid of the framework structures seen in the sectional drawing is spaced at 7.2 m. The individual warehousing functions inside the building had to be separated by approximately 4000 sq. m. partitioning bulkheads made of prefabricated elements with a height of 15.55 m. The greatest challenge of the design and construction phase was to ensure a secure counter-bracing system throughout the erection works and to choose the correct sequence of assembly of the elements. Another challenge we faced was the design and manufacturing of the 34.5 m long roof girder, which resulted from the requirement for perforations for sanitary installations. Such requirement was unknown in previous practice.

Prior to the commencement of construction several important issues had to be addressed to minimise the risk of a disaster. The most important ones were as follows:

Do the geometric features of the manufacturing mould considered for the 34.5 m long beam meet the geometric and static requirements?

The client designed a roof slope smaller than the 3 per cent normally used in Hungary. We feared that manufacturing costs of the 12 beams would have increased significantly as a result of the modification of the manufacturing mould and of the excess concrete required. The manufacturer of the supporting structure proposed beams with a 3 per cent slope as is usual in Hungary in the case of high wave corrugated steel roofing because this would have conformed to the manufacturing facilities of Hungarian prefabrication plants. However, after the contract

had been signed the client decided to insist on its original plans. The issue was solved when the Hungarian Concrete Association contacted the German Concrete Association and a joint statement was issued proposing the use of a beam with a 3 per cent slope in accordance with Hungarian practice.

Another problem apart from the beam geometry was that the client ordered two 1.3 m long and one 1.0 m long openings beyond the various other perforations seen in the sectional drawing in Fig. 10. The loading area of the beam is 7.2 m. Earlier, beams of similar span were made with a column grid of 6.0 m and no beam had ever been manufactured with perforations and openings of such dimensions before. Considering the design calculations of the openings we found some examples in foreign literature. In Germany, the problems related to concrete workability are solved by means of self-compacting concrete. Beams with improperly worked in concrete must be discarded as refuse, so there is a significant financial risk involved. At 2005 prices, remanufacturing one single beam would have cost the contractor HUF 1.15 million. For reasons of concrete placing the manufacturer employed a special concrete composition and a sufficient number of mould vibrators. In the end, there was no need to remanufacture concrete any element for reasons of surface deficiencies.

In working out the calculation model of the structure prevailing consideration were the conditions during the erection phase, allowing for the bulkheads. Accordingly, the assembly sequence and bracing system had to be designed with a view to factors of economy. The final results are illustrated in Figs. 21, 22, and 23.

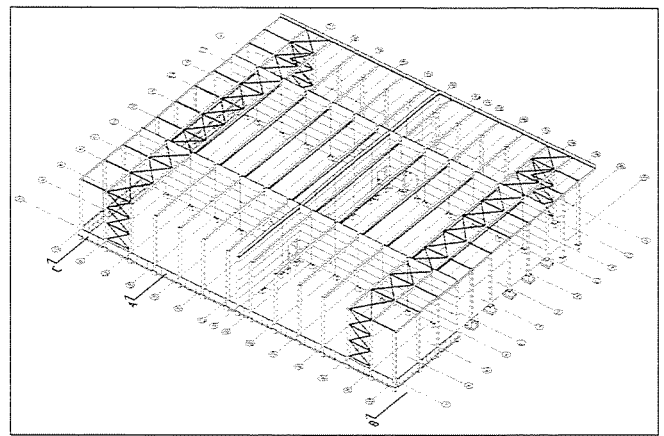


Fig. 21: LIEGL & DACHSER Space frame



Fig. 22: LIEGL & DACHSER Structural assembly

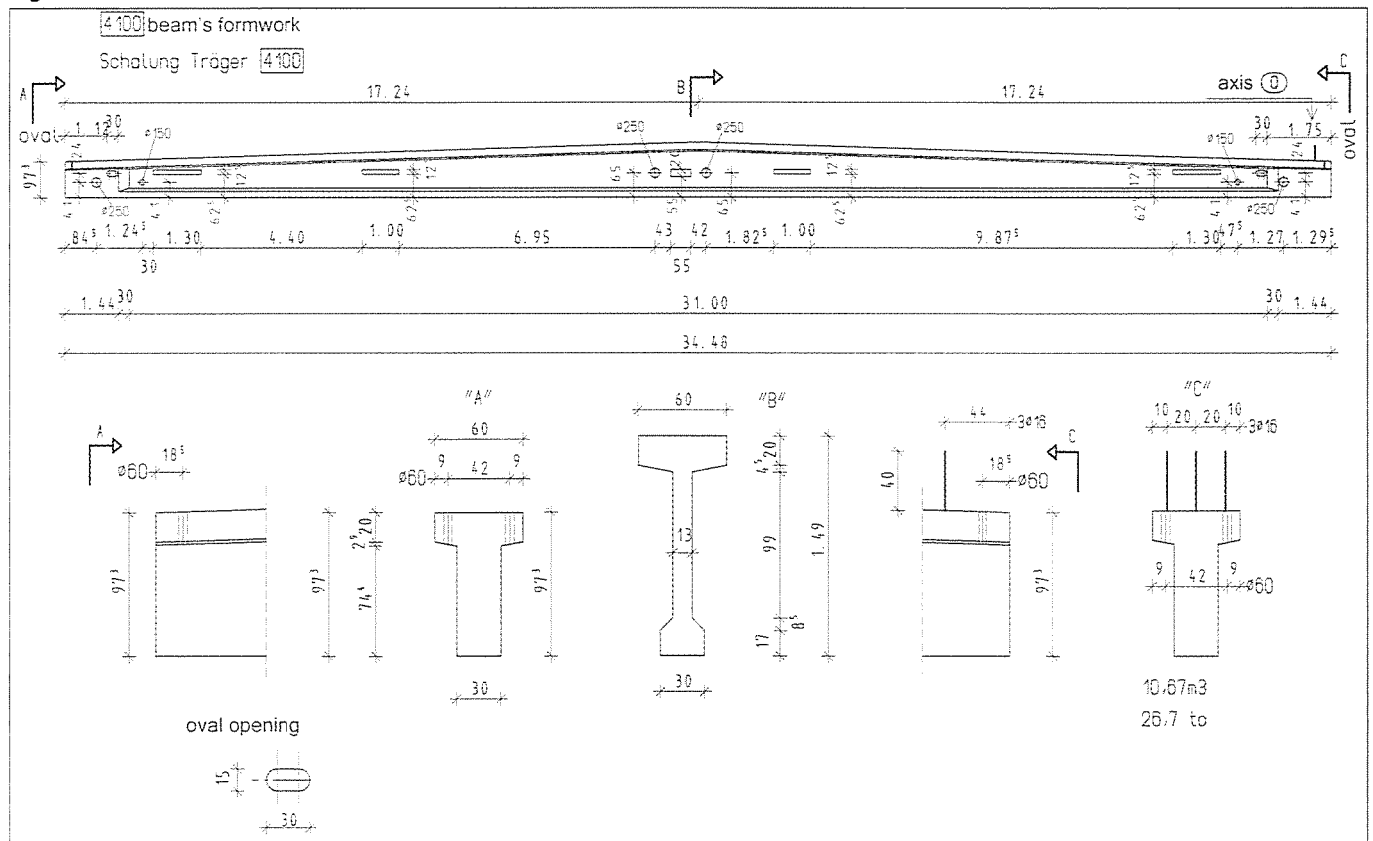
### 2.2.5 EGLO Warehouse Hall, Pásztó

EGLO has been planning to extend its warehousing and manufacturing capacity since 2001. During the design phase both concrete and steel framework plans were made. The warehouse to be constructed connects to an existing structure

by means of a three-story corridor link. Construction started in September 2005 with the technical taking-over in March 2006.

The height of the warehouse hall exceeded that of all similar structures constructed previously. The client required a two-bay

Fig. 23: LIEGL & DACHSER Beam formwork





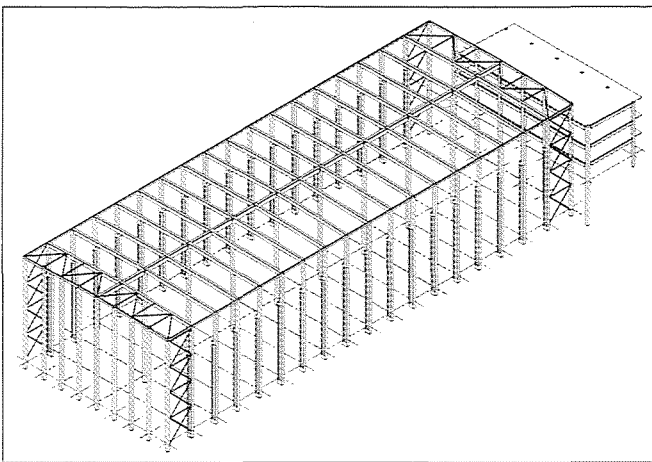


Fig. 24: EGLO Space frame



Fig. 25: EGLO Structural assembly

reinforced concrete structure with a clear height of 23.65 m (!) and a length of 110 m. The supporting structure of the hall has a framework comprising columns retained at the bottom and free at the top end.

The design challenge in this case was to choose a safe structure that can be built economically. On the manufacturing side, the main problem faced was transporting and erecting the 26 m long columns weighing 30 tons. The maximum allowable vertical declination of the top end of the erected columns was 20 mm. Otherwise, the placing of roof beams would have required the cutting of concrete at a height of about 24 m. The erection team performed the job with due care and met all erection tolerances.

When defining column cross-sections one of the requirements was to keep displacement of the structure within allowable limits (1/200) and, with a view to transport and craning costs, not to exceed the maximum component mass of 30 tons. The plan was that intermediate columns shall have a necessary and sufficient square cross-section. After having examined the related manufacturing, transport, erection and final state factors a cross-section of 600×600 mm was found to be suitable. The framework structure was braced by the columns on the long front. Compared to horizontal loads the vertical loads of the building were not significant. Several possible cross-sections had to be examined, including I and square cross sections hollowed out and filled with heat-insulation material. Design calculations revealed that 1.20×0.60 m external dimensions and an I cross-section should be used. In order to further reduce the own weight of the columns the upper 7.5 m section had to be reduced to 600×600 mm. In the transportation stage this part was designed as a cantilever in the delivery state.

During the preparation of the production plans the requests

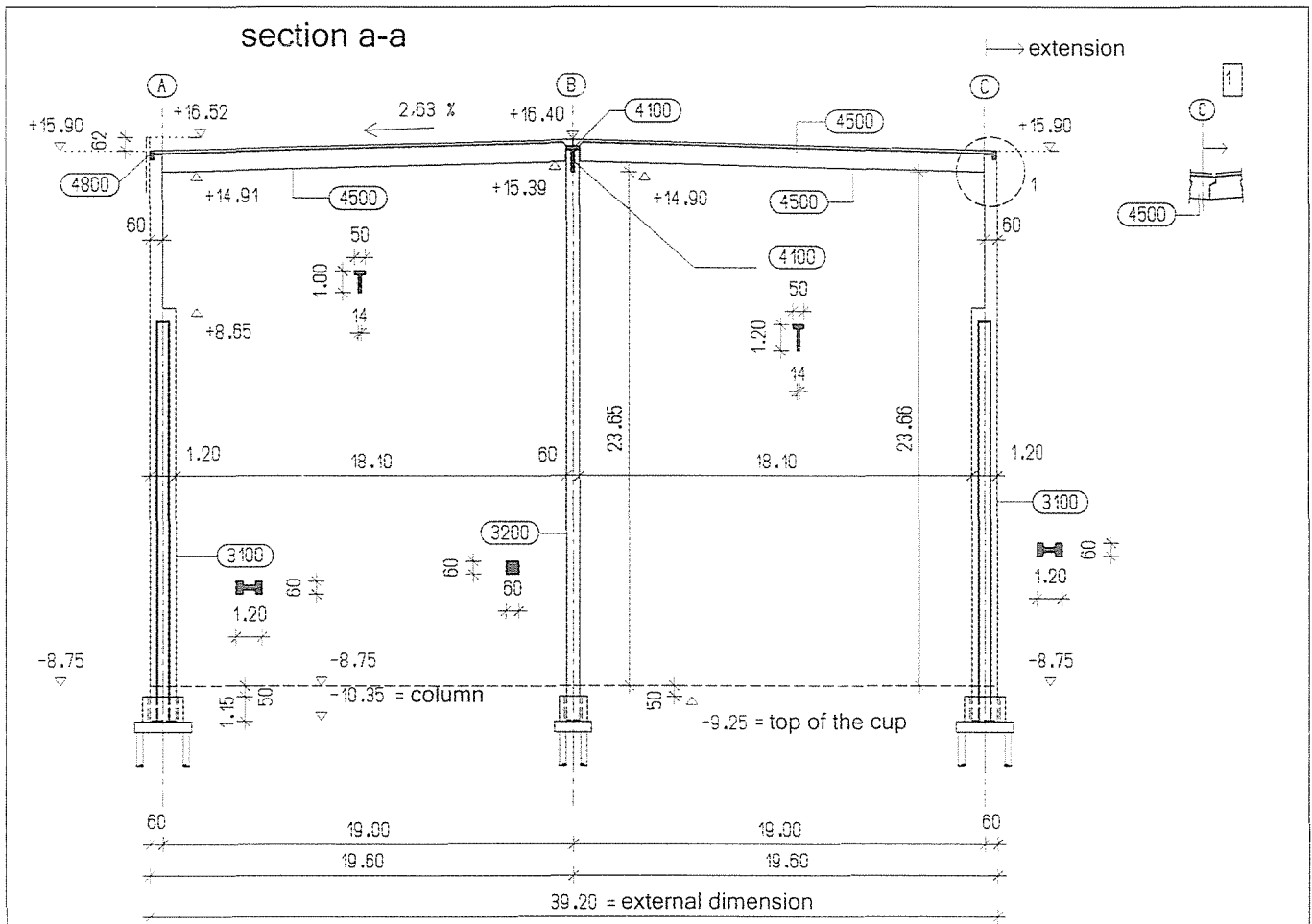


Fig. 26: EGLO Hall section



**Fig. 27:** EGLO Assembly of corridor link

of the structural contractors were also honoured: the column centralizer was placed in the centroidal axis of the column and perforations were made at specific heights to accommodate incidental stabilisers. Columns were adjusted using the traditional method of wooden wedges and concrete filling.

Details of the building are shown in *Figs. 24 to 28*.

### 3. SUMMARY

The structures of these buildings described above involved non-conventional technical methods but the lessons they taught are basically the same. In order to be able to solve technical issues literature offering answers and suitable design software are needed. For a solution of the beam openings foreign literature was consulted. Calculation of the framework structure dimensions was assisted by structural design software allowing for the behaviour of concrete (reinforced, cracked cross-section) and calculating the effects of second-order forces to be taken into consideration.



**Fig. 28:** EGLO Erection

The design process followed the provisions of EUROCODE 2. EC offered a *lingua franca* between foreign (in this case German) clients and Hungarian contractors and often made it possible to reconcile differences of opinion.

Reinforced concrete structures were calculated using structural design software (FETT, STUR) of ABACUS GmbH.

### 4. REFERENCES

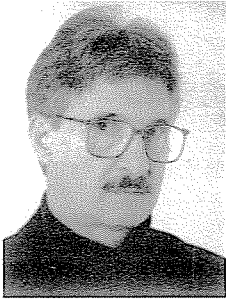
- Eligehausen, R. (1992) "Das Bewehren von Stahlbetonbauteilen", DAfStb Heft 399, Beuth Verlag  
 Reineck, K.-H. (2005) "Modellierung der D-Bereiche von Fertigteilen", Beton-Kalender 2005/2, Ernst & Sohn

**József Képes** (1967) Architect, graduated from the Technical College of University of Debrecen. From 1994 he participated in various contracting works, after 1998 he was commercial manager at BVM Mibet Ltd. prefabrication firm and from 1999 head of commercial division. In 2001 he was appointed as enterprise director, then in 2003 enterprise and commercial director.

**László Novák** (1962) structural engineer, M. Sc.: Civil Engineering Faculty of the Technical University of Budapest. 1984 – various positions related to construction and building maintenance; 1994-1996 – college lecturer at the Technical Department of Zrínyi Miklós National Defence University; 1996-98 – project engineer, VSTR-H Bp. 31 Structural Concrete Contracting Ltd.; 1998-2003 – structural designer, PLAN31 Ltd.; 2003 – managing director, STAT31 Engineering Bureau.; chief engineer, VSTR-H Bp., 31. A.É.V. Scope of activities: design of reinforced concrete structures

**László Polgár** (1943) civil engineer, M. Sc.: Civil Engineering Faculty of the Technical University of Budapest. from 1966 – site manager, product designer, chief process engineer of State Construction Enterprise No. 31; 1992 – managing director of Plan31 Engineering Ltd. and technical managing director of ASA Construction Industry Ltd. Chairman of the Association of Hungarian Concrete Element Manufacturers. Member of the Hungarian Group of *fib*. Palotás-prize holder.

# CONCRETE STRUCTURE ON ELASTIC PADS - THE BARTÓK BÉLA NATIONAL CONCERT HALL IN THE PALACE OF ARTS, BUDAPEST



Ferenc Gonda

*The irregular five-sided site on the bank of the Danube river; near to the Lágymányos Bridge and the South Railway Bridge posed many design and construction challenges. The greatest of them was the solution of noise and vibration isolation of the Theatre and the Concert Hall. This paper describes the design and construction techniques utilized to construct the Concert Hall.*

## 1. INTRODUCTION

The striking new presence in Budapest along the Danube river is the recently constructed Palace of Arts. The opening ceremony was held on 14<sup>th</sup> March, 2005. The 70.000 m<sup>2</sup> gross floor area building is located on a pentagonal building site. It houses three significant cultural institutions - the Ludwig Museum for contemporary art, the 500 seat Festival Theatre, and the 1.700 seat Bartók Béla National Concert Hall. (Fig. 1.) The complex is served by a three-level underground parking lot for 621 cars. This project represents the largest single investment in a cultural institution during the past hundred years in Hungary.

## 2. THE PALACE OF ARTS

The Palace is 21-37 m high, 168 m long and maximum 81 m wide. It completely covers the 10.000 m<sup>2</sup> area of the site (Fig. 2.). The structure of the building – columns, walls, floors - is primarily C30/37 cast-in-place reinforced concrete. Floors are typically flat slabs, 25-30 cm in depth. Part of the museum floors were precast; downstand beam-and-slab construction. The roof of the Festival Theatre and the Concert Hall (Fig. 3.) as well as the upper lobby floor (Fig. 4.) are steel structures.

To minimize the transfer of internal noise and vibration both the underground levels and the superstructure are divided by isolation joints. The three parts of the building are separated

**Fig. 1:** The Palace of Arts and the Danube River (Photo by A. Polgar, Arcadom zRt.)



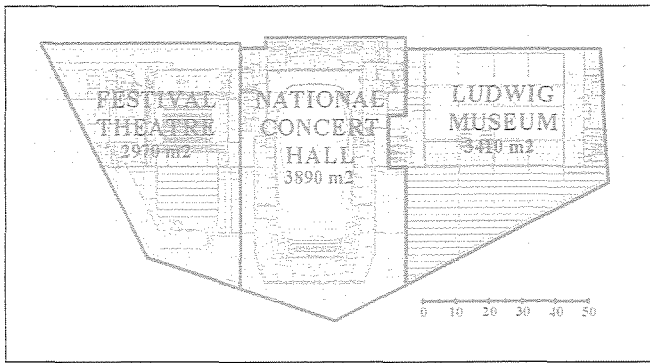


**Fig. 2:** Plan of the Palace, level +20,50 m

by 5 cm wide airspaces in two transversal lines. Vertical elements (walls and columns) are doubled at the boundaries. On Fig. 5 you can see the different phases of construction of the separated units: mat foundation of the Museum (left), the excavation of the Concert Hall (middle) and the blinding of the Festival Theatre (right).

### 3. THE CONCERT HALL

The 1.500 m<sup>2</sup> shoebox shape auditorium of the National Concert Hall is located in the centre of the building. (Fig. 2) The performance chamber is 55 m long, 29-35 m wide and 23-24 m high. The volume - including the reverberation chambers - exceeds 40.000 m<sup>3</sup>. The hall has three cantilevered seating tiers (side and rear terraces, Fig. 7) over the 825 seat main level (orchestra, rear parterre and boxes).

The minimum 30 cm deep bottom slab and the 30 cm thick walls of the “box” are in-situ concrete. Fifteen 4,5 meter deep steel trusses span the roof (Fig 3). The bottom chord carries 290 pieces of 15 cm deep precast panels (Fig. 8) forming the acoustic ceiling of the auditorium. The narrow joints of the elements were poured with self compacting concrete. The top chord supports a 20 cm deep cast-in-place concrete roof slab. The attic space created within the truss depth accommodates a great deal of equipment. The calculated self-weight of the auditorium box is 16.595 tons.

The shape of the auditorium, including the length-width-height ratio were closely determined by acoustic criteria. (Acoustic consultant: Artec Consultants Inc., New York.) Other features aimed to achieve the best acoustic performance include adjustable reverberation chambers and an acoustic canopy (Fig 9). The 600 square meter, 50 ton acoustic canopy is rigged to raise and lower in three separate parts over the concert platform. The 6.000 cubic meter volume of the reverberation

**Fig. 3:** 35 m span truss during assembly

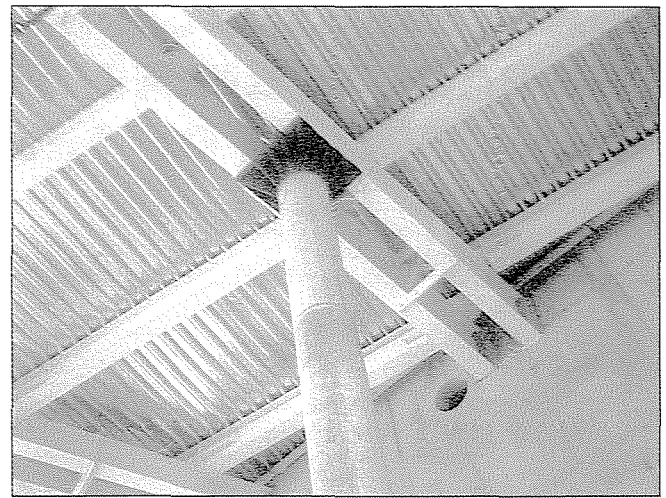
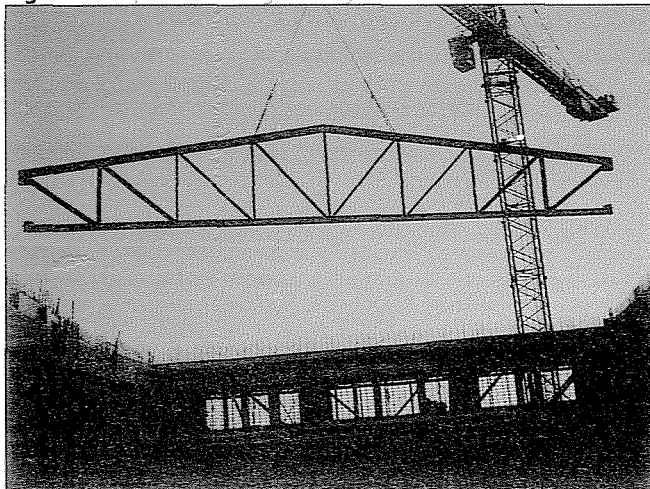


**Fig. 4:** HEM beams of the upper lobby floor



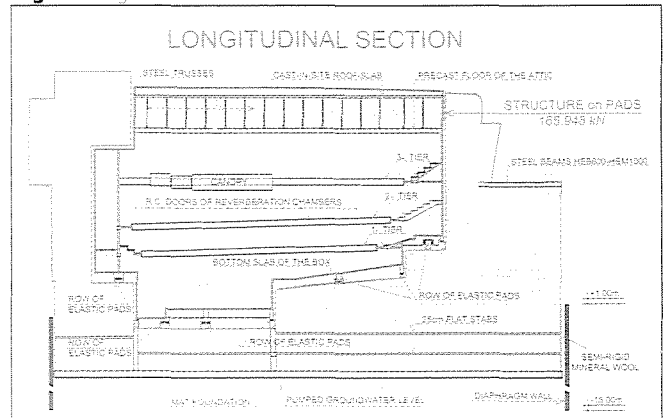
**Fig. 5:** Mat foundation divided by isolation joints

chambers can be joined to be part of the auditorium by the operation of 10 cm thick concrete doors. Between the 2,5 m wide and 3,0-7,5 m high doors we had only 50 cm space for columns. (Fig. 10)

### 3.1 System of noise and vibration isolation

All spaces within the Palace of Arts had to be protected from excessive noise or vibration. The nearby railway bridge was suspected as main source of both. Prior to designing the project, two vibration-test-piles (15,50 m deep = supposed depth of the diaphragm wall, and 10,50 m deep = supposed depth of the mat foundation) were studied. On this basis it was determined, that the entire building required complete vibration isolation.

**Fig. 6:** Longitudinal section of the Concert Hall structure



The fundamental approach to achieving this was the creation of a 10 cm isolation gap between the 65 cm thick, 18,0 m deep diaphragm wall and the 30 cm thick concrete perimeter wall of the building, further a 1,10 m deep mat foundation. The isolation gap between the diaphragm wall and the actual building structure was filled with semi-rigid, 120 kg/cubic meter density mineral wool. To prevent contact with groundwater the water is continually pumped (1-3 m<sup>3</sup>/day) to keep it's level below that of the mat foundation.

Both the concert hall and the theatre needed a second "defense line". (At this point the Hungarian acoustic consultants for the theatre had a slightly different philosophy than those in the U.S. for the concert hall. In this article we give details only for the latter.) In case of the concert hall the second line of defense is created by a 20 cm airspace (with a 5 cm loose mineral wool acoustic blanket) between the walls of the surrounding structures and the perimeter walls of the reinforced concrete auditorium box, along with vibration isolation bearings (elastic pads) between the structures. In this manner the performance chamber is completely isolated; it is protected from noise and vibration.

### 3.2 The elastic pads

The elastic pads – material and sizes - were designed by the vibration isolation consultant Wilson, Ihrig & Associates (California). They used loading data of the structural engineer Dékettő Statikus Iroda Kft., Ferenc Gonda. The material of the isolation bearings is bonded natural rubber, consisting of five 29 mm rubber layers and four 3 mm steel layers between 10 mm top and bottom steel plates. (Fig. 11, 12, 14) These types of bearings have no lateral stiffness, requiring the auditorium box to be supported by lateral bearings as well.

The vertical load pads have to carry the gravity load (165.948 kN) from the mass of the auditorium. The average

Fig. 7: Cantilevered tiers

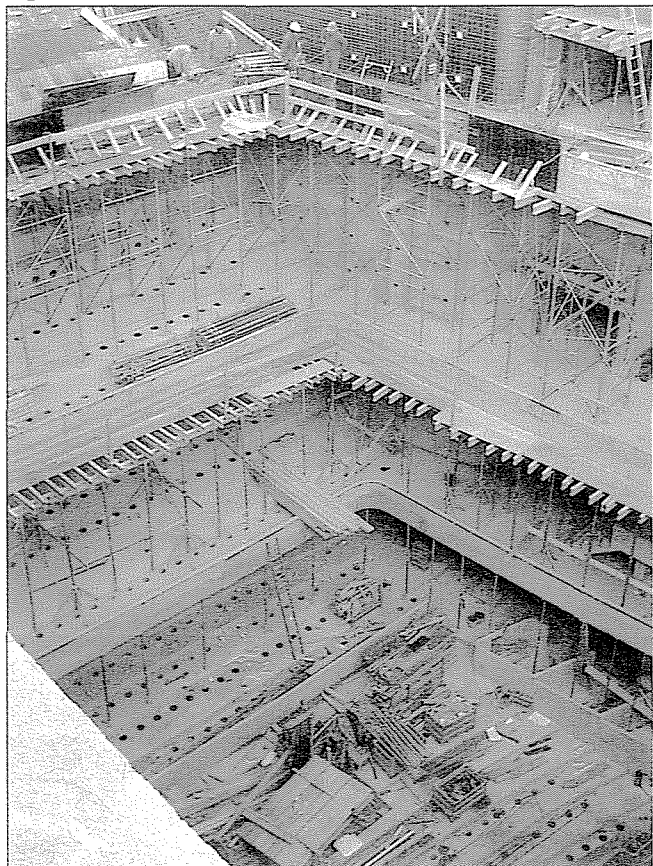


Fig. 8: Floor of the attic (precast)

load on a total of 247 vertical load bearings is 672 kN, the average deflection 8,26 mm. The very low - 0,33 kN/cm<sup>2</sup> -load stress is an important factor in achieving long life. According to the consultants the service life is not less than 100 years.

Number and size of the bearings: 316 each, 450 mm x 450 mm x 177 mm high, 19 each, 360 mm x 360 mm x 177 mm high.

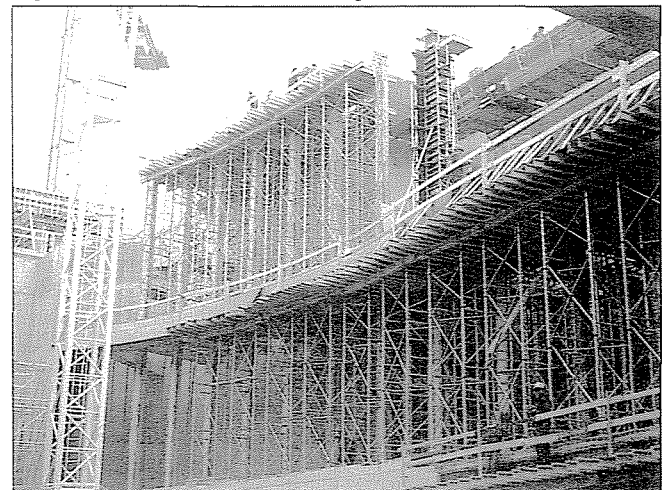
The vertical resonance frequency of the pads is 6,0Hz. The nearest structure, the auditorium floor, has double the resonance frequency, 13 Hz. To attain this in some areas, we had to increase the 30 cm depth of the slab. This was achieved in the simplest possible way, by pouring the steps needed to create a sloped orchestra level floor as structural concrete.

To minimize the load on the isolation pads, we aimed to omit all unnecessary mass from the inner auditorium box. As a result, the underside of this element, where vertical load transfer happens, comprises of a number of different levels. The concert platform area has a two-level orchestra-pit (-2 m). The main seating area consists of an orchestra level and a rear parterre (+5 m, +11,m). The reverberation chambers cease below the height of the second tier (+13 m). As a result, the gravity-load bearings are placed at four different elevations mostly under the perimeter walls (Fig. 6).

Another challenge was presented by the 30 cm thick walls requiring a 50 cm headbeam required to transfer load on to the 450 mm wide bearings. The horizontal forces resulting from the necessary eccentric load conditions were counteracted by the nearby floor-slabs.

The horizontal seismic load was calculated on the basis of 0,08 relative acceleration, the applicable design criteria for Budapest. This way the lateral load was 12% of the gravity load. To achieve isolation at the horizontal load transfer points, 2x22 pads were needed in pairs in both longitudinal and transversal directions. The total number of lateral-load-

Fig. 10: Reverberation chambers during construction



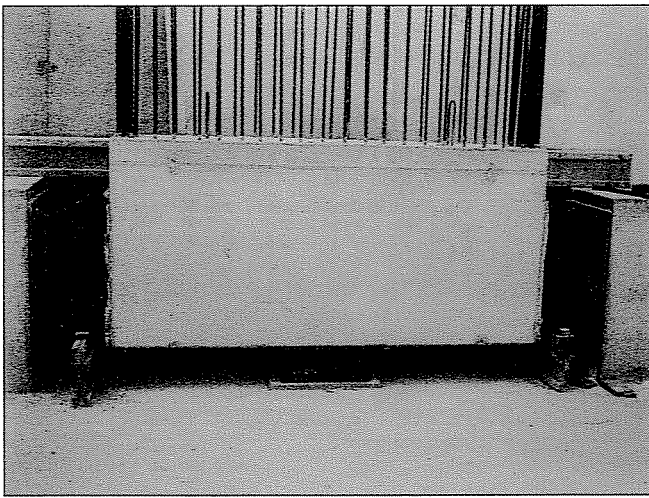


**Fig. 11:** Prefabricated downstand lug



**Fig. 12:** Lateral bearing, being precompressed

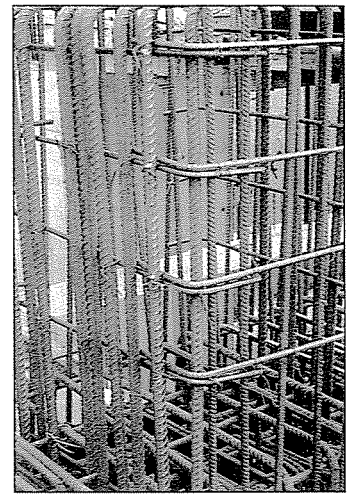


**Fig. 13:** Reinforcement of a cast-in-place upstand lug

resisting bearings was 88. The lateral bearings are placed under the perimeter walls, precompressed between upstand and downstand concrete lugs (Fig. 14). The horizontal resonance frequency is 2,7 Hz. The precompression load was 650 kN, deflection 7,6 mm. The pads remain in compression during an expected ground motion.

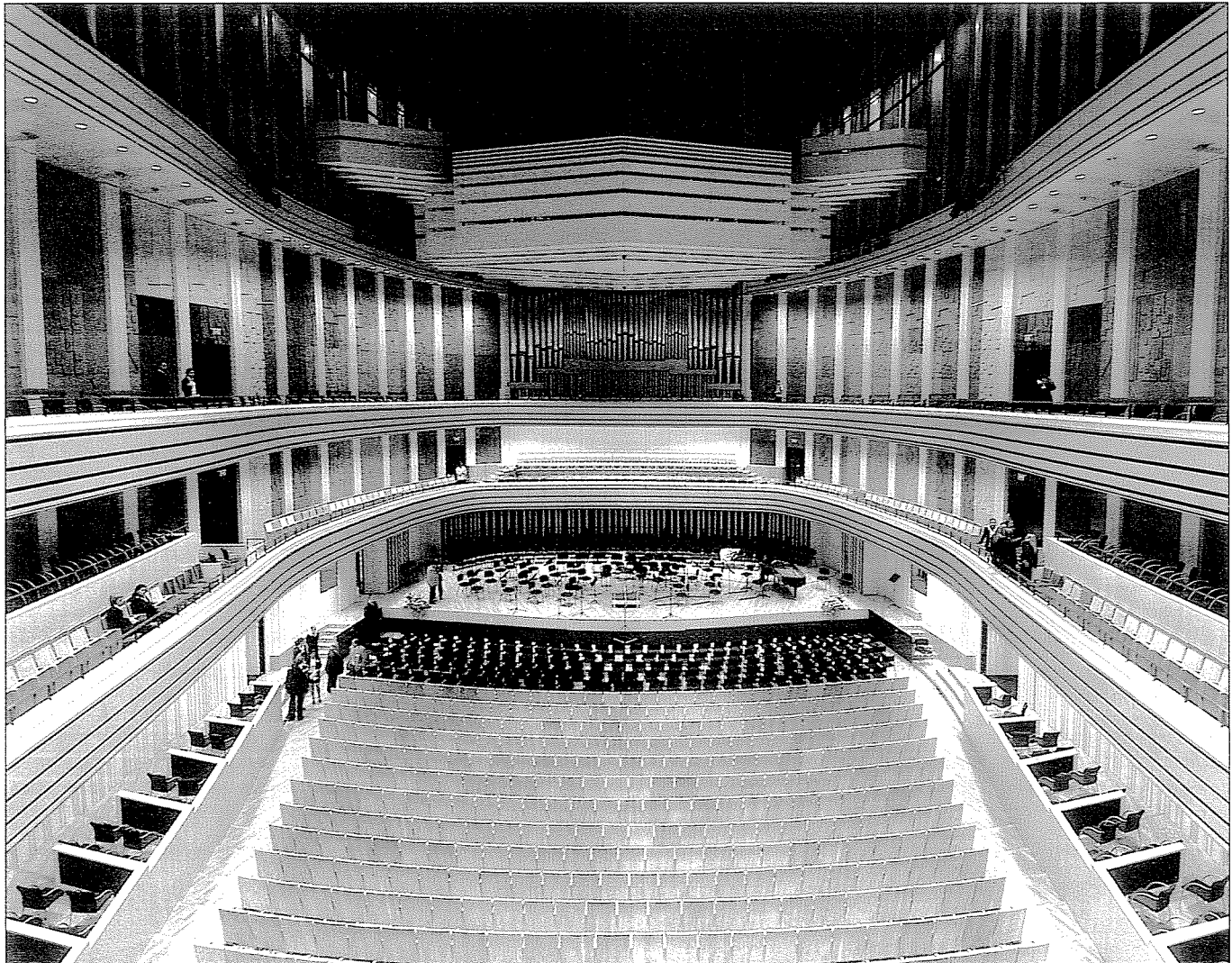
### 3.3 Construction - Challenges of the Isolation

The mineral wool insulation was generally an effective spacer between the shoring and the building structure to maintain the critical 10 cm isolation gap mentioned earlier. Not so however near the terrain level, where the diaphragm wall had to be braced against earth-pressure by a row of elastic pads.

The concrete lugs at the lateral load resisting bearings needed heavy reinforcement (Fig. 13), while maintaining a  $\pm 5$  mm tolerance. All the upstand lugs were cast-in-place while majority of the downstand lugs were precast. (Fig. 11)

The lateral bearings could abutt directly against the concrete of the lugs on one side, but on the opposite side 68 mm thick

**Fig. 9:** The auditorium: stage, canopy, reverberation chambers (Photo by A. Polgar, Arcadom zRt.)



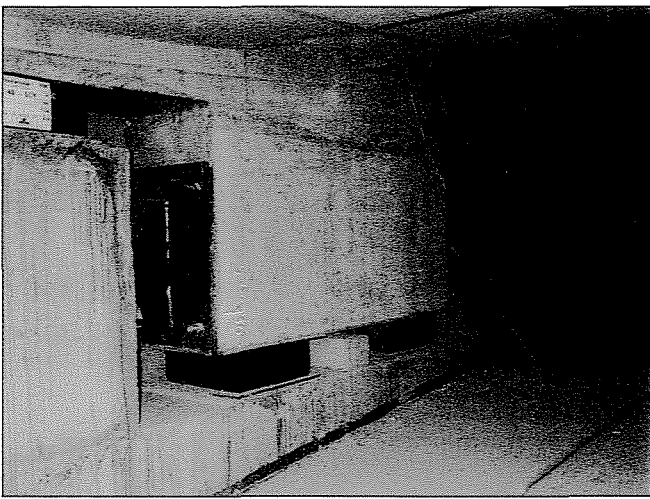


**Fig. 14:** Bearings and failsafe stops under a perimeter wall

steel plates were required to provide sufficient stiffness. The bearings were precompressed with flat jacks and the position was fixed by 6 M36 bolts (*Fig. 12*).

The construction of the „auditorium box” had to be completed and the full gravity-load compression applied on the vertical load pads prior to pre-stressing the lateral-load bearings. This prevented damage through vertical movement.

The precompression task was extremely difficult, as the space for the installation of the pads was most confined, with headroom of 1.20-1.60 m (*Fig. 15*)

The final phase was the assembly of failsafe stops between the elastic pads to prevent more than 45 mm deflection. One single 200x450x150 mm concrete stop has the bearing capacity of two elastic pads (*Fig. 14*).

The general contractor Arcadom Rt. was an ideal partner in answering the above challenges.

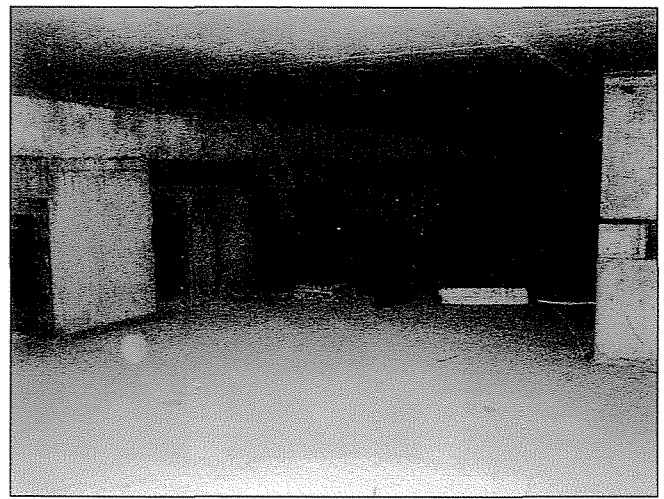


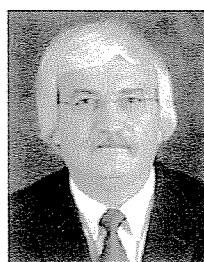
**Fig. 15:** Precompression work – “sit down, please”

## 4. CONCLUSION

Significant environmental noise and vibration at the project site made it necessary to construct the National Concert Hall as a fully isolated structure. The “box within a box” design model, using natural rubber isolation pads, further a combination of precast and cast-in-site concrete achieved a vibration- and noise-free auditorium - a perfect home for concerts.

**Ferenc Gonda** (1942) structural engineer (1966), specialised engineer in reinforced concrete (1972), head designer and managing director of DÉKETTŐ Statikus Iroda Ltd. Till 1994 he gathered experience in the design of concrete and steel structures as an employee of large state-owned planning offices: Lakóterv and ÁÉTV. In 1995 he started his own office and continued designing a big range of residential, commercial and cultural buildings. As a structural designer he was awarded a Silver Medal by the President of the Republic in 1997 (Police Headquarter, Budapest) and a Certificate of Merit by the Cultural Minister in 2005 (Palace of Arts, Budapest).

# HISTORICAL BACKGROUND OF PROBABILITY-BASED DESIGN IN HUNGARY



Prof. György Farkas - Tamás Kovács - Prof. Kálmán Szalai - Assoc. Prof. Antal Lovas

The EN 1990 “Basis of structural design” (EN 0) contains design principles that are applied in the Structural Eurocodes. The EN 0 is partly based on design methods used by the Eastern European countries, among them Hungary, during the second part of the 20<sup>th</sup> century and takes into account the related practical design experience of these countries.

The Hungarian codes introduced in 1949-51 (MSZ – Hungarian Code; and Highway Bridge Standard) already used the first version of the new design procedure, the partial safety factor method that was based on the concept of optimal safety. For more than 50 years, the fulfilment of the design requirements has been checked by this procedure. Considering their basic principles, the method serving as the root of Hungarian design codes for more than 50 years can be taken as antecedent of the reliability procedures published in the EN 0.

In the following, a survey will be given on the probability based design of concrete structures by summarizing its precedents in the former Hungarian design methods then the results of its application in Hungary will be demonstrated.

**Keywords:** safety, failure, limit states, risk, reliability

## 1. HISTORY OF THE DEVELOPMENT OF THE DESIGN PROCEDURE APPLYING PARTIAL SAFETY FACTORS

### 1.1 The periods of standardization in Hungary

The important standardization periods in Hungary are shown in Table 1. Between 1900 and 1949, verification of the adequacy of structures was described based on their elastic state, according to admissible stresses, based on Western European examples, and influence by them (Palotás, 1967).

The Temporary Highway Bridge Code (KH ‘50) of 1950 and the Countrywide Design Code for Buildings (Hungary, MSZ ‘51) prescribed to verify the ultimate limit state based on the theory of plasticity, while the analysis of serviceability limit states presupposed the validity of the theory of elasticity, all based on a semi-probabilistic design procedure applying partial safety factors (Mayer, 1926; Menyhárd, 1951; Szalai, 1987, 1996).

An overview of the targets for developing design methods

**Table 1:** Codification periods in Hungary

Time	Characteristics of the design method
1909-1910	Analysis of elastic state based on design method using admissible stresses
1931	
1949	Analysis of elastic and plastic states based on semi-probabilistic method applying partial safety factors
1949-1950	
1957	
1971	
1980-1985	

and their principles shows that at the beginning, the geometry of the structure was defined based on an understanding of the construction experience without any, or with very primitive calculations. The development of the elementary strength of materials enabled the spread of the *method of admissible stresses*.

Within this frame, calculation of stresses was carried out; the well proven dimensions were applied and then the results were compared to the admissible stresses. Parallel to the spread of knowledge in the theory of structures, the proven construction experience, that of the industrial methodology more reliable control of the load capacity of structures, a new branch of science became possible and grew as a result of this development, i. e. the theory of plasticity (and failure safety theorem).

This was followed by the spread of laboratory tests that enabled more reliable determination of load capacity  $T_i$  of the structure through the use of both theoretical calculations and experimental methods.

The optimum geometry  $L_{opt}$  of structures was developed as a result of two parallel processes. In one respect, the admissible stresses applied in the design were gradually increased, and in this way the optimum measures were approached “from below”. On the other hand, the value of the considered loads was reduced step by step, and so the optimum load capacity  $T_{opt}$  of structures (depending on the geometry  $L_{opt}$ ) was approached “from above” (Bölcskei, 1969) (Fig. 1).

The *method based on failure safety* is built upon the comparison of internal and external forces assuming a failure state in the structure. The comparative formulae contained *forces* (in given cases the loads) instead of stresses. Initially, a proportion of the value of the load bearing capacity was considered as a serviceability limit (Szalai, 1974).



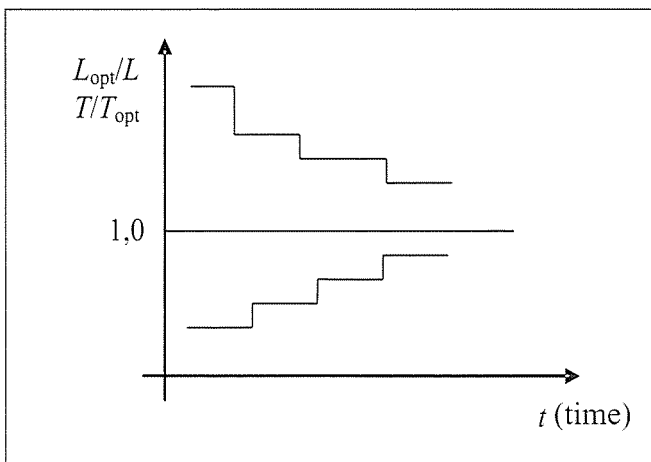


Fig. 1: Relation between  $L_{opt}/L$ ,  $T/T_{opt}$  and the time  $t$

While approaching the optimum load capacity, it became clear, that in several cases it was not the ultimate load but another unfavourable change in the structure, not closely connected to the load bearing capacity (e. g. deformation) that made the structure unusable. This concept resulted in the structural design practice in the *limit state method*. In this method, the probability of the development of the load limit states was analyzed.

The next development was the inclusion of the ultimate limit state considered from point of view of structural geometry (Gvozdev, 1949; Gyengö, Menyhárd, 1960).

## 1.2 Development of design methods based on safety factors

A common feature of design methods noted in Chapter 1.1, arose because of uncertainties occurring during the unanticipated behaviour of the structure. Safety factors were applied to protect the structure against unanticipated behaviour related to the design.

Over time, two types of safety factors were developed (Szalai, 1974).

These were called as:

- uniform safety factor, and
- partial safety factors respectively (Table 2).

The *method of admissible stresses* applies a *uniform safety factor* as well as the procedure based on *failure safety*.

The basic functions of design can be given in the following formulae:

At the method of admissible stresses

$$\sigma_{\max}(F_m, L_m) \leq \sigma_{\text{adm}} = \frac{R_m}{\gamma_1}$$

At the first version of the procedure based on the safety against failure

$$S(\gamma_2 F_m, L_m) = R(R_m, L_m).$$

I. e. in the above formulae:

- $\sigma_{\max}$  the highest stress calculated according to theory of elasticity,
- $\sigma_{\text{adm}}$  the admissible stress to characterise the material strength,
- $F_m, L_m$  and  $R_m$  mean geometry and strenght value of load (internal force),
- $S, R$  the failure load and load capacity respectively, to be determined according to the principle of theory of plasticity and theory of failure, from the expected values of the load  $F_m$  and geometry  $L_m$ , as well as the strength  $R_m$ ,
- $\gamma_1, \gamma_2$  the uniform *safety* factor, being generally variable depending on the material and the structure, and having a value changing over time, when  $\gamma_1 \geq \gamma_2$

The method of limit states applies *partial safety factors*. In this particular method, the basic functions of design can be written as:

$$Y_S(\gamma_F F_m, L_m) \leq Y_R\left(\frac{R_m}{\gamma_R}, L_m, H_a\right).$$

- Here, over the above mentioned symbols
- $\gamma_F$  and  $\gamma_R$  partial safety factors which refer to load and load capacity, which are different depending on the type of load and material.
- $Y_S$  and  $Y_R$  design internal force and limit internal force to be calculated based on geometry  $L_m$  due to loads and effects  $F_m$  – or forces, and load capacity (strength)  $R_m$  effected by these, taking into consideration the safety factors  $\gamma_F$  and  $\gamma_R$  – and from the expected value of total load capacity.
- $H_a$  cases of limit states (deformation, cracking etc.),

Table 2: Antecedents of the introduction of the design method based on partial safety factors

Year	Name/Nomination	Publication/Action
1914	G. Kazinczy	"Tests on walled in beams" (In Hungarian. Budapest, Periodical)
1926	M. Mayer	"Safety of structures and their calculation based on limit forces instead of admissible stresses" (In German. Berlin, book)
1928	G. Kazinczy	"The criticism of $\sigma_{\text{adm}}$ , the interpretation of safety" (In German, IABSE, Vienna)
1931	G. Kazinczy	"The "n (modular ratio) free design" (In German, RILEM, Zürich)
1936	A. J. Moe	"Mathematical description of the principle due to partial safety factors"
1942	G. Kazinczy	"The importance of plasticity of materials from point of view of load capacity of structures" (In Hungarian)
1943	U37-42 Soviet Technical Instruction	"Instructions to the design and construction of reinforced concrete structures" (In Russian, Moscow)
1950	Hungarian Ministry of Transport and Post (KPM)	"Temporary Code for Bridges" (In Hungarian, Budapest)
1951	Institute for Building Science (ÉTI)	"Completion and Modification of the Hungarian Code for reinforced concrete structures in buildings" (In Hungarian, Budapest)
1951	P. Gábory, I. Menyhárd, M. Rózsa	"New design method for reinforced concrete structures, design method based on safety factors and failure theory" (In Hungarian, Budapest)

in which strength plays no significant role in changes causing obstruction in the use of the structure.

### 1.3 Interpretation of the partial safety factors according to Mayer

Safety factors in the design procedure are important in control of the consequences of uncertainties of parameters affecting load capacity of structures. Building science experts, making use of error estimation based on results achieved in mathematics and surveying, were aware for some time, that the properties of structural parameters can be described mostly reliably by means of *probability laws*. M. Mayer, in his book mentioned above (1926), referring to the results of K. Jordán (mathematician of the Budapest Technical University) explains the following, assuming normal distribution. The value  $Y_s$  which can be considered in the calculation, where parameters influencing the load capacity (e.g. geometry, self weight, superimposed load), can be determined in order to calculate the resistance by taking into consideration triple standard deviation [the standard deviation multiplied by 3]

$$Y_c = D \pm 3m$$

where  $D$  is the mean value of the given parameter,  $m$  is the standard deviation.

It was of historical importance in the theory of design, to find the proposal in Mayer's book determining the load capacity or threshold load that included several independent probability variables (parameters) in the formula:

$$X = f(l_1, l_2, \dots)$$

According to the above formula, the determination of the standard deviation of the given parameter  $X$  is shown mathematically by the function:

$$M = \sqrt{\left(\frac{\partial f}{\partial l_1} m_1\right)^2 + \left(\frac{\partial f}{\partial l_2} m_2\right)^2 + \dots}$$

The threshold to be considered is:

$$X_k = X \pm 3M$$

where  $X$  is the mean value of the load or load capacity. Mayer, after publishing his book worked up results of real measurements, suggested values for partial safety factors.

Mayer considers the value calculated with the standard deviation multiplied by  $\pm 3$  to be acceptable, because, as he has written: "in practice almost 100% can be found within this interval (more exactly, considering both extremities, 99.73% of cases)".

It is significant that Mayer, reflecting on the triple standard deviation values, suggested calculations considering the following values:

1.30 for superimposed load,

in general 1.15 for self weight, in case of reinforced concrete 1.25,

for snow load 2.00.

But Mayer was not satisfied with applying the triple standard deviation values for the considered value for the strength of concrete structures. His proposal to overcome this, probably

for the sake of conforming to the „proven” geometry, contains divider of 2. This means that the calculated value for the strength of concrete according to

$$\sigma_d = \frac{D - 3m}{2}$$

## 2. SCIENCE-HISTORICAL ANTECEDENTS

### 2.1 Historical background of the introduction of the Mayer-theorem in Eastern Europe

The Mayer-theorem, like all new ideas, encountered difficulties and resistance over decades from practising engineers. This is natural, and is to be expected to occur nowadays. Namely, structural design is an engineering discipline replete with responsibility and the practical engineer will not be willing to change the well proven methods. There is some readiness, in normal circumstances, to accept research results, giving reasons for radical alterations to accepted practice, these being published in conference proceedings and periodicals. Generally an extraordinary situation is needed to introduce a new procedure, which touches on safety or radically changes the traditional approach. Such a situation developed during World War II in the Soviet Union and later, after the war in Eastern European countries. A comparable new situation is the establishment of the European Union in Western Europe.

A technical instruction was published in the Soviet Union in 1942, in which Mayer's original proposal was adopted with the alteration that at the design value  $R_d$  of strength, the factor (divider) 2 was omitted. The war situation and the corresponding state directives made it necessary to allow for (and to increase) the risk, and within this environment it was accepted by silent consent.

Hungary was the first country in the world to adopt the code built on Mayer's concept that and was first introduced in Hungary in 1950 (Menyhárd, 1951, Gyengő, Menyhárd, 1960). The extraordinary situation required for the introduction of Mayer's code was created by the political expectation inspired by adopting the Soviet example. I. Menyhárd was well acquainted with the new procedure which had previously been worked through by international scientific societies and within Hungarian scientific circles (Mayer, 1926, Kazinczy, 1914). I. Menyhárd, who was well informed and being at the top of the professional elite, recognised the extraordinary situation, and referring to the following Soviet example, proposed the introduction of the Mayer concept corrected by Gvozdev (Gvozdev, 1949) as the new Hungarian Code, MSZ '51. The Soviet-oriented Hungarian administration introduced the code. The safety level of the Hungarian code at that time was approximately equal to (or almost lower) than the previous safety level included in the method based on admissible stresses (Korányi, 1949).

### 2.2 Political antecedents of the introduction of the Soviet Code

The political precedents of the introduction of the Hungarian Code (Szalai, Lenkei, 1992) were the following.

The restricted political situation helped the introduction of the codified new design method in Hungary, and in general in Eastern Europe. The genius I. Menyhárd initiated the introduction of a revolutionary new method in Hungary, and used the advantages of references to the Soviet experience. Thus it was introduced by the decision of the National Economic Council of Hungary. It is interesting to mention as characterising the political situation that I. Menyhárd was arrested after the Fulton speech of Churchill and put under investigation and imprisoned in 1947.

I. Menyhárd was one of the founders of the endowment, by means of which the Hungarian Nobel Prize recipient, A. Szent-Györgyi was able to head a delegation of scientists, to travel in secret to Istanbul and confer with the British on the armistice.

On the other hand, it belongs to the precedents that E. Hilvert, Hungarian structural engineer travelled in the 1930s to the Soviet Union to undertake a job and returning after the war to Hungary took with him temporary instructions from the Soviet Union based on ultimate states. At that time I. Menyhárd had been working at the Scientific Institute for Building in Budapest and recognised the potential of this theory in the professional and political arenas. Referring to the Soviet experience, this new process was based in scientifically proven methodology and contained potential to generate new development. Despite the resistance in professional circles, he was able to make this new method officially accepted (Emphasised in the Liège Congress 1949 of IABSE).

When in 1952/53, the Soviets introduced this as a standard which had been developed during the war years; conservative opposition attacked the concept with both political and scientific arguments. In support of the standard, one of the most compelling arguments of A. A. Gvozdev was (as witnessed and reported by Hungarian PhD students, Gy. Deák and T. Garai,) the reference to the positive experience with the Hungarian code MSZ '51. Subsequent to the acceptance of the Soviet code, other Eastern European countries accepted the codification concept based on Mayer's idea. The formation of the present safety level of EN 0 (being lower than the earlier planned standard) were based on the result of trials carried out by 35 countries in the late 1970s as well as on the lower Hungarian Code.

The mentioned Hungarian PhD students studying in Moscow in 1952 participated as observers at the session of the scientific council of the Moscow Structural Engineering University (MISI). Prior to the session the head of the Department of Science History wrote a letter to the Central Committee of the Communist Party of the Soviet Union opposing the introduction of the code based on limit states method. As a consequence of the letter N. S. Khrushchev who was that time the party secretary of Moscow, was also responsible for the building industry, requested the scientific council of MISI to take a stand on the issue. A heated discussion developed between opponents and the submitters of the concept. The most important arguments of the opponents were that the method causes confusion among structural designers, thus harming the national economy. A. A. Gvozdev, who authored the concept, pointing at the two Hungarian PhD students, based his argument on the fact that in Hungary the method has been used without negative incidents countrywide as a code over the past two years. As a result of the discussion, the method was introduced in the Soviet Union in 1955.

## 2.3 The COMECON Code and its precedents

By end of the 1950s, following the Hungarian and Soviet experience, the limit state design was adopted in Poland, Bulgaria and Romania, also. There was an attempt to adopt this code in Czechoslovakia but the professional public opinion rejected the application. The first consultation on COMECON codes and in this context on the codes for load bearing structures, took place in Moscow in 1960. K. Szalai participated at this session. The delegate of GDR vehemently defended the method of admissible stresses referring to the DIN. In response, A. A. Gvozdev, referring again to Hungarian experience, advised in reference to the Hungarian practice, that the introduction of the method was practically without any problem. The aim of this was that the member countries should introduce it as national standard. Finally, after many attempts, a detailed draft based on the Soviet code was accepted by all other Soviet Block countries except Hungary. Hungary, there being no political constraint, did not accept the design manual. The manual was built on semi-probabilistic principles which contained in parts such experimentally produced procedures that were not supported by the theory. The other Eastern European countries introduced the Manual as national code. This created serious professional-political problems within the circle of structural engineers, e.g. in Poland. In 1978, with active co-operation from Hungary, a COMECON code was developed and published as an alternative to the Manual. This alternative had semi-probabilistic fundamentals and contained only the basic guidelines. These principles corresponded to the CEB-FIP '78 recommendations.

## 2.4 Probability-theoretical precedents

The method of applying partial safety factors per Mayer was introduced as the limit states method. This design procedure was later called semi-probabilistic method. The semi-probabilistic design procedure (or only partially based on theory of probability) essentially means that the probability of occurrence of the not desired states (being loss of load capacity, limitation of serviceability, etc.) is chosen on optimum safety levels, and the codes prescribe according to this their partial safety factors.

The limit states method is an extraordinarily expedient system, based on the findings of construction science research. Prior to the method developed by A. A. Gvozdev (Gvozdev 1949):

- Initial attempts were made to apply mathematical statistics and the theory of probability to structural engineering;
- Taking into account the characteristics of reinforced concrete, methods were developed to calculate following the theory of plasticity (failure), where the condition belonging to the load capacity exceeds the elastic range.
- The possibility of qualitative changes had been exhausted within the frames of the used design methods (based on single safety factor);
- The war effort and sustained losses created an economic imperative for better use of materials and of the load capacity of structures.

The theory of probability and mathematical statistics were relatively new fields of mathematics to be used in structural design at the beginning of the 1950s. During the 17<sup>th</sup> century, P. Fermat and B. Pascal developed the fundamentals of theory of

probability in relation to gambling. J. Bernoulli, P. S. Laplace, K. F. Gauss and A. Moivre, all enriched the probability theory by an essential statement or notion.

S. D. Poisson and A. A. Markov were the founders of theory of stochastic processes. Great scientists of mathematical statistics and theory of probability were K. Pearson and A. N. Kolmogorov. M. Mayer performed the initial structural engineering application of mathematical statistics and theory of probability in his mentioned work presumably using also the influence of the Hungarian mathematician K. Jordán (Mayer, 1926).

Among the foremost in the field was G. Kazinczy who also applied the theory of probability in the field of engineering. He explains in his study for the post-graduate engineering course (Kazinczy, 1942) his concept based on theory of probability following the ideas of Mayer and Jordán. According to this estimating the normal distribution the probability of failure can be determined. Consequently the structure has to be designed such that it maximizes economical considerations of establishment, taking also into account maintenance and refurbishment (Mihailich, Haviár, 1966).

## 2.5 The beginning of the design based on plasticity

The Hungarian, G. Kazinczy was a significant personality in the field of plasticity and the analysis of failure and load capacity of structures.

His paper on walled-in beams (Kazinczy, 1914) was an early contribution to the behaviour of structural elements in plastic state. It had a great importance because it refers firstly to the role of plastic behaviour of the material in the load capacity of the member. He explains the phenomenon of the yield mechanism and of the plastic hinge, mentioning that "...the walled-in beam can deflect if the stress is as high as the yield stress at least in three places."

He explains about the plastic hinges that "... the beam works as if at the mentioned places there were hinges, i.e. at these places the value of the moments have remained as high as it was when the iron reached the yield point."

A full series of works of G. Kazinczy has dealt with the problems of design according to the principles of plasticity.

## 3. INTRODUCTION OF THE DESIGN OF REINFORCED CONCRETE STRUCTURES BASED ON LIMIT STATES IN EASTERN EUROPE

### 3.1 The codification according to I. Menyhárd

The design method based on the failure state and applying (further on) a single safety factor with respect to reinforced concrete structures, was raised on the level of a state-wide design code in the Soviet Union in 1938.

The essence of the method assuming 3<sup>rd</sup> stress state of reinforced concrete uses calculations with an assumed value of strength. According to the guidelines, in certain cases, the plastic redistribution of forces may be considered. The proven

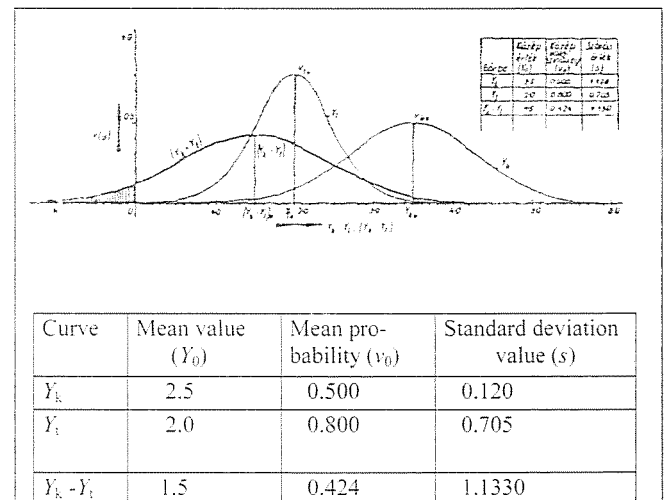
load capacity of the structure is to be divided by the single safety factor. On the other hand, the value of this safety factor was only variable between 1.5 to 2.2 depending on the ratio of the dead load and live load, and on the character of the analysed structure.

The new design method based on limit states, was essentially developed in 1949. It was supported by the experience gained via the application of Mayer's notions under war conditions. The excellent personalities of the Hungarian building science, I. Menyhárd, I. Korányi and others were informed on the Soviet prescriptions by the conveyance of Hungarian specialists who have returned from the Soviet Union, first of all E. Hilvert, as mentioned. Another resource for I. Menyhárd was the new Hungarian school for the theory of probability led by A. Rényi, who also had the opportunity to study the achievements of the Soviet-Russian results in this field (Rényi, 1954). I. Menyhárd writes (1951) about this circumstance in his book, which is nowadays unfortunately known only to a few people:

"...In the year 1950, the draft of the code for reinforced concrete structures in buildings in the Soviet Union was completed. We know details of this by means of literature contributions. The new draft code was prepared considering fully the principles related in this chapter..." (The principles are those of limit states.)

I. Menyhárd, developing this thesis based on results of research work by A. A. Gvozdev in limit states method, describes appropriate safety standards. According to this description, safety can be characterized by the failure probabilities of the structure. This can be given by the relative size of the negative section of the density function deviation for load and resistance (*Fig. 2*).

**Fig. 2:** The interpretation of safety according to I. Menyhárd (original figure with English version of table)



An interesting reference can be found in Menyhárd's book on the new standards for hydraulic structures:

"...The Soviet regulations provide the value expressing the probability of resistance of the structure due to the categories of constructions. E.g. in case of I<sup>st</sup> class structures, the probability of resistance is determined as 1/2500, for II<sup>nd</sup> class structures this value is 1/740, for III<sup>rd</sup> class structures, 1/250. The structures have to be qualified as first, second or third class, depending on the interest which is touched by the construction. A valley water dam is considered a first class construction because its failure affects a large community. Devastation by flood and failure of energy supply can be the consequences. The bottom emptying sluice of the dam can be designed as a third class structure, because if it fails, it does not cause larger loss than its own worth. ..."

## 3.2 The regulation by Gvozdev

Representatives of the construction-science school of Gvozdev – coinciding with the edition of Menyhárd's book – published explanation of their findings on the new design method based on limit states (Keldish, 1951). The authors present the conceptual fundamentals of the limit states based design method and its application for reinforced concrete, masonry, steel and timber structures as well. The first published precise introduction and explanation of the limit states (ultimate, deformation, and crack width) can be found in this book. The full series of partial safety factors appears in this work, and the explanations remain valid.

The conceptual statement of the authors with respect to the interpretation of the limit states is as follows:

"...the method of calculation according to limit states aims at demonstrating the smallest possible load capacity ..."

The authors determine the lowest (design) value of material resistance by the formula

$$R_d = R_m - 3 s_R$$

to be found at M. Mayer (Mayer, 1926) based on country-wide data. In this formula  $R_m$  is the mean value. Introduced upon this is the so called homogeneity coefficient which is given in the formula

$$k = \frac{R_d}{R_m} = 1 - 3 \frac{s_R}{R_m}$$

(This means that the factor 2 for concrete suggested by Mayer was omitted.)

The values of the homogeneity coefficient  $k$  are the following for different materials:

- for concrete  $k=0.55\sim0.65$ ;
- for steel  $k=0.85\sim0.90$ ;
- for masonry  $k=0.40\sim0.60$ ;
- for timber  $k=0.44\sim0.75$ .

The value  $R_m$  for concrete refers to prism strength and for steel to yield point.

The possible maximum value of load is to be taken into account for the analysis of ultimate state. This can be achieved by multiplication of the so called normative (basic) value of the load by its given safety factors. In case of other limit states the normative (basic) values of loads are to be considered.

## 4. OUTCOME OF HUNGARIAN RESEARCH WORKS ON MEASURES OF ACCEPTABLE RISK

### 4.1 Semi-probabilistic method

The practical introduction of the method of limit states initiated world-wide detailed theoretical and experimental research work. (Bulletin d'Information, 1978). In the following decades, representatives of Hungarian construction science actively participated in this research work, (Kármán, 1965; Mihailich, Haviár, 1966; Lenkei, 1966; Palotás, 1967; Korda, Szalai, 1973; Böleskei, Dulácska, 1974; Szalai, 1987, 1996, Bódi, Dulácska,

Deák, Korda, Szalai, 1987; Deák, 1992; Korda, 1998; Kovács, 1997; Mistéth, 2001).

It should be mentioned that in relation to reinforced concrete, prestressing was always discussed in the developed Hungarian codes. There were naturally some differences in case of bridges (e. g. two levels for service load for different requirements (Tassi, 1968). For buildings, prestressed concrete structures were codified aiming at the same level as reinforced concrete, of course with special aspects of prestressing (Tassi, Windisch, 1974).

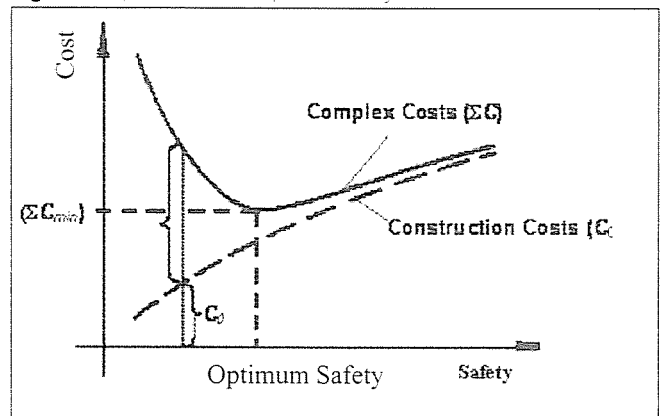
According to considered opinion, the semi-probabilistic method is essentially the same as the method of limit states with one difference being that the mean value of failure is chosen on the country level. The partial safety factors are determined due to acceptable risk, by means of the theory of probability and mathematical statistics.

### 4.2 Optimum or acceptable risk by Kármán and Mistéth

The safety factors applied in the context of the semi-probabilistic method were determined starting from the acceptable (or optimum) risk (Kármán, 1965). The acceptable risk can be determined by considering the (direct and indirect) financial losses: losses due to personal injury (Kármán, 1987), lost profit and the cost of reconstruction.

T. Kármán and E. Mistéth were looking for the optimal or acceptable risk, analysing the minimum level of complex costs (Fig. 3).

Fig. 3: Interpretation of the optimum safety



$$C = C_0 + C_1 + p_r D$$

In this function  $C_0$  is the construction cost of the structure,  $C_1$  is the maintenance cost,  $D$  the sum of loss occurring with a probability  $p_r(p_{rs})$ , which includes the loss connected with personal injuries and lost profit. According to Mistéth, the inequality

$$0 \leq t \leq T$$

is valid for the full intended lifespan of the structure

$$\text{Prob}[R(t) - S(t) = \Delta(t) \geq 0] \geq (1 - p_r)$$

The optimum i.e. acceptable risk belonging to the minimum of complex costs can be given as

$$p_{\text{opt}} = \frac{1}{b \cdot \delta} \quad (\text{T. Kármán})$$

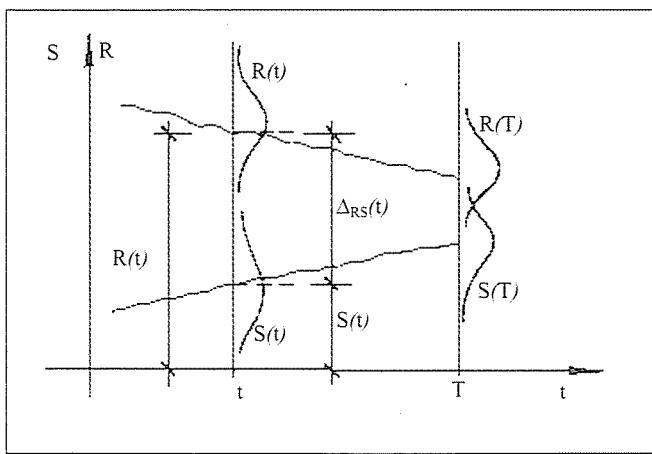


Fig. 4: The change with time of the resistance and the forces

or

$$\frac{1}{p_{opt}} = \frac{2,3}{b_1} \left( \frac{D}{C_0} + 1,5 \right)$$

In the above formulae (E. Mistéth)

- $t$  the time after construction;  
 $T$  planned lifespan of the structure;  
 $R(t)$  and  $S(t)$  effective values of load capacity and load at time  $t$ ;  
 $\delta = D/C_0$  the damage ratio  
 $D$  the value of the direct and indirect damage at the eventual failure of the structure followed by material loss and personal injury  
 $C_0$  construction cost of the structure  
 $b$  value of the factor depending on the conditions of use and construction material, furthermore on this model of analysis, its mean value is  $b=80$  (Kármán, 1987)  
 $b_1$  factor depending on the parameters serving the basis of design of the structure, the value of which, depending on the deviation of the chosen construction material, varies according to Mistéth from 0.03 to 0.10 (Mistéth, 1974).

### 4.3 The sufficient safety according to Kármán

For the sake of acceptance of concept and numerical value of optimal i.e. acceptable risk, T. Kármán formulated the following: In case of load bearing structures, the target could be producing *sufficient safety*, not "absolute" safety. The sufficient safety means the ability of the structure to function reliably for the duration of its intended lifetime for the purpose for which it was designed. The larger this reliability, the higher is the safety of the structure and lower the probability of its failure.

To determine the optimal risk ( $p_{opt}$ ) of the structure, T. Kármán was first to incorporate into his formula the value of the human factor following the eventual failure of the structure (Kármán, 1987). T. Kármán presented the method of determination of the value of optimal risk (based on his study completed 1964) and therein that of the value of human loss, at a session of a CEB meeting in 1968. The concept of measuring the damage caused by failure to personal injury and human loss was met with indignation both within Hungary and abroad - West and East - by both the religious and atheist researchers as well as official people. They declared that the loss of human

life is inestimable and is deemed to be infinitely high.

However, as T. Kármán emphasized, to determine the safety of a structure, it is possible and necessary to value the damage affecting society as a whole. The value of damage due to the full loss of work-capability or even of death of an individual, according to Kármán, is 40 years discounted gross national income per capita for developed countries. The sum calculated accordingly largely corresponded to the amount paid by western insurance companies, at that time, injuries or loss of life due to aviation accidents. The passing of decades was required for general acceptance of the concept of T. Kármán.

The measure of sufficient safety,  $p_{opt}$ , is generally different for individual structures and also for different parts of a structure. According to the analyses by T. Kármán, in cases of buildings, the value of the damage ratio is in average  $\delta=125$ . According to this, the value of sufficient safety or acceptable risk,  $p_{opt}=10^{-4}$ . The reliability belonging to this  $M=1-p_{opt}=0.9999$ , to which theoretically a safety index  $\beta_{opt}=3.719$  can be appended. It is worthwhile to note, that the measure of the designed risk in code EN-0,  $p=10^{-4}$  and the value of the safety index appended to this is  $\beta=3.8$ .

## 5. ANALYSIS OF LOAD CAPACITY OF STRUCTURES BY RELIABILITY METHOD

The proof of suitability of structural load capacity can be performed by the following procedure based on reliability theory (Szalai, 1974). The suitability of load capacity has to be proven using the predictable values of resistance  $R_m$ , and at the side of the actions the dead load  $G_m$  and live loads

$$Q_m = Q_{1m} + \sum_{i=2}^n \psi_{0i} Q_{im} \quad \text{Here } Q_{1m} \text{ is the dominant live load, } Q_{im} \text{ is the } i^{\text{th}}, \text{ non dominant live load and } \psi_{0i} \text{ is the simultaneity factor belonging to } Q_{im}.$$

### 5.1 Proof of the suitability of load capacity

The common handling and comparison of the effect

$$E_m = G_m + Q_m \quad \text{to resistance } R \text{ can be interpreted according to}$$

Fig. 5; the load capacity of the structure is satisfactory if

$$R_d - E_d \geq 0$$

where  $R_d$  - the design value of resistance, of which, with one side transformation

$$R_d = R_m \exp(-\beta \cdot \alpha_R \cdot \nu_R)$$

$E_d$  - the design value of the effect side

$$E_d = \left[ G_m (1 - \beta \cdot \alpha_G^{(-)} \cdot \nu_G) + Q_{1m} (1 - \beta \cdot \alpha_Q^{(-)} \cdot \nu_Q) \right]$$

where apart from the above written symbols  $\alpha_G$  and  $\alpha_Q$  are the so called sensitivity factors (see Chapter 5.2),  $\nu_G$  and  $\nu_Q$  are the coefficient of variation of the dead and live load (see Chapter 6.3).

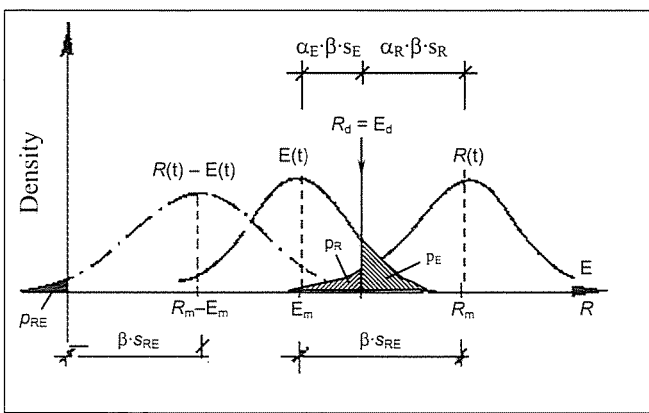


Fig. 5: Density functions of load and resistance

## 5.2 The global safety factors

The load capacity requirement is fulfilled if

$$R_m \geq \exp[\beta \cdot \alpha_R^{(+)} \cdot v_R] \cdot [G_m (1 - \beta \cdot \alpha_G^{(-)} \cdot v_G) + Q_m (1 - \beta \cdot \alpha_Q^{(-)} \cdot v_Q)]$$

where  $\alpha_i$  values are also here the sensitivity factors, which can be calculated as follows:

$$\alpha_R = \frac{R_d \cdot v_R}{\sum(\kappa_i)^2}; \quad \alpha_G = \frac{G_m \cdot v_G}{\sum(\kappa_i)^2}; \quad \alpha_Q = \frac{Q_m \cdot v_Q}{\sum(\kappa_i)^2};$$

$$\sqrt{\sum \kappa_i^2} = \sqrt{(R_d \cdot v_R)^2 + (G_m \cdot v_G)^2 + (Q_m \cdot v_Q)^2}$$

Applying the symbol  $Q_m = \mu G_m$ , and reordering the above expression, the global safety factor

$$\gamma_m = \frac{R_m}{G_m + Q_m} = \left[ \frac{1}{1 + \mu} (1 - \beta \alpha_G^{(-)} v_G) + \frac{\mu}{1 + \mu} (1 - \beta \alpha_Q^{(-)} v_Q) \right] \exp(\beta \alpha_R^{(+)} v_R)$$

takes this form, and having this as the load capacity (considering the above symbols)

$$R_m \geq \gamma_m (G_m + Q_{1m} + \sum_{i=2}^n \psi_{0i} Q_{im})$$

becomes the proof.

## 5.3 Interpretation of the coefficient of variation $v_i$

Table 3: Classification of buildings based on damage ratio according to EN-0

Class according to Damage Ratio	Description	Examples from among buildings and engineering structures
CC3	The significance of loss of human life is high; or the economic, social, environmental consequences are extraordinary significant	Tribunes, public buildings, where the damage caused by failure is high. (E. g. Concert Hall)
CC2	The significance of loss of human life is medium; the economic, social and environmental consequences are considerable	Residential, dwellings, office buildings, public institutions where the damage caused by failure is medium (as office buildings)
CC1	The significance of loss of human life is low; the economic, social, environmental consequences are not considerable or negligible	Agricultural buildings, in which people are generally not remaining (e.g. storage houses, glass houses)

Specialists who worked out the EN 0 reasoned higher partial safety factors than those accepted in Eastern Europe. They expanded the concept of the coefficient of variation due to traditional interpretation as follows.

The following three factors play a role in the coefficient of variation  $v_R$  of the *resistance side* as interpreted by EN:

- the measured coefficient of variation of the value of

$$\text{resistance: } v_{Rf} = \frac{s_R}{R_m}$$

- the uncertainty of the calculation model:  $v_{Rm0}$ ,
- the uncertainty of geometric data:  $v_{RG}$ .

In the above formulae  $s_{iR}$  is the standard deviation which can be calculated by considering the individual values and their deviations of parameters occurring in the resistance function (Szalai, 2002).

The common consideration of these uncertainties can be calculated by the pooled deviation

$$v_R = \sqrt{v_{Rf}^2 + v_{Rm}^2 + v_{RG}^2}$$

The  $v_E$  value of the coefficient of variation (similarly to  $v_R$ ), is influenced by the measured coefficient of variation of effect

$$E (v_{Ef} = \frac{s_E}{E_m}), \text{ the calculation model } m (v_{Em0}) \text{ and geometry}$$

model  $G (v_{EG})$ . Here  $s_{iE}$  is the standard deviation which can be calculated taking into consideration the individual values of the parameters at the *effect side* of the function and their deviation.

Following from these and according to the previous interpretation of the effects  $G$  and  $Q$  at the *force side*: the relative value of the pooled coefficient of variation  $G$  as

$$v_G = \sqrt{v_{Gf}^2 + v_{Gm}^2 + v_{GG}^2}$$

the relative value of the pooled coefficient of variation  $Q$  is

$$v_Q = \sqrt{v_{Qf}^2 + v_{Qm}^2 + v_{QG}^2}$$

where  $v_{Gf}$  and  $v_{Qf}$  are the coefficient of variation of the measuring data according to the interpretation of the above  $v_{Ef}$

## 5.4 The reliability (safety) index $\beta$

To select the above mentioned safety index  $\beta$  (called reliability index by EN 0) the EN 0 defines the classes of buildings according to damage ratio by means of Table 3.

Minimum values of reliability indices  $\beta$  belonging to the analysis of ultimate limit state suggested by EN 0 are found in Table 4.

The values of the reliability indices  $\beta$  as defined by EN-0, due to reliability class RC2 and to the corresponding damage ratio class in case of one year and 50 years designed lifespan

**Table 4:** Recommended values for  $\beta$  according to EN-0

Reliability class	Minimum values of $\beta$	
	1 year reference term	50 years reference term
RC3	5.2	4.3
RC2	4.7	3.8
RC1	4.2	3.3

**Table 5:** Recommended values for  $\beta$  in case of different Limit States according to EN-0

Limit state	Provided reliability index	
	1 year	50 years
Ultimate	4.7	3.8
Fatigue		1.5 – 3.8
Serviceability (Irreversible)	2.9	1.5

**Table 6:** Relation between  $\beta$  and  $p$

$p$	$10^{-1}$	$10^{-2}$	$10^{-3}$	$10^{-4}$	$10^{-5}$	$10^{-6}$	$10^{-7}$
$\beta$	1.28	2.32	3.09	3.72	4.27	4.75	5.20

respectively, are included in Table 5. This table also contains at the same time, the values  $\beta$  belonging to fatigue and serviceability limit states.

The calculated values of the function  $p=\Phi(-\beta)$  between the reliability index and the risk calculated in the case of normal distribution function is shown in Table 6. Here  $\Phi$  is the function of normal distribution.

## 5.5 Control levels according to EN 0

In the interest of complying with the above mentioned reliability level, based on the EN0, the purchaser defines the function/use of the structure which then determines RC1~RC3. Depending on the reliability classes RC1~RC3 the so called design control (DSL1~DSL3), and site control (IL1~IL3) levels are determined.

## 6. SUMMARY

After the construction tragedies in Babylon and other building disasters, it was necessary in the 20<sup>th</sup> century BC to create the Hamurabi Code. Principally for reducing construction costs, the contemporary building masters preferred to reduce with the sizes or omitted more durable and stronger materials. Thus the safety of structures was gradually decreased and the number of construction accidents increased. The analysis and evaluation of construction failures and their consequences agitated the fantasy of researchers. After the activity of G. Galilei and I. Newton, the seeking of optimum safety levels became the central topic of building science. At the end of 19<sup>th</sup>, and beginning of 20<sup>th</sup> century, the codes prescribed the control of statically satisfaction of structures assuming the elastic state, using the single safety factor and the method of admissible stresses. Parallel to the gradually decreasing geometrical data and application of more audacious structural solutions, completion of elastic calculation model built on service states took place, and the analysis of ultimate state became prominent. The Hungarian G. Kazinczy, (1914) analysed the load bearing capacity of steel beams walled in at both ends

using the elasto-plastic material model. The German M. Mayer (1926) proposed a method applying partial safety factors. The standard application of these initiatives was delayed because of the particular responsibility of structural designers. The Soviet-Russian A. A. Gvozdev proposed (1946) the application of the method based on ultimate and serviceability limit states. After World War II, at the beginning of the 1950s, in a peculiar economic-political situation, under the leadership of I. Menyhárd, Hungary changed to the application of design methods using partial safety factors. As a consequence of this codification a period of gradual reduction of structural safety began (1955-86). With the formation of the safety level in the Eurocode, the associated Eastern European experience (among others) could be utilized. In order to apply the theory of probability, the basis of the safety codes had to be incorporated into the more recent Eurocodes. (Szalai, Farkas, Kovács, 2002, Szalai 2002, Szalai 2003).

## 7. REFERENCES

- Bódi, I. Dulácska, E. Deák, Gy., Korda, J. Szalai, K. (1989) "Book of Structural Engineers" Chapter 5. Buildings. (In Hungarian), *Műszaki Könyvkiadó*, Budapest
- Bölcskei, E. (1969) "Safety of Structures" (In Hungarian), *Műszaki Tudomány*, pp. 413-414.
- Bölcskei, E., Dulácska, E. (1974) "Book of Structural Engineers" (In Hungarian) *Műszaki Könyvkiadó*, Budapest
- Bulletin d'Information No. 129 (1978), "Trial and Calculations based on the CEB/FIP Model Code for Concrete Structures", London
- Deák, Gy. (1992) "Stochastic View at the Analysis of Serviceability State" (In Hungarian), *BME Építőmérnöki Kar, Vasbetonszerkezetek Tanszéke Tudományos Közleményei*, Budapest, pp. 48-59.
- Farkas, Gy., Kovács, T., Szalai, K. (2002) "Synthesis of Safety Levels Approved in East and West Europe in the Eurocode" *Proceedings of the fib 2002 Congress on Concrete Structures in the 21st Century*, Vol.2. Session 11, Osaka
- Gvozdev, A. A. (1949), "Design of Load Capacity of Structures on Base of Limit Equilibrium" (In Russian) *GOSSTROYIZDAT Moscow*
- Gyengő, T., Menyhárd, I. (1960) "Theory, Design and Structural Formation of Reinforced Concrete Structures" (In Hungarian), *Műszaki Könyvkiadó*, Budapest
- Kármán, T. (1965), "On the Optimum Safety of Load Bearing Structures" (In Hungarian), Budapest
- Kármán, T. (1987) "Human Factors of Structural Safety" (In Hungarian), *Közlekedésépítés- és Mélyépítéstudományi Szemle*
- Kazinczy, G. (1914) "Tests on Walled in Beams" (In Hungarian), *Betonszemle*, Budapest, pp. 76-85.
- Kazinczy, G. (1942), "The Importance of Plasticity of Materials from Point of View of Load Capacity of Structures" pp. 79-110.
- Keldish, V. M. (Editor) (1951) "Calculation of Structures Based on Limit States" (In Russian), *Izdatel'stvo Stroitel'noy Literatury*, Moscow-Leningrad
- Korányi, I. (1949) "The Safety of Structures" *Magyar Közlekedés, Mély- és Vízépítés*, pp. 76-86.
- Korda, J. (1998) "The Application of the  $\bar{A}$ -Distribution Function in Tests to Characterise the Concrete Strength", *Budapesti Műszaki Egyetem Építőmérnöki Kar Vasbetonszerkezetek Tanszéke Tudományos Közleményei*, pp. 87-91.
- Korda, J., Szalai, K. (1973) "Strength Requirement of Structural Concretes and their Classification" *Mélyépítéstudományi Szemle*, pp. 117-125.
- Kovács, B. (1992) "Stiffening Analysis of Buildings Erected in the IMS System", *Department of Reinforced Concrete Structures, Technical University Budapest*, (In Hungarian), Special Issue, multiplied.
- Kovács, B. (1997) "The 'Shear-Wall' Model" (In Hungarian) *Budapesti Műszaki Egyetem Építőmérnöki Kar Vasbetonszerkezetek Tanszéke Tudományos Közleményei*, pp. 113-119.
- Lenkei, P. (1966), "Some Problems of Yield Condition for Reinforced Concrete Slabs", *ÉTI. Bulletin 2*, pp. 36-41.
- Lenkei, P. Szalai, K. (1994), "Hungarian Experience and EUROCODE 2" *Proceedings of the Workshop*, Czech Technical University, Prague.
- Mayer, M. (1926) "Safety of Building Structures and their Calculation according to Limit Forces instead of Admissible Stresses" (In German), Springer, Berlin.
- Menyhárd, I. (with Co-Authors) (1951) "New Design Method for Reinforced Concrete Structures. Design Method Based Safety Factors and Ultimate State Theory", (In Hungarian), *Építőipari Könyv- és Lapkiadó Vállalat*, Budapest
- Mihailich, Gy., Haviár, Gy. (1966), "The Beginning and First Establishments



- of Reinforced Concrete Construction in Hungary” (In Hungarian), *Akadémiai Kiadó*, Budapest
- Misztéth, E. (1974) “Statical Design on Probability Base” (In Hungarian) *ÉTK*, Budapest
- Misztéth, E. (2001) “Design Theory” (In Hungarian), *Akadémiai Kiadó*, Budapest
- MSZ-EN (1990) “Bases of Structural Design” (In Hungarian), Budapest
- Palotás, L. (1967) “Reinforced Concrete Study” (In Hungarian), *Tankönyvkiadó*, Budapest
- Rényi, A. (1954) “Theory of Probability”. (In Hungarian). *Tankönyvkiadó*, Budapest.
- Szalai, K. (1974) “Some Questions of Design Theory of Reinforced Concrete Structures” (In Hungarian) *Mélyépítéstudományi Szemle*, pp. 303-305.
- Szalai, K. (1987\*, 1996\*\*) “Reinforced Concrete Structures.” (In Hungarian), \**Tankönyvkiadó*, \*\**Műegyetemi Kiadó*, Budapest
- Szalai, K. (2002). “Components of Partial Factors for Construction Materials” (In Hungarian), *Budapesti Műszaki és Gazdaságtudományi Egyetem Építőmérnöki Kar Hidak és Szerkezetek Tanszéke Tudományos Közleményei*, pp. 155-160.
- Szalai, K. (2003), “The Introduction of the Design with Partial Safety Factors in Years 1949-51 in Hungary.” (In Hungarian), *Tartószerkezeti Kutatások Évfordulós kötet Lenkei Péter tiszteletére Pécs*, 107-115.
- Szalai, K., Farkas, Gy., Kovács, T. (2002) “Optimization of Eastern and Western European Safety Levels of Load Carrying Structures in EC Prescriptions” (In Hungarian), *Közúti és Mélyépítési Szemle*, pp. 201-210.
- Szalai, K., Lenkei, P. (1992) “Hungarian Experience in Structural Design Coding (Historical Antecedents of Eurocode-2)” *Periodica Polytechnica*, Series Civil Engineering, Vol. 36, pp. 114-122.
- Tassi, G. (1968) “On the Prescriptions in the New Code for Highway Bridges related to Prestressed Concrete Structures” (In Hungarian), *Mélyépítéstudományi Szemle*, Budapest, pp. 502-505.
- Tassi, G., Windisch, A. (1974) “Technical-Economic Impacts of the New Hungarian Code MSZ 15022/2-1971 for Prestressed Concrete Structures” (In Hungarian), *Magyar Építőipar*, pp. 97-103.
- Prof. György Farkas** (1947), Civil Eng., completed also the post-graduate course in Engineering Mathematics, PhD, Dr.-habil., Head of Department of Structural Engineering, Budapest University of Technology and Economics, former Dean of Civil Engineering Faculty, Main field of activity: Modelling and strengthening of R.C. and P.C. structures, post-tensioned floor structures, dynamics of structures, HSC and HPC structures. Member of Hungarian Group of *fib*.
- Tamás Kovács** (1974), Civil Eng., Assistant to Professor at the Department of Structural Engineering Budapest University of Technology and Economics, Main field of interest: Modelling and estimation of damages strengthening of RC and PC structures based on dynamic characteristics, strengthening of concrete bridges, HSC and HPC. Member of Hungarian Group of *fib*.
- Prof. Kálmán Szalai** (1930) Civil Eng. (1953), Doctor of Tech. Sci. (Hung. Acad. Sci. 1976), Professor Emeritus at the Department of Structural Engineering, Budapest University of Technology and Economics (till 2000), afterwards research Professor. Main field of activity: Design theory of concrete, R.C. and P.C. bridge and building structures, Quality control, surveying and strengthening, HSC, HPC. Corrosion protection of R.C. structures. Member of Hungarian Group of *fib*.
- Assoc. Prof. Antal Lovas** (1946), Civil Eng. completed also the post-graduate course in Engineering Mathematics, PhD. Dean of Civil Engineering Faculty, Budapest University of Technology and Economics. Teaches at the Department of Structural Engineering, Main field of activity: Theory of structures. Statics, dynamics and strength of concrete structures Member of Hungarian Group of *fib*.



András Árpád Sipos – Prof. Gábor Domokos

*In our paper we show a robustly convergent algorithm for the calculation of spatial deformations of cracked, elastic RC bars. Elastic deflections of RC beams can be computed by integrating the curvature along the structure where the neutral axis of each (cracked) section must be determined. Locating the neutral axis of an arbitrary cross-section under biaxial bending and compression is a highly non-linear problem.*

*The core of the algorithm is a direct recursion derived from the equilibrium conditions to calculate the neutral axis of a cracked cross-section. We proved that the 2D map associated with this iterative method has a unique, stable fixed point; the neutral axis belonging to this fixed point is the equilibrium solution. In numerical simulations we found the recursion being globally convergent.*

*We embedded this iterative method into a parallel search algorithm to calculate the deformations of reinforced concrete bars. The nonlinear effects (creep, shrinkage, etc), which are normally considered in the engineering practice, do not affect the convergence properties of the algorithm. After describing the algorithm we give numerical examples including the calculation of a prestressed beam, a cracked RC frame and the postcritical behaviour of RC columns.*

**Keywords:** spatial deformation, Parallel Hybrid Algorithm, globally convergent recursion, eccentric compression, arbitrary cross section

## 1. INTRODUCTION

In this paper we introduce a fast and efficient algorithm to calculate the spatial deformations of prestressed concrete beams or asymmetrically compressed columns. The literature on the spatial deformations of elastic rods is rich, these works are inspired as well by the engineering practice (Domokos, 1994, 1995; Domokos & Gáspár 1995;) as by the mechanical modeling of the DNA (Coleman et al. 1995; Swigon et al. 1998) and the explanation of other biological phenomena (Goriely et al. 1998, 2002). Apparently, no mathematically consistent, convergent algorithm is available for beams without (or with limited) tensile strength. The spatial deformations can be computed by the integration of the curvature along the bar axis. As the core of the algorithm one has to calculate the stress distribution of the cross sections. In the literature the latter problem is either solved by the Newton Raphson, the Quasi Newton method or by the Finite Element Method (FEM) (Brøndum-Nielsen, 1979, 1986, Consanza et al. 1997). These methods are rather complicated. FEM is, in general, not consistent with Kirchhoff rod theory, furthermore, one can show examples of divergent behaviour, therefore these methods can hardly serve as the core of a robust algorithm to calculate spatial deformations.

Here we propose an algorithm which is fully consistent with classical Kirchhoff rod theory. The stress distribution of an arbitrary cross section can be calculated by a direct recursion based on the equilibrium conditions. To the best of our knowledge the method is globally and robustly convergent. The uniqueness of solutions and the stability of the only fixed point are analytically proven in (Sipos, 2006). We embedded the recursion into the core of the PHA (Parallel Hybrid Algorithm)

(Domokos et al., 2004), which is a solver for boundary value problems. Since the PHA does not use corrective iterative steps to find the equilibrium paths the proposed method is very robust. The method is capable to be applied in the engineering practice (Sipos et al. 2005).

The first part of our paper describes the method, the analytical proofs in (Sipos et al. 2005) will only be referred to. The second part shows the equilibrium paths of a prestressed concrete beam, a column in a frame and an RC rod as examples. Finally, we draw conclusions.

## 2. DESCRIPTION OF THE PROPOSED METHOD

### 2.1 Determining the neutral axis of an arbitrary cross section

We consider a cross section of arbitrary shape, belonging to a reinforced concrete beam (or column). The concrete is assumed to be elastic, with small tensile and large compressive strength, the material law of the steel is symmetrical (Fig. 1). Locating the neutral axis is a highly nonlinear problem, since the unknown neutral axis is part of the boundary of the working (compressed) concrete area. We propose a direct recursion based on the equilibrium equations (Sipos 2006). The method can be associated with a 2D map. Although nonlinear 2D maps often exhibit chaotic behaviour, we proved that the recursion has a unique, super-stable fixed point. In numerical simulations we found our method to be *globally convergent*. Below we describe our scheme.

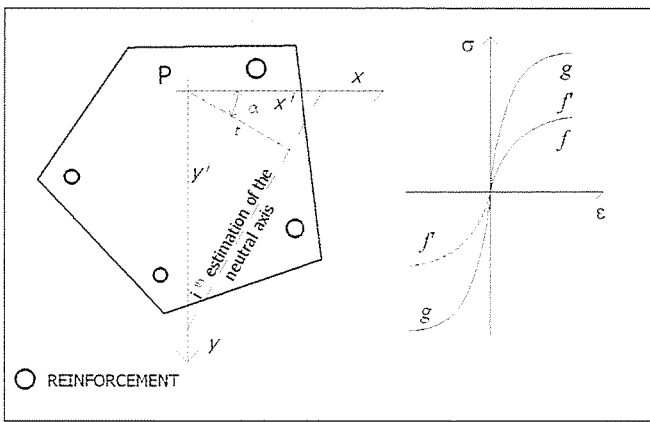


**Fig. 1:** An arbitrary RC cross section and the stress-strain relations of the concrete and the reinforcement (in different scales)

Let the compressive force be denoted by  $F$ , its point of application by  $P$  (Fig. 1). We use a global  $[xy]$  coordinate system, which is a freely chosen coordinate system having the origin at the point  $P$ . Let  $f(\epsilon)$  denote the stress-strain relation of the concrete,  $g(\epsilon)$  the stress-strain relation of the reinforcement,  $A_c$  and  $A_r$  denote the area of the concrete and the reinforcement, respectively. In each step of the iteration we calculate the neutral axis assuming (temporarily) that the concrete has tensile strength. The stress-strain relation for this case is denoted by  $f'(\epsilon)$ , where  $f'(\epsilon) = f(\epsilon)$  if  $\epsilon > 0$  and  $f'(\epsilon) = -f(-\epsilon)$  if  $\epsilon < 0$ . After identifying the  $i^{\text{th}}$  estimate on the neutral axis, intersecting  $x$  and  $y$  at  $x_i$  and  $y_i$  respectively, the total area of reinforcement  $A_r$  and the compressed concrete area  $A_c$  define the "active" part of the cross section, which is the input of the  $(i+1)^{\text{st}}$  step of the recursion. Accepting the hypothesis of plane cross sections, the strains can be expressed as

$$\epsilon = x \cos \alpha + y \sin \alpha - t, \quad (1)$$

$$\alpha = \arctan(y_i / x_i) \quad t = \frac{x_i y_i}{\sqrt{x_i^2 + y_i^2}} \quad (2)$$

The equations of equilibrium are the followings:

$$\int_{A_c} f'(\epsilon) dA + \int_{A_r} g(\epsilon) dA = F, \quad (3)$$

$$\int_{A_c} x f'(\epsilon) dA + \int_{A_r} x g(\epsilon) dA = 0, \quad (4)$$

$$\int_{A_c} y f'(\epsilon) dA + \int_{A_r} y g(\epsilon) dA = 0 \dots \quad (5)$$

As long as

$$f(\epsilon) = c \cdot \epsilon^k, \quad (6)$$

where  $c$  and  $k$  are constants, the location of the neutral axis does not depend on the absolute value of the load  $F$ , i.e. eq. (3) is independent on (4)-(5). In this case the general form of the iteration can be given as:

$$\begin{bmatrix} x^i \\ y^i \end{bmatrix} = \begin{bmatrix} F(x^{i-1}, y^{i-1}) \\ G(x^{i-1}, y^{i-1}) \end{bmatrix}, \quad (7)$$

where  $F(x,y)$  and  $G(x,y)$  are derived from eq. (4) and (5). In case of linear elasticity ( $f(\epsilon) = c\epsilon$ )  $F$  and  $G$  can be given explicitly as

$$\begin{bmatrix} x^i \\ y^i \end{bmatrix} = \begin{bmatrix} F(x^{i-1}, y^{i-1}) \\ G(x^{i-1}, y^{i-1}) \end{bmatrix} = \begin{bmatrix} (D_{xy}^{i-1})^2 - I_x^{i-1} I_y^{i-1} \\ D_{xy}^{i-1} S_x^{i-1} - I_x^{i-1} S_y^{i-1} \\ (D_{xy}^{i-1})^2 - I_y^{i-1} I_x^{i-1} \\ D_{xy}^{i-1} S_y^{i-1} - I_y^{i-1} S_x^{i-1} \end{bmatrix}, \quad (8)$$

where  $S_x, S_y, I_x, I_y, D_{xy}$  are the first and second moments of area of the actual cross section, respectively. The map given in eq. (7) has only one solution resulting there is only one fixed point. For the map given in eq. (8) we proved that this only fixed point is superstable, namely both eigenvalues of the matrix of stability for the linearized system equal zero. For a compressed, symmetrical cross section under uniaxial bending the map describing the recursion is only one dimensional. We proved the global convergence for this case provided the first estimation on the neutral axis is perpendicular to the axis of symmetry. Although we were unable to extend this proof to the general, two dimensional case, we are convinced that the same mechanism governs it as well. In systematic numerical trials we found the method to be globally convergent even for very unusual shapes.

## 2.2 The Parallel Hybrid Algorithm (PHA)

To calculate the spatial deformation of a rod with given end-conditions, one has to solve a boundary value problem (BVP). In the literature there are several path-following algorithms to solve BVPs. In our case, where detached (disconnected) branches of the equilibrium path can occur, these methods do not seem to be fully adequate. We applied the Parallel Hybrid Algorithm (PHA), an iteration-free boundary value problem solver (Gáspár et al., 1997). We describe the PHA in a simple, planar example: a homogeneous, linearly elastic cantilever beam under axial compressive load  $P$  (Fig. 2).

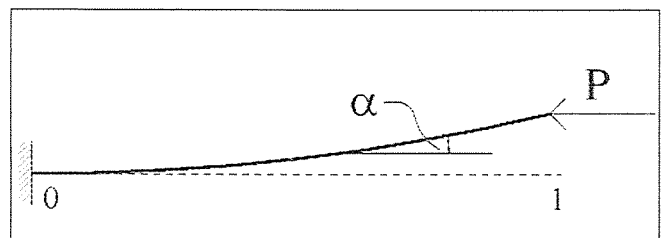


**Fig. 2:** Illustration for the PHA method. an axially loaded cantilever beam.

Here we have a simple differential equation defining the shape:

$$EI\alpha'' + P \sin(\alpha) = 0, \quad (9)$$

where  $\alpha$  denotes the slope of the bar axis,  $EI$  is the bending stiffness. In this example we have two variables (i.e. non-constant initial conditions and parameters), the initial bending moment  $\alpha'(0) = M(0)$  and the load parameter  $P$ . The far-end value  $\alpha'(1) = M(L)$  can be viewed as function  $f(P, M(0))$ , assuming that an integrator is available. (In the general case, we have  $n+1$  variables and  $n$  functions, the former define

the *Global Representation Space (GRS)* of the problem. The variables  $v_j$  are the non-constant boundary conditions at  $s=0$  (and the load parameter), the function values are the prescribed conditions at  $s=L$ .)

Now we seek the solutions of  $f=0$ . A fast and efficient parallel algorithm, the so-called *Parallel Hybrid Algorithm (PHA)* is presented in (Domokos et al., 2004) for the solution of such equation systems. The cantilever beam of Fig. 2. can be reduced to a single function, depending on 2 variables. In case of spatial deformations of a reinforced concrete beam, the system of 5 functions depending on 6 variables has to be solved (for details, see section 3.3.).

The PHA computation starts with the discretization of the GRS by choosing a symplectic grid, in case of the cantilever problem in two dimensions, this symplectic grid contains triangles. The function  $f$  is evaluated at the meshpoints and linearly interpolated in the symplectic domains. Since the calculation of two simplexes is independent, the computation can be carried out in a parallel environment.

The PHA was implemented under PVM system (Parallel Virtual Machine). Big advantage of the simplex method is that only the finite-dimensional GRS points of the bifurcation diagram are stored, not the final shape of the bar. This latter can be easily re-computed by integration for a selected point of the equilibrium path. In our work we implemented the recursion drafted in part 2.1 into the core of the Parallel Hybrid Algorithm. An application has been also developed to show the final shape and the possibly cracked zones belonging to the chosen point of the bifurcation diagram. The user interface enables users to carry out calculations in the parallel environment easily via a web browser.

## 2.3 TAKING THE MATERIAL PROPERTIES INTO ACCOUNT

Our method considers the material properties of reinforced concrete by applying the corresponding relations of the *EC2* standard. This approach is sufficient for engineering practice and enables the algorithm to handle real engineering problems in a reliable manner. As far as our current numerical simulations predict, the nonlinearities originating from creep, shrinkage, non-linear material behavior or tension-stiffening do not affect the global convergence of the proposed method. The calculation of the maximal value  $P_{max}$ , the initial value  $P_{m,0}$  of the prestressing force and the time dependent losses of prestress are also based on the *EC2*.

## 3. EXAMPLES

### 3.1 Deformations of a prestressed concrete beam

Due to the applied technologies, a slight asymmetry may occur during the prestressing of an RC beam. The asymmetry originates from the slight difference in the prestressing force in the symmetrically placed wires and from the difference in the Young's modulus of the concrete in different regions of the beam. This asymmetry can produce relatively high deformations in case of prestressed concrete bridge beams with a span higher than 30 m. Since bridge girders are prefabricated elements, these deformations can make the assembly of the structure

difficult, or even impossible. The method described in the first part is capable to predict such unfavourable deformations with very high accuracy, even in the design phase.

In this paper we give a simple example to explain the abrupt growth of deformation over a threshold in the span. Essentially, this spatial deformation corresponds to the lateral buckling of the beam. Analytical estimates for the buckling load are available (Kollár, 1991), our method can check these estimates, compute postcritical behaviour and equilibria for beams with geometrical imperfections. The beam is supposed to be unloaded except the prestress and its own weight denoted, by  $q$ . We consider  $P_{m,0}$  according to the *EC2* as a prestressing force, because the unfavourable deformations occur some days after the manufacturing, that is why the time dependent losses of the prestressing force caused by creep, shrinkage and relaxation are not taken into account.

The beam is supposed to be simply supported with planar hinges at both ends. We consider the cross section given in Fig.3. We assume the concrete has reached 80% of its designed strength. The asymmetry of the prestressing force is handled as an eccentricity denoted by  $\delta$  of the prestressing wire on the

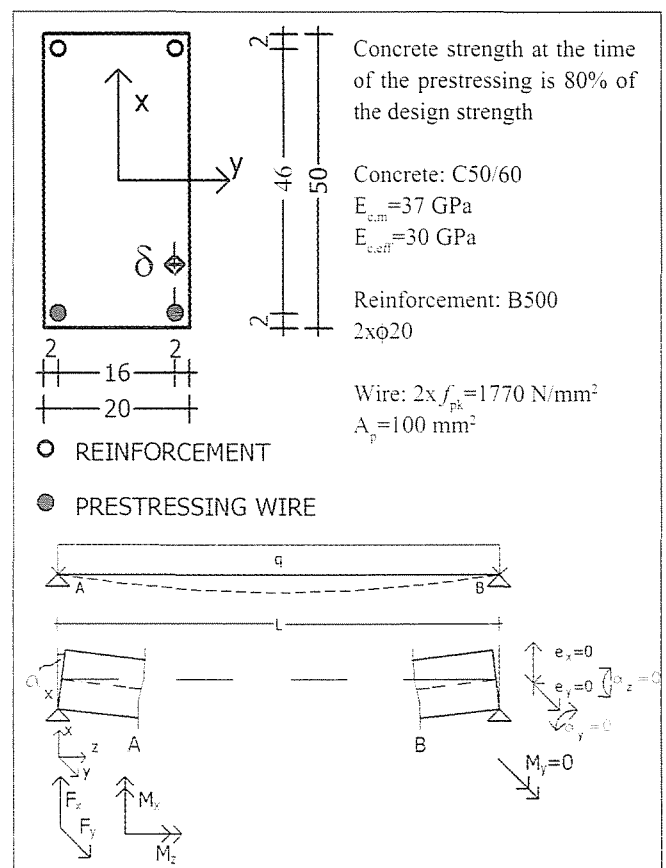
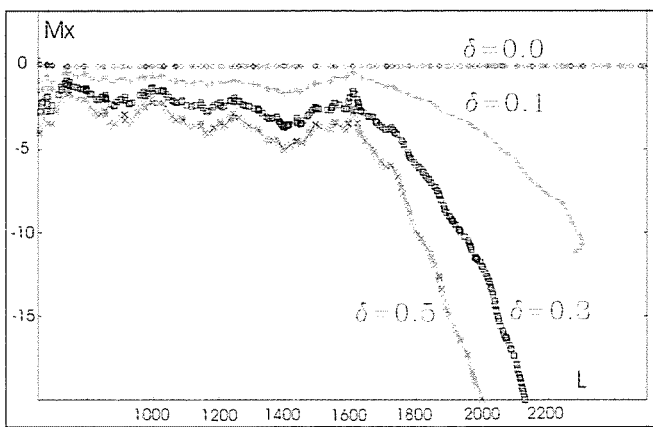


Fig. 3: A prestressed concrete beam,  $q=2.12$  kN/m

right side, resulting an eccentricity in the prestressing force in the direction  $y$ . The deformation is characterized by the middle deflection of the beam in the directions  $x$  and  $y$ .

For this problem the GRS is 6 dimensional. The variables are  $F_x, F_y, M_x, M_y, \alpha_x$  at point A and the  $L$  length of the bar. Two of the functions are the zero displacements in the directions  $x$  and  $y$  ( $e_x=0, e_y=0$ ), two are the zero rotation around axes  $y$  and  $z$  ( $\alpha_y=0, \alpha_z=0$ ) and one function prescribe zero bending moment around axis  $y$  ( $M_y=0$ ) at point B.

The equilibrium paths is plotted in Fig. 4 in the space  $[L, M_x]$  for the symmetrical and several asymmetrical cases. Observe the sharp increase of moments (and deformations) at approximately  $L=1750$  cm. This phenomenon is due to the



**Fig. 4:** Equilibrium paths of the prestressed concrete beam for symmetrical and slightly asymmetrical prestressing force in the plane of the variables  $L$  and  $M_x$ .

lateral buckling of the beam, described in (Kollár,1991). The computed critical load agreed within 10% with the analytical estimate given in (Kollár,1991). Our computations show stable postcritical behaviour. We plan to compare our results to experimental data and to determine the imperfection-sensitivity curve.

### 3.2. SECOND ORDER MOMENT OF A COLUMN IN A FRAME

RC frame structures are often built *without additional bracing*, in this case the columns are clamped at the bottom and they are connected to the horizontal beam by hinges. The columns are under compression and biaxial bending. Calculations often neglect the effect of the limited tensile strength of the concrete, in this way the second order moments are underestimated. Although some software tools are capable to calculate second order moment taking the *effective stiffness* of the columns into account, to the best of our knowledge they cannot handle prestressing force and cross sections with arbitrary shape.

In this part we apply our method to calculate the second order moments of an RC column being an element of a simple

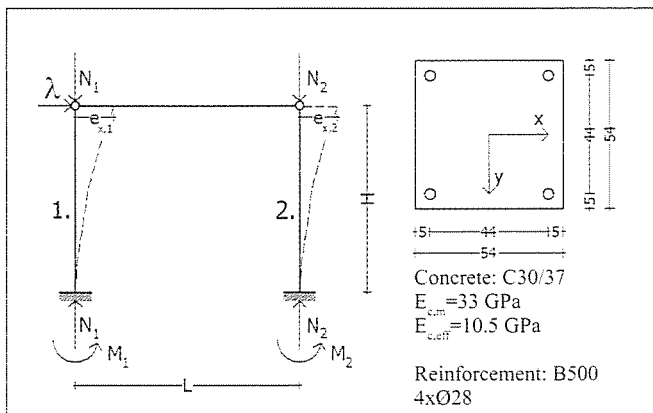


**Fig. 5:** A simple frame with clamped columns at the bottom

frame structure. The dimensions of the frame, the loads, the cross section of the columns, and the material properties are given in Fig. 5.

Assuming the deformations of the horizontal beam to be arbitrary small, the planar case can be solved as a 2 dimensional problem; the columns of the frame can be computed separately. (PHA is capable to solve the general problem, i.e. the deformations of the beam are also taken into account, this can be solved as a 6D problem.) Let  $j$  denote the serial number of a given column, in our case  $j=1,2$ . The two variables are the

horizontal force  $\lambda$  and the  $e_{x,j}$  horizontal displacement of the top point. The reactions ( $N_j, M_j$ ) can be computed from  $\lambda$  and  $e_{x,j}$  at the clamped ends. Solving the IVP from the reactions, the horizontal displacement  $e_{x,calc,j}$  of the top point can be calculated. The investigated function is  $f = e_{x,j} - e_{x,calc,j}$ .

The results of the PHA computation can be shown on a  $\lambda - e_{x,j}$  diagram for each column ( $j=1,2$ ). Since the horizontal displacement of both columns must be equal, the diagrams can be added. Having a design value for  $\lambda$ , one can get the final horizontal displacement  $e_{x,final}$  of the structure from the diagram which contains the result of all columns (Fig. 6). In this way, frames with arbitrary number of columns can be

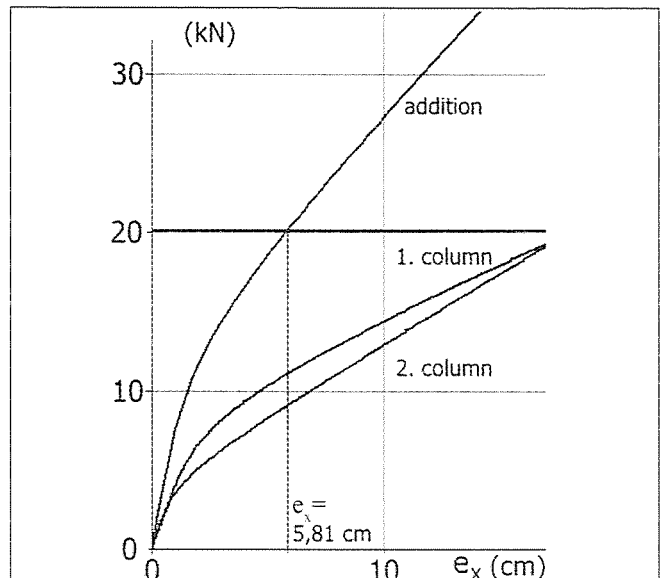


**Fig. 6:** Addition of the results

solved, even if the cross sections or the reinforcement of the columns are different (i.e.: frames having both prestressed and non-prestressed columns).

Having the final horizontal displacement, the second order moments can be determined for each column. Having the second order moments the cross section at the clamped end is checked in the ULS for compression and bending. The method is capable to handle those cases (i.e. asymmetrical cross section or reinforcement, biaxial bending with compression) where second order moments cannot be calculated by the equations given in the EC2 standard.

### 3.3 Equilibrium paths of RC rods

The method can be applied to determine the equilibrium paths of reinforced concrete rods with special boundary conditions.

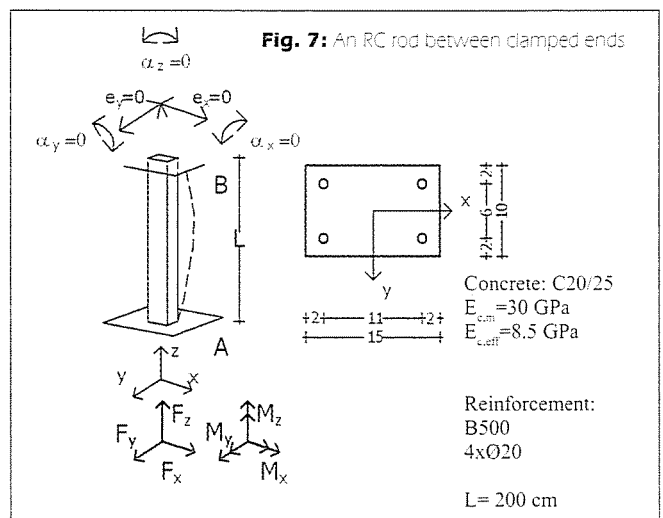


**Fig. 7:** An RC rod between clamped ends

		point A			
		Clamped	Planar hinge X	Planar hinge Y	Spatial hinge
point B	Clamped	+	-	-	+
	Free	+	x	x	x
	Planar hinge X	-	+	+	+
	Planar hinge Y	-	+	+	+
	Spatial hinge	+	+	+	-

+already implemented  
 -has not been implemented yet  
 xUnstable structure

**Table 1:** Calculating equilibrium paths of an RC rod - the considered boundary conditions

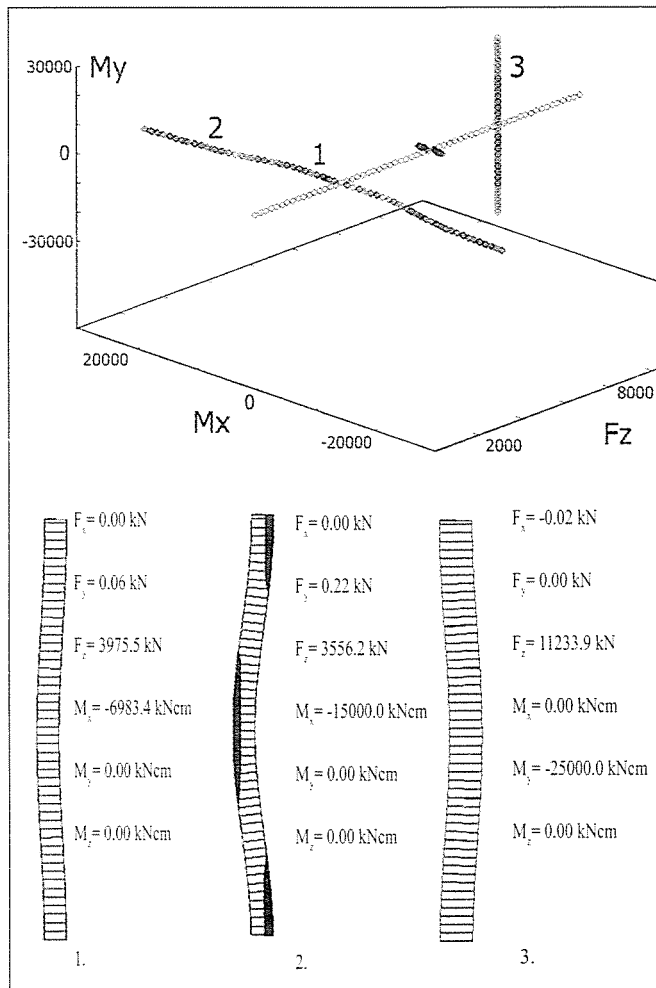


**Fig. 8:** The equilibrium path in the space of  $F_z$ ,  $M_x$ ,  $M_y$  and the corresponding shapes for points number 1, 2 and 3

Table 1. contains the cases which have been considered until now.

In this part we show the bifurcation diagram and some corresponding shapes of a rod between clamped ends. The cross section and other details are given on Fig.7. This is a 6 dimensional problem; the variables are the three reaction forces ( $F_x$ ,  $F_y$ ,  $F_z$ ) and the three reaction moments ( $M_x$ ,  $M_y$ ,  $M_z$ ) at the point A. Two from the five functions prescribe the zero displacements in both direction x and y ( $e_x=0$ ,  $e_y=0$ ), the other three prescribe zero rotation of the cross section around the three global coordinate axes ( $\alpha_x=0$ ,  $\alpha_y=0$ ,  $\alpha_z=0$ ) at point B. The critical loads belonging to the different buckling modes are not affected by the limited tensile strength of the concrete. The occurring cracks cause the unstable (decreasing) parts in the branches of the equilibrium path.

Fig.8. shows the equilibrium path in the space of the variables  $F_z$ ,  $M_x$  and  $M_y$  and three shapes belonging to the numbered points. Cracked zones are shaded. The method is

capable to determine the effective stiffness of arbitrary shaped bars under arbitrary loads.

## 4. CONCLUSIONS

In our paper we presented a method to calculate spatial deformations of reinforced concrete bars. The core of the algorithm is a globally, robustly convergent recursion which determines the neutral axis of an arbitrary reinforced concrete cross section. The recursion is capable to be used in the PHA, which is an efficient solver on boundary value problems. Using the method we investigated the spatial deformations of a prestressed beam, determined the second order moment for a column in a frame and calculated the equilibrium path for an RC rod between clamped ends.

## ACKNOWLEDGEMENT

This work was supported by OTKA grants TO46646, TS49885 and the NKFP No. 2\_009\_04. The support of BVM Épelem Ltd. is highly appreciated.

## REFERENCES

- Brøndum-Nielsen, T. (1979) "Stress Analysis of Concrete Sections Under Service Load", *ACI Journal, Proceedings*, V. 76., No. 2, pp. 195-211.
- Brøndum-Nielsen, T. (1986) "Serviceability Limit State Analysis of Cracked, Polygonal Concrete Sections Under Biaxial or Symmetric Bending", *ACI Journal, Proceedings*, V. 83., No. 2, pp. 209-218.
- Coleman, B. D., Tobias, I. & Swigon D. (1995) "Theory of the influence of the end-conditions on the self-contact in DNA loops", *J. Chem. Phys.*, 103, pp. 9101-9109.
- Cosenza, E. and Debenardi, P. G. (1997) "Calculation of Stresses, Deformations and Deflections of Reinforced and Prestressed Concrete Elements in Service", *CEB Bulletin 235 "Serviceability models" Progress Report*, pp. 105-142.
- Domokos, G. (1994) "Global description of elastic bars", *Zeitschr. Angew. Math. Mech.*, 74, pp. T289-T291.
- Domokos, G. (1995) "A group-theoretic approach to the geometry of elastic rings", *J. Nonlin. Sci.*, 5, pp. 453-478.
- Domokos, G., Gáspár, Zs. (1995) "A global, direct algorithm for path-following and active static control of elastic bar structures", *Int. J. Struct. Mech.*, 23, pp. 549-571.
- Domokos G., Szeberényi I. (2004) "A Hybrid Parallel Approach to One-parameter Nonlinear Boundary Value Problems", *Comput. Assist. Mech. Eng. Sci.* 11, pp. 15-34.
- Gáspár, Zs., Domokos, G., Szeberényi, I. (1997) "A parallel algorithm for the global computation of elastic bar structures", *Comput. Assist. Mech. Eng. Sci.* 4, pp. 55-68.
- Goriely, A., McMillien, T. (2002) "Tendril perversion in intrinsically curved rods", *J. Nonlin. Sci.*, 12, pp. 241-281.

- Goriely, A. & Tabor, M. (1998) "The mechanics and dynamics of tendril perversion in climbing plants", *Phys. Lett.*, A250, pp. 311-318.
- Kollár, L. (1991) "*Special problems in the theory of stability in engineering*" (in Hungarian), Akadémiai Kiadó, Budapest
- Sipos, A. A., Domokos G., Gáspár Zs. (2005) "The convergence features of the 2D Pelikan iteration", *Építés- és építészettudomány*, 33 (1-2), pp. 205-217 (in Hungarian)
- Sipos, A. A., Domokos G. (2005) "Asymmetrical, spatial deformations of reinforced concrete columns and prestressed beams", *fib Symposium "Keep Concrete Attractive"*, Budapest, Vol. II, pp. 693-698.
- Sipos A. A. (2006) "A robust algorithm to calculate the spatial deformations of rods without tensile strength", *Proc. Estonian Acad. Sci. Phys. Math.*, 55, 2 (in press)
- Swigon, D., Coleman, B. D. & Tobias, I. (1998) "The elastic rod model for DNA and its application to tertiary structure of DNA minicircles in mononucleosomes", *Biophys. J.*, 74, pp. 2515-2530.

**András Árpád Sipos**, (1980), received his M.Sc. architect degree from the BME in 2003. He is a PhD student at the Dept. Mechanics, Materials and Structures. He is the member of the Hungarian Group of *fib*.

**Gábor Domokos**, (1961), received his M.Sc. degree from the BME in 1986. Doctor of Sciences since 1997, adjunct professor, Dept. Theor. and Appl. Mech., Cornell University since 1999, Corresponding member of the Hung. Acad of Sci. since 2004.



Prof. György Balázs

Long term loads induce creep deformations in concrete. The so called linear creep law is valid whenever the creep deformation is proportional to the load level. Present study indicates that the linear creep law is valid up to the load till the volumetric change (obtained from measurements on concrete prisms in three dimensions) is constant. The influencing factors to the limit of constant volumetric change are also analysed in the paper.

**Keywords:** linear creep law, silica fume, polymer impregnated concrete

## 1. INTRODUCTION

Based on their experimental results in the 1980s, Glanville and Davis assumed that Hooke's law is valid also for long term deformations, i.e. twice of the creep deformation belongs to twice of the load (Fig. 1). It was then called as *linear creep law* and it was considered to be valid up to the 30-40% of the concrete prism strength.

In several codes the validity of linear creep law is limited in  $0.45 f_{ck}$ , where  $f_{ck}$  is the characteristic compressive strength of concrete measured on a cylinder of 150 mm diameter and 300 mm height.

Since long time I was interested if the limit of linear creep law can be related to a given mechanical characteristic. According to my hypothesis this limit can be related to the failure mechanism of concrete. This hypothesis is detailed herein.

## 2. FAILURE MECHANISM OF CONCRETE

At the beginning of loading concrete compressive strains are practically proportional to the stresses in longitudinal directions and transverse tensile strains are also proportional. However, these proportionalities are not available close to failure. Failure stress (strength) is just a stress value that is preceded by a failure mechanism. The  $\sigma$ - $\epsilon$  relationship of concrete loaded centrally and uncracked before loading can be classified into the following parts according to the failure mechanism (Fig. 2):

1. Up to approximately 30% of the strength, there are no-considerable bond cracks between the aggregates and the cement stone.
2. Between 30 and 50% of the strength, small bond cracks may develop.
3. Between 50 and 70% of the strength, then cracks further open. At the top of this load range the failure process of concrete is started to be accompanied by acoustic signals.
4. In the following load range the inner structure of concrete is considerably weakened. An instabil crack may form that may even grow without increasing the load. This stress range can be called as critical stress range and its lower limit can be called as critical stress ( $\sigma_{crit}$ ).
5. In the final stress range micro cracks develop in the concrete which may lead to complete failure.

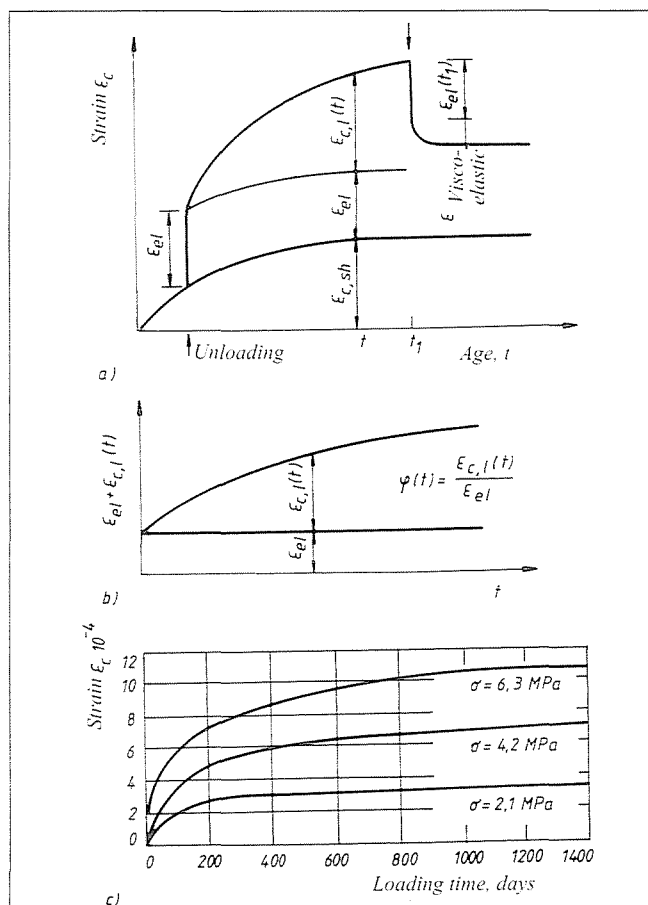


**Fig. 1:** Long term strains of concrete  
 a) Strains due to shrinkage and long term loads  
 b) Definition of creep factor  
 c) Test results by Möller and Brzesky (1937)



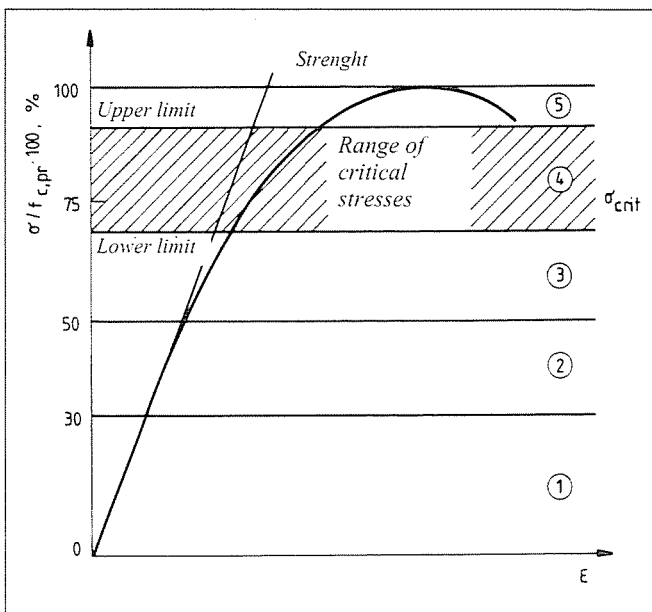


Fig. 2: Classification of failure process of compressed concrete

In order to be able to determine  $\sigma_{crit}$ , theoretical studies (Griffith, 1920; Stroeven, 1973), empirical studies (Rüsch, 1959; Rasch, 1962; Béres, 1963, 1968; Hsu-Slate-Sturman-Winter, 1963; Tamigava-Kosaka, 1975; Desayi, 1968; Egbers, 1969; Wahdan, 1974; Sasse, 1969) were carried out. I did a review of these studies in Ref. Balázs (2001).

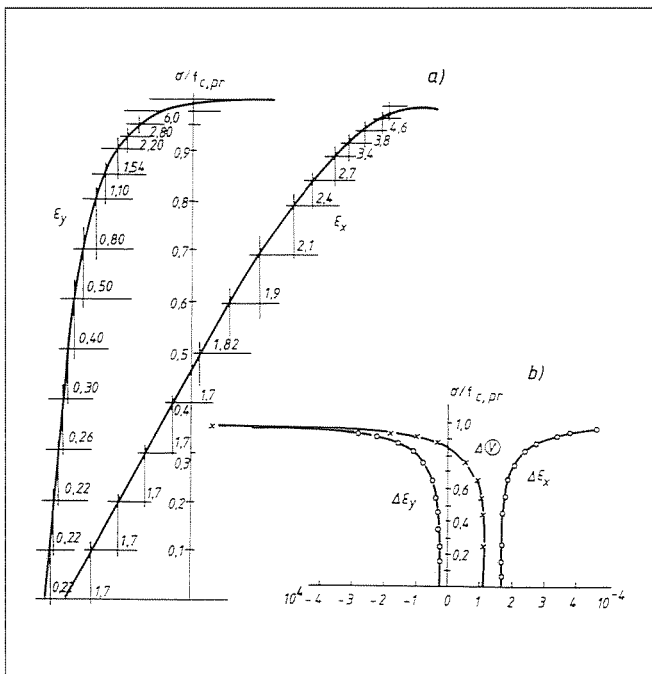
In our empirical studies we used the analysis of volumetric change (Béres, 1963, 1968).

During the evaluation of my test results I used an empirical method by measuring the longitudinal ( $\epsilon_x$ ) and transverse ( $\epsilon_y$ ) strains at middle heights of compressed prisms of 120·120·360 mm sides. Volumetric change ( $\Delta V$ ) is calculated then as:

$$\Delta V = \Delta\epsilon_x - 2\Delta\epsilon_y.$$

The evaluation is indicated in Fig. 3.  $\Delta V$  was calculated in steps of the  $\sigma$ - $\epsilon$  diagram. For relatively low loads the calculation steps were taken at 1/10 of the compressive strength, however, close to failure the steps were reduced.

Fig. 3: Calculation of the volumetric change ( $\Delta V$ ) from stress-strain measurements



The diagram of volumetric changes can have three different forms as it will be further explained in Chapter 3 (Fig. 4). In all three cases the diagrams start with a vertical branch. I call its top point as  $\sigma_{crit,l}$ . According to my hypothesis this can be considered as the maximum of the linear creep law or the lower limit of critical stress.

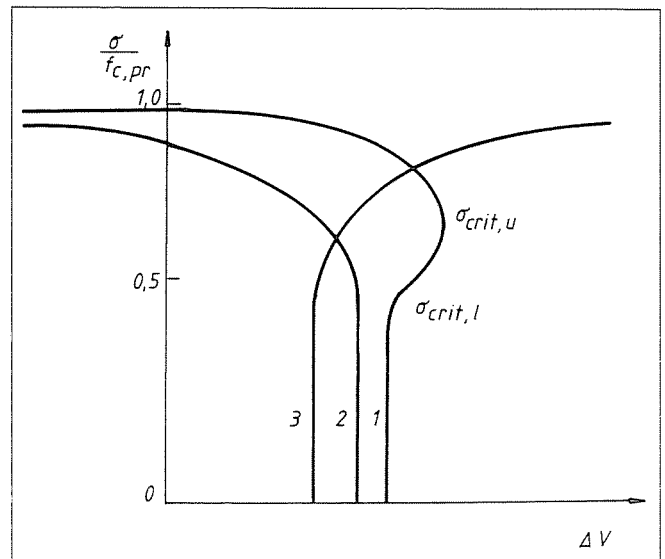


Fig. 4: Possible forms of the volumetric change diagram

### 3. INFLUENCING FACTORS OF THE VOLUMETRIC CHANGE DIAGRAM

A lot of research was carried out at the Department of Construction Materials, Budapest University of Technology between 1960 and 2000 related to the failure mechanism of concrete.

Examples will be shown indicating that  $\sigma_{crit,l}$  is not a constant value but it is influenced by various factors. In the following described *Test 1* was carried out between 1965 and 1970, *Test 2* between 1980 and 1990, *Test 3* between 1975 and 1980.

#### Test series 1

32 different concrete mixes were tested. Cement types were CEM I 42.5 and CEM I 32.5 from Tatabánya, Hungary. The aggregate was dried sand and gravel from river Danube, classified according to the diameter. Then we mixed the aggregate then to have grading curves A with maximum diameter of 8, 16 and 32 mm.

The cement content was between 100 and 160 kg/m<sup>3</sup>, the water-cement ratio was between 0.294 and 0.940. We tried to keep the same consistency it was checked by the Glanville-value (to be 0.72 and 0.82).

Cube strength was measured on 5 cubes of 200 mm sides to each mixes, prism strength was measured on prisms of 120·120·360 mm sides. In addition to them also flexural strength, splitting – tensile strength and direct – tensile strength were measured.

In Fig. 5 cube strength is presented as a function of the cement +0.25 mm diameter aggregate. These results can be approached by two lines which have a change of inclination just at the paste saturation point.

Lower ( $\sigma_{crit,l}$ ) and upper ( $\sigma_{crit,u}$ ) values of the critical stresses

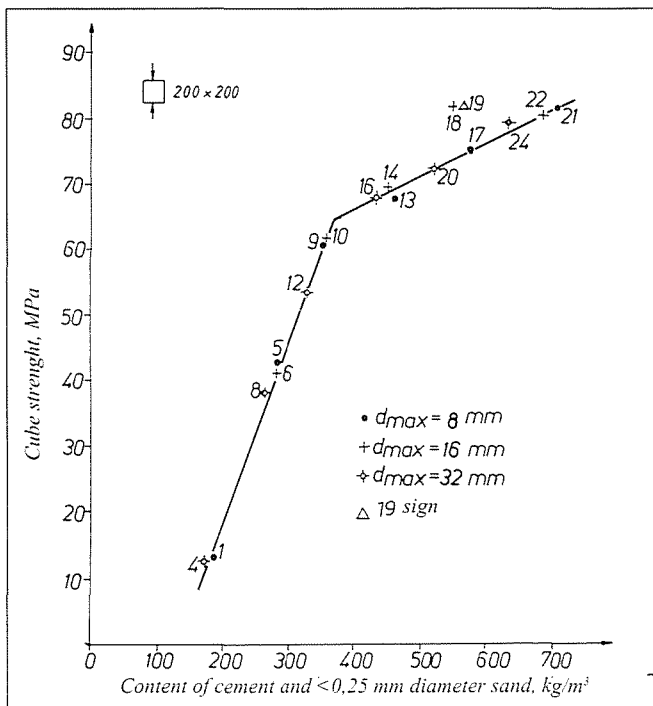


Fig. 5: Cube strenght as a function of content of cement and <0.25 mm diameter sand

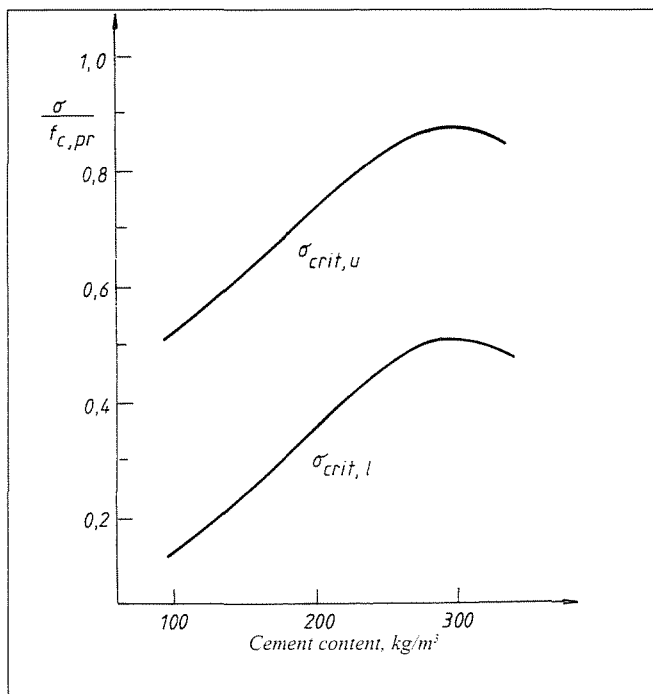


Fig. 6:  $\sigma_{crit,l}$  and  $\sigma_{crit,u}$  as a function of cement content

are presented in Fig. 6 which indicate that these values depend on the cement content.

### Test series 2

Specimens were prepared with CEM I 42.5 (produced in Beremend, Hungary). The aggregates were dry sand and gravel from river Danube with grading between A and B limit curves of  $d_{max} = 16$  mm.

Paste saturation was determined carefully. Maximal density of concrete was reached with additional 40-60 kg/m<sup>3</sup> cement compared to its theoretical value. This was considered as the practical value of paste saturation. By applying more cement, density of concrete did not increase and not even the strength owing to the increase of porosity which was counter acting.

In one of the tests the cement content (292 kg/m<sup>3</sup>) was considered to be the starting value which belonged to the theoretical value of paste saturation. Then the cement content

was stepwise increased. The water-cement ratio was decreased by keeping the consistency to be constant (being 0.82 to 0.84 according to the Glanville measurement). Fig. 7 presents the typical points of the experimentally determined volumetric change ( $\Delta V$ ) diagram. The x-axis of Fig. 7 indicates the additional amount of cement paste related to the paste saturation point. Test results indicate slight increase of  $\sigma_{crit,l}$  between 0.3 to 0.4  $f_{c,pr}$  with increasing amount of additional cement paste.

In other tests we started with the practical paste saturation (385 kg/m<sup>3</sup> cement). Then a 5 to 25% of cement was replaced by silica fume. The consistency was approximately the same, but the water-cement ratio slightly increased. The season of the increase of water-cement ratio was the high specific surface of silica fume. Fig. 8 indicates the volumetric change as a function of the silica fume content with the following conclusions:

- Addition of silica fume shifted  $\sigma_{crit,l}$  up to 0.55 to 0.6  $f_{c,pr}$ . Its probable reasons are (1) silica fume reacts with the lime hydrate which is produced during hydration and increases the amount of calcium-silicate-hydrate, on the other hand (2) silica fume improves bond of cement paste on the surface of aggregates which is a normally a relatively weak zone.
- Application of silica fume above 10% is not reasonable.
- Long term load improves crack sensitivity of concrete by increasing  $\sigma_{crit,l}$  owing to the increase in density of concrete under long term loads.

### Test series 3

In these series failure mechanism of polymer impregnated concretes (Balázs-Kovács, 1979, 1982; Balázs, 1982) were experimentally studied.

Fig. 7: Volumetric change of concrete as a function of extra amount of cement paste in addition to the paste saturation

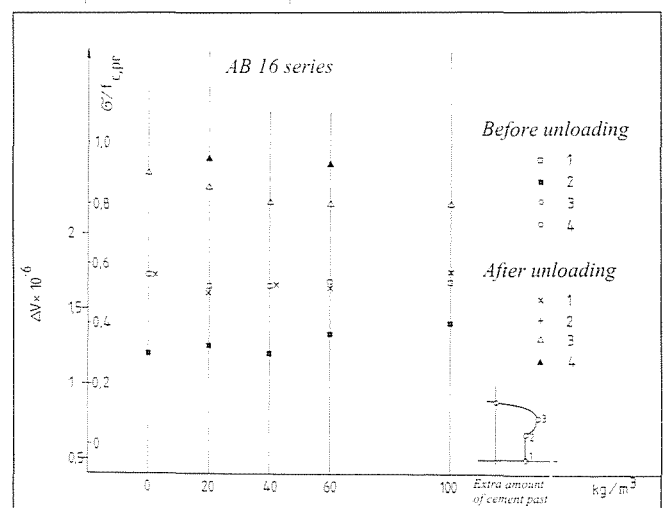
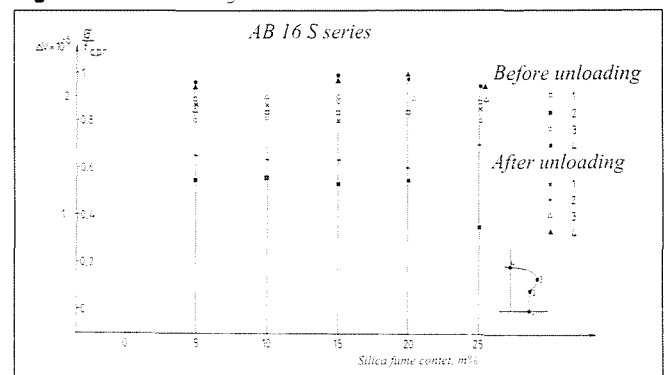
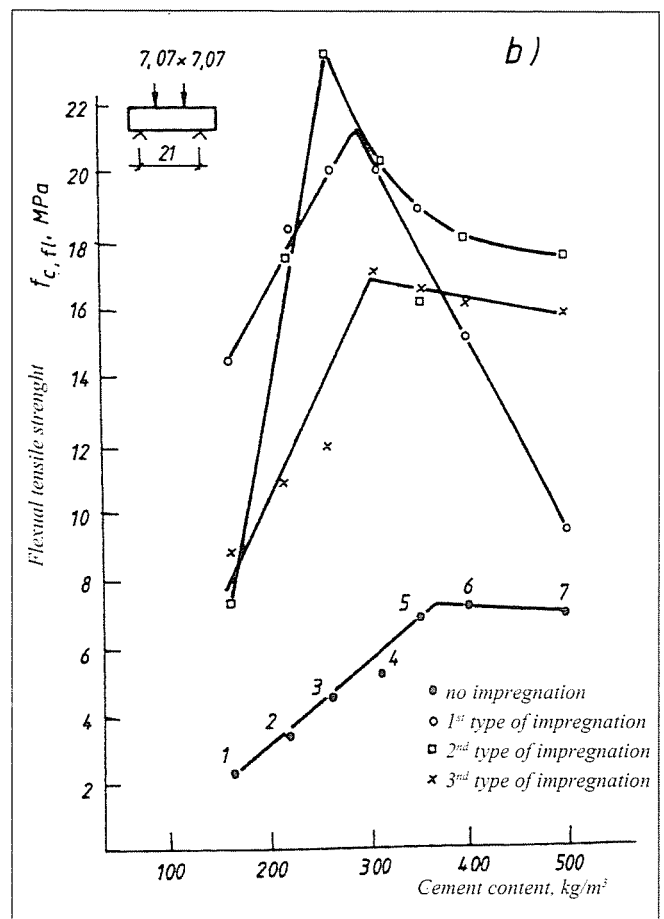
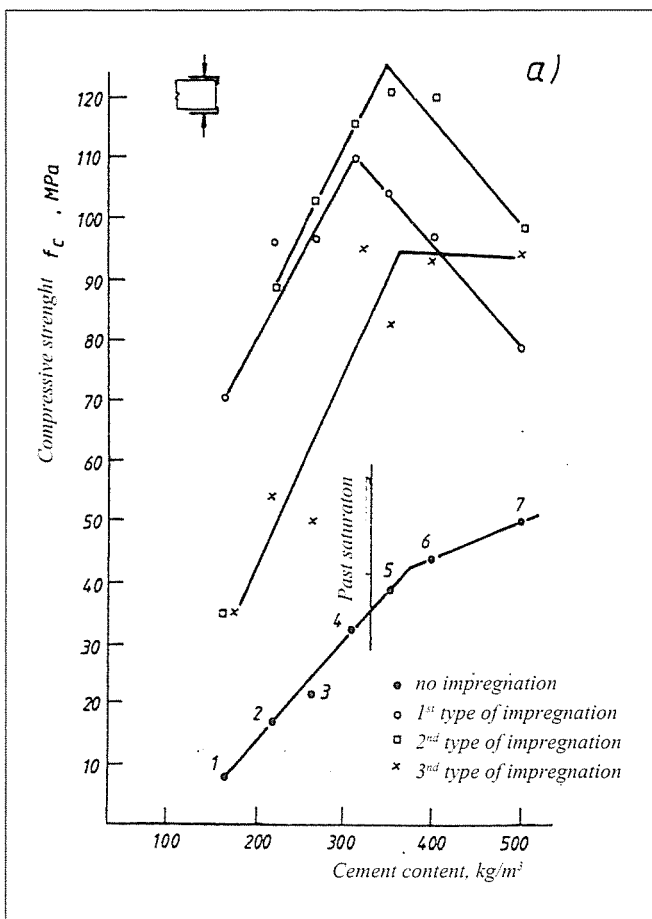


Fig. 8: Volumetric change of concrete as a function of silica fume content





**Fig. 9:** Strength of impregnated concretes (a) Compressive strength (b) Flexural tensile strength

Concretes were made with 165 to 500 kg/m<sup>3</sup> cement content, 0.81 to 0.345 water-cement ratios and Danube gravel and sand of  $d_{max} = 28$  mm with practically constant consistency. Specimens were impregnated after curing one week in water followed by 20 days in laboratory conditions and finally 24 hours drying at 150°C:

*1<sup>st</sup> type of impregnation:* 270 to 400 Pa vacuum was produced then methyl-metacrylate monomer was added to the surface and the vacuum was increased to 2700 to 4000 Pa. Then the vacuum was released continuously in 5 minutes. Specimens were then kept in the monomer for 30 minutes. Specimens

were then weighted and put into water which was heated up to 80 to 90°C. In this way the monomer was polymerized and became poly(methyl-metacrylate): PMMA.

*2<sup>nd</sup> type impregnation:* its difference to the 1<sup>st</sup> type of impregnation was that the specimens were put into boiling water before polymerization. This method was used because the slow heating up let a part of the monomer to leave.

*3<sup>rd</sup> type of impregnation:* specimens were kept for one day in MMA monomer then polymerization was carried out in water of 80°C.

Measured strength values as a function of the cement content is presented in Fig. 9. Test results indicate that both

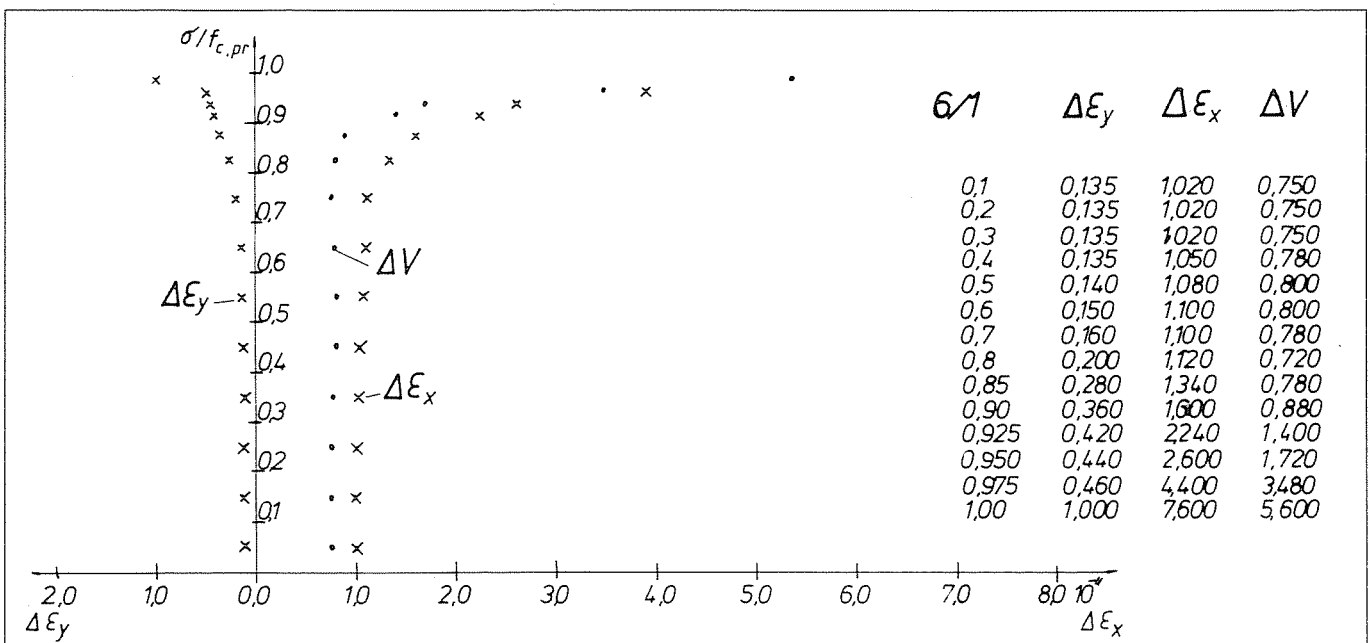


**Fig. 10:** Volumetric change diagramm (specimen Nr. 6)

compressive strength and flexural tensile strength increased considerably. We can consider as a new result that the highest increase was reached in case of paste saturated concretes.

Fig. 10 indicates the volumetric change of specimen 6 which contained 400 kg/m<sup>3</sup> cement with 0.38 water-cement ratio. Its compaction by Glanville was 0.75. Dry density of hardened concrete was 2295 kg/m<sup>3</sup>. Water absorption with gradual immersion was 3.95 V%. Fig. 10 indicates that  $\sigma_{crit.f}$  was about 75% of the failure load which is a very high value.

I take the opportunity to mention that  $\sigma_{crit.f}$  of autoclaved concrete (strength 100 to 120 N/mm<sup>2</sup>) was also high.

## 4. CONCLUSIONS

The paper presents the hypothesis that *the linear creep law* is valid up to the loads which induce constant volumetric changes of concrete in compression which is defined as:

$$\Delta V = \Delta \epsilon_x - 2 \Delta \epsilon_y$$

The presented experimental study indicated that the constant part of the volumetric change diagram depends on the paste saturation, the silica fume content, polymer impregnation or autoclave curing.

Present hypothesis indicates that the maximum load to linear creep should not be a constant portion of the design strength.

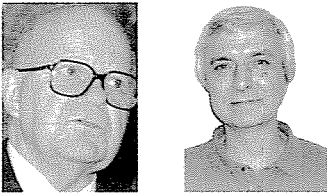
Further studies are needed to support present hypothesis.

## 5. REFERENCES

- Balázs, Gy. – Borján, J. ((1974), "High strength concrete by using gravel and sand", *BME Dept. of Construction Materials* 14/1974, KÖZDOK (in Hungarian)
- Balázs, Gy. – Kovács, K. (1979), "Influence of impregnation on concrete strength", *Journal Construction Materials* 1979/11. pp. 466-475 (in Hungarian)
- Balázs, Gy. – Kovács, K. (1982), "Polymer impregnated concrete", *Periodica Polytechnica*, Vol 26/1-2 pp. 89-98
- Balázs, Gy. (1982), "Analysis of internal structure of concrete", *Thesis for Doctor of Sciences, Hungarian Academy of Sciences* (in Hungarian)
- Balázs, Gy. – Zsigovics, I. (1991), "Theoretical studies on the durability of concrete 5. Past saturation and failure mechanism of concrete", *Research report OTKA 3000 (Hungarian Research Fund)* (in Hungarian)
- Balázs, Gy. (2001), "My own ways in concrete research", *Academy Press* (in Hungarian)
- Béres, L. (1963), "Test methods to study the macro-structural changes of concrete", *Research and development* (in Hungarian)
- Béres, L. (1968), "Structural changes of concrete under loading", *FIP Symposium*, 1968, pp. 86-90
- Bojtár, I. – Bagi, K. (1989), "Numerical analysis of state-changing process in granular assemblies", *Periodica Polytechnica Civil Engineering*.
- Desaxi, P. (1968), "A model to simulate the strength and deformation of concrete compression", *Matériaux et Construction* 1, 49.
- Eggers, G. (1969), "Die erste Ableitung von Spannungs-Dehnungs-Kurven und ihre Bedeutung bei der Ermittlung von Strukturveränderungen viskoelastischer Stoffe", *Materialprüfung* 11, 3.
- Griffith, A. A. (1920), "The phenomena of rupture and flaw in solids", *Philos. Royal Soc. of London, Serie A*, 221, pp. 163-178.
- Hsu, T. T. C. – Slate, F. C. (1963), "Tensile bond strength between aggregate and cement paste or mortar", *Journal of the American Concrete Institute*, No. 60, pp. 465-486.
- Hsu, T. T. C. – Slate, F. O. – Sturman, G. M. – Winter, G. (1963), "Micro-cracking of plain concrete and the shape of stress strain curve", *Journal of the American Concrete Institute, Proceedings*, Vol. 60, No. 2, pp. 209-224.
- Möller, K. – Brzesky, A. (1937), "Concrete and reinforced concrete", *University Press, Budapest* (in Hungarian)
- Rasch, Ch. (1962), "Spannungs-Dehnungs-Linien des Betons und Spannungsverteilung in der Biegezone bei konstanter Dehnungsgeschwindigkeit", *Deutscher Ausschuss für Stahlbeton, Heft 154*
- Rüsch, H. (1959), "Physical problems in testing of concrete", *Zement-Kalk-Gips*, 12, 1959/1, pp. 1-9.
- Sasse, H. R. (1969), "Zum Problem des Bruchverhaltens betonähnlicher Zweistoffsysteme", *Dissertation TH Aachen*
- Stroeven, P. (1973), "Some aspects of the micromechanics of concrete", *Stevin Laboratory, Technological Univ. of Delft*
- Tanigawa, Y. – Kosaka, Y. (1975), "Mechanism of fracture and failure of concrete a composite material", *Memoirs of the Faculty of Engineering, Nagoya University*, vol. 27, No. 2
- Wahdan, E. H. (1974), "Zur Übertragung bruchmechanischer Erkenntnisse auf Beton", *Dissertation TH Aachen*

**Prof. György Balázs** (1926), civil engineer (1950), Doctor of Sciences from the Hungarian Academy of Sciences, head of department (1976 to 1991) for the Department of Construction Materials at the Budapest University of Technology. His main fields of interest are: construction materials, concrete technology, theory of concrete, durability, history of concrete and reinforced concrete. He published 20 books, 6 chapters in books and 260 articles.

# GRAPHO-ANALYTICAL CALCULATION OF PARTICLE SIZE DISTRIBUTION CHARACTERISTICS OF CONCRETE AGGREGATES



Prof. Tibor Kausay – Dr. Tamás Simon

The grading of concrete aggregates (sands, sandy gravels, crushed stones, stone dusts etc.) numerically the particle size distribution is characterised namely by the mean value, the standard deviation, the variation coefficient, the average particle size, the fineness modulus and the specific surface area (by volume). The article introduces a united system for the determination of particle size distribution characteristics. The developed grapho-analytic calculation method unites the visualization of graphic methods with the consistence of the analytic methods. The application of the method means the determination of the particle size distribution characteristics by solving simple equations which represent the areas above or under the grading curves which are presented in the appropriate coordinate system. The usability of the equations is greatly helped by computerisation. The figures offer better understanding of the formulas.

Keywords: aggregate, sandy gravel, crushed stone, grading, fineness modulus, specific surface

## 1. INTRODUCTION

During research, development and high standard design of the aggregates or fillers of concretes, mortars and asphalts, the grading of the sands, sandy gravels, crushed stones and stone dusts can be numerically specified by the mean value, the standard deviation, the variation coefficient, the average particle size, the logarithmic fineness modulus and the specific surface by volume (Kausay, 1975). The determination of them is always based on the result of a sieve or a sedimentation test. The calculation however can be done in two ways that is graphically or analytically, depending on that the area under or above the curve in the coordinate system - proportional to the grading properties - is determined or we describe the values giving the grading properties. The area determination is done basically by measurement while the values are evaluated solely by calculations.

Both methods have differential and also differentia variety.

The developed method carries the signs of grapho-analytical differentia calculus. The method is grapho-analytical, because by area calculation we carry out moment determination, and differentia calculus, and because for the determination of the grading properties we use directly the results of the sieve or the sedimentation test.

## 2. THE PRINCIPLE OF THE CALCULATIONS

As a principle of the calculations we use the common property of the grading, that the value of each can be expressed depending on their characteristics using a coordinate system which has a suitably transformed  $x$  axis by the area above or under the grading curve. For this the scale on the  $x$  axis should be chosen in such a manner that in the coordinate system the areas will be proportional to the grading properties, what can be achieved by transforming the originally linear  $x$  axis suitably. The linearly scaled  $x$  axis is the carrier of the particle size, while the transformed axis carries the derivative of the particle sizes.

At first let us solve the calculation of the area in general because the determination of the grading properties can be derived from the solution of the general form of the area under the grading curve.

In the present paper under the  $p_\delta$  density function and its derivatives must always be understood a probability density function which is expressing mass proportion, while under the corresponding  $P_\delta$  distribution function and its derivatives always the relative mass distribution function should be understood even if the scaling of the  $y$  axis is in mass percentages.

According to Fig. 1. and 2. let us indicate the value of the particle size distribution by  $P$ , the boundaries of the subsets by  $\delta$ , which in case of linearly scaled  $x$  axis means  $d$ , in case of quadratic scaling  $d^2$ , in case of logarithmically scaled  $x$  axis  $\lg d$ , while in case of reciprocal  $x$  axis scaling would mean  $d^{-1}$ . The unit of  $d$  is mm. Let the indexes refer to the subset boundaries, to the first the no. 1 and  $n$  to the last which are the particle bulk's smallest and biggest particle size.

To derive the general form of the relation we should take the grading curve as consisting of straight lines and calculate the  $T_\delta$  area under the  $P_\delta$  grading curve:

$$\begin{aligned}
 T_\delta &= \int_{\delta_1}^{\delta_n} P \, d\delta = \sum_{i=1}^{n-1} T_i = \frac{1}{100} \cdot \sum_{i=1}^{n-1} \frac{P_i^\% + P_{i+1}^\%}{2} \cdot (\delta_{i+1} - \delta_i) = \\
 &= \frac{1}{100} \cdot \left[ \frac{P_1^\% + P_2^\%}{2} \cdot (\delta_2 - \delta_1) + \frac{P_2^\% + P_3^\%}{2} \cdot (\delta_3 - \delta_2) + \dots + \frac{P_{n-1}^\% + P_n^\%}{2} \cdot (\delta_n - \delta_{n-1}) \right] = \\
 &= \frac{1}{200} \cdot \left[ 100 \cdot (\delta_n - \delta_{n-1}) + \sum_{i=2}^{n-1} P_i^\% \cdot (\delta_{i+1} - \delta_{i-1}) \right] \quad (1)
 \end{aligned}$$

Following we look for the connection between the corresponding areas under the curve and the different grading characteristics.

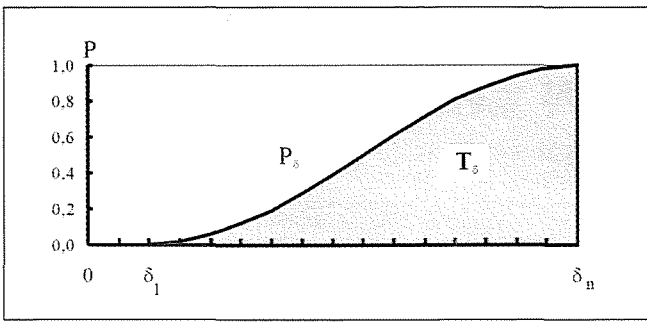


Fig. 1: The  $T_\delta$  area under the  $P_\delta$  grading curve

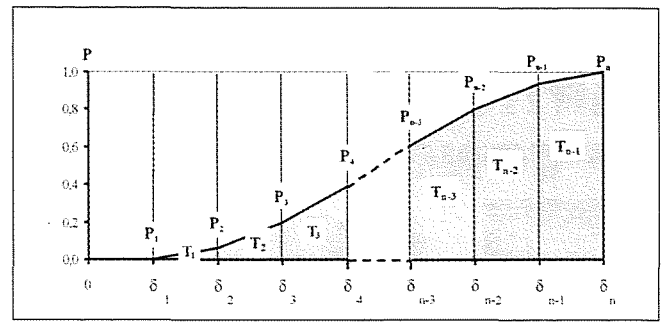


Fig. 2: Division of the  $T_\delta$  area to sub areas

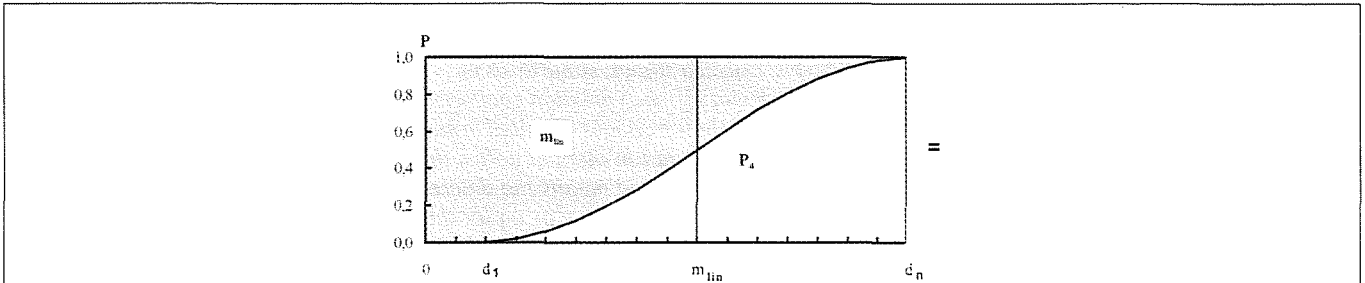


Fig. 3: The area  $m_{lim}$  above  $P_d$  grading curve

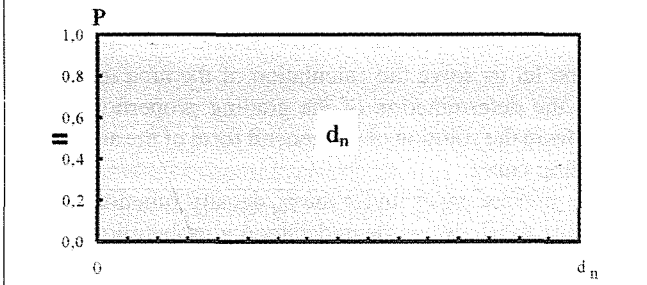


Fig. 4: The area  $d_n$  under the line  $P=1$

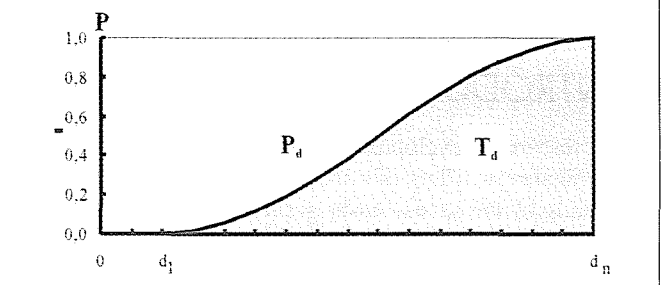


Fig. 5: The area  $T_d$  under  $P_d$  grading curve.

### 3. EXPECTED VALUE OR LINEAR FINENESS MODULUS

The expected value or in other words the linear modulus of fineness of the  $d$  particle size is equivalent to the area above the grading curve  $m_{lim}$ , which is plotted in a coordinate system having a linearly scaled  $x$  axis in the interval of  $d=0$  and  $d_n$  (formula (2) and Fig. 3 and 5.).

$$m_{lim} = v_1 = \Psi_0 = \int_{d_1}^{d_n} d \cdot p \, dd = \int_0^{d_n} dd - \int_{d_1}^{d_n} P \, dd = d_n - T_\delta =$$

$$= \frac{1}{200} \cdot \left[ 100 \cdot (d_{n-1} + d_n) + \sum_{i=2}^{n-1} P_i^{\%} \cdot (d_{i-1} - d_{i+1}) \right] \quad [\text{mm}] \quad (2)$$

The  $T_d$  expression necessary to express equation (2) can be obtained from equation (1) by inserting  $\delta=d$ . The meaning of equation (2) using the signed areas in Fig. 3., 4. and 5. is:

$$m_{lim} (=) T_{4. \text{ Figure}} - T_{5. \text{ Figure}}$$

As an explanation of equation (2) we must indicate that the  $k^{\text{th}}$  moment  $v_k$  of the area under the  $p_d$  density function to the  $x$  axis is:

$$v_k = \int_{d_1}^{d_n} d^k \cdot p \, dd \quad [\text{mm}^k]$$

and the  $(k-1)^{\text{th}}$  moment  $\Psi_{k-1}$  of the area above  $P_d$  distribution function to the  $x$  axis (if  $k$  is not a negative number):

$$\Psi_{k-1} = \int_0^{d_n} d^{k-1} \cdot (1-P) \, dd \quad [\text{mm}^k]$$

From the definition it is derived that  $v_0$  is nothing else than the area under the density function  $p_d$  and its value is  $v_0=1$  (Fig. 6).

Further, if  $k \neq 0$ , and if  $k=1$  then

$$v_{k \neq 0} = k \cdot \Psi_{k-1} \quad [\text{mm}^k] \quad \text{and} \quad v_1 = \Psi_0 = m_{lim} \quad [\text{mm}]$$

i.e. the latter also is the definition of the linear modulus of fineness.

### 4. THE SQUARE OF THE STANDARD DEVIATION

Simplifying we can say that the  $p_d$  density function and the corresponding  $P_d$  distribution function can be characterized

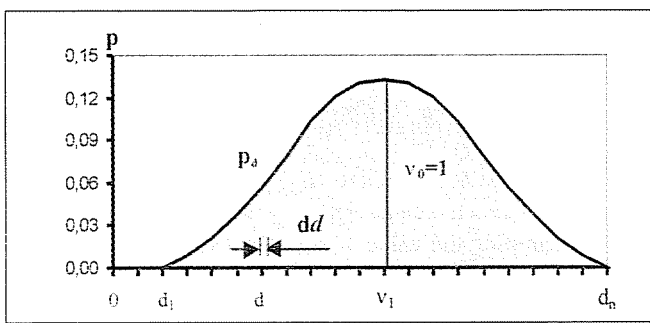


Fig. 6: The  $v_0=1$  area under the density function  $p_d$

by their expected values and square of the standard deviation. We have seen that the expected value is equal to the moment  $v_1$  of the area under the  $p_d$  density function to the  $x$  axis.

The square of the standard deviation is the secondary central moment  $\mu_2$  of the area under the density function  $p_d$  to the vertical line of the expected value. It can be proved that the square of the standard deviation i.e. the  $\mu_2$  central moment is equal to the difference of the squares of the  $v_2$  second order moment and the  $v_1$  primary moment. This is nothing else, but the difference of the squares of the double of  $\Psi_1$  primary moment (to the  $x$  axis) and of the expected value of the area above the grading curve expressed in a coordinate system having a linear  $x$  axis:

$$\sigma^2 = \mu_2 = v_2 - v_1^2 = 2 \cdot \psi_1 - m_{lin}^2 \quad [\text{mm}^2]$$

where in our case using  $k=2$ ,  $\mu_k$  in general is the  $k^{\text{th}}$  order central moment of the area under the  $p_d$  density function to the vertical line of the expected value:

$$\mu_k = \int_{d_1}^{d_n} (d - v_1)^k \cdot p \, dd \quad [\text{mm}^k]$$

If the  $P$  distribution function is presented in a coordinate system which has not a linearly but a quadratically scaled  $x$  axis then into the place of the double  $\Psi_1$  primary moment a

zero order moment will come into force. That is the square of the standard deviation is equal to the difference of the area ( $d_n^2 - T_d^2$ ) above the grading curve expressed in a coordinate system having a quadratically scaled  $x$  axis in the interval of  $d=0$  and  $d_n^2$  and the square of the expected value:

$$\begin{aligned} \sigma^2 &= d_n^2 - T_d^2 - m_{lin}^2 = \\ &= \frac{1}{200} \cdot \left[ 100 \cdot (d_{n-1}^2 + d_n^2) + \sum_{i=2}^{n-1} P_i^{90} \cdot (d_{i-1}^2 - d_{i+1}^2) \right] - m_{lin}^2 \quad [\text{mm}^2] \quad (3) \end{aligned}$$

The content of equation (3) expressed by areas can be seen in Fig. 7., 8. and 9.

$$\sigma^2 (=) T_{7, Fig} - m_{lin}^2 = T_{8, Fig} - T_{9, Fig} - m_{lin}^2$$

Using the square of the standard deviation  $\sigma^2$  can be calculated the standard deviation  $\sigma$ , the relative square of the standard deviation  $\sigma^2/m_{lin}^2$  and the relative standard deviation  $\sigma/m_{lin}$  that is the coefficient of variation.

## 5. LOGARITHMIC EXPECTED VALUE AND AVERAGE PARTICLE SIZE

The expected value or in other words the linear fineness modulus of the grading curve is interpreted in a coordinate system which has a linearly scaled  $x$  axis. If the grading curve is interpreted in a coordinate system which has logarithmically scaled  $x$  axis then instead of the previously discussed expected value we obtain the logarithmic expected value. Since the logarithmic expected value is nothing else then the logarithm to the base ten of the average particle size ( $\lg d_{average}$ ), the average size of the particles can be calculated. So the average of the particle size is interpreted in a coordinate system having a logarithmically scaled  $x$  axis and its value differs from the value of the linear fineness modulus.

The expected value is expressed by the area above the

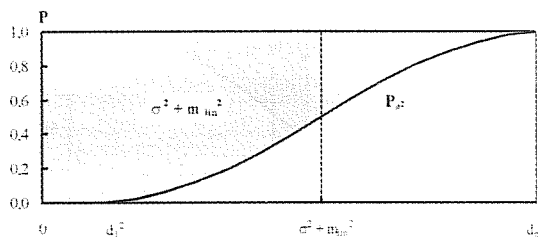


Fig. 7: The area  $\sigma^2 + m_{lin}^2$  above the  $P_d$  grading curve

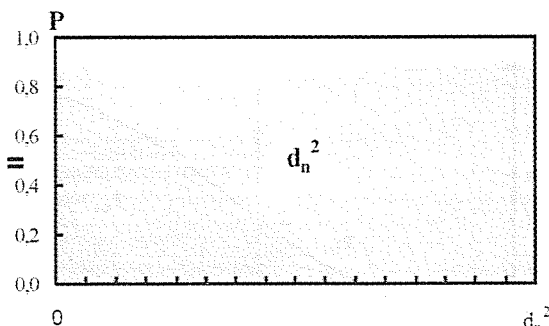


Fig. 8: The area  $d_n^2$  under the line  $P=1$

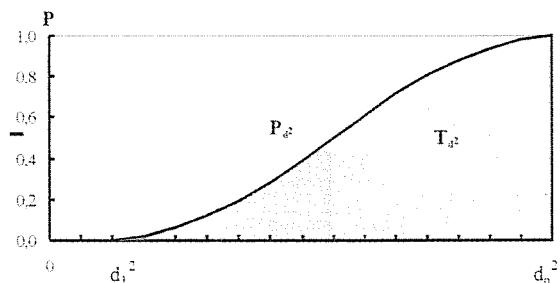


Fig. 9: The area  $T_d$  under the  $P_d$  grading curve

distribution function by definition. The boundaries of the area above the  $x$  axis having a starting point of zero is  $d=0$  and  $d_n$  which are the  $y$  axis and the maximum size of the aggregate. In case of logarithmically scaled  $x$  axis the maximum size of the particles can be found at the  $\lg d_n$  position, but the interpretation of the  $x$  axis is more complicated because the starting point – since  $\lg 0 = -\infty$  – must be different from zero. Due to this the role of the  $y$  axis is taken by a vertical at  $\lg 1 = 0$  value on the  $x$  axis, which divides the coordinate system into two parts. Since the logarithm of the numbers smaller than one are less than zero that is negative, the sign of the area left to the  $\lg 1 = 0$  point will be negative.

The grading curve of  $d_i < 1$  mm smallest particle size depending on the value of the maximum size is located in this negative area (if  $d_n < 1$  mm), or extends there (if  $d_n > 1$  mm). This later possibility is taken the most general situation in practice.

So in connection of the logarithmic expected value we may not talk about the above the curve area, but about the area bounded by the curve. Accordingly the logarithmic expected value is equal to the area bounded by the distribution function expressed in a coordinate system which has a logarithmically scaled  $x$  axis. This area is out of two parts, one is to the left from the  $x = \lg 1 = 0$  vertical, where the area under the curve is considered, while to the right of this line the area above the curve must be considered (Fig. 10.) which can be expressed as follows:

$$\lg d_{average} = \lg d_n - T_{\lg d} = \frac{1}{200} \cdot \left[ 100 \cdot (\lg d_{n-1} + \lg d_n) + \sum_{i=2}^{n-1} P_i \% \cdot (\lg d_{i-1} - \lg d_{i+1}) \right] \quad (4)$$

In equation (4) the unit of  $d$  is mm and the value of  $\lg d_{average}$  is to be considered as unit less.

Expressing the content of equation (4) by areas on Fig. 10., 11. and 12.:

$$\lg d_{average} (=) T_{Fig. 10} = T_{Fig. 11} - T_{Fig. 12}$$

The average particle size ( $d_{average}$ ) has the value of the logarithmic expected value ( $\lg d_{average}$ ) which can be calculated after determining the value of equation (4):

$$d_{average} = 10^{\lg d_{average}} \quad [\text{mm}] \quad (5)$$

By looking at the shaded area on Fig. 10. it can be seen that  $\lg d_{average}$  logarithmic expected value and the logarithmic average particle size  $d_{average}$  are independent from the starting point  $\lg d_m$  of the  $x$  axis.

## 6. THE HUMMEL AREA AND LOGARITHMIC FINENESS MODULUS

The logarithmic fineness modulus can be calculated from the logarithmic expected value. To derive it, it is necessary to calculate the Hummel area  $F_{\lg d}$  which is — according to the classical interpretation — the same as the area above the grading curve which is expressed in a coordinate system with a base ten logarithmic scaled  $x$  axis, extending until the  $\lg d_m$  starting point of the  $x$  axis Hummel (1930; 1959.). The procedure can be carried out by taking the difference between the areas represented by  $\lg d_{average}$  and  $\lg d_m$  which due to the negative sign of  $\lg d_m$  is numerically an addition:

$$F_{\lg d} = \lg d_{average} - \lg d_m = m_{\lg} \cdot \lg 2. \quad (6)$$

The unit of  $d_{average}$  and  $d_m$  is mm, while the value of  $F_{\lg d}$  and the logarithmic fineness modulus  $m_{\lg}$  are both unitless numbers. The content of expression (6) by the areas signed in Fig. 13., 14. and 15. is:

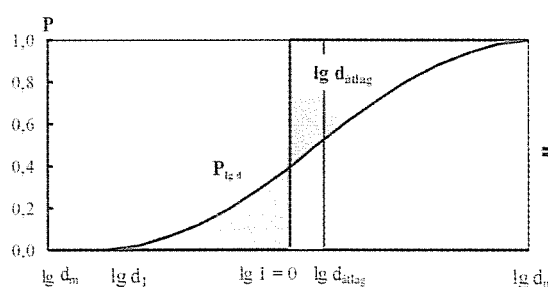


Fig. 10: The area  $\lg d_{average}$  bounded by the grading curve  $P_{lg d}$

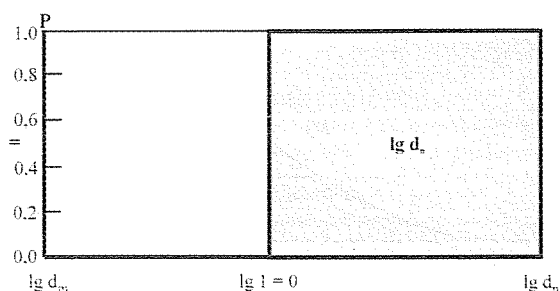


Fig. 11: The area  $\lg d_i$  under line  $P = 1$

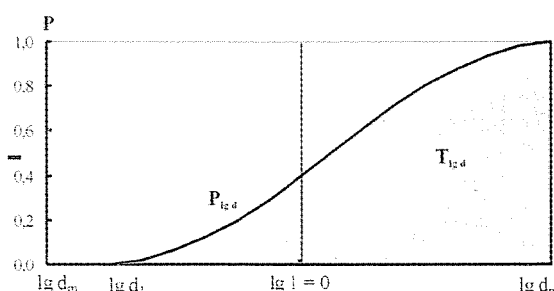


Fig. 12: The area  $T_{lg d}$  under the grading curve  $P_{lg d}$



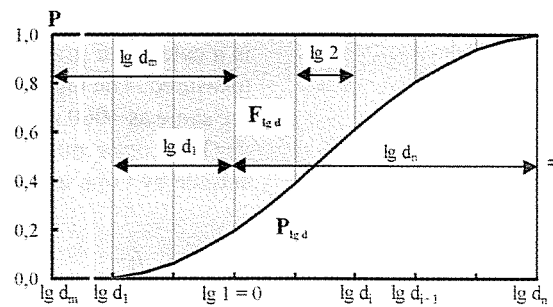


Fig. 13: The Hummel area  $F_{lgd}$  above  $P_{lgd}$  grading curve

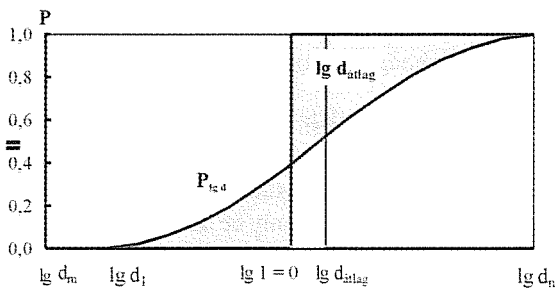


Fig. 14: The area  $lg d_{average}$  bounded by the grading curve  $P_{lgd}$

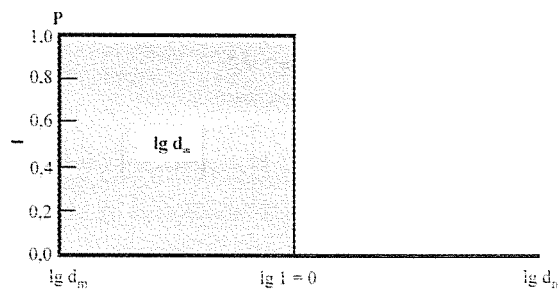


Fig. 15: The area  $lg d_m$  under  $P=1$  straight line

$$F_{lgd} (=) T_{Fig. 13} = T_{Fig. 14} - T_{Fig. 15}$$

On Fig. 13 it can be well seen that the magnitude of the Hummel area and consequently it's derivatives alike the logarithmic fineness modulus greatly depend on the initial value  $lg d_m$  of the  $x$  axis, which bounds the Hummel area or the magnitude of the corresponding value of the  $d_m \neq 0$  particle size, which is to be agreed upon Popovics (1952; 1953).

For the examination of the particle size distribution Abrams (1918) used the American Tyler sieves the characteristics of which is that the finest sieve size — that is the starting point of the  $x$  axis — is 0.147 mm and the further sieves have the size always the double of the previous one that is  $0.147 \cdot 2^{(i-1)}$ , where  $i = 1, 2, 3, \dots, n$ . Taking the logarithms of them the sieve sizes  $(lg 0,147) + (i-1) \cdot (lg 2)$  on a logarithmically scaled  $x$  axis would be equally distanced ( $lg 2$ ), a constant value (Fig. 13.).

By using this property of the Tyler scaled  $x$  axis the Hummel area ( $F_{lgd}$ ) can be derived as the sum of partial areas which all have a base length of ( $lg 2$ ) and the height can be calculated from the  $y$  values ( $1-P_i$ ) Fig. 2. and 13. To derive formula (6) we followed this method:

$$F_{lgd} = \sum_{i=1}^{n-1} \frac{(1-P_i) + (1-P_{i+1})}{2} \cdot lg 2 = m_{lg} \cdot lg 2 \quad \text{from here:}$$

$$m_{lg} = \frac{F_{lgd}}{lg 2} \quad (7.1)$$

which is the logarithmic modulus of fineness, having no unit.

From this the usual practice of characterizing the grading of concrete aggregates differs certainly which is using also the  $y$  values ( $1-P_i$ ) belonging to  $lg 2$  base length — that is the summarized relative retained masses over doubled sieve sizes — taking the height instead of the side of the partial area.

Then the qualifying value of the aggregate by the Hummel area is:

$$F = \sum_{i=1}^n (1-P_i) \cdot lg 2 = m \cdot lg 2 \quad \text{where: } m = \sum_{i=1}^n (1-P_i) \quad (7.2)$$

the fineness modulus as the product qualifying value which generally is simply called the fineness modulus. It's value slightly differs from the theoretical value derived from expression (7.1) but in the practice it is neglected. The fineness modulus has also no unit.

Accordingly the value of the logarithmic fineness modulus and the product qualifying greatly depend on the starting value of the  $x$  axis. In Hungary in concrete technology the starting point of the  $x$  axis presently in practice and generally if  $d_i \geq d_m$  — due to the lack of other any other condition — is always chosen as  $d_m = 0,063$  mm.

## 7. SPECIFIC SURFACE BY VOLUME AND BY MASS

The specific surface by volume is the total surface area of a unit body volume of the particles, that is the quotient of the sum of the exterior area of the individual particles of the particle bulk and the sum of the volume of the particles, which mostly also contain pores. The analysis of graphic calculation was carried out by Fáy and Kiss (1961).

The  $f_v$  specific surface of a particle set can be expressed in case of spherical or cubic — that is idealised — shaped particles as six times the (-1) order  $v_{-1}$  moment of the area under the  $p_d$  distribution function to the  $y$  axis:

$$f_v = 6 \cdot v_{-1} = 6 \cdot \int_{d_1}^{d_n} d^{-1} \cdot p \, dd \quad [\text{mm}^{-1}]$$

By introducing  $u = d^{-1}$  [ $\text{mm}^{-1}$ ] and substituting the

corresponding values into the above expression it can be proved that:

$$f_V = 6 \cdot v_{-1} = 6 \cdot \left( \int_0^{u_n} du + \int_{u_n}^{u_1} P_u du \right) \quad [\text{mm}^{-1}]$$

According to this the specific surface by volume is equal to six times the area under the grading curve which is expressed in a coordinate system having a reciprocally scaled  $x$  axis, that is:

$$\begin{aligned} f_V &= 6 \cdot (d_n^{-1} + T_{d^{-1}}) = \\ &= \frac{3}{100} \cdot \left[ 100 \cdot (d_{n-1}^{-1} + d_n^{-1}) + \right. \\ &\quad \left. + \sum_{i=2}^{n-1} P_i^{90} \cdot (d_{i-1}^{-1} - d_{i+1}^{-1}) \right] \quad [\text{mm}^{-1}] \end{aligned} \quad (8)$$

The content of equation (8) are the marked areas on Fig. 16., 17. and 18.:

$$f_V (=) 6 \cdot T_{\text{Fig. 16}} = 6 \cdot (T_{\text{Fig. 17}} + T_{\text{Fig. 18}})$$

The specific surface by volume of the particle bulk is very sensitive to the size and quantity of the fine particles. As an extreme example in case of the bulks having  $d_f=0$  as the smallest particle size the calculation of the specific surface by volume is facing problems, because in this case if  $d_f=0$  then  $u_f=\infty$  and  $f_V=\infty$ , that is the specific surface by volume would be infinite. Due to this reason a condition is usually drawn, which is  $d_f \geq 0,001$  mm and  $u_f \leq 1000$  mm<sup>-1</sup>. Although this condition is arbitrary, the values can be accepted because in the aggregate for concrete the finest particles are the clay particles (which have a particle size less than 0.002 mm), and the quantity of them we limit deliberately.

In construction practice the area of a unit amount of the bulk is more liked to be expressed instead to the volume, by the specific surface by mass and is simply called the specific

surface Nischer (1996). The reason of it is simply in the measuring techniques. While the specific surface by volume is a calculated grading property, the specific surface can be measured. The unit of the specific surface is m<sup>2</sup>/kg, which is the same as 1000 mm<sup>2</sup>/g.

The connection between specific surface  $f$  and specific surface by volume is described by the expression (9).

$$f = 10^3 \cdot \frac{f_V}{\rho_T} \quad [\text{m}^2/\text{kg}] \quad (9)$$

where:

$f_V$  = specific surface by volume [1/mm]

$\rho_T$  = the average body density of the particles of the bulk [kg/m<sup>3</sup>]

The specific surface also depend on the body density of the material. For this reason — unlikely the specific surface by volume — cannot be considered as a grading property, since the specific surface can only be used directly to compare bulks having the same particle body density.

## 8. CONCLUSIONS

The advantages of the developed grapho-analytical calculation method of the grading properties are that their principle have a standard structure, makes it possible to use arbitrarily chosen sieve sizes for the sieve tests and to examine arbitrary particle sizes during sedimentation tests. It makes it unnecessary to derive the grading function, eliminates the necessity of area or the proportional distance measurement and actually does not really require the compilation of the grading curve which belongs to the total examination. The application of the calculation method is simple, by solving equations of similar form which can be computerized. The standardisation of the method in Europe is not expected, in Hungary however a standard deals with it which has been accepted and it's sign is MSZ 18288-5:1981. Hopefully this standard will remain in force since no other may substitute it.

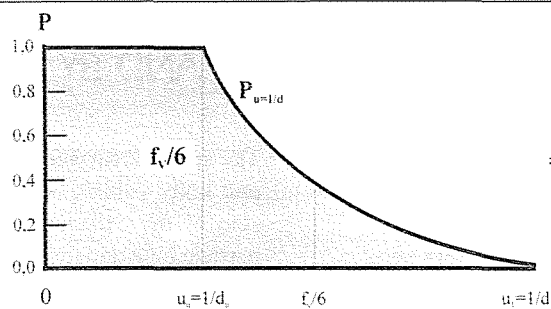


Fig. 16: The area  $f_V/6$  under the grading curve  $P_{u=1/d}$

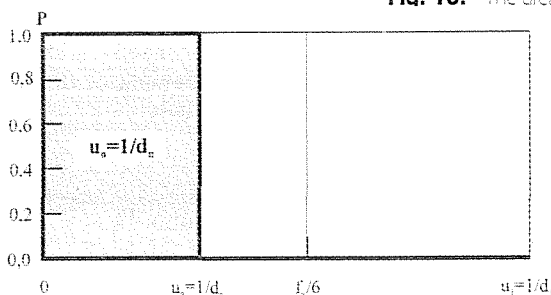


Fig. 17: The area  $1/d_n$  under the line  $P=1$

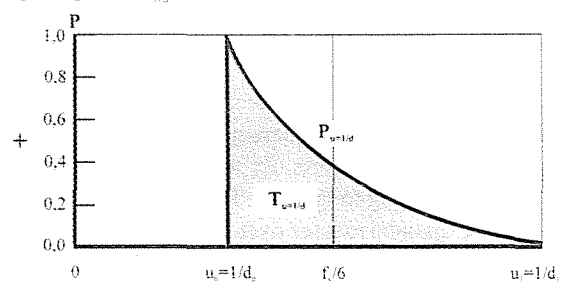


Fig. 18: The area  $T_{u=1/d}$  under the grading curve  $P_{u=1/d}$

## 9. MOST IMPORTANT NOTATIONS

$d$	nominal particle size, independent variable
$d_{average}$	average particle size in case of logarithmically calibrated $x$ axis, the $lgd_{average}$ is the number of the logarithmic expected value
$d_i$	$i^{th}$ particle subset size limit
$d_m$	value of the starting point of the $lgd_m$ $x$ axis, the corresponding particle size is for the calculation of the logarithmic fineness modulus
$f$	specific surface (by mass)
$f_v$	specific surface by volume
$F$	practical qualifying value of the <i>Hummel</i> area
$F_{lgd}$	the <i>Hummel</i> area
$k$	order of moment of the area under a function
$lgd_{average}$	the logarithm to the base ten of the average particle size, the logarithmic expected value
$lgd_m$	value of the starting point of the logarithmically scaled $x$ axis
$m$	the practical product qualifying value of the logarithmic fineness modulus
$m_{lg}$	the logarithmic fineness modulus
$m_{lin}$	expected value, in other words the linear fineness modulus
$n$	the number of the examined particle sizes
$p_d$	the density function
$p_\delta$	the density function transformed according to $\delta$
$P_d$	the distribution function, in other words the grading curve
$P_\delta$	the distribution function or grading curve transformed according to $\delta$
$P_i$	distribution function value belonging to the $i^{th}$ particle subset boundary
$T_{Fig. z}$	area marked on <i>Fig. z</i>
$T_\delta$	area under the transformed distribution function $P_\delta$
$\delta$	the value of $d$ particle size transformed proportionally with the grading properties
$\mu_2$	the second order central moment of the area under $p_\delta$ density function to the vertical line of the expected value
$\mu_k$	the $k^{th}$ order central moment of the area under $p_\delta$ density function to the vertical line of the expected value
$V_0=1$	area under the density function $p_\delta$
$n_{-i}$	the $(-1)^{th}$ order moment of the area under the density function $p_\delta$ to the $y$ axis
$V_i = \Psi_i$	the first order moment of the area under the density function $p_\delta$ to the $y$ axis, which is equal to the area above the distribution function $P_\delta$
$V_2$	the second order moment of the area under the density function $p_\delta$ to the $y$ axis
$V_k$	the $k^{th}$ order moment of the area under the density function $p_\delta$ to the $y$ axis

$\rho_T$	average particle body density of dry particle bulk
$\sigma$	standard deviation
$\sigma^2$	square of standard deviation
$\sigma/m_{lin}$	coefficient of variation
$\sigma^2/m_{lin}^2$	the relative standard deviation square
$\Psi_i$	first order moment of the area above the distribution function $P_\delta$ to the $y$ axis
$\Psi_{k-1}$	the $(k-1)^{th}$ order moment of the area above the distribution function $P_\delta$ to the $y$ axis (if $k$ is positive)

## 10. REFERENCES

- Abrams, D. A. (1918), "Design of concrete mixtures", *Bull. 1. Structural Materials Research Laboratory, Lewis Inst., Chicago*
- Hummel, A. (1930), "Die Auswertung von Siebanalysen und der Abrams'sche Feinheitensmodul", *Zement, H. 15*. pp. 355-364.
- Hummel, A. (1959), "Das Beton-ABC. Ein Lehrbuch der Technologie des Schwerkonzrets und des Leichtbetons", *Verlag von Wilhelm Ernst & Sohn, Berlin*
- Kausay T. (1975), "Analytic determination of grading properties of sandy gravels and crushed aggregates" *Mélyépítéstudományi Szemle, XXV. volume 4.*, pp. 155-164. (in Hungarian)
- MSZ 18288-5:1981 (Hungarian Standard), "Particle distribution and cleanness of construction stones. Calculation of grading properties." *Hungarian Standards Institution*. 6 p.
- Nischer, P. (1996), "Verbesserung der Betoneigenschaften durch Optimierung der Betontechnologie", *Beton + Fertigteil-Jahrbuch, 44. Ausgabe, Bauverlag GmbH, Wiesbaden und Berlin*, 78-85. pp.
- Popovics S. (1952), "Numerical qualification of concrete aggregate particle distribution", *Hungarian Academy of Sciences, volume 1952/7., 1-3.* ", pp. 45-75. (in Hungarian)
- Popovics S. (1953), "Methods to derive grading properties of concrete aggregate", *Lecture Notes of the Institute of Postgraduate Engineering Education, Felsőoktatási Jegyzetellátó Vállalat, Budapest. (in Hungarian)*
- Tibor KAUSAY** (1934), M.Sc civil engineer (1961), specialisation in reinforced concrete (1967), university doctor (1969), candidate of technical sciences (1978), Ph.D. (1997), associate professor of department of Building Materials, Technical University of Budapest (1985), honorary professor at the department of Construction Materials and Engineering Geology, Budapest University of Technology and Economics (2003). Member of the Hungarian Group of *fib* (2000), gróf Lónyay Menyhért priced Honorary member of the Szabolcs-Szatmár-Bereg county Scientific Organisation of the Hungarian Academy of Sciences (2003). Main research fields: concrete technology, stone industry. Author of about 120 publications.
- Tamás SIMON** (1956), M.Sc civil engineer (1983). Between 1983 and 1990 consultant of VIZITERV Consulting Engineering Company for Water Engineering. For two years, between 1990 and 92 developing and constructing engineer of „kas” Insulation-techniques Developing and Constructing Incorporated Company. Since 1992 senior lecturer of Budapest University of Technology and Economics, Department of Construction Materials and Engineering Geology. Since 2005 lecturer of Ybl Miklós College of Technology, Department of Building Materials and Quality Control. Main fields of interest: concrete and reinforced concrete structures, concrete technology, quality control. Member of the Hungarian Chamber of Engineers and the Hungarian group of *fib*.

# ASPECTS OF MIX DESIGN OF LIGHTWEIGHT AGGREGATE CONCRETE



Dr. Rita Nemes – Assoc. Prof. Zsuzsanna Józsa

Several new cellular pellets appeared on the market as lightweight aggregate in the last 10 years. The amount of products made out waste material is growing up. The most important one of these is the expanded glass. Previously the expanded glass pellets were aggregates only of concrete blocks. Nowadays there are other demands in addition to low density. A lot of properties are controllable under the manufacture. The properties of aggregates have strong influence on mix design. Our test results cover mainly expanded glass pellets. For comparison expanded clay pellets were also tested.

**Keywords:** lightweight aggregate, lightweight concrete, expanded glass aggregate, compressive strength, Young's modulus, mix design

## 1. INTRODUCTION

Load bearing structures can be constructed of concrete with various shapes, however the relatively low strength-to-weight ratio of concrete can be considered as a disadvantage. The self-weight of concrete structures may be considerable compared to the live loads. The technology of lightweight concrete is progressively developing to increase the heights of buildings and bridge spans. Use of lightweight aggregate concrete (LWAC) is also advantageous in refurbishment, as a result of less additional load. In cases of prefabricated structures, lightweight concrete can simplify the mounting technology, enables to produce larger elements or use smaller cranes.

Possible solutions can be, either to increase the strength (High Strength Concrete) or to decrease the selfweight of concrete (Lightweight Concrete), or to find the optimal solution between the requirements (Falikman, Sorokin, 2005 and Müller, Haist, Mechtcherine, 2002). The density of structural concrete is between 800 and 2000 kg/m<sup>3</sup> (Table 1) and the compressive strength class is between LC8/9 and LC80/88 (Table 2) according to EN 206-1 European Standard. All of these concretes are lightweight aggregate concretes where the designed air content is assumed being only inside the aggregate; the cement mortar matrix fills the gaps. Density of aggregate influences mainly the density of concrete since the volume of the aggregate is significant in the mixture.

**Table 1:** Classification of lightweight concrete by density according to EN 206-1 (European Standard)

Density class	Density [kg/m <sup>3</sup> ]
D1.0	800-1000
D1.2	1000-1200
D1.4	1200-1400
D1.6	1400-1600
D1.8	1600-1800
D2.0	1800-2000

**Table 2:** Compressive strength classes for lightweight concrete according to EN 206-1 (European Standard)

Compressive strength class	Minimum characteristic cylinder strength $f_{ck,cyl}$ N/mm <sup>2</sup>	Minimum characteristic cube strength $f_{ck,cube}$ N/mm <sup>2</sup>
LC8/9	8	9
LC12/13	12	13
LC16/18	16	18
LC20/22	20	22
LC25/28	25	28
LC30/33	30	33
LC35/38	35	38
LC40/44	40	44
LC45/50	45	50
LC50/55	50	55
LC55/60	55	60
LC60/66	60	66
LC70/77	70	77
LC80/88	80	88

## 2. PRINCIPLES OF DESIGN

Basic data for the normal weight concrete are the compressive strength classes. The most important is the water-cement ratio. The first step of mix design is to choose the water-cement ratio. If the water-cement ratio is increasing, the compressive strength is strongly decreasing, but the main load bearing part of concrete is the aggregate skeleton. No significant difference

can be realized between the crushing resistances of the normal weight aggregates (natural quartz gravel, crushed stones), so this is not a variable of the concrete mix design. The strength of normal weight aggregate can be taken as a constant, so in design the modulus of fineness is the only parameter. The method of design of lightweight aggregate concrete is different due to two reasons. One is the load-carrying mode (the load carrying part is the mortar matrix and not the aggregate skeleton). It is very important to find an aggregate that is matching to the matrix stiffness, as it is shown in Ref. *Bremner, Holm (1986)*. Second reason is the different strength of lightweight aggregates. The crushing resistance of several lightweight aggregates can be considerably different. Usually it is much lower than the crushing resistance of natural stones, but it can achieve that of natural quartz gravel, as well. The water-cement ratio is also important for lightweight aggregate concretes, because the load bearing part is the cement stone, but the concrete strength depends mainly on crushing resistance of lightweight aggregate (*Table 3*).

Density of concrete is the basic information for design similarly to compressive strength of concrete. However, these are opposite requirements. If the strength of aggregate is higher, the particle density of aggregate is higher. It can reach different values in case of lightweight aggregates from several materials. The crushing resistance of lightweight aggregates limits the compressive strength of lightweight aggregate concrete. Normal weight and lightweight aggregate can be applied mixed. The most common combination of aggregates for structural lightweight concrete is, when the sand fraction (lower than 4 mm) is normal weight and gravel fraction is lightweight aggregate. In case of using different types of aggregates with different particle densities the calculation of grading in volume percent (instead of the usual mass percent) is necessary. The aim is not the paste-saturated concrete. Lightweight aggregate concrete have to be over saturated.

**Table 3:** Differences in mix design between normal weight and lightweight concrete

	Normal weight concrete (NWC)	Lightweight aggregate concrete (LWAC)
Requirement	compressive strength	compressive strength + density
Strength depends strongly on	water-cement ratio	water-cement ratio + crushing resistance of LWA
Grading	percent by mass	percent by volume
Optimal strength	by paste-saturated concrete	by over saturated concrete

The strength of lightweight aggregate concrete depends on crushing resistance of lightweight aggregate and strength of cement mortar. If the crushing resistance of lightweight aggregate is very low (under 1 to 2 N/mm<sup>2</sup> according to EN 13055-1:2002), the influence of aggregate particles can be

neglected during mix design of concrete. (These lightweight aggregates are used to structural concrete together with natural sand.) In this case it is necessary to know the gap ratio of lightweight aggregate bulk. The over saturation should be minimum 10 to 20 % by volume. Lightweight aggregates are usually artificial products with round form and equal diameter. Here the theoretical gap ratio is 23 % by volume, accordingly the suggested maximum value of lightweight aggregate for over-saturated concrete is approximately 60 to 65 % by volume.

### 3. PROPERTIES AND SELECTION OF LIGHTWEIGHT AGGREGATES

#### 3.1 Aggregates in general

Lightweight aggregates (LWAs) have two main groups. It can be a natural material (the aggregate of historical lightweight concrete structures) or the more popular artificial products. Modes of manufacturing can be either the crushing or the heat treatment of the raw material. Most frequently the combination of these two processes are used. The manufactured material can be made out of natural material (for example clay or shale) or can be industrial by-product or waste. Wastes have two subgroups, wastes from building industry (used as crushed brick) or communal waste (used as expanded glass).

General requirements of LWAs are (*EN 13055-1:2002*): low bulk density (max. 1200 kg/m<sup>3</sup>) and low particle density (max. 2000 kg/m<sup>3</sup>), pressure resistance, thermal insulation capability, mechanical and chemical resistance, fire-resistance, frost-resistance, shape keeping. The most popular and well-known lightweight aggregates are the clay and shale products.

**Expanded clay pellet** (*PCR 2004:x*) is a natural product manufactured from special clay. The clay is dried, heated and fired in rotary kilns where at a temperature of approx. 1200 °C it is expanded into lightweight aggregate. The products may have applications within the area of building construction and horticulture.

**Expanded glass pellet** (*Józsa, Nemes, 2004*) is a special product of lightweight aggregates. The expanded glass is fabricated and applied similarly to expanded clay products. Glass pellets can be made out of waste glass. It is not necessary to select and clean the raw material. The waste glass is ground to a powder, granulated and burned in rotary furnace, with a patented method. The use of expanded glass pellets is favourable from economic and environmental point of view. The recycling of waste and industrial by-products in the construction industry is more and more important nowadays.

#### 1.2. Water absorption of LWAs

The water absorption of aggregates is not the same, but the difference is not considerable and the value is low in case of normal weight aggregates. Water absorption capacity of LWAs is usually high as the result of their high porosity. The result is, that the water absorption and the porosity is higher, if the particle density lower. This is the behaviour of the lightweight aggregates *type A* (*Fig. 1, Table 4*), where aggregates have open

capillary pores. This high water absorption can reach 50 % by mass, usually it results disadvantages in concrete technology (e.g. need extra water to be added (Lin, Chen, Peng, Yang, 2005), the concrete can not be pumped). On the other hand it has an internal water curing effect. The normal process against this phenomenon is to cover the expanded clay aggregates with cement paste on the surface before mixing. It is an extra step in concrete technology (Müller, Haist, 2005); it is time consuming and needs extra costs. In case of expanded glass pellets the surface coating can be produced during the manufacturing process. So *type B* can be reached, where water-absorbing capacity is inversely depending on the particle density, but the water absorption is not higher than 10 % by mass. The water absorption can be independent from particle density with this coating, as well. For *type C* the water-absorbing capacity of the pellets is very low, under 2 % by mass, and it is available under water pressure, too. (Józsa, Nemes, 2002)

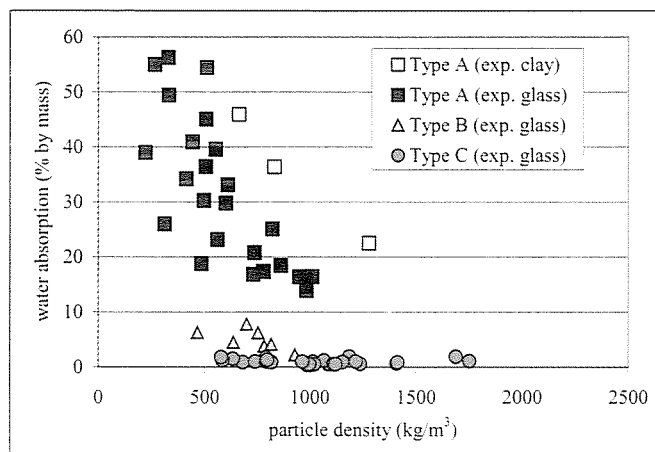


**Fig. 1:** Relationship between the particle density and the water absorption of aggregate

### 3.2 Strength of LWAs

In case of expanded clay and expanded glass products the relationship between crushing resistance and particle density (except the very low densities (<500 kg/m<sup>3</sup>)) is linear (Fig. 2). The crushing resistance of aggregate may reach 70 % of crushing resistance of natural quartz gravel. The results measured on quartz gravel can be represented on the same line so it is possible to give the strength of lightweight aggregate in percentages of the strength of normal quartz gravel. This property is independent on water absorption capacity and raw material (Fig. 3).

## 4. SIGNIFICANT PROPERTIES FOR MIX DESIGN

The most significant property and the input data for design is the crushing resistance of aggregate and the relationship between the crushing resistance and the particle density of

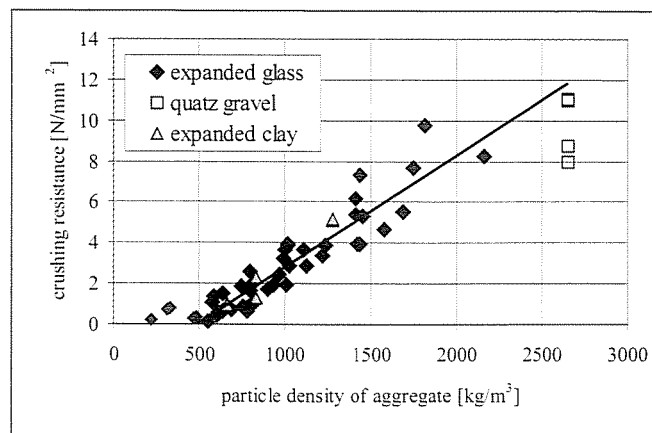


**Fig. 2:** Relationship between the particle density and the crushing resistance of aggregate

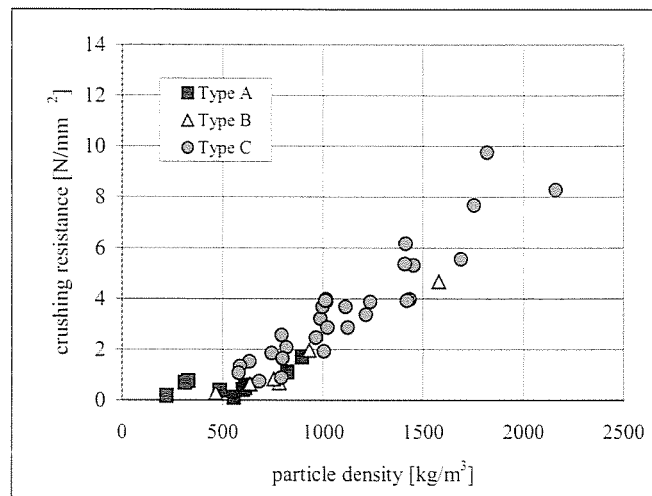


**Fig. 3:** Relationship between the particle density and the crushing resistance in case of different water absorption types of expanded glass aggregates

lightweight aggregate. Advantages of artificial products are the better and more constant quality.

### 4.1. Laboratory tests

In experimental program 18 types of expanded glass (from three different manufacturers) and two types of expanded clay products (produced by one manufacturer) were tested. The reference aggregate was natural quartz gravel. The specimens were cubes with edge 150 mm and 70 mm. Strength tests were carried out at the age of 28 days. Samples were stored under lime-saturated water until testing.

### 4.2. Effect of strength of cement mortar

Strength of LWAC depends primarily on the strength of the cement mortar, as the main load bearing part is the matrix in LWAC. The importance of the strength of the mortar is more considerable in case of LWAs with low self-weight. During the

**Table 4:** Water absorption and particle density of different types of LWAs and NWAs

	Water absorption		Particle density LWA [kg/m <sup>3</sup> ]	Particle density NWA [kg/m <sup>3</sup> ]
	% by mass	% by volume		
Type A	10-60	8-30	200-1800	---
Type B	2-10	2-5	450-1200	2000-2600
Type C	< 2	< 3	500-2000	2600-3000

**Table 5:** The measured compressive strength (on cubes 70 mm, average values) – three different cement mortar mixtures without gravel, with natural quartz gravel and with four different expanded glass aggregates

		Cement mortar	With quartz gravel	With LWA			
				No. 1	No. 2	No. 3	No. 4
Average density of concrete [kg/m <sup>3</sup> ]		2250	2400	2000	1700	1590	1400
Particle density of aggregate [kg/m <sup>3</sup> ]		-	2650	1600	635	600	310
Compressive strength of concrete [N/mm <sup>2</sup> ]	No. 1	63.8	60.6	44.3	32.8	20.8	14.4
	No. 2	59.2	55.7	35.0	30.0	16.1	9.3
	No. 3	30.1	36.9	24.6	21.3	11.8	7.1

tests were used three cement mortar mixtures with natural quartz gravel, with four different expanded glass pellets and without gravel (Table 5). The cement was the same and the aggregate content was 47 volumetric percent in all cases. Aggregate under diameter of 4 mm was natural sand. Consistency was set by water reducer admixture (superplasticizer). If the compressive strength of mortar is increasing, the compressive strength of LWAC is increasing. The rate of change in compressive strength of LWAC is independent from the type of LWA, if the volumetric ratio of the aggregate is constant (Fig. 4). Respectively the strength of concrete the higher the density of aggregate is, the more important the strength of cement stone is.

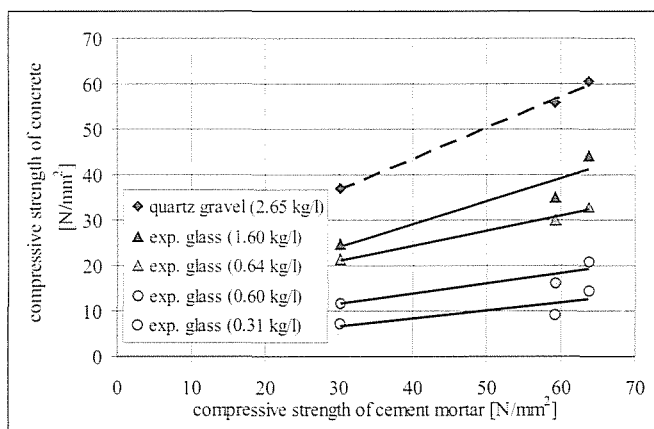


**Fig. 4:** Relationship between strength of cement mortar and strength of concrete in case of application of different LWAs and natural quartz gravel, amount of LWA is 47 % by volume, (average values, measured on 70 mm cubes)

### 4.3 Effect of amount of aggregate

Volumetric ratio of aggregate was applied on the widest possible range. Lower and upper limits can be defined for the volumetric ratio of aggregates. Lower limit is found around 30 to 33 percent by volume. Upper limit can be determined belonging to a paste-oversaturated mixture. Slight paste-oversaturation is needed to ensure the interaction force flow. Paste-saturated condition can be determined based on the gap ratio of the aggregate (50 to 60 percent by volume). These series of tests were carried out exclusively with same mortar mixtures (No.1 Table 5). Aggregate content of test specimens was 36 to 56 percent by volume. Fig. 5 indicates results for one type of expanded glass aggregate (particle density: ~1000 kg/m<sup>3</sup>) at different volumetric ratio of aggregate. If the volume of aggregate exceeds 56 percent by volume, compaction of fresh concrete started to be impossible resulting low strength. In the

range of 48 to 50 percent by volume an increase in density leads to an increase in strength. Under 46 percent by volume the values of strength seemed to be not influenced by the decrease in the volumetric ratio of aggregate. Bilinear curves were found experimentally to demonstrate the relationship between density of concrete and compressive strength. It can be concluded that concrete has almost the same compressive strength with further increase in density after reaching the inclination point. Based on this relationship, the optimum situation can be defined at the point where maximum strength is available at minimum density. This behaviour is similar in the case of expanded glass and expanded clay aggregate concretes. Defining bilinear curves are advantageous for design. Bilinear curves can be the basis of LWAC mix design methods in the future, based on this new approach.

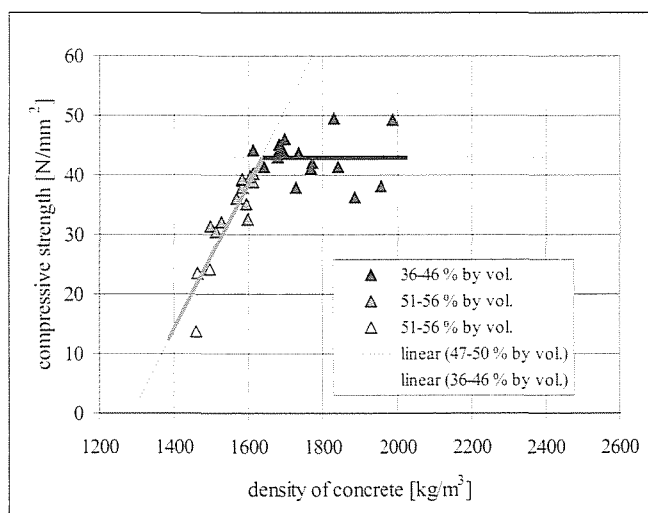


**Fig. 5:** Compressive strength vs. density of concrete in case of different amount of one type of expanded glass pellet (same cement mortar, 150 mm cube, individual values)

### 4.4. Effect of strength of aggregate

Influence of crushing resistance of the aggregate is essential on the strength of LWAC. The strength of the particles should be neglected whenever the aggregates have very low crushing resistance. In this case the main load bearing part of the LWAC is the mortar. If the aggregate has relatively high strength then the behaviour of LWAC is similarly to the NWC. The particle density depends strongly on the crushing resistance (Fig. 2). In present test series we defined three classes of expanded glass aggregates according to their particle densities (300 to 600 kg/m<sup>3</sup>, 800 to 1200 kg/m<sup>3</sup> and 1200 to 2000 kg/m<sup>3</sup>). In

all cases the relationship between concrete density and cube strength was found to be similar to that of the first series (in which effect of amount of aggregate was tested), if the amount of lightweight aggregate was changed (Fig. 6). In case of aggregates with low particle density (300 to 600 kg/m<sup>3</sup>) a maximum concrete strength of 20 to 25 N/mm<sup>2</sup> was realised. In this case the strength of aggregate can be practically neglected for the prediction of the strength of LWAC. The conventional model of lightweight concrete can be used here, supposing that the mortar-skeleton carries all the loads. The optimal concrete density was found about 1350 kg/m<sup>3</sup>, where the aggregate amount is about 53 to 54 % by volume. In case of aggregates with medium particle density (800 to 1200 kg/m<sup>3</sup>) to the optimum of mix belong higher compressive strength and lower amount of aggregate. If the density and the crushing resistance of lightweight aggregate is higher (1200 to 2000 kg/m<sup>3</sup>), then the compressive strength can reach the strength of normal weight concrete, and to the optimum belongs less lightweight aggregate (41 to 43 % by volume).

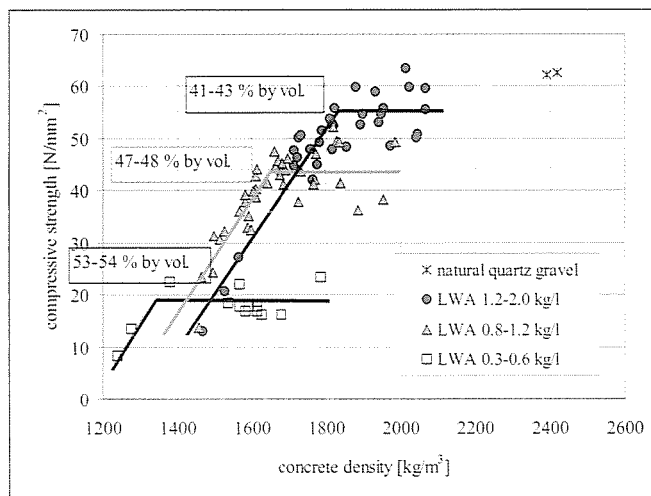


Fig. 6: Relationship between concrete density and compressive strength in case of LWAs of different particle density groups (150 mm cube, individual values)

## 4.5 Young's modulus

According to several standards it is possible to calculate the Young's modulus. Normally it is calculated from the Young's modulus of normal weight concrete by a reducing factor according to the density of LWAC. (This factor is not the same in several countries/standards.)

Measured values of Young's modulus are shown by a filled symbol on Fig. 7 versus measured compressive strength on the same specimen. Calculated values according to MC 90 (CEB-FIP MODEL CODE 1990) are drawn with empty symbols on Fig. 7 where the formula for LWAC according to (fib, 2000) is the following.

$$E_c = 2.15 \cdot 10^{-4} \cdot \left(\frac{f_{cm}}{10}\right)^{1/3}, \text{ by rearrangement: } E_c = 10 \cdot \sqrt[3]{f_{cm}} \quad (1)$$

where:  $E_c$ : Young's modulus in N/mm<sup>2</sup>  
 $f_{cm}$ : mean cylinder strength in N/mm<sup>2</sup>

$$\eta = \left(\frac{\rho}{2200}\right)^2 \quad (2)$$

where:  $\eta$ : reduction factor for LWAC

$\rho$ : density of LWAC in kg/m<sup>3</sup>

Our test results indicate the estimation possibility of Young's

modulus directly from compressive strength, without explicit formulation of density. For these cases a new formulation of Young's modulus is presented in the followings.

$$E_m = 3700 \sqrt{f_{cm}^*} \quad (3)$$

where:

$E_m$ : average value of Young's modulus in N/mm<sup>2</sup>

$f_{cm}^*$ : mean compressive strength on prism (120x120x360 mm) measured in N/mm<sup>2</sup>

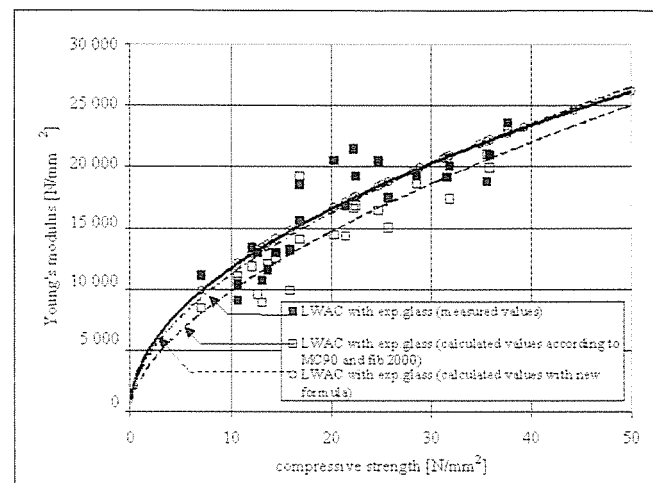


Fig. 7: Young's modulus vs. compressive strength measured and calculated values with different methods

## 5. CONCLUSIONS

Strength of LWAC is influenced by the crushing resistance of the LWA as well as by the strength of the cement mortar. Crushing resistance can be accurately predicted from particle density that is easy to measure.

Aim of mix design is to be able to reach the lowest density of LWAC with the possibly highest available strength. For this purpose, an optimum volumetric ratio of aggregate particles should be defined. Strength of LWAC can be predicted from the properties of the constituents and their mixing ratio.

Present paper proposes a new formula for the estimation of Young's modulus of LWAC.

## 6. ACKNOWLEDGEMENT

Authors wish to express their gratitude to Geofil Ltd. (Tatabánya, Hungary) for the collaboration and financial support and to Liapor Ltd. and Solvadis Austria for supplying aggregates.

## 7. REFERENCES

- Bremner, T.W., Holm, T.A. (1986). "Elastic Compatibility and the Behaviour of Concrete", ACI Journal March-April/1986, pp. 244-250
- CEB-FIP (1993). CEB-FIP MODEL CODE 1990. Thomas Telford Services Ltd.
- EN 13055-1:2002 Lightweight aggregates – Part 1: Lightweight aggregates for concrete, mortar and grout
- EN 206-1:2000 Concrete – Part 1: Specification, performance, production and conformity
- Falikman, V.R., Sorokin, Y.V. (2005) "High-Strength Lightweight concrete for Cast-in-Place Construction" Proceeding of fib Symposium Keep Concrete Attractive, 23-25 May 2005, Budapest, Hungary, Eds.: Balázs, G.L. and Borosnyói, A., pp. 391-396
- fib (2000). "Lightweight Aggregate Concrete. Recommended extensions to Model Code 90: Case studies" fib bulletin 8 Sprint-Druck Stuttgart



- Józsa, Zs., Nemes, R. (2002) „Recycled Glass Aggregate for Lightweight Concrete”, *Concrete Structures*, 2002, pp. 41-46.
- Józsa, Zs., Nemes, R. (2004), “An Innovative Material from Recycled Glass to Lightweight Concrete”, *Proceeding of 1rd International Symposium Innovative Materials and Technologies for Construction and Restoration*, 6-9 June 2004, Lecce, (Italy) Eds.: La Tegola, A. and Nanni, A., pp. 229-240.
- Lin, C-K, Chen, H-J, Peng, H-S, Yang, T-Y. (2005) “Properties of Self-Compacting Lightweight Aggregate Concrete”, *Proceeding of fib Symposium Keep Concrete Attractive*, 23-25 May 2005, Budapest, Hungary, Eds.: Balázs G.L. and Borosnyói, A., pp. 945-950
- Müller, H.S., Haist, M. (2005), “Pumpable Self-Compacting Lightweight Concrete”, *Proceeding of fib Symposium Keep Concrete Attractive*, 23-25 May 2005, Budapest, Hungary, Eds.: Balázs G.L. and Borosnyói, A., pp. 368-373
- Müller, H.S., Haist, M., Mechtcherine, V. (2002) “Selbstverdichteter Hochleistungs-Leichtbeton”, *Beton- und Stahlbetonbau*, Heft 6, Juni/2002, pp. 326-333
- PCR 2004:x –Expanded Clay Light Weight Aggregates in the form of “Tout Venant” ([www.escsi.org](http://www.escsi.org))

**Rita NEMES** (1978) MSc in civil engineering, postgraduate diploma in concrete technology, assistant lecturer at the Department of Construction Materials and Engineering Geology at Budapest University of Technology and Economics. Her main field of activities are: concrete technology and testing, testing of ceramics and wall elements. Her research topics are structural lightweight aggregate concrete. She wrote her PhD Thesis on the subject of lightweight concrete with expanded glass aggregate. She is a member of Hungarian Group of *fib* and Scientific Society of Silicate Industry.

**Zsuzsanna JÓZSA** (1950) PhD, associate professor at the Department of Construction Materials and Engineering Geology at Budapest University of Technology and Economics, architect, postgraduate diploma in building reconstruction. Her main field of activities are lightweight aggregate concrete, non-destructive concrete testing, concrete corrosion and repair, thermal and moisture properties of materials, thermal insulation and water-proofing, roof tiles, wall construction, bricks and tiles, aerated concrete, environmental compatible building materials. She is Hungarian representative of Member of IASS WG 18 “Environmental Compatible Structures and Structural Materials”, Member of Association for Building Biology, Hungarian Scientific Society of Building, Scientific Society of Silicate Industry, Hungarian Group of *fib*, and was member of TG 8.1: Lightweight aggregate concrete.

# SERVICEABILITY ASPECTS OF CONCRETE MEMBERS PRESTRESSED WITH FRP – HUNGARIAN EXPERIENCES



Dr. Adorján Borosnyói – Prof. György L. Balázs

*Present paper intends to review Hungarian experiences on Fibre Reinforced Polymers (FRP) for concrete structures and to discuss design considerations by applying FRP bars or tendons embedded in concrete as prestressed or non-prestressed reinforcement. Test results on FRP indicate high tensile strength, high fatigue strength as well as low relaxation and creep, however, due to lower transverse strength special anchoring devices can be needed. On the other hand, special attention should be taken against brittle failure due to the linear elastic behaviour of FRP. Service design of FRP reinforced or prestressed concrete members can be based on the conventional way of design of reinforced concrete members, however, special considerations are needed and modifications of existing approaches can be developed.*

**Keywords:** Fibre Reinforced Polymer (FRP) reinforcement, durability, serviceability, deflection, cracking

## 1. INTRODUCTION

Corrosion of steel reinforcement is resulted in increasing maintenance costs (especially in bridges) in the last decades. Practicing engineers, researchers and authorities are looking for possible improvements to reduce or even eliminate corrosion of embedded reinforcement in concrete structures. For a long time, concrete was supposed to have infinite service life; therefore, early design codes did not contain any recommendation or limitation on durability of reinforced or prestressed concrete structures. Due to the development of industry and transportation as well as the use of de-icing salts from the 1960s, the environment of human is started to become considerably polluted. Aggressive atmosphere and subsoil water increases the risk of corrosion of embedded reinforcement in concrete. Chloride content of de-icing salts accelerates it. The situation is more dangerous for prestressing tendons in thin-wall precast prestressed girders. Deterioration of highway concrete bridges due to corrosion has a developing tendency, resulting the necessity of frequent structural diagnosis and high maintenance costs. Accordingly, in Hungary more than 2000 are exposed to regular use of de-icing salts from about 6000 highway concrete bridges (Balázs, 1995). Structural engineers – dealing with durability of concrete – greatly concern about possibilities to improve service life of embedded reinforcements. Several proposals have been presented so far from the developments of concrete technology to the use of epoxy coated reinforcements. However, these did not always lead to the expected results. Idea of using Glass Fibre Reinforced Polymer reinforcement instead of steel reinforcement in concrete structures has already appeared in the 1950s, beam tests were also carried out (Rubinsky, Rubinsky, 1959). These pioneering trials were unsuccessful, because glass fibre reinforcements available at that time did not have adequate bond performance. After a long silent period, use of Fibre Reinforced Polymers as reinforcements appeared again in the 1970s. In Germany, Japan and some other countries main field

of research focused on Glass Fibre Reinforced Polymer. Bayer AG (Germany) produced the first commercially available non-metallic prestressing tendon, with the brand name Polystal<sup>®</sup> HLV (Hochleistung-Verbundstab). The supplier developed the full prestressing system with the use of Glass Fibre Reinforced Polymer tendons and anchoring devices. Applicability of the new material was investigated on full-scale experiments (Balázs, Borosnyói, 2000). In the 1980s several experimental and full-scale applications could be found all over the world of Glass Fibre Reinforced Polymer reinforcements in bridges (Sweden, Soviet Union, Japan, USA, etc.). However, the widespread use stopped due to the simple fact, that ordinary glass fibres were not alkaline resistant enough, therefore, suffered considerable deterioration in the alkaline environment of concrete. Nowadays, there is again interest on Glass Fibre Reinforced Polymer reinforcements. These reinforcements consist of glass fibres of special chemical composition as well as special resin matrix (e.g. urethane-modified vinyl ester) that makes the reinforcement alkaline resistant. Manufacturers guarantee the resistance against alkalinity. Such alkaline resistant Glass Fibre Reinforced Polymer reinforcement is C-BAR<sup>®</sup> (Marshall Composites Inc., USA) which is developed for non-prestressed use (European supplier: Schöck Bauteile GmbH, brand name: ComBAR<sup>®</sup>).

As a result of the research work in the 1980s aramid (aromatic polyamide) and carbon fibres were developed. Because of their high price these new fibres were used in the beginning mainly for aerospace research and military purposes (e.g. bullet-proof vests). Gradual price reduction made possible civil aircraft, automotive, electronics (e.g. loudspeakers) and sport equipment (e.g. skis, tennis rackets) applications as well. For civil engineering purposes (i.e. reinforcement for concrete structures) the first Aramid Fibre Reinforced Polymer bars (FiBRA<sup>®</sup>, Technora<sup>®</sup>) and Carbon Fibre Reinforced Polymer bars (CFCC<sup>®</sup>, Leadline<sup>®</sup>) were manufactured in Japan. Highest quantities of these reinforcements are still produced in Japan. In Europe manufacturers can be found in Italy (Arapree<sup>®</sup>,

Carbopree®) or in The Netherlands (Carbon-Stress®). Main advantages of aramid and carbon fibres – besides their high tensile strength – their excellent fatigue strength and resistance to all kinds of aggressive environments. Carbon fibres are completely alkaline resistant, while aramid fibres can be considered alkaline resistant during their service life. In North America, Japan and Europe more and more new bridges are constructed with non-metallic reinforcements. With increasing experiences of these alternative applications the use of FRPs – mainly CFRP – can spread in addition to probably more price reductions.

Civil engineers are currently studying possible applications of FRP reinforcing bars and FRP prestressing tendons. Mechanical properties of FRPs differ from those of conventional prestressing steel leading to different behaviour and design aspects. FRP tendons show linear elastic behaviour and brittle failure with considerable release of elastic energy. Tensile strength of CFRP tendons is generally higher than that of steel prestressing tendons but their Young's modulus and ultimate strain is usually minor to steel prestressing tendons. Owing to the linear elastic behaviour of FRP tendons almost all of the stored energy during loading is elastic, which releases suddenly by failure. Difference in surface configurations of non-metallic reinforcements can also influence structural behaviour.

For concrete members reinforced or prestressed with FRP reinforcement governing parameters of design are often the requirements on serviceability limit states owing to the relatively low Young's modulus of FRP – minor to that of steel. Evaluation of deflections and crack widths need accurate, however, simple methods. Due to the linear elastic reinforcing material a bilinear load vs. deflection response can be observed under service loads that can be modelled in a simple way. On the other hand, due to different surface configurations of FRP reinforcements the cracking behaviour can be also different from that of conventional RC/PC members.

## 2. HUNGARIAN EXPERIENCES

Present paper deals with an experimental programme completed at the Budapest University of Technology and Economics, Faculty of Civil Engineering to study service behaviour of concrete beams prestressed with CFRP tendons in terms of both load vs. deflection responses and cracking behaviour (Borosnyói, 2002). Results of experiments provide valuable information on serviceability limit state to develop future design recommendations for concrete members prestressed with CFRP tendons. Simplified calculation of deflections was introduced with a bond parameter evaluated for sand coated CFRP tendons used for present laboratory tests. Very limited data are available on pivot hysteresis behaviour of flexural members as well as on the influencing parameters. Present research provided information on pivot points of loading-unloading moduli of steel or CFRP prestressed concrete members under repeated loads. Importance of surface configuration of prestressing material on cracking behaviour due to different bond and tension stiffening were also studied.

### 2.1 Materials

Stress-strain responses of prestressing wires (both steel and CFRP) are indicated in Fig 1. Mechanical characteristics are summarised hereafter.

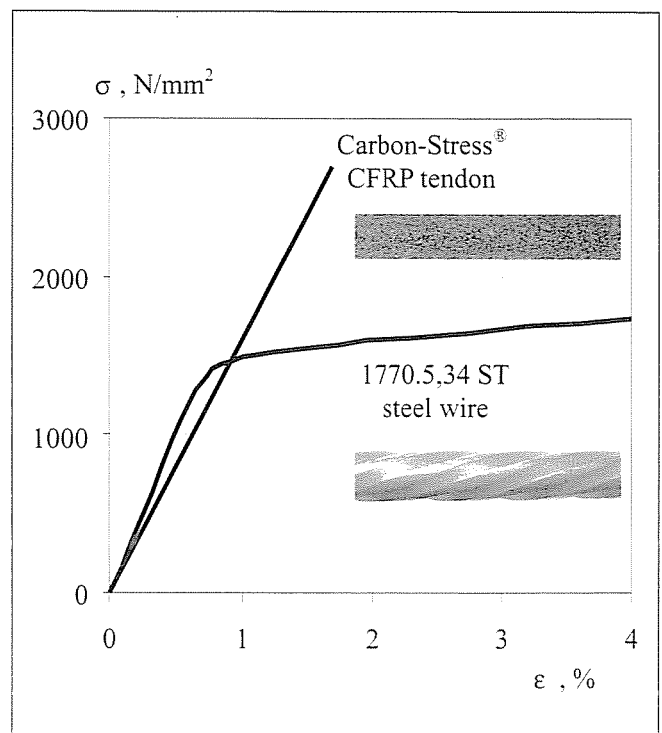


Fig. 1: Stress-strain diagrams of CFRP and steel prestressing wires used in tests

#### A) steel prestressing wires (1770.5,34ST produced by D&D, Hungary)

indented surface pattern,

nominal diameter

$$\varnothing_p = 5.34 \text{ mm}$$

tensile strength

$$f_{ptk} = 1770 \text{ N/mm}^2$$

proof stress

$$f_{p0.1} = 1450 \text{ N/mm}^2$$

ultimate strain

$$\varepsilon_{pu} = 3.5 \%$$

Young's modulus

$$E_p = 195\,000 \text{ N/mm}^2$$

relaxation loss

$$\rho = 2.5 \%$$
 (1000 h, 20°C, under  $0.7f_{ptk}$ )

coefficient of thermalexpansion

$$\alpha_f = 10 \times 10^{-6} \text{ m/m/}^\circ\text{C} \text{ (longitudinal and transverse).}$$

#### B) CFRP prestressing wires (Carbon-Stress® produced by NEDRI, NL) (Nedri, 1998)

sand coated surface pattern,

nominal diameter

$$\varnothing_f = 5.0 \text{ mm}$$

tensile strength

$$f_{tu} = 2700 \text{ N/mm}^2$$

ultimate strain

$$\varepsilon_{tu} = 1.7 \%$$

Young's modulus

$$E_f = 158\,800 \text{ N/mm}^2$$

relaxation loss

$$\rho = 1.0 \%$$
 (under  $0.7f_{tu}$ )

Poisson's ratio

$$\nu = 0.3$$

coefficient of thermal

expansion

$$\alpha_f = 0.2 \times 10^{-6} \text{ m/m/}^\circ\text{C}$$

(longitudinal)

$$\alpha_f = 23 \times 10^{-6} \text{ m/m/}^\circ\text{C}$$

(transverse).

Specimens were prepared by Pfeleiderer Precast Concrete Company, Lábatlan, Hungary. Maximum aggregate size of 16 mm of continuous grading curve is indicated in Fig 2. (fineness modulus,  $m = 6.30$ ). Applied water-cement ratio was 0.35 with CEM II/A-V32,5R (500 kg/m<sup>3</sup>) without any admixtures. Characteristic compressive strength of concrete cubes was  $f_{ck} = 57.4 \text{ N/mm}^2$  at the age of 28 days, stored under water for the first 7 days (with  $f_{cm} = 65.0 \text{ N/mm}^2$ ).

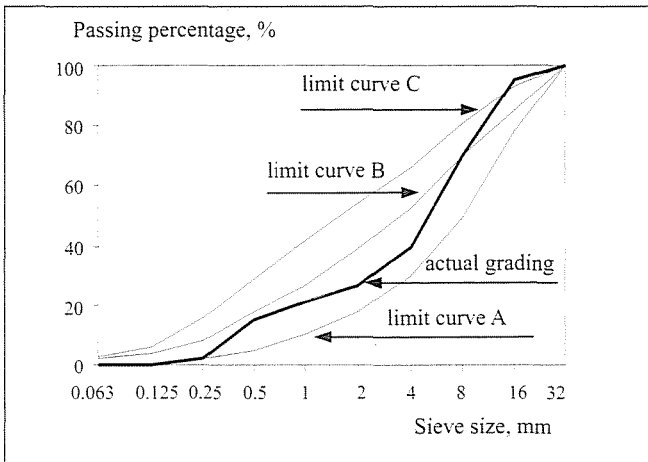


Fig. 2: Grading curve of aggregate used for concrete in tests

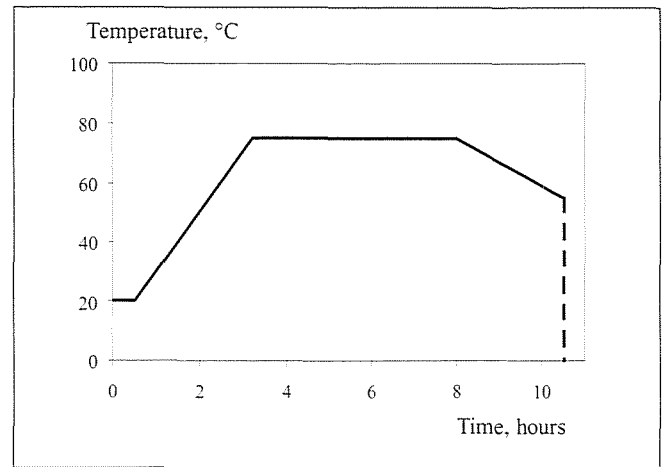


Fig. 4: Temperature development during heat curing

## 2.2 Preparation of test specimens

For test specimens the configuration of a typical prestressed concrete girder was chosen (i.e. considerable compression zone, relatively thin web, etc.). A conventional Hungarian prestressed concrete floor girder system, the so-called E-type pre-tensioned concrete girder was adopted for testing purposes. Specimens were prepared by Pfeleiderer Precast Concrete Company, Látatlan, Hungary. Test beams had an I-cross-section with relatively thin web and did not contain any other longitudinal reinforcement but prestressed pre-tensioned tendons (Fig 3). Beams had the same cross section, with minimum concrete cover of 12 mm. Number of prestressing wires was 1, 2 or 4. For comparison non-prestressed elements were also cast with 2 tendons. Test beams were steam cured for ten hours at a maximum temperature of 75°C. Temperature development of curing process is presented in Fig 4.

Application of prestressing force on the CFRP wires required special attention owing to their relatively low transverse strength compared to their high axial strength. CFRP wires used for present tests are not supplied with anchorages for prestressing. Therefore, the following technique was developed for prestressing the CFRP wires. Steel tubes with a length of 150 mm were glued to both ends of the CFRP wires by Sika Icosit KC220/60 epoxy resin (Fig 5). Prestressing force was applied by a conventional prestressing jack suitable to prestress  $\varnothing$  12.8 (1/2 in) strands. Six beams were cast in each turn separated by hard rubber profiles. Each tendon was pre-tensioned to a 26.3 kN load, that means 1340 N/mm<sup>2</sup> and

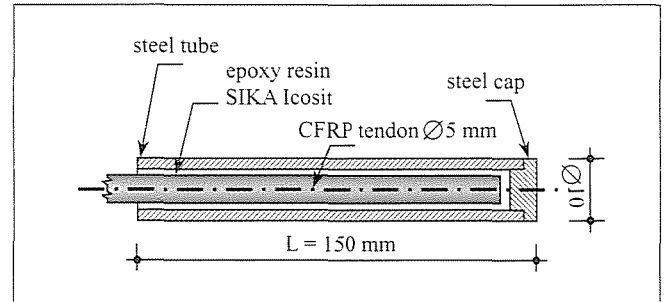


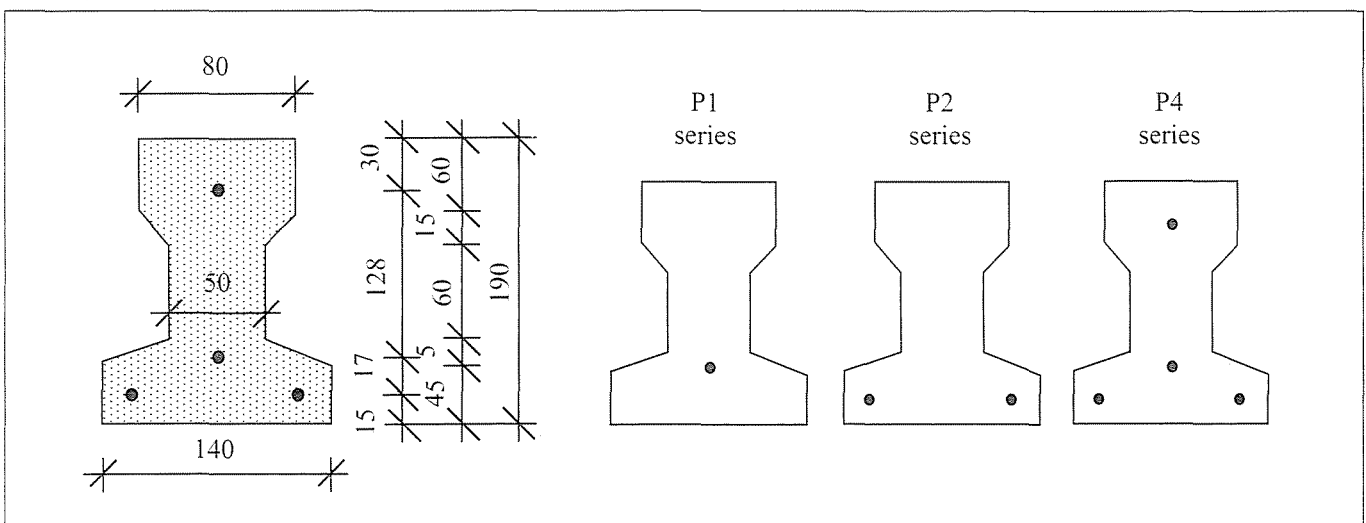
Fig. 5: Anchoring device

1174 N/mm<sup>2</sup> initial prestress in the CFRP and steel wires, respectively. After steam curing prestressing force was released by flame cutting of steel wires and sawing of CFRP tendons. First observation after steam curing and tension release was that neither temperature difference during steam curing, nor sudden release of prestressing force initiated longitudinal cracks in any beam.

## 2.3 Test method and evaluation

Beams were tested with a clear span of 3.0 m under four-point bending (loads acting at the third points). Loads were applied by means of two hydraulic jacks at the third points. Load cells recorded quasi-static monotonic loads. Deflection was continuously registered with an LVDT at the mid-span. Four loading-unloading cycles were applied at specified deflection levels (i.e. right after cracking and at mid-span deflections

Fig. 3: Typical cross sections of beam specimens



of 10, 20, 30 and 40 mm) before loading up to failure. Load vs. deflection responses were continuously followed by a portable computer (presented real-time on screen) and recorded digitally. Every crack width was measured at the level of the prestressing tendons by hand microscope at each load step.

## 2.4 Aim of studies

In present research work detailed analyses were given on the following fields:

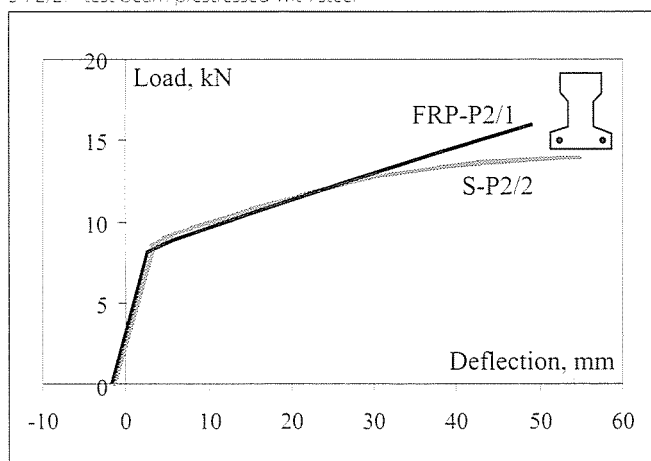
- Presentation of a new bilinear proposal for the calculation of deflections of CFRP prestressed concrete flexural members based on own experimental results and verified on experimental results available by other researchers,
- Proposal for a possible modification to the CEB method for the calculation of deflections in the case of CFRP reinforced or prestressed concrete flexural members,
- Analysis of load vs. deflection pivot behaviour under repeated loads,
- Detailed analysis on the flexural cracking behaviour of concrete members reinforced or prestressed with sand coated CFRP wires,
- Proposals for possible modifications of parameters of code formulae on crack spacings and crack widths for sand coated CFRP wires or indented steel wires.

## 3. EXPERIMENTAL RESULTS AND DISCUSSION

In present test programme load vs. deflection responses of both steel and CFRP prestressed concrete members were linear before reaching the cracking load with almost equal flexural stiffness. Exceeding the cracking load, the load vs. deflection diagrams of CFRP prestressed members remained practically linear with lower stiffness on the contrary to steel prestressed members, which showed slight non-linearity. The decrease of flexural stiffness was a function of the applied reinforcement ratio. Bilinear behaviour of CFRP prestressed members was due to the linear elastic behaviour of CFRP prestressing tendons. Comparative load vs. deflection responses are indicated in Fig 6.

In present experimental programme measured cracking load as well as the mid-span deflection at failure were not found to depend on the type of prestressing material. The mode of failure has changed from tendon failure (in case of one tendon)

**Fig. 6:** Comparative load vs. deflection responses  
FRP-P2/1: test beam prestressed with CFRP  
S-P2/2: test beam prestressed with steel



to crushing of concrete (in case of four tendons). Most of the beams failed in shear because no shear reinforcement was used. CFRP tendons broke during the shear failure on the contrary to steel wires, which kept the failed parts together. So the dowel action of CFRP tendons was found to be negligible.

Recommendations of CEB-FIP Model Code 1990 (MC90) were used for the calculations of cracking moments and ultimate moments in terms of Young's modulus and flexural tensile strength of concrete based on mean compressive strength of concrete ( $E_c = 40.1 \text{ kN/mm}^2$ ,  $f_{ct,fl} = 6.3 \text{ N/mm}^2$ ). It could be realised that cracking moments can be estimated reasonably well by using flexural tensile strength of concrete calculated by recommendations of MC90.

## 3.1 Deflection control

Load vs. deflection responses of concrete beams prestressed with CFRP tendons are practically bilinear. Based on present experimental data a new bilinear approach could be developed for the simplified calculation of deflections of CFRP prestressed concrete beams. In uncracked elastic state (*State I*) moment of inertia ( $I_1$ ) and deflections can be predicted accurately using the assumptions of CEB-FIP Model Code 1990 by simple substitution of mechanical properties of CFRP reinforcement. Evaluation of the cracking moment ( $M_r$ ) is also accurate (see above). Reaching the cracking load ( $M_r$ , calculated according to MC90) use of the following effective moment of inertia is proposed (Fig 7):

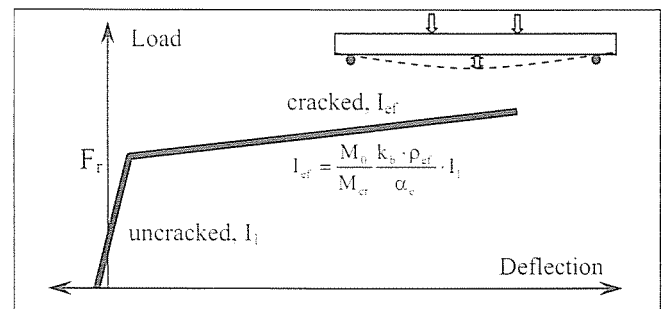


**Fig. 7:** illustration for the developed bilinear formula

$$I_{ef} = \frac{M_0 \cdot k_b \cdot \rho_{ef}}{M_r \cdot \alpha_c} \cdot I_1 \quad (1)$$

$$\text{where } M_0 = -N \cdot x_{12} \frac{1/r_2}{1/r_2 - 1/r_1}, \text{ and } x_{12} = x_1 - x_2 \quad (2)$$

$$N = A_r \cdot \sigma_{p,ef} \quad (3)$$

$$\rho_{ef} = \frac{A_r}{A_{c,ef}} \quad (4)$$

$$\alpha_c = \frac{E_r}{E_c} \quad (5)$$

In Eq. (1) parameter  $k_b$  takes bond properties of the CFRP tendon into consideration. Evaluation of present test results by the method of least square errors gave the value of the bond parameter ( $k_b$ ) for sand coated CFRP prestressing tendons to be:

$$k_b = 50.$$

The model introduced herein can provide accurate estimation of load vs. deflection responses of CFRP prestressed concrete beams in service conditions (Fig 8). Further analysis can be found elsewhere (Borosnyói, 2002).

### 3.2 Crack control

Cracks are formed in reinforced concrete members when the principal tensile stress from loads or restraint forces reaches the tensile strength of concrete. Cracks can be avoided only in fully prestressed members. Formation of cracks of flexural members can be distinguished into two phases: the *crack formation phase* and the *stabilised cracking phase* (CEB, 1985). During *crack formation phase* cracks form at random positions according to the locally weak sections. The compatibility of strains between concrete and reinforcement is no more maintained at a crack as concrete stress dropped to zero. With increasing the distance from the crack the tensile stress in the concrete increases as force is transferred by bond stresses. At some distance the compatibility of strains between concrete and reinforcement is again recovered. The better the bond properties of the reinforcing tendon, the shorter the length for re-establishing strain compatibility. At the crack formation phase the disturbed zones are independent from each other and increase of load causes the decrease of the average crack spacing. The so-called *stabilised cracking phase* is reached when no more new cracks may form. Under this condition cracks are so close to each other that the disturbed zones can not be independent. At the stabilised cracking phase the average crack spacing remains constant. Increase of load causes increase of only the crack widths. The average crack spacing at stabilised cracking phase is a function of bar diameter, bond properties, concrete tensile strength and effective reinforcement ratio.

Present test results demonstrated that sand coated surface of CFRP prestressing tendons gives favourable cracking behaviour of close cracks with small widths. High bond strength of these tendons allows tensile stresses to be transferred along a very short distance adjacent to cracks. In this way the average crack spacing can be much less than that of steel prestressed members. Fig 9 shows the crack distribution of beams prestressed either with CFRP or steel tendons close to failure (midspan deflection = clear span/75). In Fig 9. columns give the positions of cracks and heights of columns represent crack widths.

Cracking force of CFRP prestressed members can be predicted accurately using formulae of MC 90 as studied before. Further question is the load level at reaching the stabilised cracking phase. The MC90 recommends the following ratio

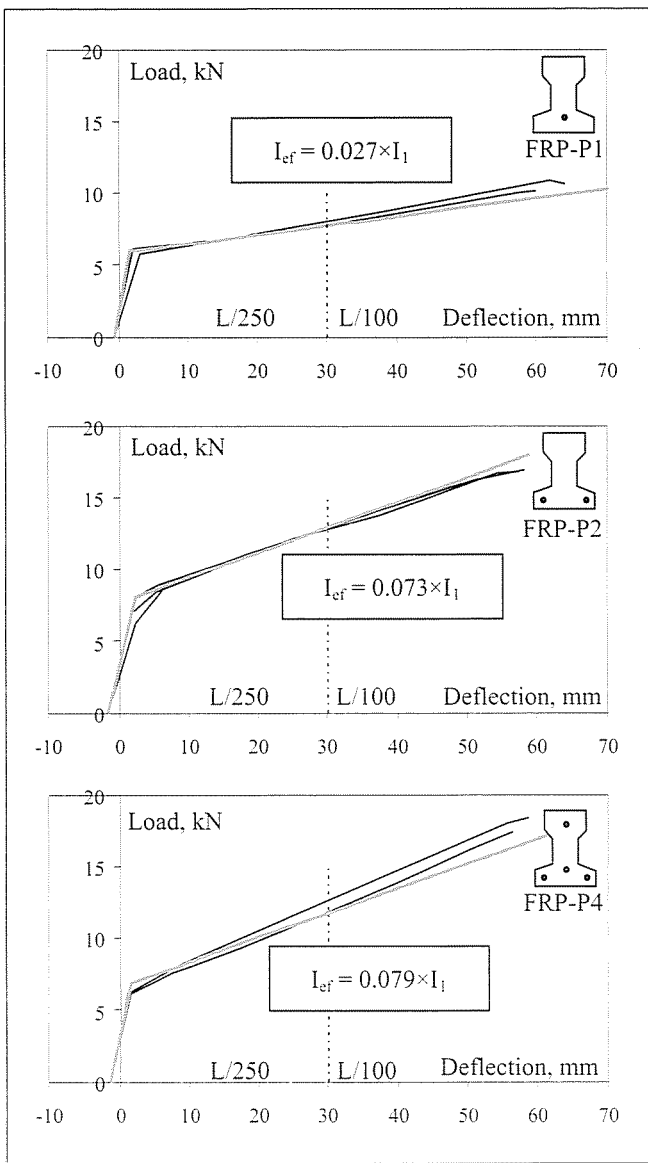
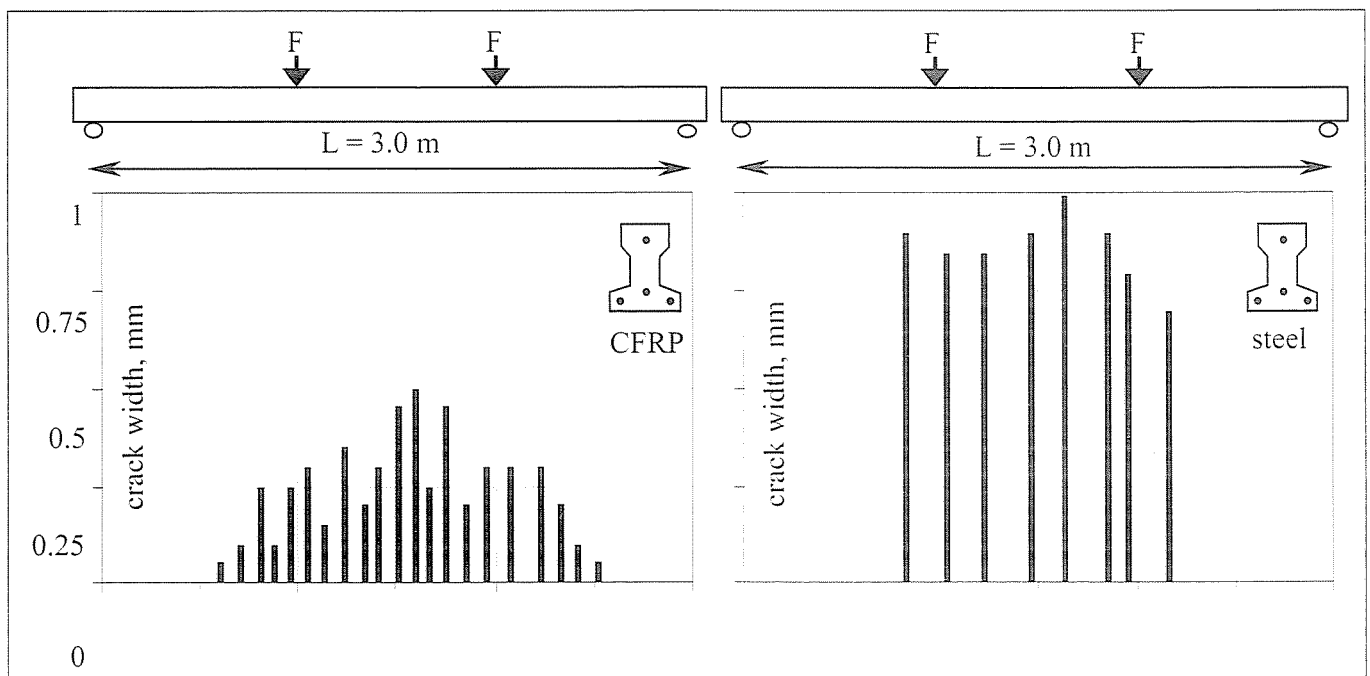


Fig. 8: Evaluation of load vs. deflection responses for the tested members with the developed bilinear formula

Fig. 9: Crack distribution of beams prestressed either with four CFRP or with four steel wires (at a midspan deflection of L/75)



for cracking load and load at reaching stabilised cracking phase [MC90 Clause 3.2.3, p. 91, Eq. (3.2-7)]:

$$F_m = 1.3 F_r$$

Fig 10 represents experimental data on the ratio of cracking load and load at reaching stabilised cracking phase as a function of applied effective reinforcement ratio both for steel and CFRP prestressed elements. Results for steel prestressed members with ratio of  $F_m/F_r = 1.303$  can prove the above assumptions. However, results for CFRP prestressed members with ratio of

$$F_m = 1.46 F_r$$

may indicate the importance of other parameters on the load level at reaching stabilised cracking phase such as Young's modulus (was 158 800 N/mm<sup>2</sup> for CFRP) or high bond capacity of sand coated surfaces.

Development of cracking can be also described by following the increase in the number of flexural cracks under increasing loads (or as a function of average strain of reinforcement). If it is supposed that the average strain of reinforcement is constant along the constant moment zone the following definition of the average strain of reinforcement can be applied:

$$\varepsilon_{sm,r} = \frac{w_m}{s_{sm}}$$

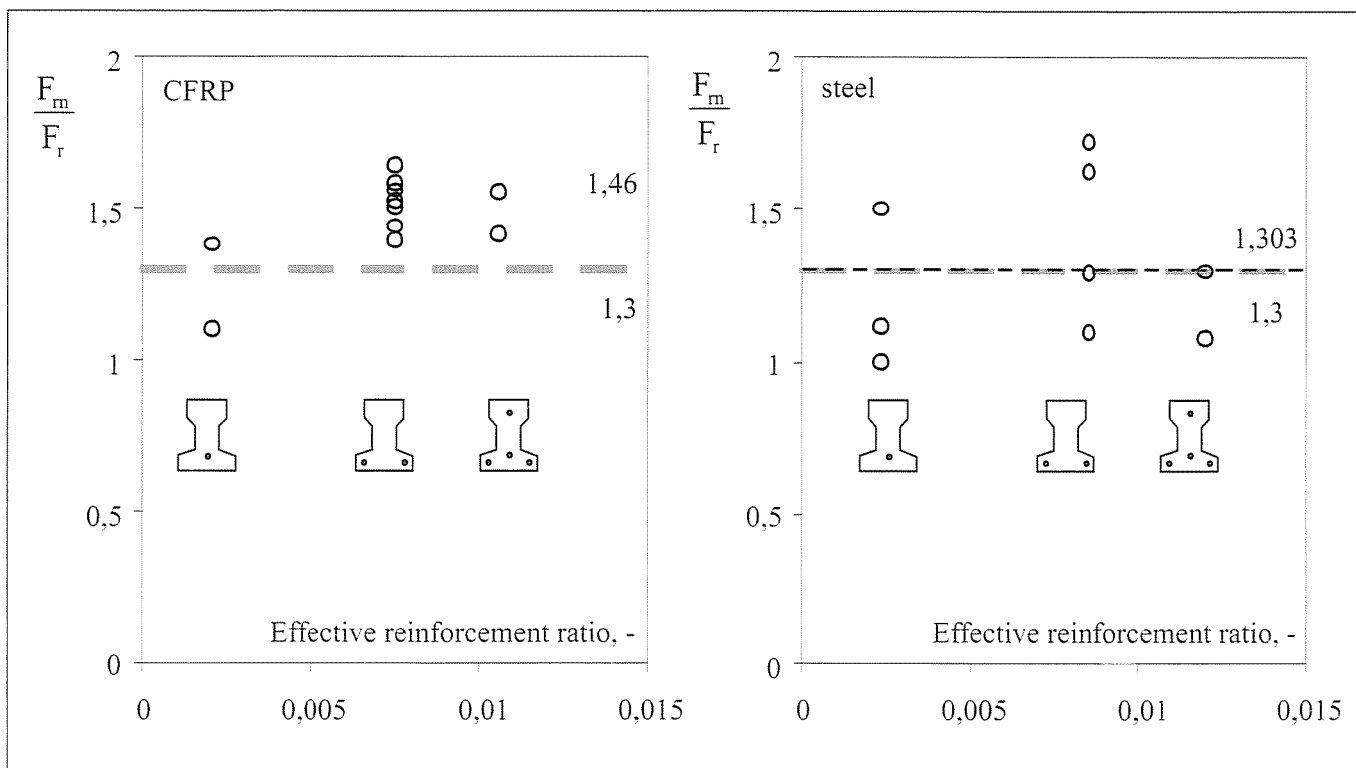


Fig. 10: Ratios of cracking load and load at reaching stabilised cracking phase

Fig. 11a: Number of flexural cracks and average tendon strains ( $\varepsilon_{sm,m}$ )

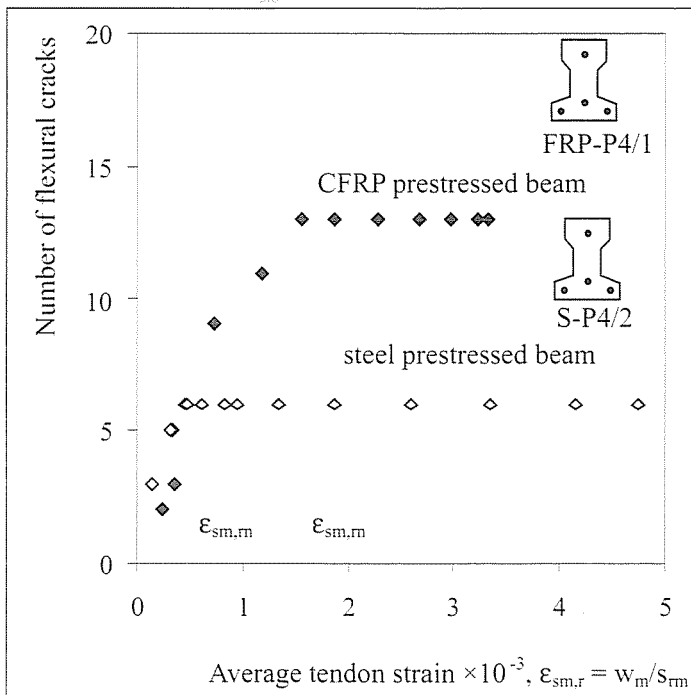
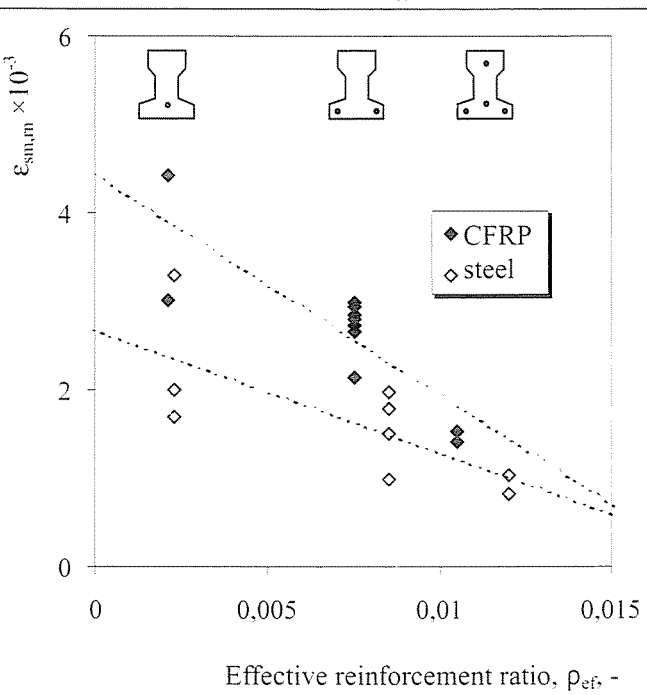


Fig. 11b: Effective reinforcement ratio and  $\varepsilon_{sm,r}$



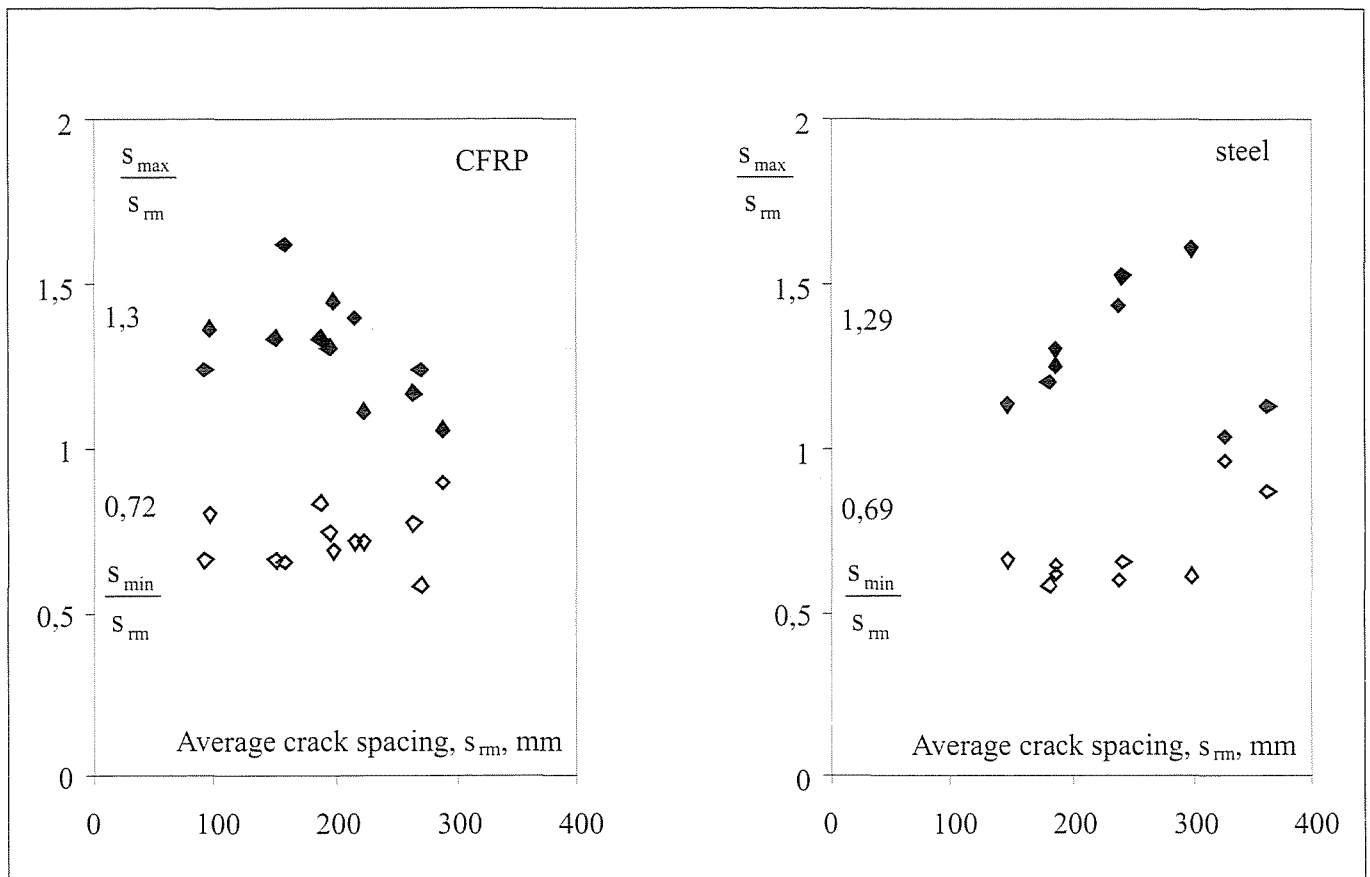


Fig. 12: Ratios of minimum vs. average and maximum vs. average crack spacings

where  $w_m$  – average crack width along the constant moment zone  
 $s_{rm}$  – average crack spacing along the constant moment zone

Fig 11 represents increase in the number of flexural cracks vs. average tendon strain for beams prestressed with four tendons. Result indicates that in the case of steel prestressed members stabilisation of crack pattern is reached under much lower average strain of reinforcement ( $\epsilon_{sm,m}$ ) than in the case of CFRP prestressed members. This behaviour is due to the high bond capacity of sand coated surfaces of CFRP tendons.

In present tests occurrence of flexural cracks was found to be

random in the constant moment zone, as indicated above. Fig 12 represents experimental data on the ratios of minimum vs. average crack spacings as well as maximum vs. average crack spacings both for steel and CFRP prestressed elements.

Based on present test results extensions of code formulae can be developed for the estimation of crack spacings. Proposals for CEB-FIP Model Code 1978, Eurocode 2 (1991), CEB-FIP Model Code 1990 and Japan Society of Civil Engineers (JSCE, 1997) are summarised in Table 1.

Based on experimental results the ratios of  $w_{max}/w_m$  and  $w_{min}/w_m$  can be represented as a function of effective reinforcement ratio. It can be concluded that ratio of  $w_{max}/w_m$  seems to be a function of bond characteristics of applied

Fig. 13: Ratios of maximum vs. average crack widths and minimum vs. average crack widths for all test members as a function of effective reinforcement ratio

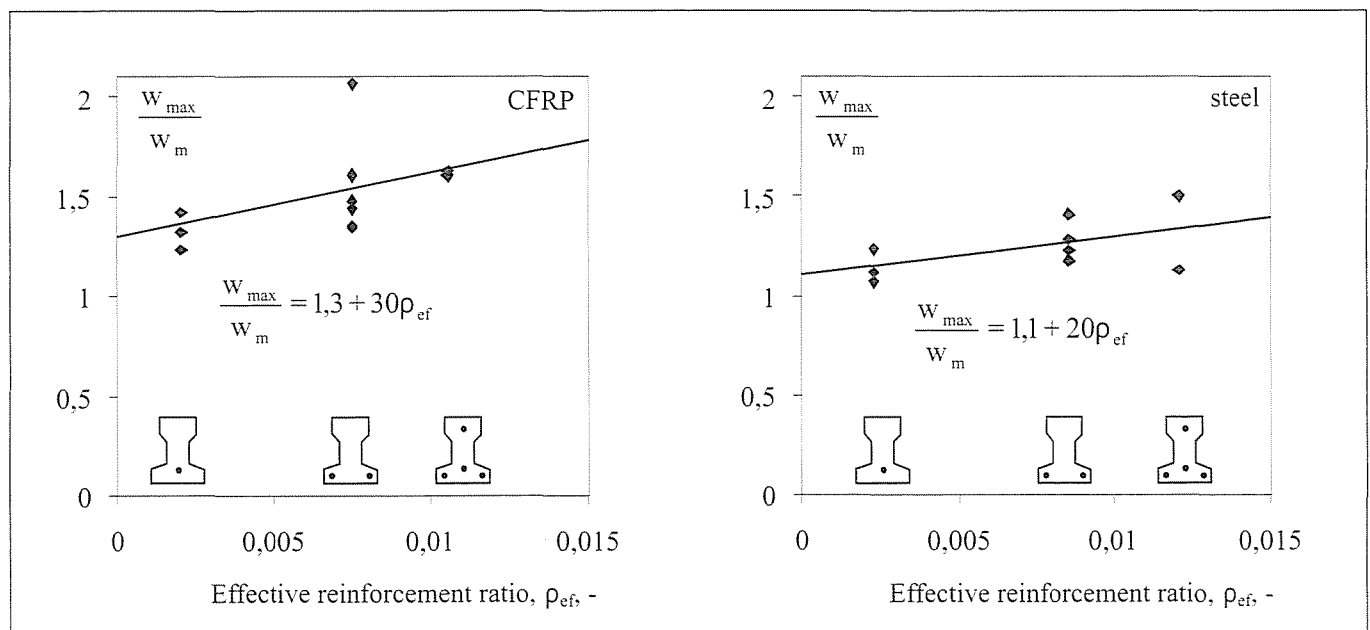




**Table 1:** Proposals for the extensions of average crack spacing ( $s_{rm}$ ) estimation

General form of formula	Original value of parameter (for deformed steel bars)	Proposed new value of parameter	
		sand coated CFRP tendon	indented steel wire
$s_{rm} = 2(c + \frac{s}{10}) + \kappa_1 \kappa_2 \frac{\sigma_s}{\rho_{ef}}$	$\kappa_1 = 0.4$	$\kappa_1 = 0.7$	$\kappa_1 = 1.08$
		$\kappa_1 = 0.4 + 40\rho_{ef}$	$\kappa_1 = 0.4 + 90\rho_{ef}$
$s_{rm} = 50 + 0.25k_1 k_2 \frac{\sigma_s}{\rho_{ef}}$	$k_1 = 0.8$	$k_1 = 2.58$	$k_1 = 4.17$
		$k_1 = 0.8 + 200\rho_{ef}$	$k_1 = 0.8 + 400\rho_{ef}$
$s_{rm} = \frac{2}{3} \frac{f_{ctm}(t) \cdot \sigma_s}{2\tau_{bm} \cdot \rho_{ef}}$	$\tau_{bm}/f_{ctm}(t) = 1.8$	$\tau_{bm}/f_{ctm}(t) = 2.18$	$\tau_{bm}/f_{ctm}(t) = 1.54$
$s_{rm} = k[4 \cdot c + 0.7(s - \sigma_s)]$	$k = 1.0$	$k = 1.42$	$k = 1.7$

**Table 2:** Ratios of maximum vs. average and minimum vs. average crack widths for test members

	$\frac{W_{max}}{W_m}$	$\frac{W_{max}}{W_m}(\rho_{ef})$	$\frac{W_{min}}{W_m}$
sand coated CFRP wire	1.51	$1.3 + 30\rho_{ef}$	0.53
indented steel wire	1.24	$1.1 + 20\rho_{ef}$	0.74

reinforcing material. Present results for sand coated CFRP tendons (with high bond capacity) fit well to experimental results that was introduced in the technical literature. However, results for indented steel wires (with limited bond capacity) were found to be minor to that was introduced in the technical literature. This influence should be taken into account during prediction of characteristic crack width as multiple of the average crack width. Results also indicate that reinforcement ratio has a strong influence on the ratio of  $w_{max}/w_m$ . Linear functions (based on evaluations by the method of least squares) are presented in Fig 13 and Table 2. Further analysis can be found elsewhere (Borosnyói, 2002).

## 4. CONCLUSIONS

Use of non-metallic (FRP) reinforcements can provide a promising alternative to avoid corrosion in reinforced concrete. By applying non-metallic (FRP) reinforcements there is no ferrous material to corrode in reinforced concrete.

Present paper reviewed Hungarian experiences on Fibre Reinforced Polymers (FRP) for concrete structures. An experimental programme completed at the Budapest University of Technology and Economics, Faculty of Civil Engineering to study service behaviour of concrete beams prestressed with CFRP tendons in terms of both load vs. deflection responses and cracking behaviour. Detailed deflection control and crack control was presented with introduction of new simplified formulae and extension of existing code proposals to CFRP materials.

## ACKNOWLEDGEMENTS

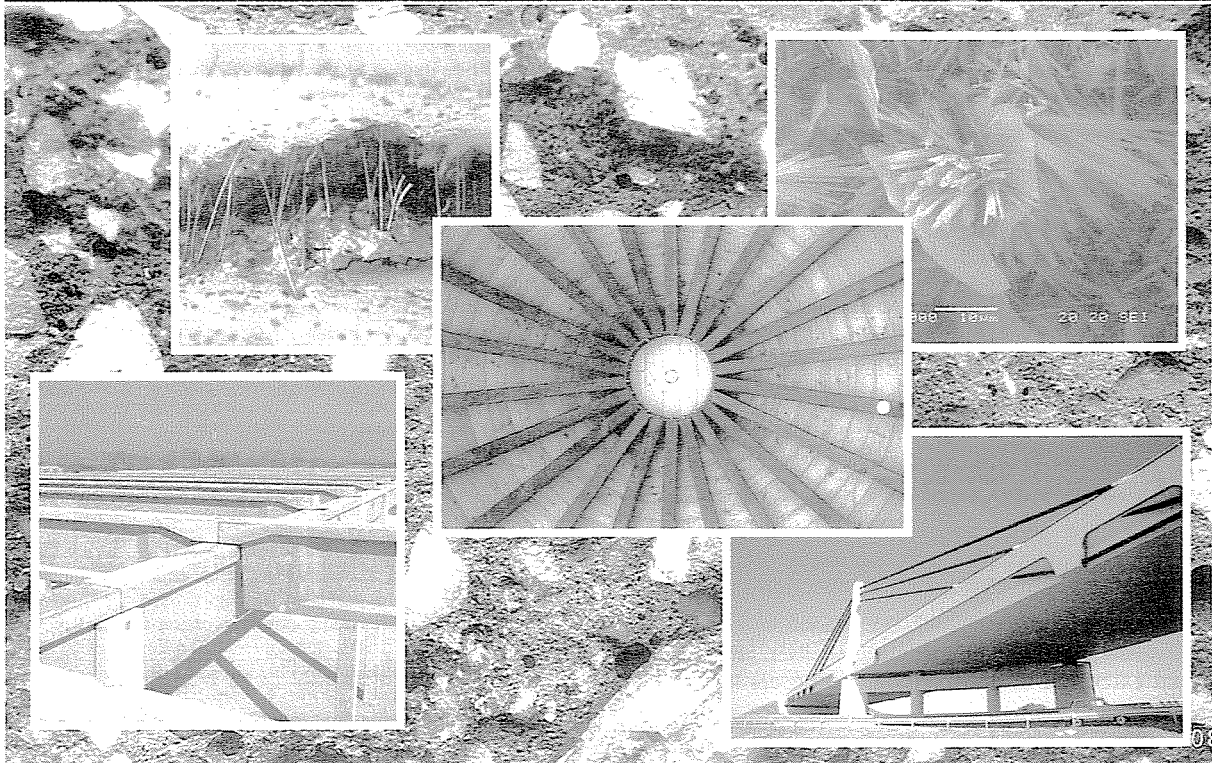
Authors gratefully acknowledge the financial support of the Hungarian Ministry of Education (OM, Contract No. 18657/2005, OM PÁL 94/2005) and that of the Hungarian Research Fund (OTKA F61685).

## REFERENCES

- Balázs, Gy. (1995) „Concrete and Reinforced Concrete. Volume 2: History of Concrete and Reinforced Concrete Structures in Highway-, Bridge- and Infrastructure Engineering”, Akadémiai Kiadó, Budapest, 1995. (in Hungarian)
- Balázs L. Gy., Borosnyói A. (2000b) „Non-metallic (FRP) reinforcements for bridge applications”, Vasbetonépítés, Vol. 2., No. 1., 2000/1. pp. 45-52. (in Hungarian)
- Borosnyói, A. (2002) „Serviceability of CFRP Prestressed Concrete Beams”, PhD Thesis, Budapest University of Technology and Economics
- CEB (1978) “CEB-FIP Model Code 1978 – Design Code”, Comité Euro-International du Béton, Thomas Telford, London, 1978 (CEB Bulletin d'Information No. 124/125.)
- CEB (1985) “Design Manual on Cracking and Deformations”, CEB Bulletin, Ed. Favre, École Polytechnique Fédérale de Lausanne, Suisse, 1985
- CEB-FIP (1993) “CEB-FIP Model Code 1990 – Design Code”, Comité Euro-International du Béton, Thomas Telford, London, 1993 (CEB Bulletin d'Information No. 213/214.)
- CEN (1991) “Eurocode 2: Design of Concrete Structures, General Rules and Rules for Buildings”, European Prestandard ENV 1992-1-1, Dec 1991
- JSCE (1997) “Recommendation for Design and Construction of Concrete Structures Using Continuous Fiber Reinforcing Materials”, Edited by Machida, Concrete Engineering Series Vol. 23, JSCE, Tokyo, 1997.
- Nedri Spanstaal BV (1998), „Nedri Product Range: Carbon-Stress®”, Manual, Venlo, the Netherlands
- Rubinsky, A., Rubinsky, I. A. (1959) “A Preliminary Investigation of the Use of Fiber Glass for Prestressed Concrete”, Magazine of Concrete Research, Sept. 1959, pp. 71-78.
- Dr. Adorján Borosnyói** (1974) MSC (CEng), PhD, senior lecturer at the Budapest University of Technology and Economics. His main fields of interest: serviceability and durability of reinforced concrete and prestressed concrete structures, application possibilities of non-metallic (FRP) reinforcements in reinforced or prestressed concrete, bond in concrete, strengthening with advanced composites. In his PhD Thesis he deals with serviceability of CFRP prestressed concrete members. Member of *fib* TG 4.1 “Serviceability Models” and the Hungarian Group of *fib*.
- Prof György. L. Balázs** (1958) PhD, Dr. habil, professor in structural engineering, head of Department of Construction Materials and Engineering Geology at the Budapest University of Technology and Economics. His main fields of activities are: experimental and analytical investigations as well as modelling reinforced and prestressed concrete, fiber reinforced concrete (FRC), fiber reinforced polymers (FRP), high performance concrete (HPC), bond and cracking in concrete and durability. He is convener of *fib* Task Groups on “Serviceability Models” and “*fib* seminars”. In addition to he is a member of several *fib*, ACI, and RILEM Task Groups or Commissions. He is president of the Hungarian Group of *fib*. Member of *fib* Presidium.



# Central European Conference on Concrete Engineering



Visegrád, Hungary  
17-18 September 2007



**INNOVATIVE MATERIALS AND TECHNOLOGIES  
FOR CONCRETE STRUCTURES**

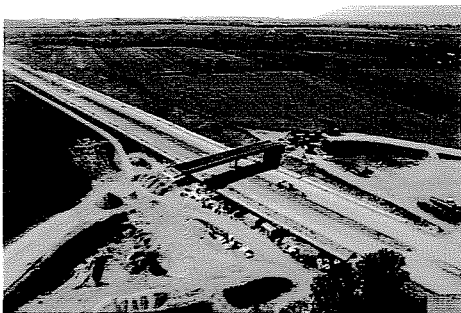


## The STRABAG Company in Hungary

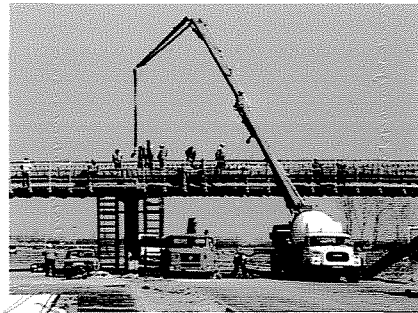


The Road and Bridge Construction Division of STRABAG has gained new impetus when the new Hungarian motorway program – directed by NA Rt. – was launched in 2003. The new sections of M7 motorway and M70 highway between Becsehely – Letenye – Tornyiszentmiklós and the south-eastern section of M0 motorway in December, 2005 were opened to traffic in the framework of the new program.

We participated and still participate in the construction of M5 motorway between Kiskunfélegyháza and the State Border. At present we are also executing the road, bridge and different concrete structure construction works of motorways M35 between Görbeháza – Debrecen and M7 between Zamárdi – Balatonszárszó.



STRABAG, having 200 billion HUF annual turnover and 3500 employees, has become a leading market provider of the construction sector in Hungary.



Whether it is motorways, bypasses, construction or rehabilitation works of local transport networks, construction of motorway bridges, building of business centers, hotels, gas stations,



commercial and industrial establishments, waste-management plants or sewage-treatment plants, STRABAG is always present.

# STRABAG

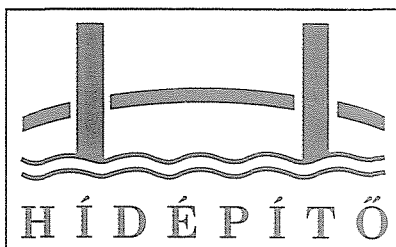
STRABAG, the Hungarian company of the international Strabag Group, was established in 2001 by the merger of two prestigious construction companies: Magyar Aszfalt Ltd. and STRABAG. The activities of STRABAG cover the fields of road and bridge construction and overground engineering.



### STRABAG Építő Zrt.

Road and Bridge Construction Division  
Division Director: Appelshoffer József

H-1135 Budapest, Szegedi út 35-37.  
Phone: 00-36-1-270-8581, Fax: 00-36-1-270-8583



ÉPÍTŐIPARI  
MESTERDIJ 1996

# HÍDÉPÍTŐ RÉSZVÉNYTÁRSASÁG

H-1138 Budapest, Karikás Frigyes u. 20. Mailing address: H-1371 Budapest 5 P. O. B.: 458  
Phone: +36 1 465 2200 Fax: +36 1 465 2222

## Extension of the South-Pest Wastewater Treatment Plant



The State-owned Hidépitő Company, the professional forerunner of Hidépitő Részvénytársaság was established in year 1949 by nationalising and merging private firms with long professional past. Among the professional predecessors has to be mentioned the distinguished Zsigmondy Rt., that participated, inter alia, in the construction of the Ferenc József (Francis Joseph) bridge which started in year 1894.

The initial purpose of establishing Hidépitő Company was to reconstruct the bridges over the rivers Danube and Tisza, destroyed during the Second World War, and this was almost completely achieved.

The next important epoch of the "Hidépitők (Bridge Builders)" was to introduce and to make general the new construction technologies.

Even among these can be judged to outstanding the bridge construction by balanced cantilever method, the experts having participated in it were awarded the State Prize. By this technology were constructed five bridges in the region of rivers Körösök and this was applied at the flyover of Marx square (today Nyugati square) in Budapest, still the most up-to-date two-level crossing in the capital requiring the minimum maintenance works.

The next big step was the introduction of the so-called cast-in-situ cantilever bridge construction method. This technology was applied for four bridges constructed over great streams, among them can be found the bridge with largest span (120 m) in Hungary made of stressed reinforced concrete, the road bridge over river Tisza at Szolnok.

An important result of the technologic development in the bridge construction was the intro-

duction of the so-called incremental launching method. In the period from year 1989 up to now yet 22 bridges were constructed by this method, mainly on the base of the designs prepared by the Company's own Technical Department.

Among them distinguishes itself the viaduct made of stressed reinforced concrete in length of 1400 m on the Hungarian-Slovenian railway

In the recent two years a great number of important professional recognitions were awarded the high level activity in the fields of bridge construction and bridge designing.

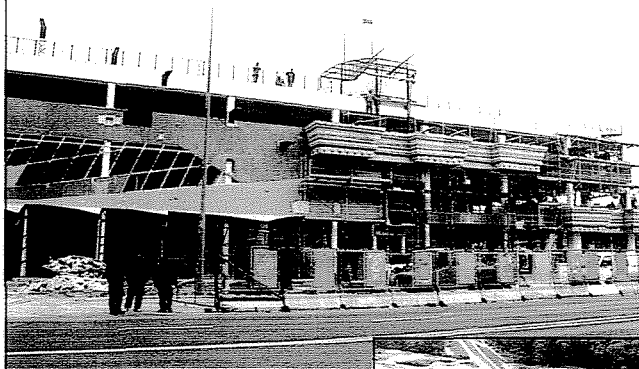
- High standard Prize of Building Industry for designing and constructing a bridge in length of twice 187 m on the section accessing Budapest of the motorway M5 (2000),

- Innovation Grand Prix for designing and constructing in record-time (one year) viaducts in length of 1400 m and 200 m on the Hungarian-Slovenian railway line at Nagyrákos (2001),

- Prize of Concrete Architecture for designing the viaducts at Nagyrákos (2001).

Nowadays, beside the high level activity in the field of bridge construction, the Company has extended its scope of activity by taking part in winding up the backwardness in infrastructure, construction of drinking water treatment plants, wastewater treatment plants, solid waste spoiling areas and sewers as well as by the introduction of the architectural engineering profile.

## The Market Hall "Lehel" in progress of construction



line, near the Slovenian State Border, constructed in one year using the incremental launching method.

Beside the bridge construction, important results were achieved by the "Hidépitők (Bridge Builders)" in the field of foundation's technological development as well, in the introduction and general use of the bored piles with large diameter, of jet grouting and of CFA (Continuous Flight Auger) pile preparation, further also a new method, subject of patent protection, was developed for very quick and economic constructing bridge piers in living water.

The Company was privatised (bought by the French Company GTMI) in year 1993. Following the multiple merger of the foreign interest parent Company, today Hidépitő Rt. belongs to the multinational Company "VINCI".



The 1400 m long viaduct on the Hungarian-Slovenian railway line at Nagyrákos

By working in good quality the Company makes efforts to inspire the confidence of the Clients. For this purpose have been introduced and operated the Quality Assurance and Environment Controlling Systems meeting the requirements of the international Standards ISO 9001:1994 and ISO 14001:1997, justified by international certificates.

The Company is hopefully awaiting the new tasks in order to enhance the reputation of the "Hidépitők (Bridge Builders)".